Author/s:
Zulkifli, Ahmad Azri

Title:
Understanding and overcoming resistance to epidermal growth factor receptor therapy

Date:
2020

Persistent Link:
https://hdl.handle.net/11343/251867

Understanding and Overcoming Resistance to Epidermal Growth Factor Receptor Therapy

Ahmad Azri Zulkifli

ORCID: 0000-0003-0543-365X

Doctor of Philosophy

June 2020

Faculty of Medicine, Dentistry, and Health Sciences

Department of Surgery

Royal Melbourne Hospital

Submitted to The University of Melbourne in total fulfilment of the requirements of the degree of Doctor of Philosophy

ABSTRACT

Colorectal cancer (CRC) is the fourth most common cancer diagnosed in Australia. Current standard treatment includes surgery, chemotherapy, and targeted therapy. Cetuximab is often used as part of the clinical management of unselected patients until a subset of patients were found to harbor KRAS mutations that conferred intrinsic resistance to Cetuximab. In addition, some patients are resistant to Cetuximab despite having wild-type KRAS. Using RNA-sequencing data and differential expression analysis, we discovered five potential biomarkers for predicting resistance to Cetuximab in CRC with wild-type KRAS. After generating 3 CRC models of acquired resistance to Cetuximab, we also employed proteomics analysis to determine potential biomarkers of acquired Cetuximab resistance in CRC cells with wild-type KRAS. In addition, we generated pre-clinical data for the repurposing of Carfilzomib (CFZ) as a novel drug to overcome Cetuximab resistance in metastatic colorectal cancer patients. In conclusion, this study provides a Cetuximab resistant model that can be used for further studies coupled with possible resistance mechanism as well as a novel drug to overcome Cetuximab resistance.

DECLARATION

This declaration is to certify that:

i. The thesis comprises only their original work towards the Ph.D. except where indicated in the preface.

ii. Due acknowledgement has been made in the text to all other material used.

iii. The thesis is fewer than 100,000 words in length, exclusive of tables, maps, bibliographies, and appendices.

Royal Melbourne Hospital

Department of Surgery

The University of Melbourne

PREFACE

The experimental data described in this thesis comprises only my original work, except for the following results, obtained in collaboration:

- Proteomic analysis of cell line SW48 and SW48 C225 was performed by Magdalene Montgomery from Department of Physiology at School of Biomedical Sciences, University of Melbourne.
- RNA-sequencing data used in Chapter 4 was obtained from Professor John Mariadason, Olivia Newton-John Cancer Research Institute (ONJCRI).

During the candidature, I was the recipient of Melbourne Research Scholarship (Stipend and Fee Offset) from The University of Melbourne.

ACKNOWLEDGEMENT

First and foremost, I would like to thank my supervisor Dr. Rodney Luwor for his continuous effort in supervising me throughout the 4 years of my PhD candidature. It has been a long and difficult journey, but he is always available every time I need his advice. Every so often I would feel overwhelmed with the project but upon having a meeting with him, I would feel calm and relieved. I would not have been able to complete this PhD without his wisdom and guidance. I would also like to thank my co-supervisor Dr. Stanley Stylli for his help and guidance over the years. His presence in the lab would always bring laughter to me and a lot of encouragement. All the stories that we shared makes going to the lab more fun. To my committee members, Dr Hong Jian Zhu, and Prof. Frederic Hollande, I am very thankful for all the advices and supports you have given me over my candidature. Your knowledge and encouragement have truly been invaluable.

I would also like to thank my fellow lab members. Over the years, there have been changes in the lab with people leaving and new people joining but these people made working in the lab more enjoyable. A special thanks to Lucy Paradiso for all her help in teaching me to do experiments in the lab, especially qPCR. Also listening to you is always entertaining.

I would also like to thank my family for the encouragement they gave me throughout my PhD years. Lastly, I would like to thank my close friends who also doing their PhD and I have someone to share the experience. Thank you!

TABLE OF CONTENT

LIST OF ABBREVIATIONS

Abbreviation	Full name
ADAMS	a disintegrin and metalloproteinase
KRAS	Kirsten RAt Sarcoma
APC	Adenomatous polyposis coli
ATP	Adenosine Triphosphate
BSC	Best supporting Care
CAPOX	Capecitabine (CAP) and Oxaliplatin (OX)
CK1α	Casein kinase 1α
CHAC2	Cation transport regulator homolog 2
CIN	Chromosomal instability
CRC	Colorectal cancer
CRY2	Cryptochrome 2
DNA	Dioxyribonucleic acid
ER	Endoplasmic Reticulum
EGF	Epidermal growth factor
EGFR	Epidermal growth factor receptor
ErbB	Erythroblastic leukaemia viral oncogene
ERK	Extracellular signal regulated kinases
FAP	Familial adenomatous polyposis
FOLFIRI	Folinic acid (FOL), 5-Fluorouracil (F) and Irinotecan (IRI)
FOLFOX	Folinic acid (FOL), 5-Fluorouracil (F) and Oxaliplatin (OX)
FDA	Food and Drugs Administration
GSK3	Glycogen synthase kinase 3
HNPCC	Hereditary nonpolyposis colorectal cancer
HER	Human epidermal growth factor receptor
IBD	Inflammatory bowel disease
IL-11	Interleukin 11
IL-11Rα	Interleukin 11 Receptor alpha
IL-6	Interleukin 6
JAK	Janus tyrosine kinase
LS	Lynch's syndrome
MSI	Microsatellite instability
MMR	Mismatch repair
MAPK	Mitogen-activated protein kinase
SMAD4	Mothers against decapentaplegic homolog 4
MM	Multiple myeloma
NSCLC	Non-small cell lung cancer

NAA25	N-Terminal Acetyltransferase B Complex Subunit
ORR	Objective Response Rate
OS	Overall survival
PTEN	Phosphatase and tensin homolog
PBS	Phosphate buffered saline
P-STAT3	Phosphorylated signal transducer and activator of transcription 3
PTB	Phosphotyrosine binding
PCR	Polymerase chain reaction
PFS	Progression-free survival
PIAS3	Protein Inhibitor of Activated STAT3
PP2A	Protein phosphatase 2A
RTK	Receptor tyrosine kinase
RPM	Revolutions per minute
RNA	Ribonucleic acid
POLR2A	RNA Polymerase II Subunit A
Src	Sarcoma-family kinases
STAT3	Signal transducer and activator of transcription 3
SLC	Small cell lung cancer
SOS	Son of sevenless
SF3A1	Splicing Factor 3a Subunit 1
SH2	SRC-homology 2
SHP1/2	Src-Homology domain-containing Tyrosine Phosphatase 1/2
SOCS3	Suppressor of cytokine signaling 3
TGF-α	Transforming Growth Factor Alpha
TKI	Tyrosine kinase inhibitor
UPS	Ubiquitination-proteasome system
UPR	Unfolded Protein Response
BRAF	v-Raf murine sarcoma viral oncogene homolog B
WT	Wild type
Wnt	Wingless-related integration site

LIST OF FIGURES

LIST OF TABLES

CHAPTER 1:

Introduction

1 Chapter 1: Introduction

1.1 Background (Colorectal Cancer)

1.1.1 Epidemiology

Around the world, colorectal cancer (CRC) is the fourth most common diagnosed cancer with an incidence rate of 10.2% and mortality rate of 9.2% of the total cancer cases in both sexes [1]. The growing concern of CRC incidence is overwhelming with nearly 1.8 million new cases diagnosed in 2018. In Australia, it is the third most common cancer (2017) with incidence rate of 67.3 per 100,000 males and 49.4 per 100,000 females [2]. Similarly, it is projected that more than 140,000 people will be diagnosed with CRC and 50,000 people will succumb to the disease in the USA (2019) [3]. The common aspect of these countries is that they are highly developed leading to earlier diagnosis of the disease. Furthermore, earlier detection of CRC leads to lower mortality rate.

1.1.2 Risk Factors

The risk of developing CRC increases due to personal traits or habits or some inherent factors that could not be changed. The main risk factor is age, where both men and women of age approaching 50 years have higher risk of developing polyps or CRC. The median age of CRC diagnosis is about 70 years old for men and 72 years old for women though the range of age is wide due to early onset CRC [4]. Inherent factors that could increase the chances of CRC is personal history of CRC or inflammatory bowel disease (IBD). People with ulcerative colitis and Chron's disease have higher risk of developing CRC with 1.4%[5] and 2.5%[6] respectively. IBD patients often have dysplasia which are not malignant but can become anaplastic and progress to a malignant phenotype. Familial history also plays a part in inherent risk factors. Patients who have relatives diagnosed with CRC would have a higher chance of developing CRC themselves [7].

Other risk factors that associated with the development of CRC are related to lifestyle. Healthy eating habits as well as active physical lifestyle play a role in CRC risk [8]. A sedentary lifestyle has been associated with increased risk of developing CRC although the link is not clearly defined [9]. It has been shown however, that moderate physical activity improved the metabolic

rate and gut motility leading to increase gut health [10]. Lack of physical activity coupled with high food intake often lead to obesity which is one the important risk factors for CRC [11].

1.1.3 Pathogenesis

Colorectal cancer was largely sporadic compared to inherited disease among people who are older than 50 years of age. 20% of colorectal cancer cases arise from germline mutations which can be differentiated into Familial adenomatous polyposis (FAP) and Hereditary nonpolyposis colorectal cancer (HNPCC) (previously known as Lynch's syndrome (LS)).

FAP is known to be caused by germline mutations of adenomatous polyposis coli (*APC*) gene located on chromosome 5q21 [12]. This gene acts as a tumor suppressor in CRC patient and is important in regulating cell adhesion, signal transduction and transcriptional activation. Deletion, insertion, and nonsense mutations lead to FAP, while other mutations can lead to classic FAP which forms more than 100 adenomas of various sizes or more mild form FAP (adenomas<100). Polyps can be formed in affected people from a young age accumulating and forming multiple adenomas and eventually diffused all over the colorectum (**Figure 1.1**).

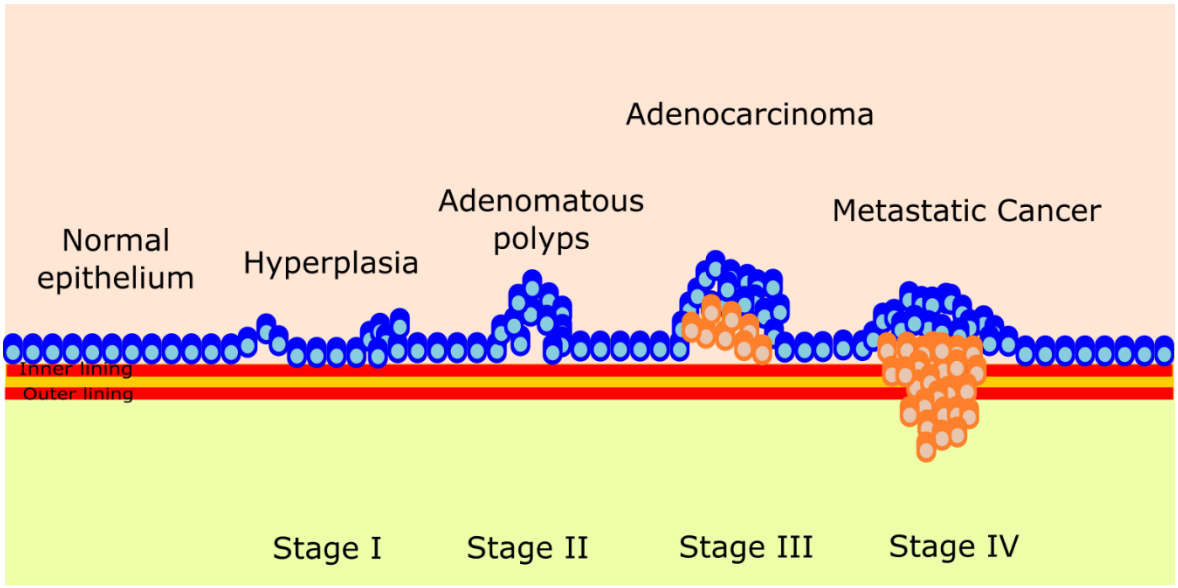

Figure 1.1: Stages of colorectal cancer.

The schematic representation of stages of colorectal cancer from normal epithelial cells to formation of polyps to formation of adenocarcinoma to ultimately formation of cancer. Blue cells represent normal epithelial cells, orange cells represent cancerous cells.

The majority of patients with FAP develop adenomas by age 35 years old [13] and colorectal cancer by the age of 40-50 years. FAP patients have high risk of developing colorectal cancer due to *APC* gene mutations. However, only one in 100,000 people have tumors arising from the colorectal epithelial cells [12]. According to Knudson's hypothesis, tumor from FAP patients developed additional somatic *APC* mutations suggesting that loss of *APC* gene was only the first step to colorectal adenocarcinoma formation [14]. This was followed by additional genetic mutations that include *KRAS, TP53* and *SMAD4* [15]. Knudson's hypothesis was strengthened with animal models from several studies that showed combination of *KRAS*, *TP53* and *SMAD4* mutations or stand-alone mutations did not initiate tumor formation unless *APC* mutations was introduced [16, 17]. The mechanism which *APC* mutations contributed to CRC formation was through the Wnt signaling pathway. The canonical pathway of Wnt involves the translocation of β-catenin into the nucleus for various functions which includes regulation of cell cycle, cell division and cell adherence [18-20]. In the absence of Wnt signaling, accumulated β-catenin is phosphorylated through a complex of proteins including Axin, adenomatosis polyposis coli (APC), protein phosphatase 2A (PP2A), glycogen synthase kinase 3 (GSK3) and casein kinase 1α (CK1α) (**Figure 1.2**). After phosphorylation β-catenin is degraded by the proteasome [20]. FAP patients lack the ability to degrade β-catenin leading to its accumulation and activation of Wnt signaling [21, 22].

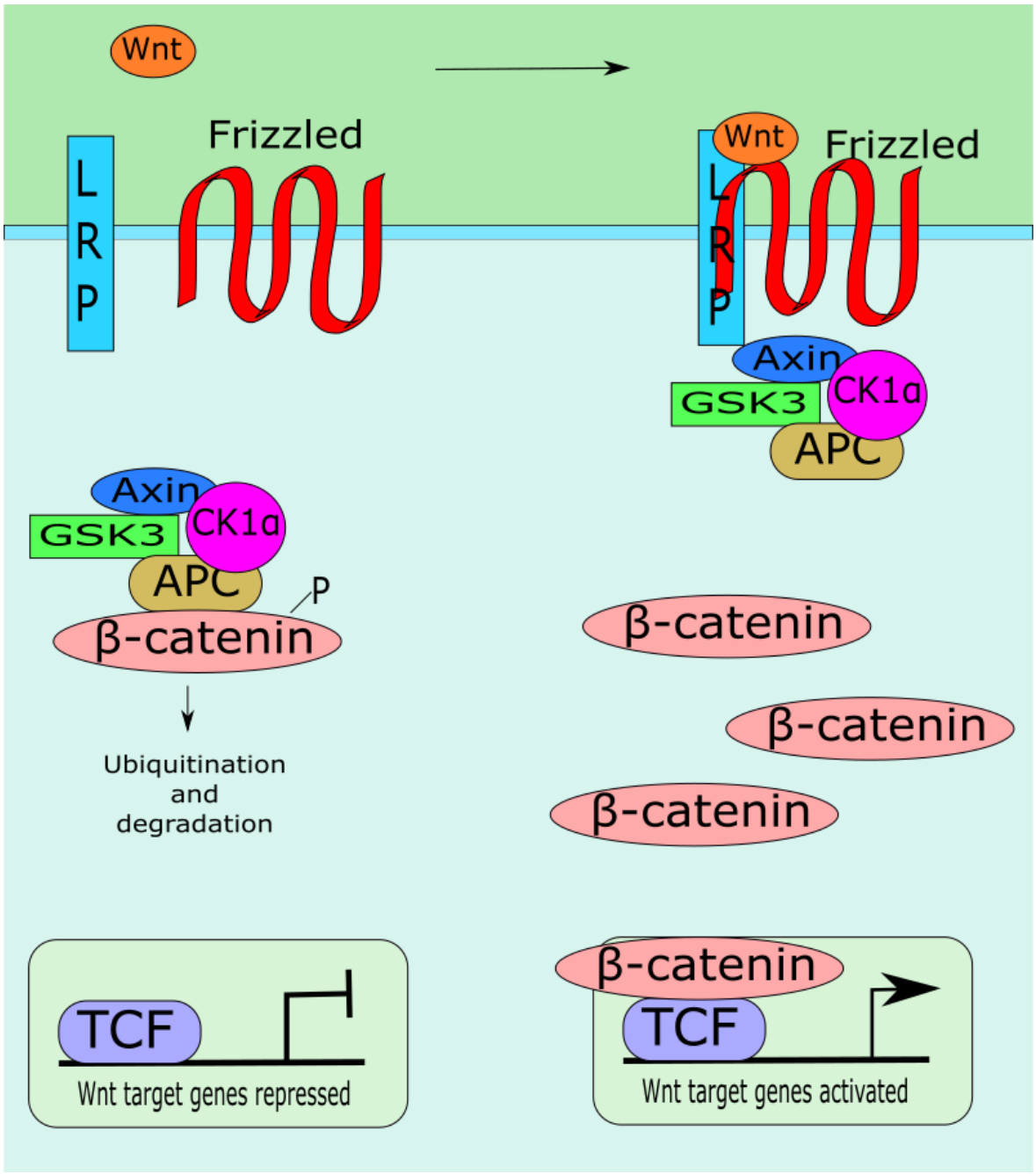

Figure 1.2: Wnt Signaling pathway

Schematic representation of the canonical Wnt signaling pathway. B-catenin is being targeted for degradation in the absence of Wnt ligand. When Wnt ligand binds to the Frizzled receptor, it releases B-catenin from suppression and activates Wnt target genes.

Lynch's Syndrome (LS) or HNPCC is an autosomal dominant syndrome that implicated 2-4% of CRC patients [23, 24]. LS developed from a germline mutation in one of the mismatch repair (MMR) genes which include *MLH1, MSH2, MSH6, PMS2* or the *EpCAM* gene causing the tumor to be characterized as Microsatellite Instability (MSI). Defects in these genes are caused through the insertion of repetitive sequence (microsatellite) that affects the correction of the DNA during replication. *MLH1* and *MSH2* are the most common mutations which take up to 90% of the LS population, followed by *MSH6* (10%) and *PMS2* [25, 26]. *EpCAM* mutation is much rarer in LS patients with the gene silencing *MSH2* upstream of the signaling pathway. LS patients have high risk of developing cancer though the risks varies according to the mutations in MMR genes [24]. The average diagnosis age of LS patients also varied between mutations with *MLS1* and *MSH2* have younger diagnosis. Given that LS patients have 50% chance of developing CRC, they lacked the development of adenomatous polyps which are known to be precursors to CRC [27]. As compared to FAP patients (adenomas >100), LS patients develop fewer adenomas by the age of 50 years old (adenomas < 3)[13, 28]. MMR inactivation was thought to precede the progression of adenomas to carcinomas, but insufficient evidence has made this uncertain.

1.1.4 Current Treatment

Standard care of treatment for colorectal cancer involves surgery, radiotherapy, and chemotherapy regiments. Several chemotherapies regiments were administered to CRC patients which includes fluorouracil (5FU), Oxaliplatin and Irinotecan. These drugs produce their anti-tumor effect by inhibiting the rapidly dividing cancer cells, but unfortunately also display cytotoxic effects on normal cells that also divide.

The first combination therapy for treating CRC patients is FOLFOX. FOLFOX is an abbreviation of the regiments that includes **Fol**inic acid, **F**luorouracil and **Ox**aliplatin [29]. Several different FOLFOX regiments are available (FOLFOX-4, FOLFOX-6, and FOLFOX-7) which differ in term of doses and administration. It is implemented in patients for 12 cycles biweekly. Common side effects include risk of infection, fatigue, breathlessness, pain and nausea [30, 31]. FOLFOX was administered as first-line treatment in CRC patients [32, 33] though it has been used as second-line treatment [34-36]. A similar treatment regimen with FOLFOX was FOLFIRI. Involving the combination of the same drug as FOLFOX except with Oxaliplatin replaced with Irinotecan. Both are currently being used as first-line treatment of CRC patients. The choices between which regiments were decided upon is based on the side effects that may occur [29]. CAPOX, another regiment that

combines the drugs **Cap**ecitabine and **Ox**aliplatin. has similar efficacy to FOLFOX and is also used in first-line treatment [37]. However, some of the side are more severe with CAPOX [38]. However, a retrospective study showed even though there was no difference in disease-free survival (p=0.598), FOLFOX displayed more toxicity compared to CAPOX [39].

1.2 Background (Non-Small Cell Lung Cancer)

1.2.1 Epidemiology

As of lung cancer, it has a higher rate of incidence at 11.6% and much higher mortality rate at 18.4% for both men and women [1]. More cases are being diagnosed every year with Asia region have the most reported incidence in 2018 at 58.5% of total cases. In accordance with the incidence, higher mortality as well as 5-year prevalence rate were also observed in Asia. Furthermore, more developed region has higher rate of incidence compared to less developed region of the world (884,313 new cases vs 15,006 new cases respectively).

1.2.2 Risk Factors

The leading risk factor for lung cancer is tobacco smoking. Tobacco has been used widely around the world as part of their culture or economics driver [40]. Commonly used in pipes, tobacco is now available in the form of cigarettes making it easier to use. After 50 years, the number of cigarettes smoked per person has increased from 100 per year (1900) to 3500 per year (1960s) [41]. The risk of smoking tobacco and its carcinogenic properties have been studied since the early 1950s [42]. According to a report by the US public health service, 70% of age-related death in male was associated with cigarette smoking [43]. Some studies showed higher risk of protracting lung cancer in women as compared to men [44, 45]. Long term smokers have higher risk of developing lung cancer compared to short-term smokers though the relative risk was reduced for ex-smoker [46]. Heavy smokers have higher risk of developing lung cancer as compared with average smoker [47].

1.2.3 Pathogenesis

The pathogenesis of lung cancer is similar with other cancers with the initiation mutations induced by carcinogen followed by long progression into cancers. Cigarette smokes contain carcinogen which initiate the process. The mutations that occur in smokers happened early in the

progression based on a study that showed similar genetic mutations in smokers and former smokers [48]. The onset of cancer is long which required 20-25 years after the initiation.

Lung cancer has several histology types that includes Small cell (SLC) and non-small cell (NSCLC) lung cancer [49]. NSCLC which make most of the diagnosed lung cancer can be further divided into three subtypes; adenocarcinomas, squamous cell carcinomas and large-cell lung carcinomas [49-51]. The current knowledge of NSCLC pathogenesis is more profound for squamous cell carcinomas than adenocarcinomas and large-cell lung carcinomas. For adenocarcinomas, studies performed to investigate the molecular pathogenesis of NSCLC revealed two proteins that were affected in smokers versus non-smokers. *KRAS* mutations has been strongly associated with tobacco consumption [52, 53] while the *EGFR* mutations in exon 19 and exon 21 were associated with non-smokers and more common in women [54, 55]. In squamous cell carcinomas, the changes involved *KRAS, PTEN* and *TP53* mutations, coupled with loss of heterogeneity and microsatellite instability driving the cancer progression [56-59].

1.2.4 Current Treatment

In NSCLC, the first line of treatment includes surgery, radiation, and chemotherapy regiments. Surgery is the most commonly medical intervention for treating a solid tumor especially in patients who have Stage I, II and III of NSCLC. The surgical rate has increased from 9% to 17% over the years [60]. Based on the biopsies and medical imaging, the tumor could be resected by removing a lobe or a portion of the lung [60]. In addition to surgery, patients were also treated with adjuvant therapies that include radiation and chemotherapy to kill remaining cancer cells prolonging patient's survival [61, 62]. Radiation therapy uses a highly concentrated beam to target the DNA of cancer cells, eliminating a specific part of the tumor. This therapy is used on patients who do not respond to surgery and chemotherapy or as adjuvant treatment. A technique was developed to deliver a more concentrated and highly focused radiation treatment called stereotactic body radiation therapy (SBRT). This technique was used on inoperable Stage I patients and results showed higher rate of control of the tumor [63].

The usage of these chemotherapy regiments had shown great success among many cases of cancer patients. However, some patients developed resistance and show severe side effects towards these therapies leading to the need to use targeted therapies. Targeted therapies are treatment regiments that make use of a molecule to target a specific component of a signaling

pathways that are maintaining the tumor cells' survival. One of the most targeted tyrosine kinase receptors is the Epidermal Growth Factor (EGF) receptor.

1.3 Epidermal Growth Factor Receptor

1.3.1 Structure

The Epidermal Growth Factor Receptor (EGFR) is a receptor tyrosine kinase (RTK) that belongs to the ErbB family and is one of the most widely studied tyrosine kinases. EGFR or ErbB1 is part of a family of four subfamily receptor tyrosine kinase which includes Her2 (Neu or ErbB2), Her3 (ErbB3) and Her4 (ErbB4). The receptors have an extracellular ligand-binding domain, transmembrane domain and cytoplasmic tyrosine kinase domain [64] (**Figure 1.3**). They also have conserved cysteine-rich clusters which are denoted as CRI and CRII forming the ligand binding domain. Within the cytoplasmic region, there are three conserved domains that are critical for downstream signaling. The juxtamembrane region is involved in negative feedback mechanism of protein kinase C (PKC). The Src-homology domain 1 (SH1) is important in autophosphorylation of the RTK on the tyrosine residues. The phosphorylated tyrosine served as a binding spot for a protein with SH2 domain or phosphotyrosine binding (PTB) domain. Finally, in the carboxy tail of the receptor, there is a motif that is involved in internalization and degradation of EGFR.

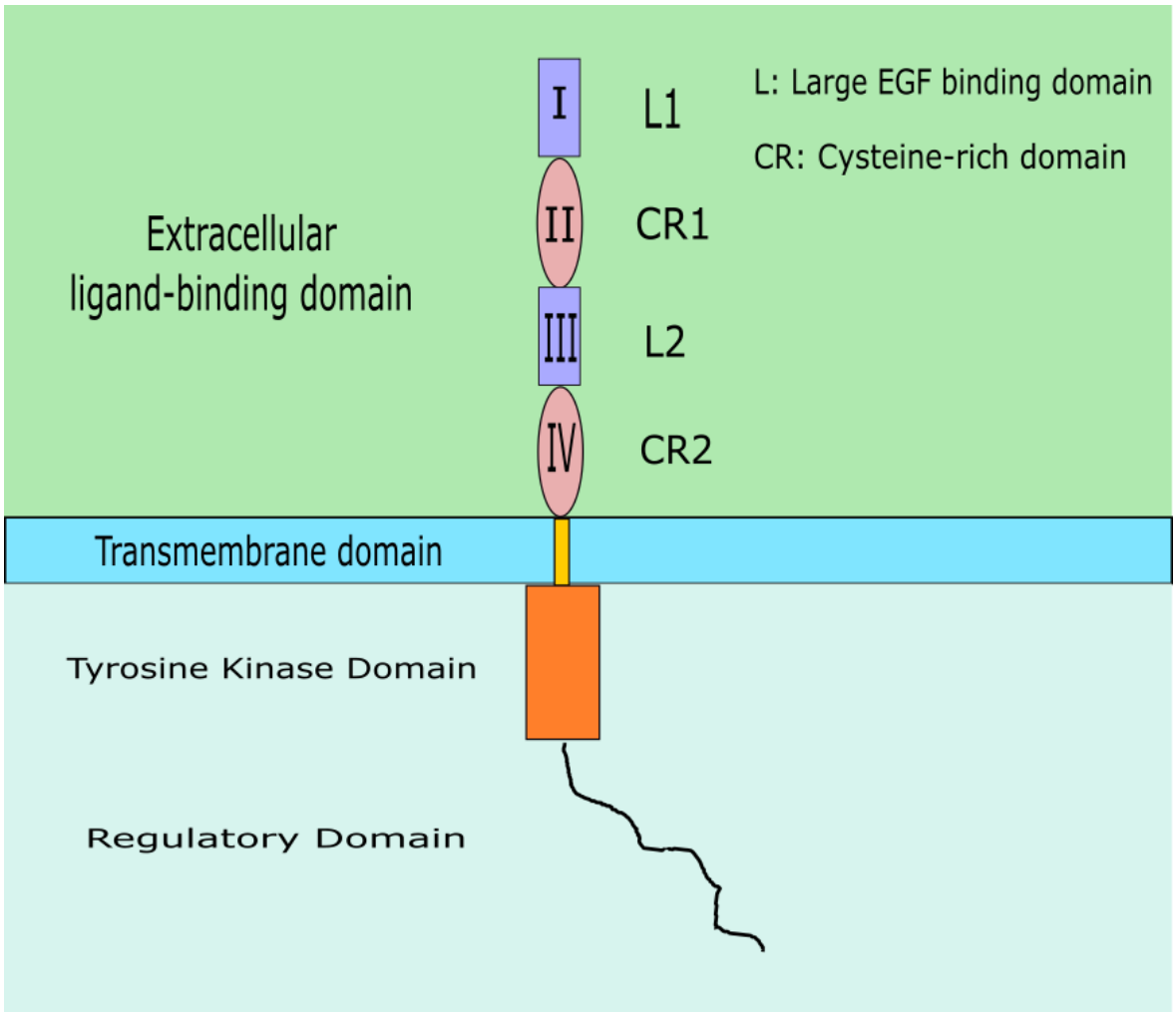

Figure 1.3: Structure of EGFR

Schematic representation of the structure of EGF receptor. There are several domains including extracellular ligand-binding domain, transmembrane domain, tyrosine kinase domain and regulatory domain. Four motifs make up the extracellular domain: two large binding domains and two cysteine-rich domains.

1.3.2 Mechanism

EGFR exist as monomers before activation occurs via oligomerization and binding with ligands. EGFR can be activated by several ligands including Epidermal Growth Factor (EGF), amphiregulin, Transforming Growth Factor Alpha (TGF-α), Heparin-binding EGF-like growth factor, Betacellulin and Epiregulin [65]. All the ligands are expressed in a precursor form and transported to the cell membrane before being cleaved into its active form [66]. The ligands are cleaved by proteases including ADAMS (a disintegrin and metalloproteinase) and released from the cell membrane. Upon ligand binding, the EGFR undergoes a conformational change that allows the residue Lysine-721 in the kinase domain to be accessible by the ATP [67]. Upon ATP binding, the kinase domain is phosphorylated and serves as binding site for several key regulators in multiple pathways. The pathways include RAS-RAF-MEK-ERK1/2 pathways, PI3K-AKT-mTOR pathway, and Src-Signal Transducer and Activator of Transcription (STAT) pathway. These pathways will trigger the activation of numerous genes that are involved in cellular activities including proliferation, survival, differentiation, cell polarity, morphology adhesion and migration [64] (**Figure 1.4**).

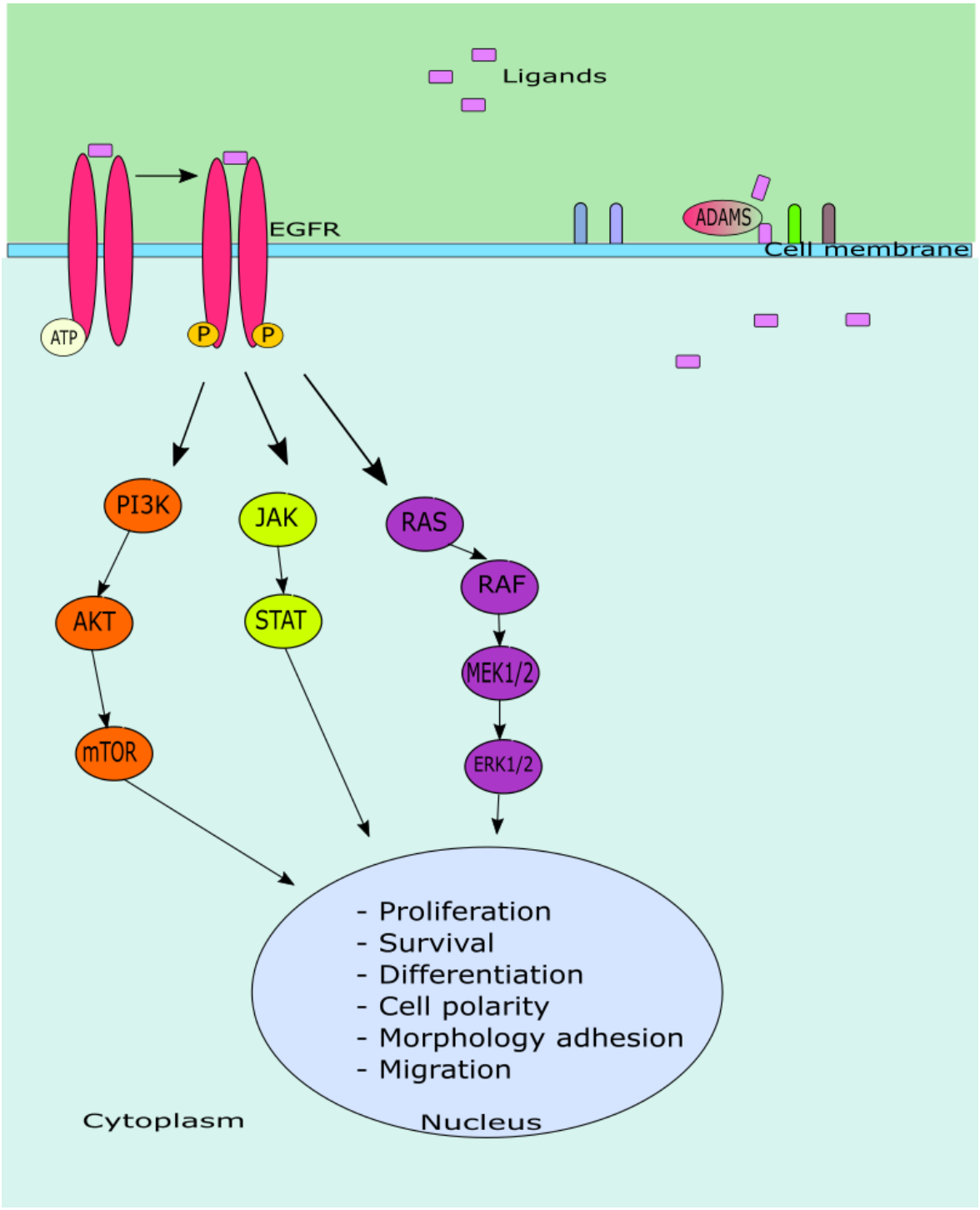

Figure 1.4: EGFR signaling pathways

Schematic representation of the EGFR signaling pathways. EGFR is activated through several ligands including EGFR, TGF-α, amphiregulin, Epiregulin, Betacellulin, and Heparin binding EGF-like growth factor. Downstream network including PI3K/AKT, JAK/STAT3 and MAPK signaling pathways are activated after the receptor was phosphorylated.

1.3.3 Downstream Molecular Pathways

1.3.3.1 JAK/STAT3 Signaling Pathway

STAT3 belongs to the STAT family of transcription factors which include six other members: (STAT1, STAT2, STAT4, STAT5A, STAT5B, and STAT6). Its role as a transcription factor and signal transducer in driving tumor progression makes it one of the most studied STAT proteins. STAT3 is made up of 770 amino acids and has several domains that are critical to its function. One of the domains is an SH-2 domain where STAT3 can bind to JAK and be subsequently phosphorylated at residue Y705. Phosphorylated STAT3 then can form a homodimer or heterodimer with other STAT proteins and translocate into the nucleus [68] though phosphorylation is not necessary for the dimerization and translocation process [69, 70] (**Figure 1.5**). STAT3 protein is further phosphorylated at residue S727 and fully activated before driving increased gene expression that is involved in tumor progression [71]. STAT3 also acts as a downstream substrate for several cytokine pathways including IL-6, IL-11, Oncostatin-M (OSM) and Leukemia Inhibitory Factor (LIF) [72]. Besides JAK, STAT3 can be activated by non-receptor tyrosine kinases such as src kinase. STAT3 activity is regulated at several steps within the pathway. The most common STAT3 regulator is Suppressor of Cytokine Signaling 3 (SOCS3). *SOCS3* is a target gene specifically driven by STAT3 activity [73]. SOCS3 protein interacts directly with the tyrosine kinase domain of the receptor or JAK kinases leading to reduction in STAT3 phosphorylation [74]. Another protein regulator called Src-Homology domain-containing Tyrosine Phosphatase 1/2 (SHP1/2) interact similarly with JAK, STAT3 and the receptor. Another STAT3 regulator is the Protein Inhibitor of Activated STAT3 (PIAS3) which acts when STAT3 is translocated into the nucleus. PIAS3 has a conserved PINIT domain that allows nuclear retention of PIAS3 [75]. This domain is important as it plays a role in binding and inhibits STAT3 activity. In lung cancer, it was shown to have an inhibitory effect on growth by blocking STAT3 phosphorylation [76].

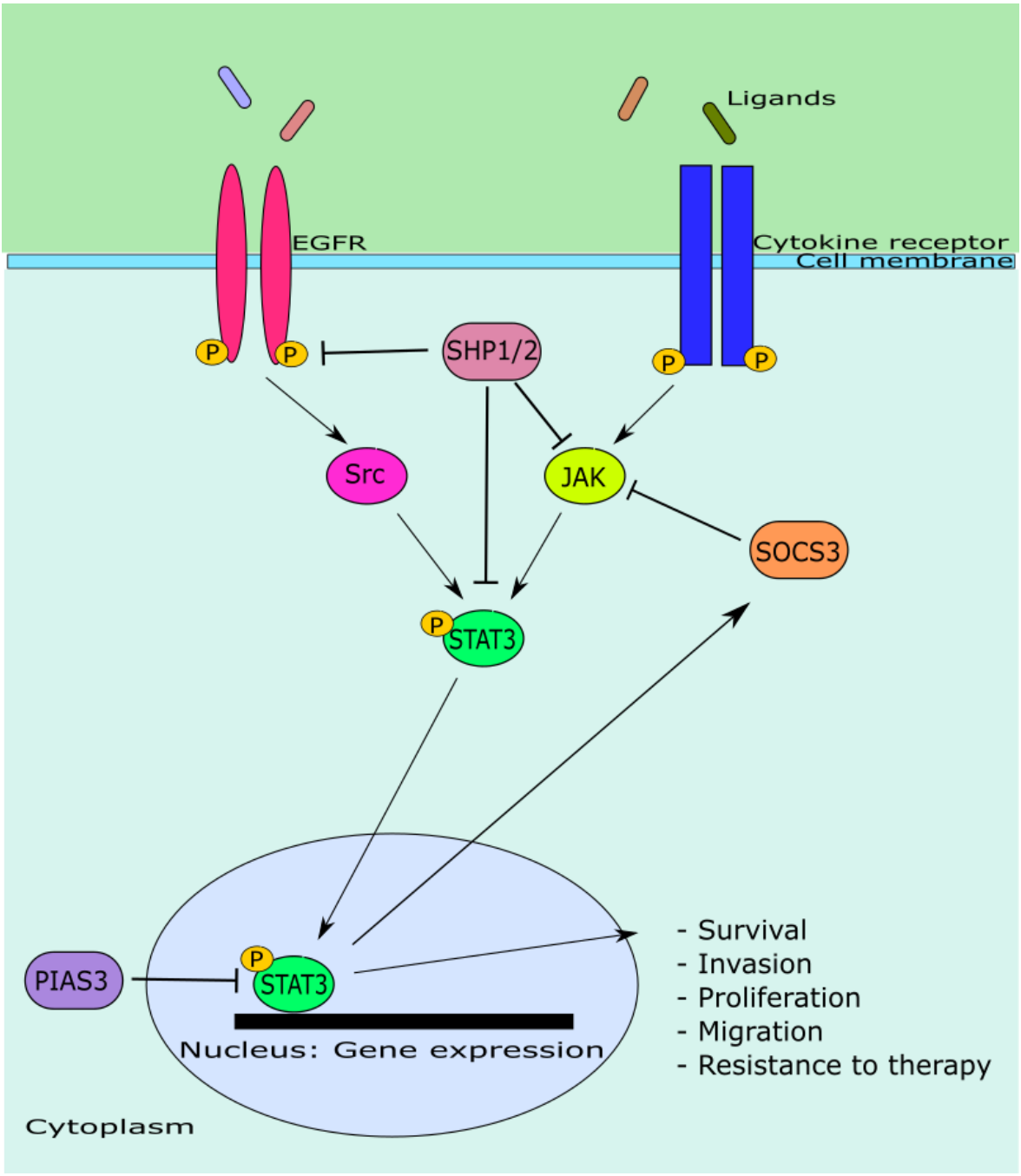

Figure 1.5: JAK/STAT3 signaling pathway

Schematic representation of JAK/STAT3 signaling pathway. Upon activation from either EGFR or cytokine receptor such as IL-6/IL-11 receptor, JAK or Src kinases are phosphorylated. The kinases would phosphorylate STAT3, activating it before translocating into the nucleus to drive gene expression. Several negative regulators including SHP1/2, SOCS3 and PIAS3 play a role in regulating the pathway.

1.3.3.2 MAPK Signaling Pathway and PI3K/AKT Signaling Pathway

The downstream molecules of the MAPK signaling pathway is activated when the RTK recruits Shc and Grb2 adaptor protein through its SH2 domain (**Figure 1.6**). Through these adaptor proteins, Son of sevenless (SOS) is recruited from the cytosol to the plasma membrane. SOS is a guanine nucleotide exchange factor (GEF) which can facilitate the conversion of Ras-GDP to Ras-GTP leading to activation. RAS protein belongs to the small GTPase family that regulates a downstream signaling cascade governing several cellular processes such as proliferation, migration and adhesion [77]. Different isoform of RAS protein could be found mainly in the form of KRAS, NRAS and HRAS [77]. The active form of Ras will activate a series of signaling cascade including Raf, Mek1/2, and Erk1/2 [78]. Phosphorylation in the kinase domain is the key in activating the subsequent molecule in the pathway. Phosphorylated Erk1/2 can now activate several substrates in the cytosol and translocate into the nucleus to phosphorylate transcription factors that regulate important gene expression. Due to its importance in regulating multiple cellular responses, over-activation or constitutively active MAPK signaling can cause the cell to be tumorigenic.

The PI3K/AKT network is another pathway that is activated by the EGFR (**Figure 1.6**). PI3K belongs to a family of lipid kinases that can phosphorylate phosphatidylinositol which is an important signaling molecule in the pathway. PI3K is made up of two subunits, p110 and p85 subunit [79]. Upon activation by EGFR or Ras, the catalytic subunit p110 can convert phosphatidylinositol-4,5-bisphosphate (PIP2) to phosphatidylinositol-3,4,5-bisphosphate (PIP3). Located on the plasma membrane, PIP3 will then recruit protein that has pleckstrin-homology (PH) domain including AKT and PDK1. Once recruited, AKT is phosphorylated by PDK1 at Threonine-308 and fully activated when phosphorylated by mTORC2 at Serine-473 [80]. AKT is involved in activating numerous substrates including mTOR that lead to increased proliferation, angiogenesis, and cellular growth. mTOR is a serine/threonine kinase which acts in the cell through two complexes: mTORC1 and mTORC2. The main targets of mTORC1 are the translational regulator eukaryotic initiation factor 4E-binding protein 1(4E-BP1) and S6K, which are important in cancer pathogenesis. S6K is involved in one of the negative feedback mechanism of the pathway by inhibiting mTORC2 thus blocking AKT from being fully activated [81]. The most studied negative feedback protein is phosphatase and tensin homolog (PTEN). PTEN catalyze the conversion of PIP3 to PIP2 preventing the recruitment of AKT to the membrane [82].

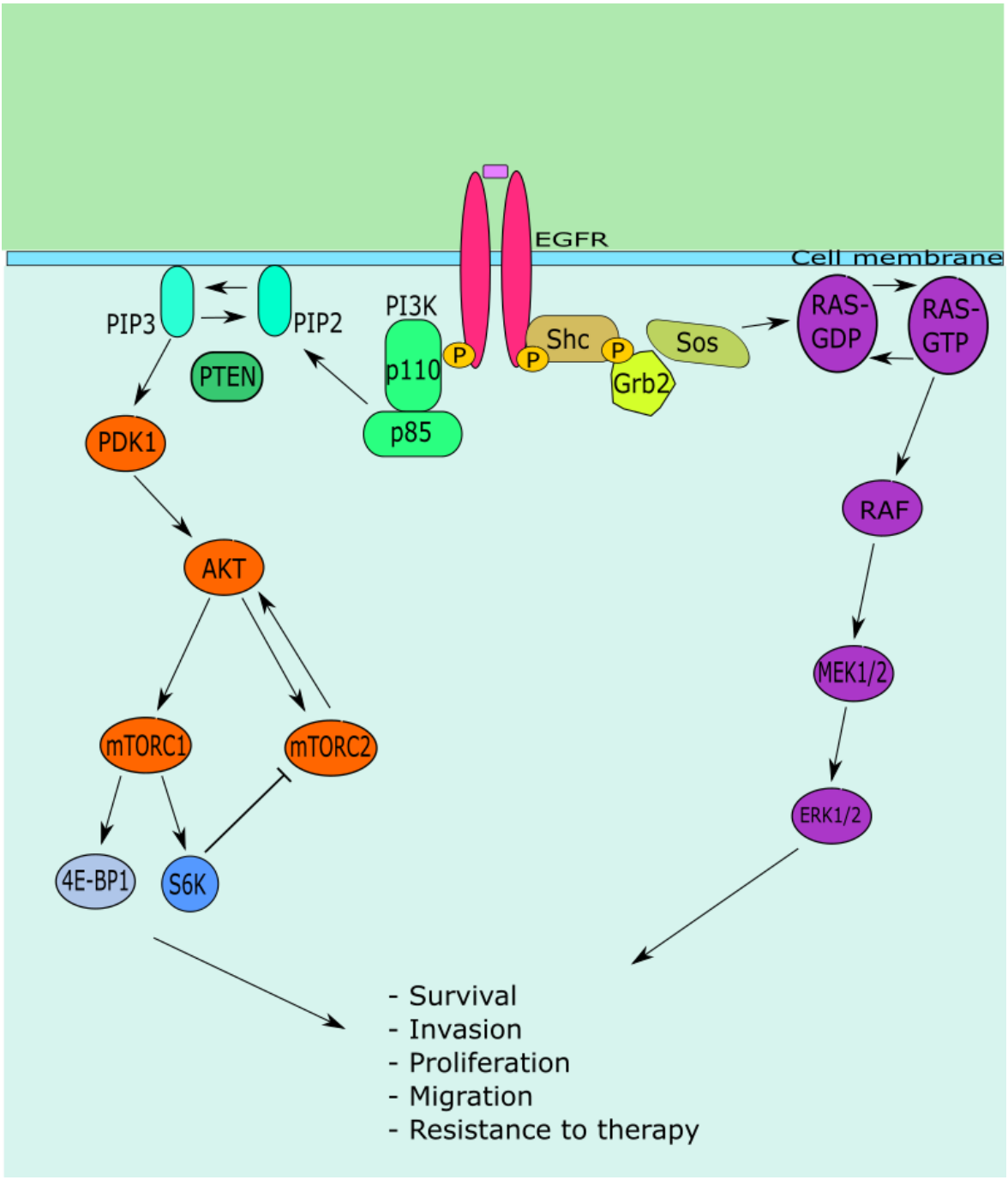

Figure 1.6: PI3K/AKT and MAPK signaling pathways

Schematic representation of PI3K/AKT and MAPK signaling pathways. Upon EGFR activation, two pathways could be activated. Through a series of signaling cascades, the pathways would be able to activate several cellular responses that are involved in increasing survival, invasion, proliferation, migration, and resistance to therapy.

1.3.4 EGFR-Targeted Therapy

1.3.4.1 Cetuximab

Cetuximab is a chimeric (murine/human) monoclonal antibody that targets the extracellular domain of EGFR and blocks ligand binding and subsequent EGFR activation (**Figure 1.7**) [83]. Cetuximab was approved by the Food and Drugs Administration (FDA) in 2004 for the use in metastatic colon cancer irinotecan refractory patients. However, many of these patients were either intrinsically resistance or soon developed resistance towards Cetuximab. An activating mutation in *KRAS* (exon 2) was discovered as a possible mechanism of resistance in some patients. Therefore, Cetuximab is now only used in patients that have wild-type KRAS [84]. More recent studies also discovered lack of response towards Cetuximab for patients harboring other *KRAS* (exon 3 & 4) mutations and *NRAS* mutations [85, 86]. The current treatment uses Cetuximab either as a monotherapy or combinational treatment with chemotherapy. In colorectal cancer, common chemotherapy regimens used in combination with Cetuximab are FOLFOX (5-Fluorouracil (5-FU), Leucovorin (LV) and oxaliplatin), FOLFIRI (5-Fluorouracil (5-FU), Leucovorin (LV) and irinotecan) and CapeOX (Oral capecitabine plus Oxaliplatin). Results from clinical trials (CRYSTAL study; Cetuximab plus FOLFIRI), (OPUS study; Cetuximab plus FOLFOX) showed that combination treatment improved response rate (RR) and Progression Free Survival (PFS) of patients compared to chemotherapy alone [30]. Another study was performed comparing Cetuximab monotherapy and/or Best supporting Care (BSC) in pretreated metastatic colorectal cancer patients. Patients receiving Cetuximab treatment showed improved Overall survival (OS)(6.1 months) compared to BSC (4.6 months) only [87].

1.3.4.2 Panitumumab

Panitumumab is a humanized monoclonal antibody that targets the extracellular region of EGFR [83]. It binds competitively with EGF and inhibits auto-phosphorylation thus blocking the activation of EGFR mediated downstream signaling pathways (**Figure 1.7**). Panitumumab was first approved in 2006 by the FDA for the use in metastatic colorectal cancer with wild-type KRAS [88]. KRAS has been a predictive biomarker for the use of Cetuximab and Panitumumab in colorectal cancer patients. Wild-type *KRAS* patients responded better to these monoclonal antibodies than mutated *KRAS*. To get a better outcome, combination treatment was applied to patients. The combination of Panitumumab and FOLFOX4 produced an improvement in PFS (10.1 months) and OS (26.0 months) in comparison with FOLFOX4 alone (PFS: 7.9 months, OS: 20.2 months) [32]. A

similar observation was recorded in another randomized phase III trial of Panitumumab with FOLFIRI. PFS was significantly improved (Panitumumab + FOLFIRI: 5.9 months vs FOLFIRI: 3.9 months) although OS was not [89]. As a monotherapy, Panitumumab was administered after Cetuximab and it showed better PFS and OS. Other than therapies targeting extracellular region of EGFR, inhibitors have been developed to target the intracellular region of EGFR to better inhibit EGFR signaling.

1.3.4.3 Gefitinib

Gefitinib is a reversible tyrosine kinase inhibitor (TKI) that targets the kinase domain of EGFR. Gefitinib binds competitively to the ATP-binding site inhibiting ATP binding and receptor activation (**Figure 1.7**). The antitumor effect of Gefitinib is due to EGFR not able to form a dimer and blocks autophosphorylation rather than internalization of the receptors. The used of Gefitinib was approved by the FDA in 2003 as a third-line treatment of non-small cell lung carcinoma (NSCLC) but later was withdrawn after no benefits was observed for OS in INTAC2 trial [90]. It was approved based on two randomized Phase II trials; Advanced Non-Small Cell Lung Cancer (IDEAL)-1 trial and IDEAL-2 [91]. In IDEAL-1, patients have undergone chemotherapy before receiving Gefitinib. At 250 mg/day, patients showed improved RR, OS, and PFS. Similar results were observed in IDEAL-2 trials where the RR was improved [92]. These patients have been treated with Gefitinib after the failure in platinum-based and docetaxel chemotherapies. However, the dosage used in IDEAL-2 resulted in more side effects compared to IDEAL-1 [93]. In another PHASE III trial, treatment of Gefitinib with BSC resulted in no improvement in OS leading to the decision of using Gefitinib after the patients have undergone chemotherapy [94]. Comparison of docetaxel and Gefitinib in a PHASE III trial in the USA showed a comparable improvement in overall survival [95]. Nevertheless, Gefitinib is much well-tolerated compared to Docetaxel. Following that, Gefitinib was used in additional studies with patients harboring *EGFR* mutations [96-99].

1.3.4.4 Erlotinib

Erlotinib is a TKI to the EGFR with a mode of action similar to that of Gefitinib. It competitively binds to the ATP-binding site preventing receptor dimerization (**Figure 1.7**). Erlotinib was first approved for the use in NSCLC patients in 2004 (FDA). Cancer Institutes of Canada conducted clinical trials that showed a reduction in cancer symptoms in NSCLC patients after Erlotinib treatment [100]. Erlotinib was shown to work best after four cycles of platinum-based chemotherapy of which improved PFS (2.2 months vs 1.8 months) and OS (6.7 months vs 4.7

months) were observed when compared to the placebo group [101]. Erlotinib also performs better in patients with *EGFR* mutations (exon 19 deletions or exon 21 L858R mutations) (FDA). Given that Erlotinib works as a first-line treatment, it also is being used in second and third-line treatment. As a second-line treatment, the effect of Erlotinib was observed to be more effective in older NSCLC patients [102]. The treatment improved various aspects of the patient's condition. The combination of Erlotinib with docetaxel and pemetrexed chemotherapies also showed similar effectiveness [103]. As a third-line treatment, Erlotinib showed much improvement on patient's quality of life while having minimum side-effects. Both Erlotinib and Gefitinib belong to the first-generation EGFR-TKI that is well-established in treating NSCLC patients. However, these two EGFR-TKIs face the same challenge where patients eventually developed resistance after continuous treatment. To circumvent the resistance, second-generation EGFR-TKI such as Afatinib and third generation inhibitors have been developed and marketed.

1.3.4.5 Afatinib

Afatinib is an irreversible tyrosine kinase inhibitor that binds covalently to specific cysteine residues in the EGFR kinase domain (**Figure 1.7**). Binding of Afatinib prevent the dimerization of EGF receptor, HER2 and HER4 thus inhibiting downstream signaling [104, 105]. Afatinib is a second-generation EGFR-TKI designed to overcome the acquired resistance from first-generation TKI driven by T790M mutations. In the LUX-Lung 1 trial, patients that have disease progression after receiving first-generation TKI treatment were treated with Afatinib. Afatinib and BSC treatment showed improved PFS compared to patients receiving BSC only [106]. However, no complete response was noted. Another clinical trial combining Afatinib and Cetuximab together showed better OR in patients harboring T790M mutation compared to those without the mutations [107]. This indicates that Afatinib is more effective in patients with *EGFR* mutations. Furthermore, in LUX-Lung 2 trial, Afatinib showed 61% of the patients had an objective response with EGFR mutations. A combined posthoc analysis of LUX-Lung 2, LUX-Lung 3 and LUX-Lung-6 revealed that Afatinib worked better in NSCLC that has uncommon mutations such as Leu861Gln and Ser768Ile [108]. Combination treatment of Afatinib with other EGFR TKIs and chemotherapies are being explored. LUX-Lung 5 trial used Afatinib alone for 12 weeks followed by combination with paclitaxel. This trial showed that combination treatment has improved PFS and Objective Response Rate (ORR) compared to Afatinib stand-alone treatment (32.1% vs 13.2%; P=0.005) [105]. Another study used co-treatment of Afatinib with Cetuximab on NSCLC patients which proved more effective than the combination

of Erlotinib and Gefitinib with Cetuximab [104]. Despite these, Afatinib produces more side effects such as severe diarrhea and mouth ulcers than other EGFR TKI as well as developed resistance.

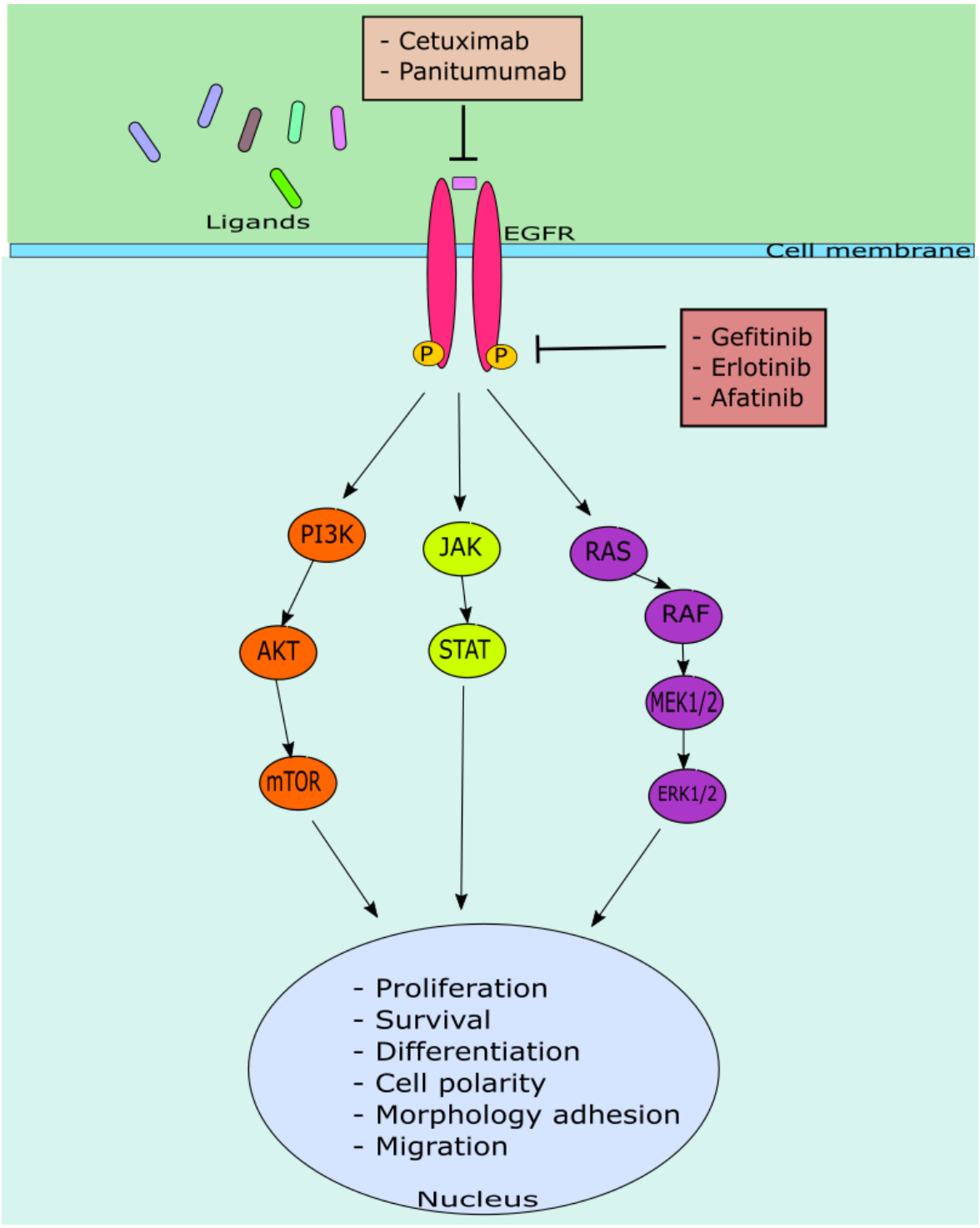

Figure 1.7: EGFR-targeted therapies

A schematic representation on how EGFR-targeted therapies act on the receptors. Cetuximab and Panitumumab target the ligand binding site by competing with other ligands. Gefitinib, Erlotinib and Afatinib target the ATP binding-site by inhibiting the conversion of energy ATP to ADP.

1.4 Resistance to Treatment in CRC

Colorectal cancer (CRC) is the third leading cause of cancer-related deaths annually worldwide. The 5-year survival rate is increasing with 65% in high-income countries such as Australia, USA, and Canada [109]. The onset of CRC could be due to several risks factors which include old age and sedentary lifestyle [110]. Alterations in the molecular pathway are the underlying mechanism in CRC pathogenesis. Chromosomal instability (CIN) is one of the alterations that is commonly observed in CRC cases [111]. The mechanism behind CIN including DNA damage response is affecting the normal function of the cells. Mutations in genes such *KRAS* and *PI3K* leads to over activation of the MAPK and AKT pathways. The heterogeneity of CRC is a challenge to improve prognosis and treatment for these patients. Current treatment of CRC involves regimens of chemotherapies including FOLFOX, FOLFIRI, and CapOX. These chemotherapies are not effective which leads to the development of monoclonal antibody targeting specific pathway. Combinations of chemotherapies and EGFR-targeted therapy have improved the treatment of CRC patients. Nevertheless, patients eventually developed resistance towards these therapies.

1.4.1 Resistance Mechanism towards EGFR-targeted therapy in CRC

Both intrinsic and acquired tumor resistance have been well reported in mCRC patients following Cetuximab treatment through several proposed mechanisms. These mechanisms involve alterations in molecular pathways underlying CRC pathogenesis. The most common resistance mechanism is alterations in molecules involved in the MAPK pathway. RAS belongs to a family of GTPase which include KRAS, NRAS, and HRAS that function upstream of MAPK protein [112]. The main function of KRAS is to transmit signals from activated growth factors receptor including EGFR to subsequent downstream molecules in the pathway. Mutations occurring in *KRAS* gene are often found in exon 2 codons 12 and 13 [113]. These mutations cause the ATPase to be dysfunctional leading to constitutively active KRAS and activation of the MAPK pathway even when upstream receptors such as EGFR are not activated. Results from clinical trials showed that patients harboring *KRAS* mutations responded poorly to Cetuximab [114]. This leads to the usage of Cetuximab only in

patients harbouring wild-type KRAS only. BRAF is a serine/threonine protein kinase that is mutated in approximately 15% of CRC patients [115]. The most common mutation V600E accounted for 80% of these mutations. The prognostic role of *BRAF* mutations in CRC is well established though not reliable as a predictive marker. There is no significant correlation between *BRAF* V600E mutations and patient's response when treated with EGFR-targeted therapy and chemotherapy together [115]. Similar combinations were used in several Phase III trials showing that there is no association between improvement in OS, PFS or OR and patient harbouring *BRAF* mutations [116]. Alterations in the AKT pathway can also lead to resistance towards anti-EGFR treatment. *PIK3CA* mutations often occur in exon 9 and 20 and were found in 10-20% of CRC patients. Interestingly, exon 20 mutations were found to be a predictive marker of Cetuximab inefficiency in wild-type KRAS patient while exon 9 mutations were associated with *KRAS* mutations [113]. In earlier studies, *PIK3CA* mutations were shown to have a significant association with primary resistance to anti-EGFR therapy [117]. Besides *PIK3CA* mutations, loss of PTEN also activates the AKT pathway. This mutation is found in 30% of CRC patients and it is associated with shorter OS in wild-type KRAS patients receiving Cetuximab treatment [118, 119]. In another study combining Cetuximab and Irinotecan treatment revealed that PTEN staining by immunohistochemistry varied between primary and metastases tumors. In metastases tumors, patients who harbour *PTEN* mutations showed less response to treatment. However, another study showed that there is no significant association in *PTEN* mutations and outcome of Cetuximab treatment [120]. These two mutations have not yet been validated as a predictive biomarker because they are always found together with *KRAS* or *BRAF* mutations.

Other than alterations in the molecular pathways discussed above, epigenetics also plays a part in conferring resistance to EGFR-targeted therapy. However, the exact mechanism is still being discussed. Aberrant modifications made other than at the genomic level which include DNA methylation, histone modifications and expression of miRNA contribute to the formation of CRC [121] and resistance towards treatment. Abnormal DNA methylation in a specific CpG island can leads to the formation of CpG Island methylator phenotype (CIMP). The CIMP at a promoter region is able to repress the expression of certain gene such as mismatch repair gene 1 (*MLH1*) [122, 123]. There have been many studies investigating CIMP as a biomarker of treatment. A study has shown that patients with CIMP-negative tumors have longer disease-free survival (DFS) after 5FU treatment [124]. Another study performed by Ouchi et al. 2015 showed that low methylated CRC subgroup have better clinical outcomes compared to high methylated CRC subgroup in a cohort of

patients who received anti-EGFR treatment (response rate, 35.7% vs 6.3%, P = 0.03; disease control rate, 75% vs 31.3%, P = 0.005; hazard ratio for progression-free survival, 0.27; 95% confidence interval, 0.13–0.57, P < 0.001; overall survival, 0.19; 95% confidence interval, 0.06–0.54, P < 0.001) [125]. Epigenetic alterations also involve aberrant expression of miRNA which is a short single stranded RNA that functions by regulating target mRNA through degradation or inhibiting its translation [126]. The role of microRNA in carcinogenesis has been studied extensively over a period of a decade. A study by Lu et al. 2017 revealed that overexpression of MIR100HG, miR-100, and miR-125b were observed in Cetuximab-resistant colorectal cancer which suppressed negative regulators of WNT signaling pathway [127]. Another study also showed colorectal cancer cell's metastasis was inhibited and Cetuximab sensitivity was restored when mir-302a was overexpressed [128]. Based on the studies that have been performed, epigenetics study could potentially reveal its role in identifying resistance mechanism to anti-EGFR therapy.

1.5 STAT3 Signaling and Resistance

Commonly proposed resistance mechanism involves two main pathways downstream of EGFR, MAPK pathway, and AKT pathway. The mutations in these two pathways give the tumor the capability to resist the effect of EGFR-targeted therapies. STAT3 signaling is one of the pathways that are involved in maintaining cells survivability but is less studied in term of a mechanism of tumor resistance. STAT3 can be activated by several pathways and it mediates many cellular activities including proliferation, metastasis, cell differentiation and apoptosis. Multiple cancers have shown to have elevated STAT3 activity including colorectal and lung cancer. Given the importance of STAT3 in mediating cellular functions, it is likely to play a role in cancer resistance against EGFR targeted therapy.

1.5.1 STAT3 signaling in primary tumor confers resistance towards EGFR-targeted therapy

STAT3 signaling has been associated with primary and acquired resistance towards EGFR-targeted therapy. A study was performed by Dobi et al 2013 using immunohistochemistry to measure the level of STAT3 phosphorylation in mCRC patients who received Cetuximab treatment. They found that tumor samples with negative phospho-STAT3 staining associated with longer PFS and OS [129]. Haura et al 2010 found that despite the high level of Gefitinib after treatment in the

tumor, the patient failed to respond to the treatment. Upon closer analysis, high level of STAT3 activity and low level of EGFR phosphorylation was detected [130]. This indicates that even though Gefitinib managed to block EGFR, another compensatory pathway may have been activating STAT3. In a more recent study, the level of phospho-STAT3 was measured before and after a combination treatment with Cetuximab and Lapatinib. Patients who have disease progression showed elevated STAT3 activity compared to those who have partial response [131]. These findings based on clinical samples were supported by experiments using cancer cell lines. Li et al 2015 used a panel of colon cancer cell lines and showed that STAT3 phosphorylation is associated with Gefitinib sensitivity. A STAT3 regulator called nuclear pyruvate kinase isoform M2 (PKM2) is also correlated with increased Gefitinib resistance [132]. In another study by Li et al 2014, Gefitinib resistance is increased when STAT3 activity was elevated through IL-6 signaling in NSCLC PC9 EGFR TKI sensitive cell line [133]. Similar results were obtained when a constitutively active STAT3 was transfected into head and neck carcinoma cell line UM-22B which increase the resistance towards EGFR TKI PD153035 [134]. STAT3 knockdown leads to increase sensitivity of head and neck carcinoma cell line UM-SCC-5 and hepatoma cell lines to Cetuximab [135, 136]. Our lab has shown that the efficacy of Cetuximab or Erlotinib is associated with their ability to inhibit STAT3 in colorectal cancer cell lines and *in vivo* xenograft models [137]. Another study revealed the treatment of Erlotinib in Erlotinib refractory patient had elevated STAT3 activity despite reducing the activity of EGFR, Erk, and AKT [138]. Therefore, continuous activation of STAT3 could potentially drive the resistance towards this therapy.

1.5.2 STAT3 signaling in acquired tumor resistance towards EGFR-targeted therapy

The clinical evidence pertaining to STAT3 signaling in acquired tumor resistance towards EGFR-targeted therapy is well explored. Gao et al 2016 collected tumor samples prior and after patient acquired resistance towards Erlotinib or Gefitinib treatment [139]. The activation of STAT3 was observed and they found that STAT3 level was increased in patient samples who acquired resistance to treatment. Another cohort of treatment resistance sample showed elevated STAT3 activity, but it was not known if the STAT3 level increased prior or after treatment due to lack of pre-treatment samples. Similarly, head and neck cancer patients, who showed resistance to Cetuximab contained elevated STAT3 activity in their tumors. However, the comparison between pretreated and post treatment was performed on non-matched samples. Nevertheless, these

results showed STAT3 potentially induce resistance in EGFR targeted therapy. *In vitro* experiment revealed similar results as seen in patients. Upon continuous treatment with Erlotinib in HCC827 NSCLC cell lines, Li et al 2013 found that STAT3 phosphorylation at basal level is higher than sensitive HCC8227 parental cell lines [140]. Yao et al 2010 conducted a similar experiment where they measured the expression of several biomarkers between H1650 NSCLC Erlotinib resistant cell lines and H1650 parental cell lines. They found that genes involved in TGFβ signaling were upregulated in resistant cell lines [141]. The expression level of IL-6, a target gene for TGFβ, was significantly elevated leading to the increased of STAT3 activity. This suggests that TGFβ signaling promotes resistance to Erlotinib through the IL-6/STAT3 pathway. Another study used NSCLC A549 cell line that has acquired Gefitinib resistance and showed higher STAT3 activity compared to sensitive A549 cell lines [142]. A much more recent study cultured pancreatic cell line BxPc3 in Erlotinib or Afatinib for more than 6 months. The cell lines developed resistance to Erlotinib and Afatinib and displayed higher STAT3 activity than their parental cell lines [143].

1.6 Novel Biomarker for Resistance

Current FDA approved anti-EGFR drugs can successfully inhibit receptor activation. Despite this, patients still have poor response to these drugs, unable to fully inhibit tumor growth. Cetuximab treatment only resulted in marginal increase in overall survival despite the high cost of administration. Therefore, the need to identify molecular mediators of anti-EGFR resistance is required. In this study, we have identified five candidate genes that predict resistance in colorectal cancer cell lines (**Chapter 4**). We will briefly outline the function of each of these five genes: *CHAC2*, *NAA25, POLR2A, SF3A1* and *CRY2* below in way of an introduction.

1.6.1 Cation Transport Regulator Homolog 2

Cation transport regulator homolog 2 (CHAC2) belongs to the CHAC family and encodes for γ-glutamyl cyclotransferase protein. This protein catalyzed the conversion of Glutathione (GSH) to 5-oxoproline and cysteinglycine. CHAC2 is the third protein found to be involved in the degradation of GSH besides CHAC1 and GGT [144]. Both CHAC1 and CHAC2 are important in cystosolic GSH degradation while GGT degrades non-cytosolic pools of GSH. The degradation of GSH disrupts the REDOX balance in the cell causing Endoplasmic Reticulum (ER) stress due to accumulation of unfolded/misfolded protein [145]. This stress activates an adaptive signaling pathway called the Unfolded Protein Response (UPR) that is mediated by ER sensors [146] (**Figure 1.8**). In a study

performed by Liu et al. 2017, they found that *CHAC2* is frequently downregulated in gastric and colorectal cancer. The high expression of *CHAC2* found in colorectal cancer patients correlate with increase survival. Furthermore, the study showed that the characteristic of *CHAC2* indicates that it's a tumor suppressor gene [147]. Due to limited studies that have been performed on CHAC2 in cancer, there have been no studies investigating the correlation between CHAC2 and resistance towards any treatment in cancer.

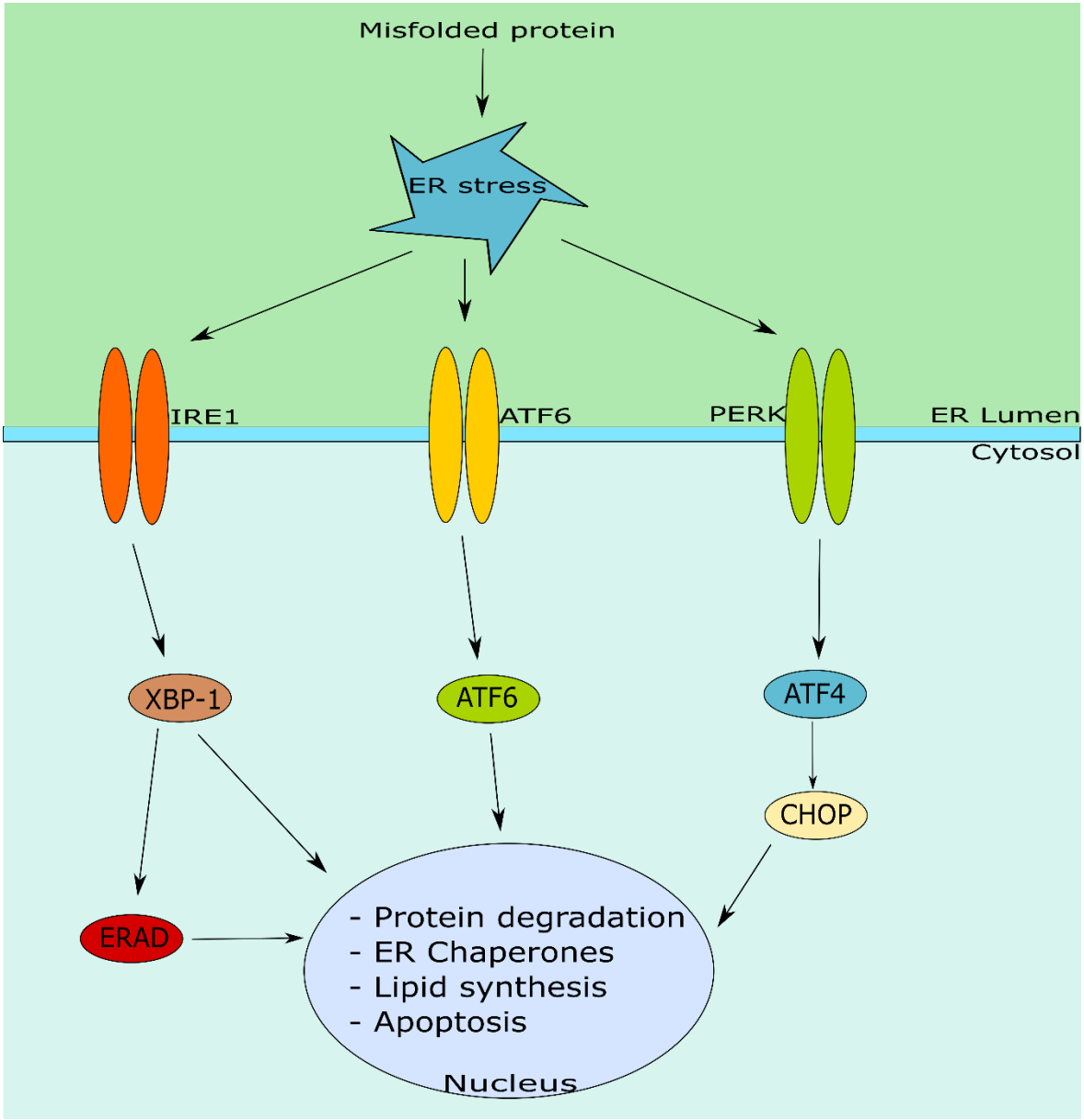

Figure 1.8: Unfolded Protein Response (UPR)

A schematic representation of the unfolded protein response pathway. Accumulation of misfolded proteins would cause ER stress which activates several molecules including XBP-1, ATF6, ATF4, ERAD, and CHOP. Downstream signaling cascade activates cellular response that facilitates protein folding or apoptosis.

1.6.2 N-Terminal Acetyltransferase B Complex Subunit

N-Terminal Acetyltransferase B Complex Subunit (NAA25) is an auxiliary subunit of NatB complex together with catalytic Nat5 subunit which formed an N-terminal acetyltransferase. NAA25 is also known as Mdm20, C12orf30 and NAP1. The functions of NAA25 and Nat5 subunits in mammalian cell are still not well understood. In yeast, the protein complex NatB involved in stabilizing actin cytoskeleton and acetylation of N-terminal methionine in protein during *de novo* protein synthesis [148]. Studies performed by Yasuda et al. 2015 showed that NAA25 is important in modulating the remodeling of actin through mTORC2 pathway (**Figure 1.9**). The activity of mTORC2 was suppressed through reduction in Rictor expression by NAA25 leading to decreased AKT phosphorylation [149]. Furthermore, knockdown of NatB through siRNA was shown to inhibit the cell growth and cell cycle progression. Similarly, to CHAC2, there is limited studies performed assessing the role of NAA25 in cancer settings and resistance towards treatment. The correlation between NAA25 and its potential to be a biomarker may be due to its capability in modulating AKT phosphorylation through mTORC2 pathway.

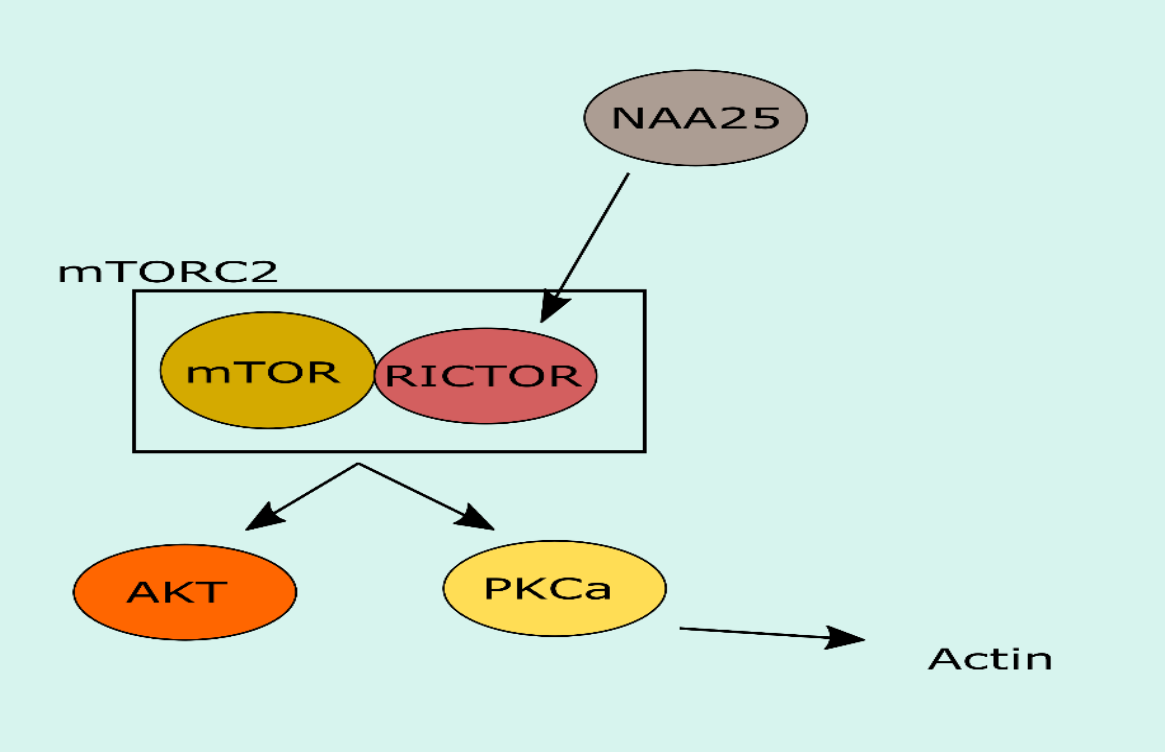

Figure 1.9: The mechanism of NAA25

A schematic representation of NAA25 pathway. NAA25 modulate the formation actin through RICTOR and mTOR.

1.6.3 RNA Polymerase II Subunit A

RNA Polymerase II Subunit A (POLR2A) makes up the biggest subunit of RNA Polymerase II complex that is important in mRNA synthesis. This gene is crucial such that homozygous deletion of *POLR2A* is lethal in all type of cells [150, 151]. In colorectal cancer, mutation of *POLR2A* is often found together with hemizygous *TP53* [152]. The genomic deletion of tumor suppressor gene often affects the neighboring essential genes causing them to be more susceptible to treatment. Studies performed by Liu et al. 2015 showed that the knockdown of hemizygous *POLR2A* inhibit proliferation more than normal *POLR2A*. Moreover, inhibition of hemizygous *POLR2A* enhanced the effect of chemotherapy drugs compared to normal *POLR2A* [153]. The potential of POLR2A to become a biomarker could be related to its expression. Based on the study by Liu et al 2015, higher expression of POLR2A could potentially cause resistance towards treatment of α-aminitin-

conjugated anti-EpCAM, a cell surface marker [153, 154]. However, whether its over-expression relates to resistance to anti-EGFR inhibitor is not known.

1.6.4 Splicing Factor 3a Subunit 1

The spliceosome is made up of 5 small nuclear RNA (snRNA); U1, U2, U4, U5 and U6 [155]. Of the 5 snRNA, Splicing Factor 3a Subunit 1 (SF3A1) is important to U2 snRNA. This gene encodes for subunit 1 of the heterotrimer splicing factor 3A complex. SF3A protein complex involved in converting the 15s U2 snRNA to its active form 17s U2 snRNA prior to pre-mRNA splicing [156] (**Figure 1.10**). There are few studies that show an association of SF3A1 with multiple cancers including colorectal, pancreatic, and hepatocellular cancers [157-159]. However, the studies only demonstrate association with no further characterization of the protein's role in those cancers. A study performed in mouse macrophages showed that the inhibition of SF3A1 reduced the production of cytokines including IL-6 and IL-10. Moreover, among the many genes and pathway affected by SF3A1 inhibition, innate immune signaling pathways such as MAPK and Toll-like Receptor signaling pathways are the one that are significantly altered [160].

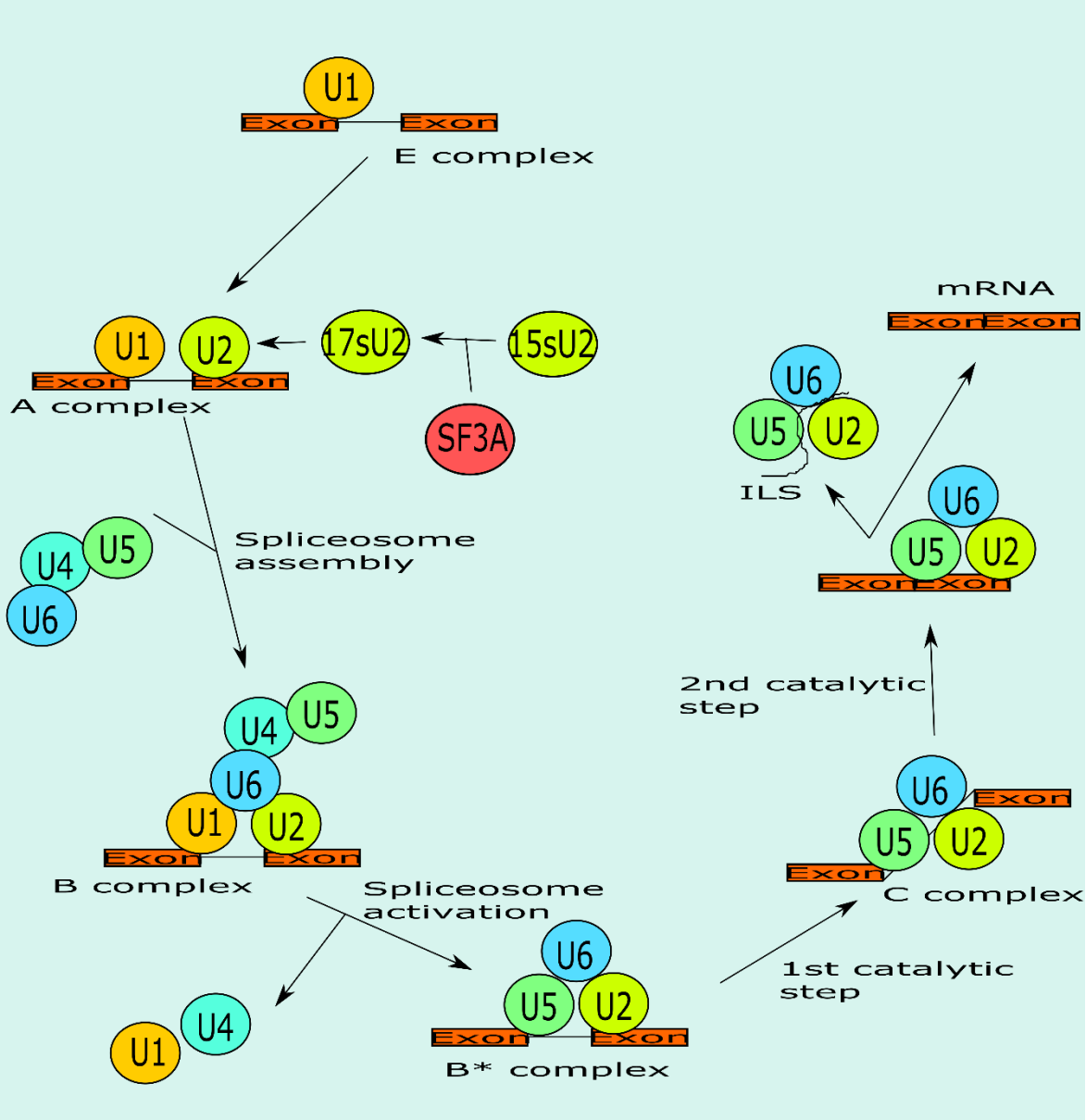

Figure 1.10: The mechanism of splicing

A schematic representation of splicing mechanism. Splicing is a complex process which involves several steps: the assembly, activation and two catalytic steps. snRNAs (U1, U2, U4, U5, and U6) were recruited during the assembly process before the complex is activated. Upon completion of the catalytic steps, the mRNA would be splice.

1.6.5 Cryptochrome 2

Circadian clock is an important biological mechanism that regulates the internal changes in the environment according to the day-night cycles. It is a core mechanism to drive the circadian rhythm through activation of transcriptional activator and repressor forming a feedback loop. Circadian clock which is also known as biological clock has been shown to affect multiple metabolic processes. In some cancers including breast, prostate and colorectal, interruption of circadian clock seems to elevate the risk of these tumors [161-163]. Cryptochrome 2 (CRY2) is a circadian clock protein that formed a feedback loop together with Period (PER), CLOCK and BMAL1. CLOCK and BMAL1 are transcriptional activators which activates the transcription of *CRY* and *PER* genes. The two PER and CRY2 proteins then associate and translocate into the nucleus to inhibit the activity of CLOCK/BMAL1 [164] (**Figure 1.11**). The expression of CRY2 was shown to be correlated with the resistance to chemotherapy in colorectal cancer patients [165]. CRY2 was found to be important in regulating the expression of genes involved in DNA damage checkpoint control [166]. Furthermore, mutation in *CRY2* increases the rate of apoptosis when treated with genotoxic drugs [167]. One of the potential roles of CRY2 to be a biomarker is that it involved in degrading c-MYC [168]. Huber et al. 2016 showed that CRY together with FBXL3 bind and promotes c-MYC ubiquitylation while loss of CRY2 stabilized the protein. The importance of c-MYC in cell proliferation could potentially make CRY2 a viable biomarker.

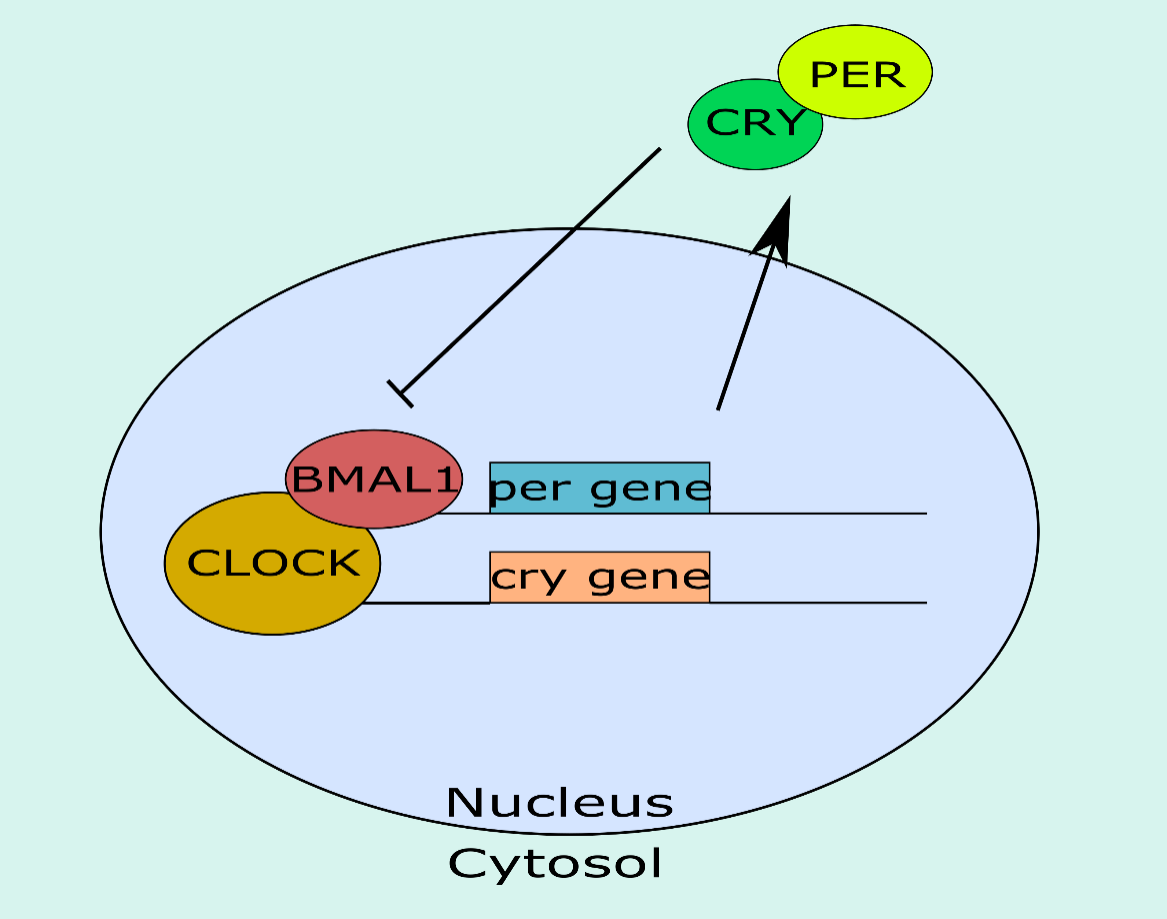

Figure 1.11: Circadian rhythm feedback loop

A schematic representation of the feedback loop of the circadian rhythm regulators. CRY2/PER protein complex inhibits CLOCK/BMAL complex from activating the transcription of cry and per genes. Reduction of CRY and PER protein would drive CLOCK and BMAL1 into activating the expression of per and cry genes forming a feedback loop.

1.7 Proteasome as Target for Therapy

The proteasome has been the target for cancer treatment for many years. The primary function of the proteasome is to regulate the removal of protein that has been targeted for degradation. Many signaling proteins are involved in the degradation cycle making it a desirable target for treatment. Anticancer drugs have been developed and approved by the FDA primarily for treatment of Multiple Myeloma and liquid tumors using proteasome inhibitors.

1.7.1 Structure and Function

The proteasome forms a system with ubiquitination to perform its function of degradation of proteins. This ubiquitination-proteasome system (UPS) maintain the cellular homeostasis by removing unwanted proteins that were involved in various cellular processes including cell cycle, apoptosis, DNA damage/repair, angiogenesis and cell differentiation [169-174]. UPS has 2 steps for the degradation process. The first step is the ubiquitination of the protein through the binding of a small molecule called ubiquitin to the protein. The process was followed by the translocation of the ubiquitinated protein to 20S proteasome for degradation.

Ubiquitin is a small molecule made of 76 amino acids. The process of ubiquitination is important in tagging the protein substrate to be degraded. Ubiquitin is covalently linked to the substrate protein through a series of steps involving several enzymes [175]. The first ubiquitin molecule was activated and added to E1 enzyme forming a complex. Ubiquitin was then transferred to carrier E2 enzyme before being added to the substrate protein. This process would be repeated to form a polyubiquitin chain on the protein marked for degradation. The ubiquitin chain usually would have four or more additional ubiquitin molecules before being transferred to 20S proteasome [176]. Other than poly chain, the protein could also be monoubiquitinated which could be a substrate used in cell signaling [177]. While monoubiquitinated protein is thought not to be degraded, it has been suggested that short monoubiquitinated protein (<150 amino acids) would be degraded by the 26S proteasome [178].

26S proteasome is a protease complex that is made of two subunits: 19S and 20S proteasome. 19S subunit function as a lid and binds to either side of 20S proteasome forming the 26S proteasome. 19S proteasome itself is comprises of a lid and a base made of multiple subunits. Having multiple subunit, 19S proteasome performed several important functions that includes

ATPase, ubiquitin-binding and deubiquitination [175]. Each subunit has their own specific function to ensure the ubiquitinated protein can enter the proteasome. The 19S lid contain nine Rpn subunits which function is to cleave ubiquitin from the protein substrates [179]. As ubiquitin unable to enter the proteasome, it needs to be deubiquitinated by the enzyme found on 19S lid. The base of 19S has ten subunits which consist AAA-ATPase. The ATPase function to convert energy to chaperone the unfolding of the protein and facilitate into the 20S proteasome [180].

The structure of 20S proteasome consists of outer and inner rings which composed of two α_1-α_7 heptameric ring and two β_1-β_7 heptameric ring respectively [175, 180]. The α rings encompass the β rings forming a barrier that separate the catalytic site and cytoplasm. Substrates binding sites are present on the α rings while the β rings housed the catalytic site. On the β subunit, there is a N-terminal threonine that plays an important role in cleaving the peptide bond of protein substrates. The catalytic sites have three different type of catalytic activities. They are the chymotrypsin-like activity, trypsin-like activity and peptidyl glutamyl peptide-hydrolysing-like activity [181]. Each activity targets different residues on the protein substrates. The resulting cleavage produced oligopeptides with length not more than 15 amino acids [179] (**Figure 1.12**).

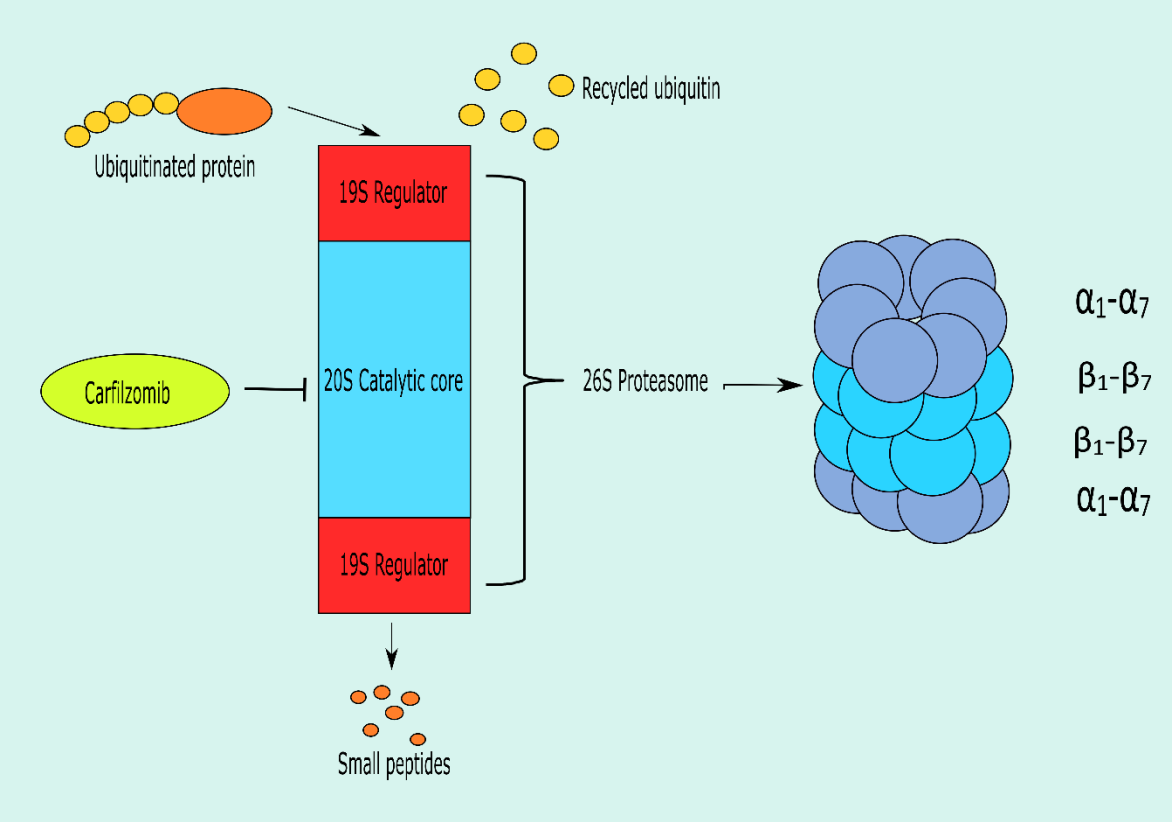

Figure 1.12: The structure and mechanism of proteasome.

A schematic representation of the structure of proteasome and its mechanism. Proteasome is made up of two heptameric α chain which made up the 19S regulator and two heptameric β chain which made up the 20S catalytic core. Ubiquitinated protein would enter the proteasome before being degraded, producing small peptides and recycled ubiquitin molecules.

1.7.2 Proteasome Inhibitors

The development of proteasome inhibitors stemmed from the effect of highly elevated levels of proteasome which affects the normal cellular activities. One of the hallmark of cancers is proliferation and apoptosis which proteasome plays a key role [169, 170]. Increasing level of 26S proteasome in cancer has been reported in several studies [182, 183]. High level of proteasome was shown to enhance survival through circumvention of apoptotic pathway [183]. Therefore, proteasome inhibitors were developed as a targeted therapy in cancer. Further studies on the inhibitor showed cancer cells have higher sensitivity to proteasome inhibitor as compared to normal cells [184, 185]. There were many proteasome inhibitors that have been developed with Bortezomib becoming the first to be approved by the FDA, subsequently, for the treatment of multiple myeloma in 2012, the second-generation inhibitor Carfilzomib was also approved.

1.7.2.1 Bortezomib

Bortezomib is the first-generation proteasome inhibitor that was approved by the FDA to be used in Multiple Myeloma patients. Bortezomib binds reversibly to the 20S proteasome inhibiting its chymotrypsin-like activity [186]. Its selectively bind the proteasome with high affinity and without having off-target effect to other proteases [187, 188]. Bortezomib managed to inhibit the proteasome thus affecting cellular processes needed for the cells to survive. Stabilising p53, inhibition of NF-κB, and elevated JNK lead to increasing level of apoptosis [189-192]. In multiple myeloma, Bortezomib was able to increase the overall survival of patients compared to dexamethasone single treatment [193]. The efficacy of Bortezomib was shown in clinical trials until it was approved by the FDA in 2003 as a third-line treatment in multiple myeloma [193-196]. Although Bortezomib has a great effect as a single agent, it was commonly used in conjunction with other drugs including Dexamethasone, Thalidomide and Lenalinomide. The combination therapies produced great results while having tolerable toxicity [197, 198]. In colorectal cancer, Bortezomib was showed to be effective in combination with Leucovorin by enhancing apoptosis synergistically both *in vitro* and *in vivo* [199]. Similarly, Kretowski et al. 2015 showed elevated level of apoptosis in colon cancer cell line in both hypoxic and normoxic conditions [200].

1.7.2.2 Carfilzomib

Carfilzomib is a second-generation proteasome inhibitor which was approved in 2012 by the FDA. The difference between Bortezomib and Carfilzomib is that Carfilzomib irreversibly bind to the 20S proteasome inhibiting its chymotrypsin-like activity [201]. This design of Carfilzomib

ensures a more efficient inhibition of the proteasome as well as minimal off-target activity [202]. As Bortezomib treatment eventually causing resistance in patients, Carfilzomib managed to overcome it by inducing apoptosis [203]. *In vitro* experiments demonstrate that Carfilzomib can inhibit non-solid tumor cells, such as myeloma cells more efficient than solid tumor cells [203]. Carfilzomib was also evaluated in clinical trials ranging from Phase 1 through Phase III trials. In a Phase I trial, 14 (39%) patients have stabilized disease after treatment with Carfilzomib. The effect of Carfilzomib was well tolerated upon consecutive treatment days [204]. A Phase II trial showed the effect of increased Carfilzomib dose from 20 to 27 mg/m^2 displayed an increase in ORR of 23% [205]. The ORR is higher compared to another trial which used the dose of 20 mg/m^2 resulting in ORR of 16.7% [206]. As a single agent, Carfilzomib showed positive effect which lead to Phase III trial that involved combination treatment. ASPIRE study compares the combination of Carfilzomib with lenalinomide and dexamethasone with lenalinomide and dexamethasone alone [207]. Another study focused on combination of dexamethasone with either Carfilzomib or Bortezomib [208].

1.8 Relevance and Importance of this Study

Cancer treatment has improved over the years with the used of targeted therapies as monotherapy or combination with chemotherapy to achieve better response in patients. Nevertheless, patients who initially respond well to these treatments often develop resistance. The heterogeneity of cancer leads to the discovery of several resistance mechanisms towards these therapies. Mutation of *KRAS* is one of the most common resistance mechanisms towards EGFR targeted therapies. It occurs in 40% of colorectal cancer patients leading to the use of Cetuximab only in patients who harbor tumors with wild-type KRAS expression. However, over 30% of wild-type KRAS patients still response poorly to Cetuximab suggesting resistance through other mechanisms. Therefore, deeper understandings of those resistance mechanisms are needed in order to develop effective treatment and prolonging the patients' survival.

The first aim of this study was to verify the role of STAT3 signaling in mediating resistance to EGFR targeted therapy by using a colorectal cancer human cells with Cetuximab-acquired resistance. Characterization of these cell lines which were developed in our lab is presented here. In term of Cetuximab-resistance mechanisms, STAT3 signaling is one of the least studied pathways. STAT3 signaling is important in regulating cellular function that involves in cell proliferation, migration,

and survival. Aberrant STAT3 signaling could potentially induce cancer development and progression. Furthermore, elevated STAT3 signaling has been shown in multiple cancers including colorectal, lung and brain cancers. Elucidating the role of STAT3 signaling in cancer resistance to EGFR targeted therapy will allow for the improvement of the treatment regimens for current patients.

The second aim of this study was to search for a potential novel biomarker for resistance towards EGFR targeted therapy. Resistance towards a treatment can involve several signaling pathways. These pathways usually are crucial to the cell's survivability. Inhibitors were then designed to target specific protein in the pathway thus restoring the cell's sensitivity to the treatment or bypassing the original treatment completely. Investigating novel pathways will further our understanding in resistance that occur after or before a treatment.

The third aim of this study was to identify a novel or repurpose a current inhibitor that could potentially restore the resistant cells sensitivity to EGFR targeted therapy in colorectal cancer. New drugs are continuously being developed and studied in order to provide better treatment to patients. This process could take a long time to be translated into the clinical. By analyzing a panel of FDA-approved drug for repurposing, we can shorten the process.

CHAPTER 2:

Materials and Methods

2. Chapter 2: Materials and Methods

2.1. Cell Culture

2.1.1. Cell Lines.

Cell lines were obtained from Walter and Eliza Hall Institute of Medical Research (WEHI). The criteria for choosing these cell lines were based on the mutational status of KRAS protein. All cell lines had wild-type KRAS protein and were adherent cells. The cell lines are as followed:

Table 2.1: Colorectal cell lines

Cell Lines

LIM1215	**GEO**	**HT115**
SW48	**HT55**	**CCK81**
CACO2	**HDC-54**	
DIFI	**HCA-7**	
SNU175	**KM12**	
C70	**COLO320**	

2.1.2. Acquired Resistant Cell Lines Generation.

Cell lines LIM1215, SW48, and CACO2 were made to acquire resistant to Cetuximab through continuous treatment of Cetuximab over the period of 6 months. All cell lines were treated with Cetuximab starting at a low dose and gradually increasing it until it reached concentration of 20µg/ml. The cell lines were denoted as LIM1215 C225, SW48 C225 and CACO2 C225.

Cell line H1650 was made to acquire resistant to Gefitinib through similar method. H1650 cell line was treated continuously over the period of 6 months with Gefitinib. Starting with low doses of Gefitinib, the concentration was increased gradually until it reaches 5µM. The cell line was denoted as H1650 GR.

2.1.3. Revival of cells from cryopreservation

Cell lines were thawed from cryopreservation at room temperature before immediately transferred into a 10 ml tube containing pre-warm culture media. The tube was centrifuged at 1300 revolutions per minute (RPM) for 3 min. Supernatant was discarded leaving the pellet in the tube. The pellet was resuspended in 10 ml culture media before being transferred into a T75 flask.

2.1.4. Cell culture maintenance

All cell lines were cultured in DMEM culture media supplemented with fetal calf serum at 5% concentration and 0.5 % of penicillin and streptomycin. The flasks containing the cell lines were maintained in an incubator at 37°C and 10% concentration of carbon dioxide. The water reservoir in the incubator were mixed with Aqua clean solution to prevent fungus from growing. Every 2-3 days, if the cells have achieved 80% confluence, the cell culture was passaged to ratio suitable for the cell lines. The culture media in the flask was aspirated and 1.5 ml of trypsin was added. After ensuring the trypsin has covered all surface, the flask was incubated in incubator at 37°C and 10% concentration of carbon dioxide for 5-15 min depending on cell lines. After incubation, the flask was agitated to dislodge any cells that still stuck down to the bottom of the flask. The flask was then observed under light microscope to check for cells dispersion. After, 3.5 ml of media was added to stop the activity of trypsin. The mixture was split according to suitable ratio and 10 ml of culture media was added. The flask was then returned to incubator to grow until the next passage.

2.1.5. Cell Culture Seeding

Cell lines that were going to be used in experiment were seeded onto 24, 12, 6-wells plate or a 10cm^2 dish. The number of cells used varied according to experiment. The culture media in the flask was aspirated and 1.5 ml of trypsin was added. After ensuring the trypsin has covered all surface, the flask was incubated at 37°C and 10% concentration of carbon dioxide for 5-15 min depending on cell lines. After incubation, the flask was agitated to dislodge any cells that still stuck down to the bottom of the flask. The flask was then observed under light microscope to check for cells dispersion. After, 3.5 ml of media was added to stop the activity of trypsin. An appropriate volume was transferred into a 10 ml tube and centrifuged at 1300 RPM for 3 min. Supernatant was discarded leaving the pellet in the tube. The pellet was then resuspended in DMEM culture media. 10µl of the cell's mixture was used in cell counting using a hemocytometer.

2.1.6. Cell culture vessel

Depending on the experiment or the growth nature of the cells, the flasks that were used to grow the cell lines were different. Small flasks (25cm^2) were used to grow cells that were going to be used for experiment that required small number of cells. Some cell lines that has trouble growing in early phase were also grown in the small flasks. Medium flasks (75cm^2) were the standard vessels that were used in the cell culture. Large flasks (175cm^2) were used in *in vivo* experiment when large number of cells were needed.

2.1.7. Cryopreservation of Cell Lines

After the cell lines have been thawed from cryopreservation, the first passage of those cell lines were preserved again for future use. The culture media in the flask was aspirated and 1.5 ml of trypsin was added. After ensuring the trypsin has covered all surface, the flask was incubated in incubator at 37°C and 10% concentration of carbon dioxide for 5-15 min depending on cell lines. After incubation, the flask was agitated to dislodge any cells that still stuck down to the bottom of the flask. The flask was then observed under light microscope to check for cells dispersion. After, 3.5 ml of media was added to stop the activity of trypsin. 4 ml of the mixture was added into a 10 ml tube and centrifuged at 1300 RPM for 3 min. Supernatant was discarded leaving the pellet in the tube. The pellet was resuspended in a mixture of 10% DMSO in culture media before being transferred into a cryogenic tube. The cryogenic tube was stored in -80°C freezer for short term preservation or in liquid nitrogen storage for longer term preservation.

2.2. Protein Extraction

2.2.1. Protein extraction

Proteins were extracted from cells that was seeded onto a plate or a dish. Culture media was aspirated, and the cells were washed with cold 1x Phosphate Buffered Saline. After the PBS has been aspirated, a volume of Triton-X lysis buffer was added. The amount of lysis buffer added were different according the size of the plate and dish. 60µl of lysis buffer was added to 12-wells and below plate, 100µl for a 6-wells plate and 300µl for a 10cm^2 dish. The plates were then put on a shaker at 4°C or on ice for 15 min. For a 6-well plate and bigger, a scrapper was used to dislodge all cell from the plate. For 12-wells plate and smaller, normal pipette tip was used to wash over the

cells for a few times before transferred into an Eppendorf tube. The tubes were then centrifuged at 1300 RPM for 15 min. The supernatant was collected for protein estimation. The cell lysates were then kept in -20°C freezer for future use.

2.2.2. BCA Protein Estimation Assay

After protein extraction, the concentration of protein was measured by using BCA protein estimation assay kit (Thermo Fisher). The assay was conducted according to the manufacturer's instruction in a 96-well plate. Briefly, the assay was done by mixing a ratio of 1:4 sample/water before adding a working reagent at a ratio of 1:8 sample/working reagent. The plate was then incubated at 37°C for 30 min. After, the plate was read using a plate reader. The absorbance values (color intensity) of the protein were quantified and plotted against a set of protein standards to determine protein concentrations.

2.3. Western Blotting

2.3.1. Sample Preparation

The concentration of protein that used was in the range of 10-50µg/µl. Each sample was prepared by mixing together an appropriate volume of LDS Sample buffer (4X), denaturing agent (10X) and sample cell lysate. The total volume of each sample was 50µl. The sample mixture was heated at 95°C for 5 min and cooled down. If the samples were to be run on the same day, the mixture was cooled on ice, vortexed and centrifuged. For longer term storage, the samples were kept in -20°C freezer for no longer than one week.

2.3.2. Protein separation

The proteins were separated by using Sodium Dodecyl Sulphate polyacrylamide gel electrophoresis. Samples lysate were loaded into 10, 12, or 15-wells gel (Thermo Fisher) at 15µl per well. The gels were NuPAGE 4-12% Bis-Tris (Thermo Fisher) and was run at 120V for 2h in NuPAGE running buffer. After the run has finished, the gel was transferred to a nitrocellulose membrane using a wet transfer system.

2.3.3. Membrane Blocking and Antibodies

After transfer, the membrane was trimmed and washed in PBS/T 3 times for 3 min each. The membrane was then blocked in 5% skim milk dissolved in Phosphate Buffer Saline Tween (PBS/T) for 1h. After blocking, the membrane was washed with PBS/T 3 times for 3 min each. Next, the membrane was incubated with primary antibodies for desired protein overnight at 4°C **(Table 2.2**).

Table 2.2: Primary and Secondary antibodies used in Western blotting

ANTIBODIES	DILUTION	SOURCE
PRIMARY ANTIBODIES		
ANTI-GAPDH RABBIT POLYCLONAL	1:1000	Cell Signaling Technologies
ANTI-STAT3 RABBIT POLYCLONAL	1:1000	Cell Signaling Technologies
ANTI-PHOSPHO STAT3 MOUSE POLYCLONAL	1:1000	Cell Signaling Technologies
ANTI-ERK1/2 RABBIT POLYCLONAL	1:1000	Santa Cruz Biotechnology
ANTI-PHOSPHO ERK1/2 RABBIT POLYCLONAL	1:1000	Santa Cruz Biotechnology
ANTI-POLR2A MOUSE POLYCLONAL	1:1000	Thermo Fisher Scientific
ANTI-SF3A1 RABBIT POLYCLONAL	1:1000	Thermo Fisher Scientific
ANTI-NAA25 RABBIT POLYCLONAL	1:1000	Thermo Fisher Scientific
ANTI-CRY2 RABBIT POLYCLONAL	1:1000	Thermo Fisher Scientific
ANTI-CHAC2 RABBIT POLYCLONAL	1:1000	Thermo Fisher Scientific

SECONDARY ANTIBODIES		
MOUSE ANTI-GOAT IGG HRP CONJUGATE	1:5000	Bio-Rad
RABBIT ANTI-GOAT IGG HRP CONJUGATE	1:5000	Bio-Rad

2.3.4. Membrane Imaging

After overnight incubation, primary antibodies were poured into 10ml tubes for future use. The membrane was washed 3 times for 3 min each. Secondary antibodies (HRP- Rabbit or mouse) were prepared according to their primary antibodies' species. The membrane was then incubated with the secondary antibodies for 1h on a shaker at room temperature. Secondary antibodies were made in PBS/T with 1:5000 dilution. Following incubation, the secondary antibodies were discarded. The membrane was washed 3 times for 3 min each. In preparation for imaging, the membrane was incubated with ECL reagent that was prepared according to the manufacturer's instruction. The membrane was incubated for 1 min before being transferred into a cassette. By using Fuji Film, the membrane was exposed to the film in a dark room over a range of time points. The film was developed by the developer (AGFA). Developed film was scanned to keep the file digitally.

2.3.5. Membrane Stripping

If needed, the membrane was stripped from all the antibodies to make way for another primary antibody. The membrane was incubated with 10ml of stripping buffer (2% SDS, 62.5nM Tris-HCL, pH 6.8) for 10 min at 50°C inside a water bath. Following stripping, the membrane was blocked again with 5% Skim milk/PBST for 30 min. Next, the membrane was probed with different antibodies overnight at 4°C.

2.3.6. Analysis

ImageJ software was used to analyze the intensity of the bands of a Western Blotting. The method used to quantify the band's intensity was adapted from Miller 2010 [209]. Briefly, the bands were measured by using ImageJ software resulting in a profile plot with peaks for different bands. The height of each peaks was different according to intensity of the bands. i.e darker band has higher peak and wider signals. Area under the curve for each curve was measured producing an

arbitrary value. These values represented the intensity of each bands i.e. higher values represented darker bands. Values obtained were normalized against a control band i.e. a housekeeping gene to get a normalized value for the band. These values were used to compare between other normalized bands

2.4. Cell Viability Assay

Cell lines were seeded onto a 96-well plate at cell density of 1000 cells per well in a triplicate. The plate was incubated at 37°C and 10% CO_2 for 24 h. After 24 h, the cells were treated with drugs at various concentrations for 3 days. For treatment with Cetuximab, the concentrations that were used were 10 and 20µg/ml. For treatment with Carfilzomib, the concentrations were 1, 2.5, 5, 7.5 and 10 nM. After the treatment period, the media was aspirated and 50µl of Cell Viability lysis buffer (Cell Titer-Glo kit (Promega)) was added. The plate was incubated at room temperature for 10 min. Next, 40µl of cell/lysis buffer mixture was transferred to a white 96-well plate. The plate was then read by using a luminometer (GloMax).

2.5. Colony Formation Assay

The Colony Formation Assay was adapted from 'Clonogenic assay of cells *in vitro'* by Franken et al 2006 [210]. Cell lines were seeded on a 24-well plate at cell density of 100 cells per well in a triplicate. The plate was incubated at 37°C and 10% CO_2 for 2 h before treatment was added. Carfilzomib and Cetuximab at concentration of 10nM and 20ug/ml respectively were added. The plate was incubated for 10-14 days at 37°C and 10% CO_2. After the treatment period, the media was removed the cells were washed with PBS. 2-3ml of a mixture of 6.0% glutaraldehyde and 0.5% of crystal violet were added for 30 min. The glutaraldehyde and crystal violet mixture were removed, and the plate was rinsed by slowly submerging it in tap water. The plate was left to dry at room temperature before colonies counting. Quantification method of the colonies was adapted and utilized using ImageJ Plugin [211].

2.6. Cell Migration Assay

Cell lines were seeded onto a 12-well-plate at cell density of 10 x 10^5 cells per well. The cells were grown until 100% confluent. Once the cells are confluent, the media was aspirated, and serum free media was added for 24 h to starve the cells. After 24 h, the media was aspirated, and 5 mg/ml

of Mitomycin C was added for 2 h. The purpose of adding Mitomycin C is to prevent mitosis from occurring. After 2 h, the cells were washed with sterile 1x PBS and a scratch was made using a pipette tip. A picture at 0 h was taken before drug was added. The concentrations for Cetuximab were 10 and 20µg/ml while Carfilzomib were 5 and 10 nM. Images for the wound was taken every 24 h for maximum of 5 days. Fresh doses of drugs were added every day until the end of experiment.

2.7. Knockdown using siRNA

Cells were trypsinized and 6 x 10^4 cells were added to 1.7 ml of serum-free media. The cells were prepared in a microfuge tube separately from the siRNA/HiPerfect master mix. The master mix was prepared by mixing siRNA to 100µl of serum-free media in a microfuge tube. Two concentrations of siRNA; 20nM and 40nM were used. Scramble sequence was used as Control siRNA. HiPerfect transfection reagent was added later at double the volume of siRNA used. The siRNA/HiPerfect master mix was then added dropwise into the tube containing the cells. The cells mixture was divided for cell viability and western blot. For cell viability assay, 50µl of cells mixture were seeded per well in a triplicate. The plate was incubated at 37°C and 10% CO_2 for 24 h. After 24 h, the cells were treated with Cetuximab at concentrations of 5, 10 and 20µg/ml. After the treatment period, the media was aspirated and 50µl of Cell Viability lysis buffer was added. The plate was incubated at room temperature for 10 min. Next, 40µl of cell/lysis buffer mixture was transferred to a white 96-well plate. The plate was then read by using a luminometer (GloMax). For western blot, the remaining of the cell's mixture was seeded on a 12 well-plate. The plate was incubated at 37°C and 10% CO_2 for 48 h before protein were extracted for western blotting.

Table 2.3: List of siRNAs

Target gene	Code	Product	Source
STAT3	sc-29493	A pool of 3 target specific	Santa Cruz Biotechnology
ERK1/2	sc-35335	Target specific	Santa Cruz Biotechnology
AKT	sc-29195	Target specific	Santa Cruz Biotechnology
CRY2	Hs.532491	Target specific	ThermoFischer Scientific

2.8. Quantitative Polymerase Chain Reaction (qPCR)

2.8.1. Plate preparation

Cells were seeded into a 6-well plate at cell density of 1 x 10^6 per well. The plate was incubated at 37°C and 10% CO_2 for 24 h. After incubation, the media in each well was aspirated and replaced with serum free media. The plate was incubated at 37°C and 10% CO_2 for 24 h. After incubation, the cells were treated with Carfilzomib at 0, 5, and 10nM. The plate was return to incubator for incubation for another 24 h. After incubation, the media was aspirated, cells were washed with cold 1X PBS and put on ice for immediate RNA extraction or frozen in -80°C freezer for later extraction.

2.8.2. RNA Extraction

The extraction was performed using Qiagen RNA mini kit following the manufacturer's instruction. Briefly, cells were lysed using a mixture of 2-Mercaptoethanol/RLT buffer and centrifuged at 1300 RPM at 4°C for 3 min. The supernatant was mixed with 70% ethanol, transferred to a mini column provided and centrifuged at 1300 RPM for 30 s. The mini column was washed with RW1 buffer before DNase 1/RDD buffer was added for 15 min. Following that, the mini column was washed with RPE buffer and the RNA was eluted with RNase-free water. Extracted RNA was kept in -80°C freezer for long term storage.

2.8.3. RNA concentration

The concentration of RNA was measured by using NanoDrop Spectrophotometer (Thermo Scientific). RNA was kept on ice for the whole procedure. The NanoDrop machine was set to measure RNA concentration. Before measuring the samples, the machine was set to blank by putting water to the NanoDrop. Following that, the RNA concentrations were measured and recorded.

2.8.4. Reverse Transcription Polymerase Chain Reaction

After the concentration of RNA for each sample was measured, the RNA was reverse transcribed into cDNA. The cDNA was prepared by using High Capacity RNA to cDNA kit according

to the manufacturer's instruction. Briefly, 2µg/µl was the maximum amount of RNA that was used. A mixture of RT buffer, enzyme mix, RNA free water and RNA were prepared for the reaction. The sample mixture underwent 1 cycle of 60 minutes at 37°C and 5 minutes at 95°C in GeneAmp PCR System 2400 (Perkin Elmer, Waltham, MA, USA). The cDNA produced were kept in -20°C freezer for long term storage.

2.8.5. Quantitative Polymerase Chain Reaction

Quantitative PCR was done using Taqman Pre-amp Master Mix (Applied Biosystem) according to the manufacturer's instruction. Briefly, a master mix of primers, enzyme, and nucleotides, were prepared. cDNA was added into 384-wells plate in duplicates followed by Master mix of specific primers. After the plate was sealed, the amplification was done on ViiA 7 Real-Time PCR system (Applied Biosystems).

Table 2.4: List of primers

Target gene	Code	Source
SOCS3	Hs02330328_s1	**ThermoFisher Scientific**
IL-6	Hs00174131_m1	
IL-11	Hs01055414_m1	
IL11-R	Hs00234415_m1	
GAPDH	Hs02758991_g1	
POLR2A	Hs00172187_m1	
SF3A1	Hs01066327_m1	
NAA25	Hs00405839_m1	
CRY2	Hs00323654_m1	
CHAC2	Hs00378072_m1	

2.8.6. Analysis

The results obtained from the qPCR were the amplification of the genes in the form of CT-value. Lower CT-value represented higher expression level of the genes and vice versa. The CT-values were normalized to housekeeping gene (CT-values gene – CT-values housekeeping gene =

ΔCT) before being analyzed. The 2-tailed standard t-test analysis was performed using normalized CT-values (ΔCT) for each gene in.

2.9. *In vivo* mouse experiment

This research project was approved by the Animal Ethics Committee of the University of Melbourne (Ethics agreement number 1613824.3)

2.9.1. Carfilzomib dose testing

An initial experiment was performed to investigate the right dose of Carfilzomib on mice. LIM1215 C225 was chosen as the cell line for pilot study. 5 mice were allocated each into Vehicle group, Carfilzomib (2mg/kg) and Carfilzomib (4mg/kg) after the injection of the cell line. After the tumor had grown to an appropriate size, mice were randomly picked and treated with either Carfilzomib according to the concentrations or (10 mM sodium citrate, 10% (2-hydroxypropyl)-β-cyclodextrin, pH 3.5) as control. The tumors were measured every day for 3 weeks or until the tumor has achieved the maximum size which was 1000mm^3. Following that, the mice were culled, and measurements were taken. The effects of Carfilzomib on tumor and mice well-being were analyzed based on the different concentrations.

2.9.2. Carfilzomib Treatment

2 cell lines were used in this experiment to investigate the effect of Carfilzomib on colorectal cancer. They were Cetuximab Acquired Resistant Cell lines; LIM1215 C225 and SW48 C225. 5 mice were allocated each randomly into the vehicle group, and treatment group after subcutaneous injection into the mice right flank. After the tumor had grown to an appropriate size, mice were randomly picked and treated with either Carfilzomib (4mg/kg) or (10 mM sodium citrate, 10% (2-hydroxypropyl)-β-cyclodextrin, pH 3.5) as control. The tumors were measured every day for 3 weeks or until the tumor has achieved the maximum size which was 1000mm^3. Following that, the mice were culled, and measurements were taken before the tumors were processed for subsequent experiments including slices for immunohistochemistry, samples for western blotting and qPCR.

2.9.3. *In vivo* animal testings

6-10 weeks old BALB/c Nude mice were injected subcutaneously with 5-10 x 10^6 of human colon cancer cells per cell line. Mice were swabbed with 80% ethanol (v/v) at the site of injection followed by the subcutaneous injection of tumor cells in 100µl of culture media using 29-gauge insulin syringe into ventral flanks, anterior to hind leg. The mice were monitored twice a day for 48 hours for signs of any unexpected adverse effect. Tumors were allowed to grow until they reached 100mm^3 before randomly separated into 3 groups. The groups were vehicle control, Carfilzomib 2mg/kg and Carfilzomib 4mg/kg. (10 mM sodium citrate, 10% (2-hydroxypropyl)-β-cyclodextrin, pH 3.5) was used as the dilution agent and as treatment for vehicle control. Carfilzomib were administered daily for 3 weeks intraperitoneally. Tumor volumes were recorded manually with electronic calipers on a daily basis. This volume was measured using the formula (length x $width^2$)/2, where the length was the longest axis, and the width was measured at right angles to the length. All healthy mice were culled at the end of 4 weeks post-treatment or tumor volume had reached maximum volume which was 1000mm^3.

2.10. RNA-Sequencing Analysis

2.10.1. Data generation

RNA- sequencing data was obtained from out collaborator Professor John Mariadason for Olivier-Newton John Institute.

2.1.1. Differential Gene Expression Analysis

Using the RNA sequencing data, differential gene expression analysis was performed to between two groups of cell lines; intrinsically sensitive and resistant cell lines towards Cetuximab. Software XLSTAT was used to perform the analysis using Differential Expression tool. The method was adapted from XLSTAT tutorial website. Briefly, the tool allowed us to set the parameters for the analysis. One-way ANOVA was used as a statistical test and Benjamini-Hochberg as the post-hoc corrections with p-value of 0.05% for significance. Tukey's test was used as multiple pairwise comparison to compare the genes and cell lines. A 50% threshold was set to eliminate 50% of the genes that has low variability. The software generated a table that showed a list of the genes with their p-values.

2.11. Statistical Analysis

All statistical analyses were performed and generated using the program GraphPad Prism 6 (Prism 6.04, CA, USA). Figure 3.2, 3.3, 3.4, 3.5, 4.1, 4.2, 4.4, 4.5, 5.1, 5.2, 5.3, 5.4, 5.5, 5.8, 5.9, 5.10, and 5.11 were analyzed using 1-way ANOVA for overall statistical significance. Tukey's post-test was performed for comparisons between groups. Figure 3.6, 3.7, 3.8, 3.9, 3.13, 3.14, 4.8, 5.6, and 5.7 were analyzed using 2-way ANOVA for overall statistical significance. Bonferroni's post-test was performed for comparisons between groups. Figure 3.10, 3.12, 4.6, and 4.7 were analyzed using standard 2-tailed student t-test for statistical significance. P- value less than 0.05 was considered as significant and was indicated by the "*" symbol. * indicates $p<0.05$, ** indicates $p<0.01$, and *** indicates $p<0.001$.

CHAPTER 3:

Characterization of Cetuximab-resistant Colorectal Cancer Cell Lines

3. Chapter 3: Characterization of Cetuximab-resistant Colorectal Cancer Cell Lines

3.1. Introduction

Patient's response to both standard and targeted therapies is one of the most important parameters in cancer management and therefore is the focus of many laboratories over several decades. Each therapeutic agent displays varying efficacy even in patients from presumably the same cohort, where some patients respond well, and others do not. The success of these agents also differs according to the type of cancer being targeted. This effect could be due to tumor resistance where tumor cells contain pre-existing mediators of resistance or where cells adapt or acquire advantageous alterations to become refractory to treatment, they were originally sensitive to. However, the molecular drivers of Cetuximab resistance in wild-type KRAS patients are not completely known and therefore further research (such as that undertaken in this thesis) needs to be conducted to elucidate the cause and effect of the tumor resistance.

3.1.1. Establishing Resistant Cell Line Model

To elucidate the possible mechanisms of acquired Cetuximab-resistance in CRC we initially developed a resistance model of cancer treatment *in vitro*. There are two methods to create a resistant cell line model. The first was by altering a known gene in a pathway to induce the cells to use alternative pathways to survive [212]. This method uses genetic modification that involves cDNA/siRNA transfection into cancer cells which is widely used in cancer research. Using a genome wide shRNA screen, Eichhorn et al. 2008 discovered that PTEN was able to modulate Lapatinib sensitivity [213]. Another study transfected lentivirus expressing wild-type kinases such as Src, and EGFR or kinases with gatekeeper mutations into cells. They discovered that dasatinib was able to target Src and EGFR and T790M mutation caused the cells to be resistant to dasatinib as well [214]. The second method is to challenge the cells *in vivo or in vitro* with a drug of choice until a sub-population of the cells overcome the anti-tumor activity of this agent and able to proliferate in the presence of the chosen agent [212]. For example: Ciardiello et al. 2004 created resistant cell lines by injecting cells into mice and treating them with Bevacizumab. Surviving cells were collected and

grown in culture [215]. By creating a resistant cell line model, it would enable the researcher to study how the cells react to the administered drug.

3.1.2. STAT3 Signaling and Resistance

STAT3 signaling is one of the pathways that is involved in maintaining cell survival but is less studied as a mechanism of tumor resistance. STAT3 can be activated by several pathways and it mediates many cellular activities including proliferation, metastasis, cell differentiation and apoptosis. Multiple cancers have shown to have elevated STAT3 activity including colorectal and lung cancer [137, 141, 216]. Given the importance of STAT3 in mediating cellular functions, it is likely to play a role in cancer resistance against EGFR targeted therapy.

3.2. Relevance and Importance of Study

Cancer treatment has improved over the years with the used of targeted therapies as monotherapy or combination with chemotherapy to achieve better response for the patients. Nevertheless, patients who initially responded well to these treatments often develop resistance. The heterogeneity of cancer leads to the discovery of several resistance mechanisms towards these therapies. Mutation of KRAS is one of the common resistance mechanisms towards EGFR targeted therapies. It occurs in 40% of colorectal cancer patients leading to the use of Cetuximab only in patients who harbor tumor with wild-type KRAS expression. However, over 30% of wild-type KRAS patients still responded poorly to Cetuximab suggesting resistance through other mechanisms. Therefore, deeper understandings of those resistance mechanisms are needed in order to develop effective treatment and prolonging the patients' survival.

In term of resistance mechanisms, STAT3 signaling is studied far less than the RAS/MAPK or PI3K/AKT pathways. STAT3 signaling is important in regulating cellular function that involves in cell proliferation, migration, and survival. Aberrant STAT3 signaling could potentially induce cancer development and progression. Furthermore, elevated STAT3 signaling has been shown in multiple cancers including colorectal, lung and brain cancers. Elucidating the role of STAT3 signaling in cancer resistance to EGFR targeted therapy will allow for the improvement of the treatment regimens for current patients.

Clinical and laboratory-based studies report that STAT3 plays an important role in incurring resistance to EGFR targeted therapy. However, there are not many studies that have been

performed in colorectal cancer and lung cancer settings specifically in acquired resistance. The first aim of this study was to characterize colorectal and lung cancer cell lines with acquired resistance to anti-EGFR inhibitors. Furthermore, we will study the role of STAT3 signaling in mediating resistance to EGFR targeted therapies. Establishing STAT3 signaling as a critical resistance mechanism will provide proof-of-principle evidence for STAT3 specific therapeutics on their own or in combination with EGFR targeted therapies.

3.3. Results

3.3.1. Validation of Resistance in Acquired Resistance Cell Lines

Cell lines LIM1215, SW48 and CACO2 with acquired resistance to Cetuximab were generated as described in the method section (**Chapter 2**). **Figure 3.1** showed an overview of the development of resistant cell lines. Sensitive cell lines were treated with increasing concentrations of Cetuximab over a 6-month period until cells proliferated even in the presence of 20µg/ml of Cetuximab. The resistant sub-population of cells were denoted as LIM1215 C225, SW48 C225 and CACO2 C225.

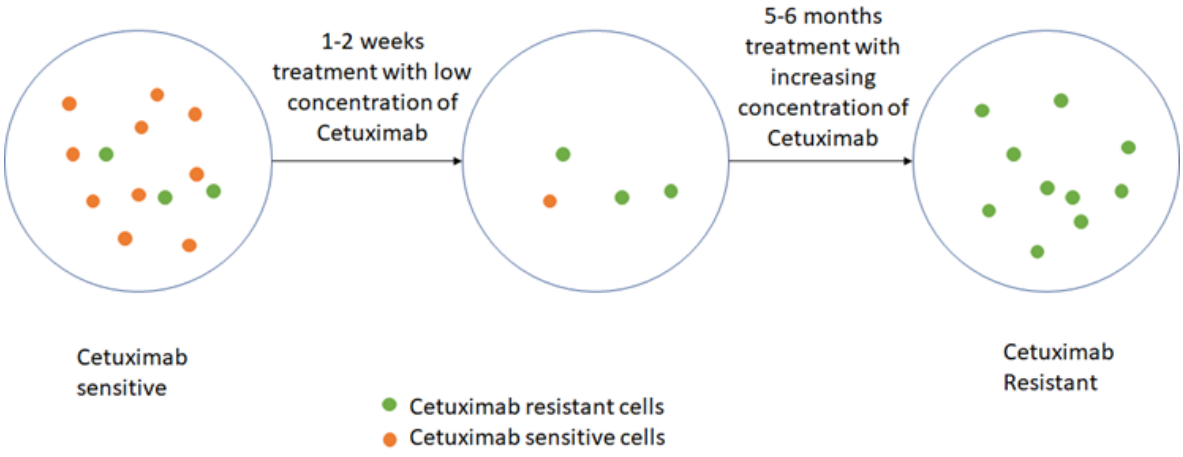

Figure 3.1: Development of resistant cell lines

Population of Cetuximab resistant cells were selected under the challenge of Cetuximab and cultured.

Cetuximab (20µg/ml) did not significantly inhibit LIM1215-C225, SW48-C225, and $CACO_2$-C225 all over a 7-day treatment period while Cetuximab significantly reduced the cell's viability of all parental cell lines at day 5 and 7 (**Figure 3.2**)

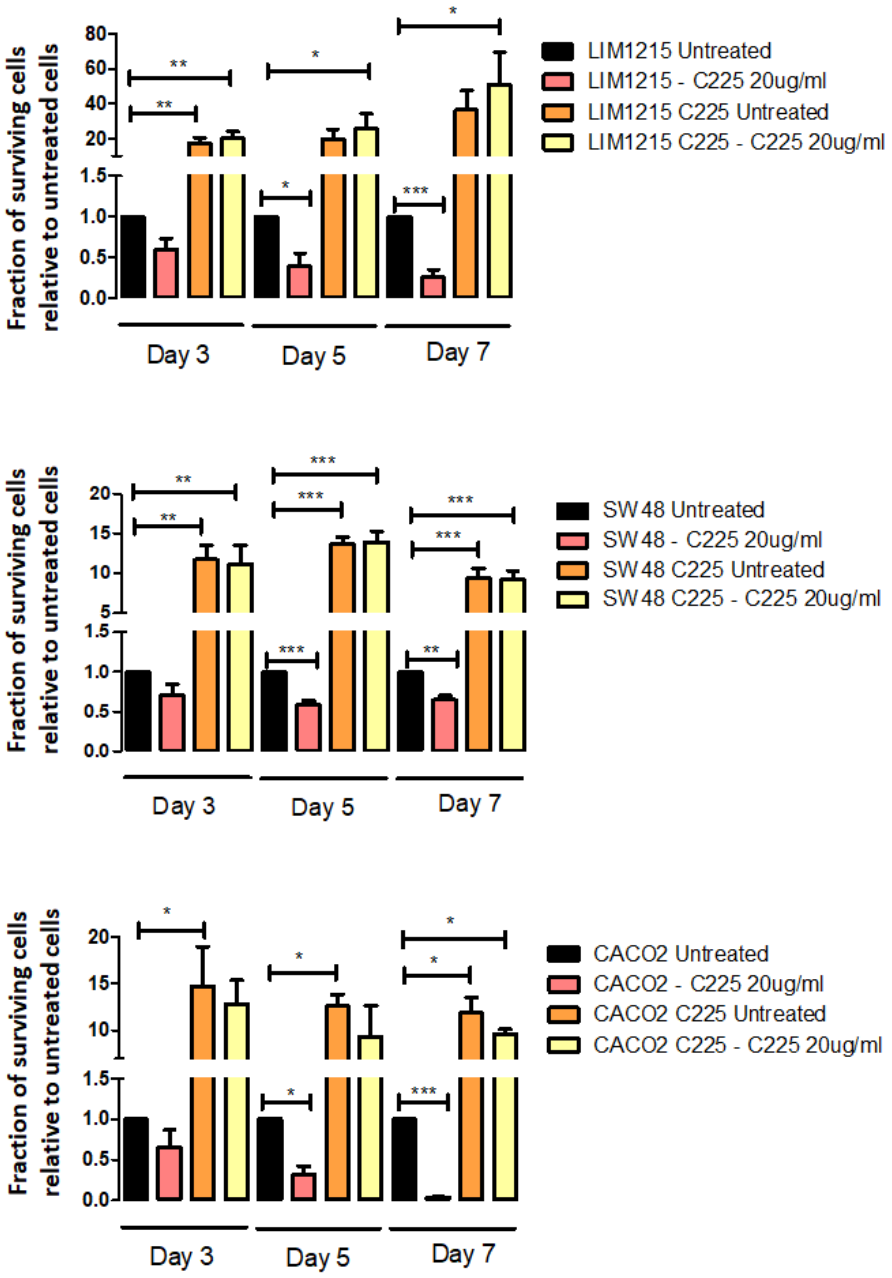

Figure 3.2: Cell viability assay of resistant cell lines.

*Cell lines LIM1215, LIM1215 C225, SW48, SW48 C225, CACO2, and CACO2 C225 were treated with Cetuximab (C225) (20ug/ml) for 7 days. Cell viability was measured using a luminometer at Day 3, Day 5, and Day 7. The data are presented as relative change of cell number to untreated sensitive cell line specifically at respective days. 1-way ANOVA was carried out for overall statistical significance. Post-hoc test, Tukey's test was performed for significance between untreated sensitive cell line group with other groups; * indicates p<0.05, ** indicates p<0.01, *** indicates p<0.001. Error bars are represented by SEM. n=3*

In addition to colorectal cancer cell lines, one NSCLC cell lines (H1650) was made resistant to Gefitinib, an RTK inhibitor through continuous treatment similar to that discussed in the previous section. The resistant cell line was denoted as H1650 G-R. Using cell viability assay, the cell lines were tested for their resistance towards Gefitinib. An increasing concentration of Gefitinib was subjected to the cell lines over the period of 3 days. The H1650 G-R cell line showed higher level of tolerance to Gefitinib compared to the parental cell line (**Figure 3.3**).

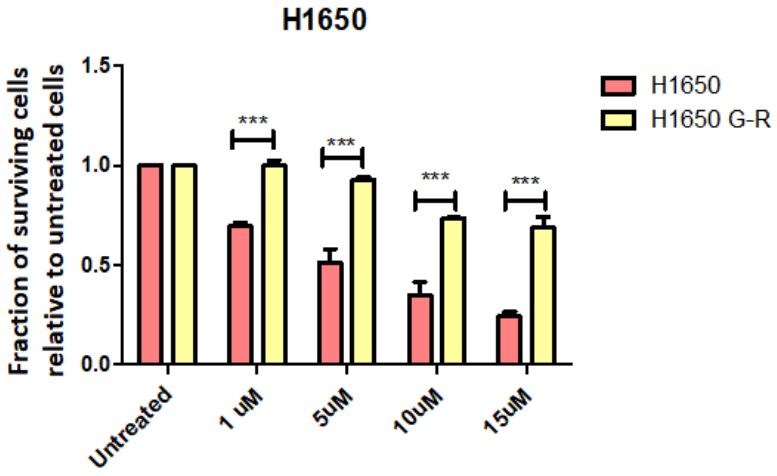

Figure 3.3: Cell viability assay of H1650 and H1650 GR

*Cell lines H1650 and H1650 G-R were treated with Gefitinib in increasing concentration for 3 days. Cell viability was measured using a luminometer at Day 3. The data are presented as relative change of cell number to untreated sensitive cell line. 1-way ANOVA was carried out for overall statistical significance. Post-hoc test, Tukey's test was performed for significance between untreated sensitive cell line group with other groups; *** indicates p<0.001. Error bars are represented by SEM. n=3*

3.3.2. Acquired Resistance Cell Lines Have Enhanced Growth

LIM1215-C225, SW48-C225, $CACO_2$-C225 and H1650-GR and their parental counterpart were assessed for their growth capability under normal growth condition (DMEM + 5% FCS) for a period of 7 days. Similar results were observed across all three resistant cell lines. The growth of the resistant cell lines peaked at day 5. At day 7, the number of viable cells has started to decrease but the data shown was not significant. The rate of growth for resistant cell lines were significantly higher than parental cell lines (**Figure 3.4 A(i-iii)**). After 3 days, the number of viable cells for resistant cell lines has grown 10 times more than the parental cell lines. A similar assay was conducted with the NSCLC resistant cell lines (**Figure 3.4B**). The growth of H1650 was higher than its resistant counterpart on Day 3 but started to decrease after Day 5. There was no significant difference in growth rate of between the H1650 and H1650 GR cell lines.

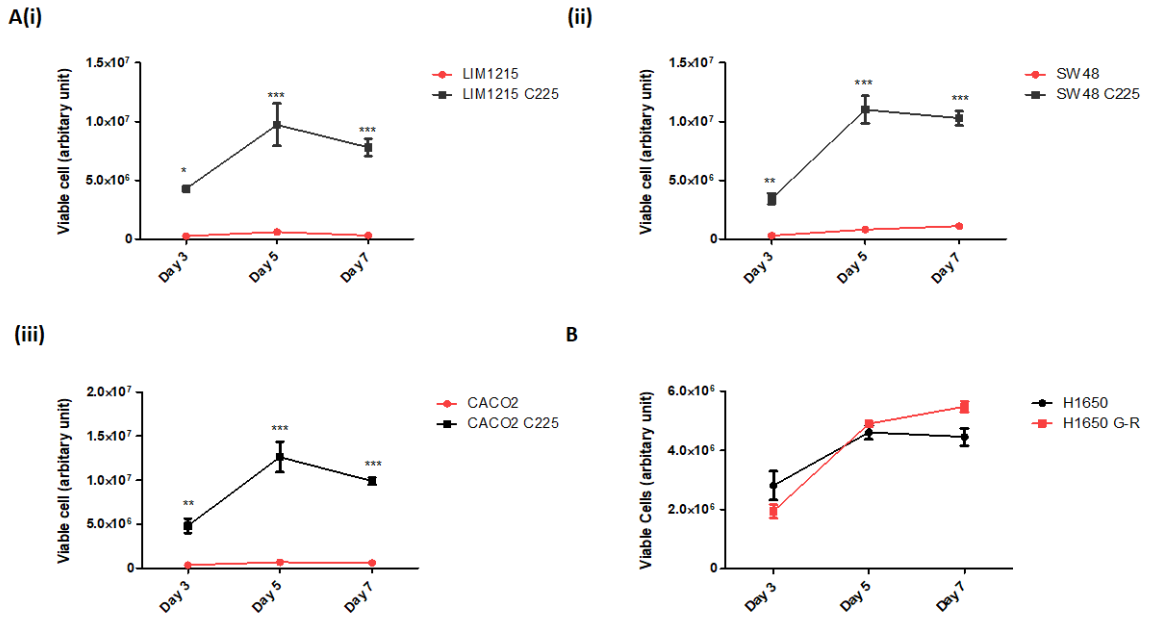

Figure 3.4: Cell viability assay

*(A(i-iii)) Cell lines LIM1215, LIM1215 C225, SW48, SW48 C225, CACO2, CACO2 C225, (B) H1650 and H1650 G-R were grown for 7 days. Cell viability was measured using a luminometer at Day 3, Day 5 and Day 7. The data are presented as the amount of viable cell for each cell lines. 1-way ANOVA was carried out for overall statistical significance. Post-hoc test, Tukey's test was performed for significance between untreated sensitive cell line group with other groups. * indicates p<0.05, ** indicates p<0.01, *** indicates p<0.001. Error bars are represented by SEM. n=3. All resistant cell lines showed higher growth rate compared to parental cell lines.*

3.3.3. Colony Formation Assay

To further characterized the cell lines, colony formation assay was performed to assess the cell lines ability to form colonies. Resistance cells showed very high capability in forming colonies after 7 days (**Figure 3.5A**). In contrast, the parental cells grew quite sparsely. The percentage of tissue culture well area covered by resistant cells were significantly higher than the parental cells (**Figure 3.5B**).

A

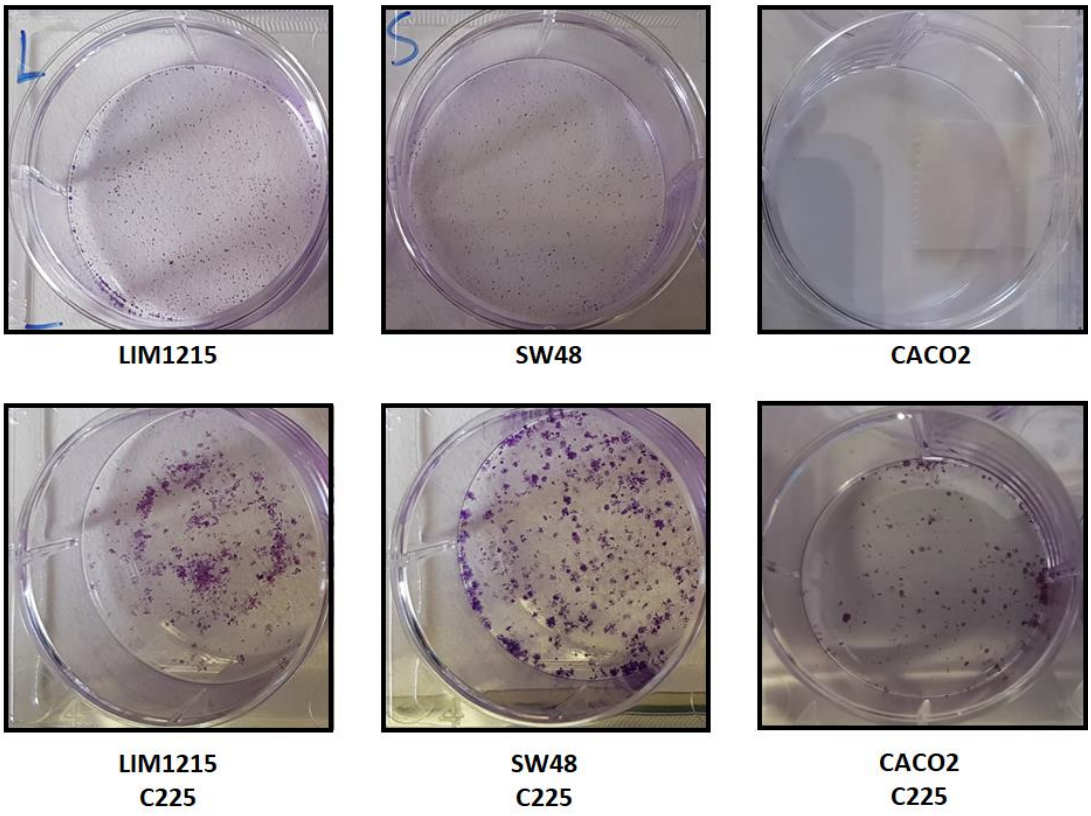
LIM1215
SW48
CACO2
LIM1215 C225
SW48 C225
CACO2 C225

B

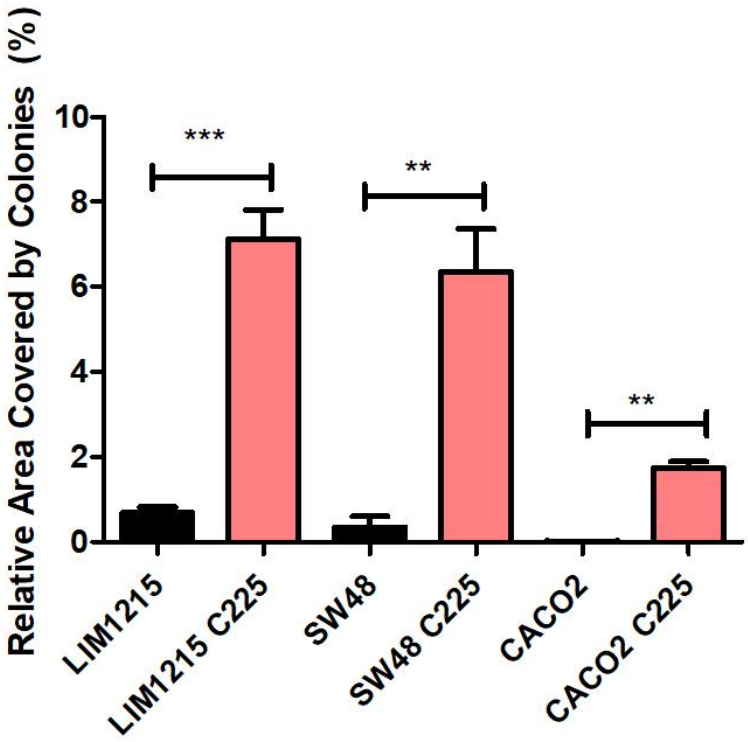
Relative Area Covered by Colonies (%)
10
8
6
4
2
0
***
**
**
LIM1215
LIM1215 C225
SW48
SW48 C225
CACO2
CACO2 C225

Figure 3.5: Colony formation assay of resistant cell lines.

*(A) LIM1215, LIM1215 C225, SW48, SW48 C225, CACO2, and CACO2 C225 were seeded at concentration of 1000 cells and grown for 7 days. Crystal violet staining was performed, and images were taken. (B) Analysis of colony efficiency was done using ImageJ. The data presented in form percentage of area covered by cells colony. 1-way ANOVA was carried out for overall statistical significance. Post-hoc test, Tukey's test was performed for significance parental and resistant cells; ** indicates p<0.01, *** indicates p<0.001. Error bars are represented by SEM. n=3*

3.3.4. Acquired Resistance Cell Lines Have Enhanced Cell Migration

Next, we investigated whether the resistant cell lines had differential migration potential compared to parental cell lines by cell scratch assay. The area of the wound was measured and compared between the parental and resistant cell lines. The result showed that all resistant cell has enhanced rate of cell migration (**Figure 3.6-3.9**). The wound had completely closed within 3 days of Cetuximab-resistant cells compared to parental cell lines which took longer. Unlike the parental cell lines which Cetuximab inhibited wound closure, the rate of wound closing for resistant cell lines when treated with Cetuximab was similar to untreated resistant cell lines. Similar results were observed when comparing parental cell H1650 with Gefitinib-resistant H1650 cells.

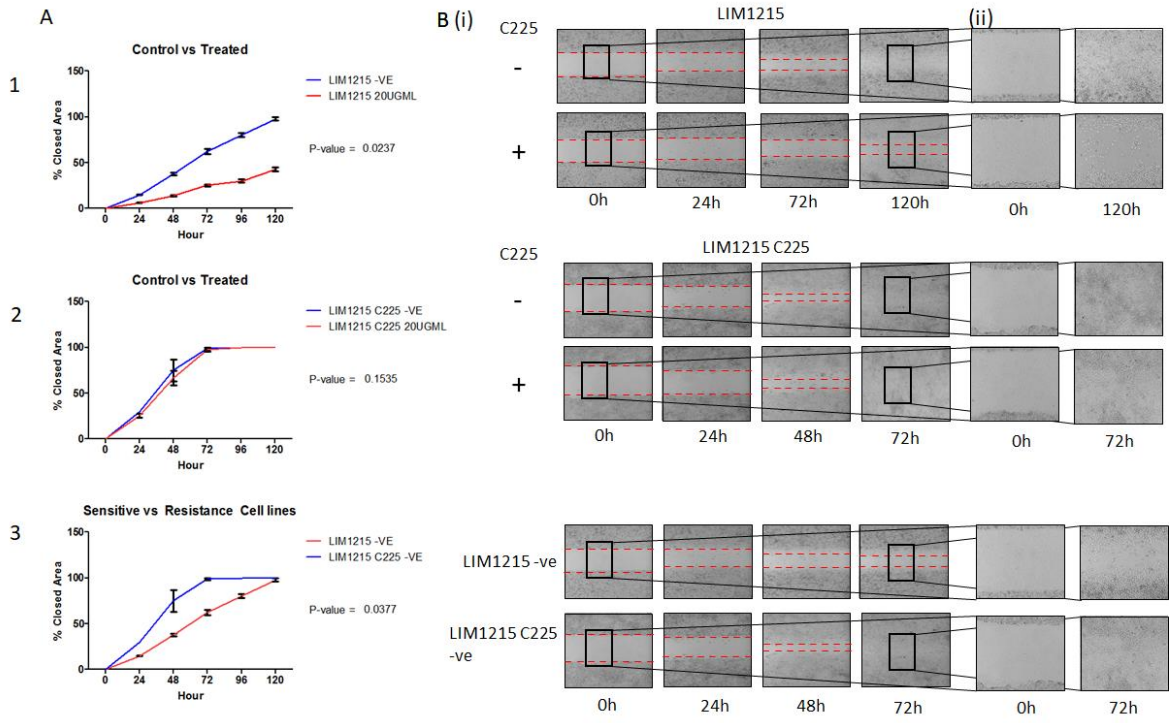

Figure 3.6: Cell scratch assay for LIM1215 and LIM1215 C225.

Cell lines LIM1215 and LIM1215 C225 were seeded and grown until 100% confluent before a scratch was made. The cell lines were treated with Cetuximab (20ug/ml) for 5 days. The area of scratch was measured every day. (A) Graphs representing the % of wound area closed over a period of five days between: 1) LIM1215 –ve vs LIM1215 20ug/ml, 2) LIM1215 C225 –ve vs LIM1215 C225 20ug/ml, 3) LIM1215 –ve vs LIM1215 C225 –ve. 2-way ANOVA was carried out for statistical significance; P-value < 0.05, n=3. Error bars represented SEM. (B)(i) The graphical representative of the area of wound closing from 0h to 72h. LIM1215 –ve vs LIM1215 20ug/ml showed graphical representative of the area of wound closing from 0h, 24h, 72h and 120h. (ii) The enlarged figure of the wound at 0h and 72h. (1) showed enlarged figure of the wound at 0h and 120h.

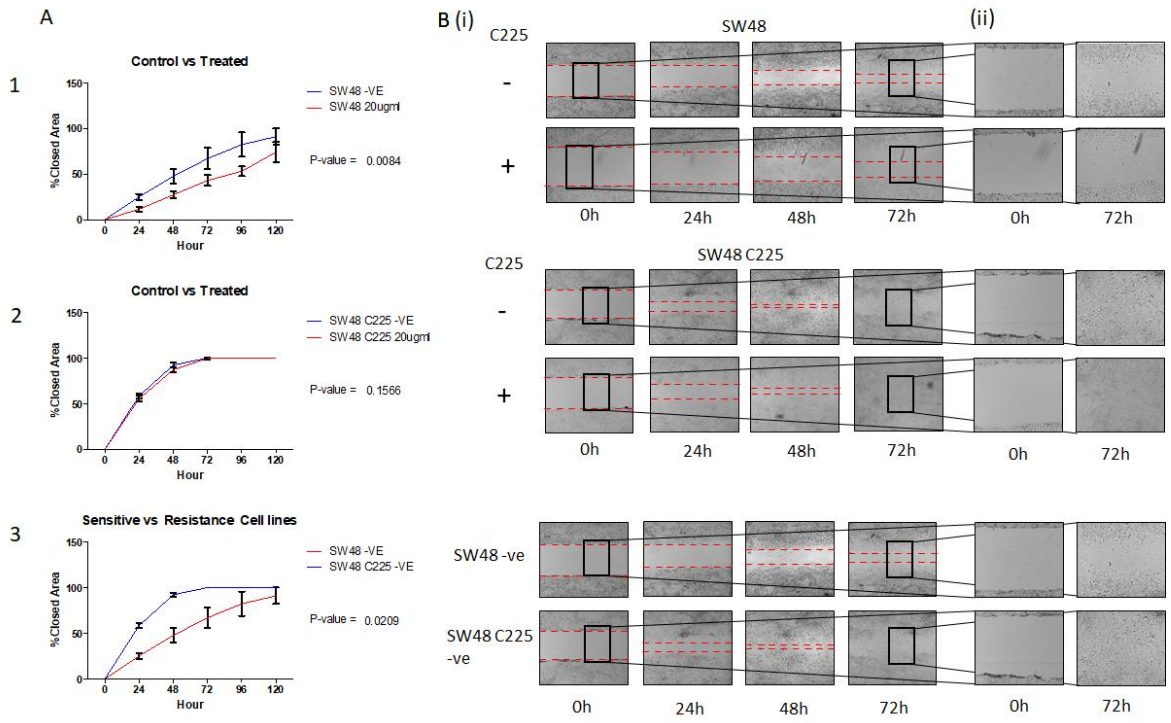

Figure 3.7: Cell scratch assay for SW48 and SW48 C225.

Cell lines SW48 and SW48 C225 were seeded and grown until 100% confluent before a scratch was made. The cell lines were treated with Cetuximab (20ug/ml) for 5 days. The area of scratch was measured every day. (A) Graphs representing the % of wound area closed over a period of five days between: 1) SW48 –ve vs SW48 20ug/ml, 2) SW48 C225 –ve vs SW48 C225 20ug/ml, 3) SW48 –ve vs SW48 C225 –ve. 2-way ANOVA was carried out for statistical significance; P-value < 0.05, N=3. Error bars represented SEM. (B)(i) The graphical representative of the area of wound closing from 0h to 72h. (ii) The enlarged figure of the wound at 0h and 72h.

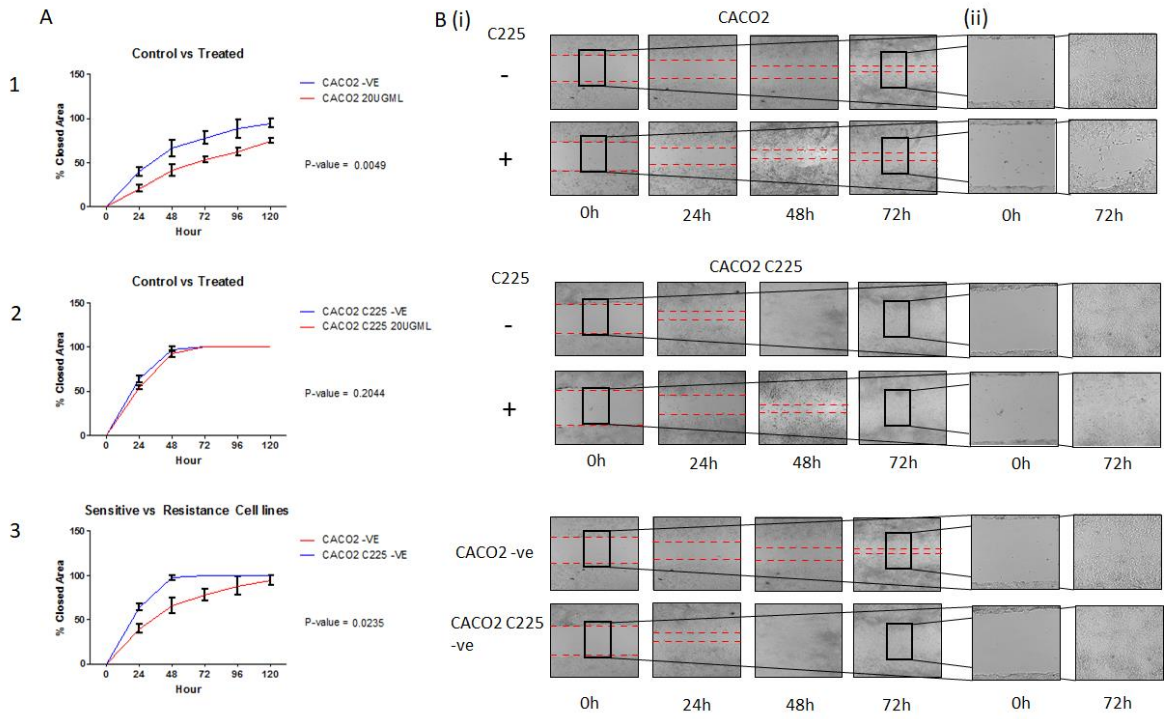

Figure 3.8: Cell scratch assay for CACO2 and CACO2 C225.

Cell lines CACO2 and CACO2 C225 were seeded and grown until 100% confluent before a scratch was made. The cell lines were treated with Cetuximab (20ug/ml) for 5 days. The area of scratch was measured every day. (A) Graphs representing the % of wound area closed over a period of five days between: 1) CACO2 –ve vs CACO2 20ug/ml, 2) CACO2 C225 –ve vs CACO2 C225 20ug/ml, 3) CACO2 –ve vs CACO2 C225 –ve. 2-way ANOVA was carried out for overall statistical significance; P-value < 0.05, N=3. Error bars represented SEM. (B)(i) The graphical representative of the area of wound closing from 0h to 72h. (ii) The enlarged figure of the wound at 0h and 72h.

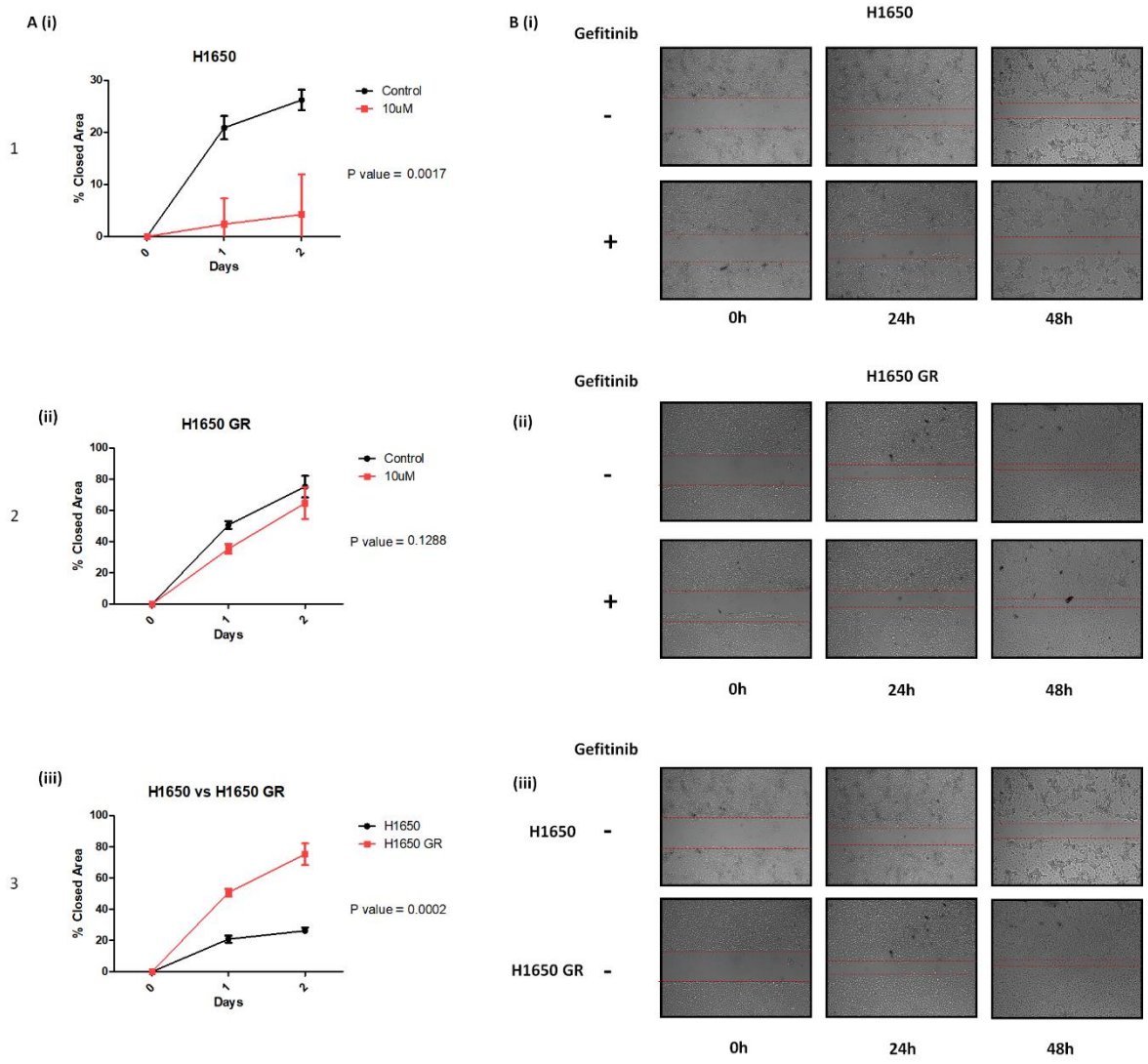

Figure 3.9: Cell scratch assay for H1650 and H1650 GR.

Cell lines H1650 and H1650 GR were seeded and grown until 100% confluent before a scratch was made. The cell lines were treated with Gefitinib (10uM) for 2 days. The area of scratch was measured every day. (A) Graphs representing the % of wound area closed over a period of 2 days between: 1) H1650 control vs H1650 Gefitinib, 2) H1650 GR control vs H1650 GR Gefitinib, 3) H1650 control vs H1650 GR control. 2-way ANOVA was carried out for overall statistical significance; P-value < 0.05. Error bars represented SEM. (B)(i-iii) The graphical representative of the area of wound closing from 0h to 48h. n=3.

3.3.5. Acquired Resistance Cell Lines Have Enhanced Growth *In vivo*

In vitro experiments have revealed that the resistant cell lines have much higher proliferative and migration capability. Next, we investigated the characteristic of these resistant cell lines *in vivo.* Parental and resistant cell lines were injected into the flank of the mice subcutaneously. The cells were allowed to grow into tumor until it reached the maximum size allowed. The tumors were measured every day before the mice were culled. **Figure 3.10** showed the growth curve of the resistant cell lines against the parental. Cell lines LIM1215 C225 and SW48 C225 showed higher growth rate compared to the parental. Furthermore, treatment of LIM1215 C225 and SW48 C225 with Cetuximab showed no visible reduction in tumor growth in resistant cells. These results corresponded with our *in vitro* assay where resistant cell lines were more proliferative and resistant to Cetuximab.

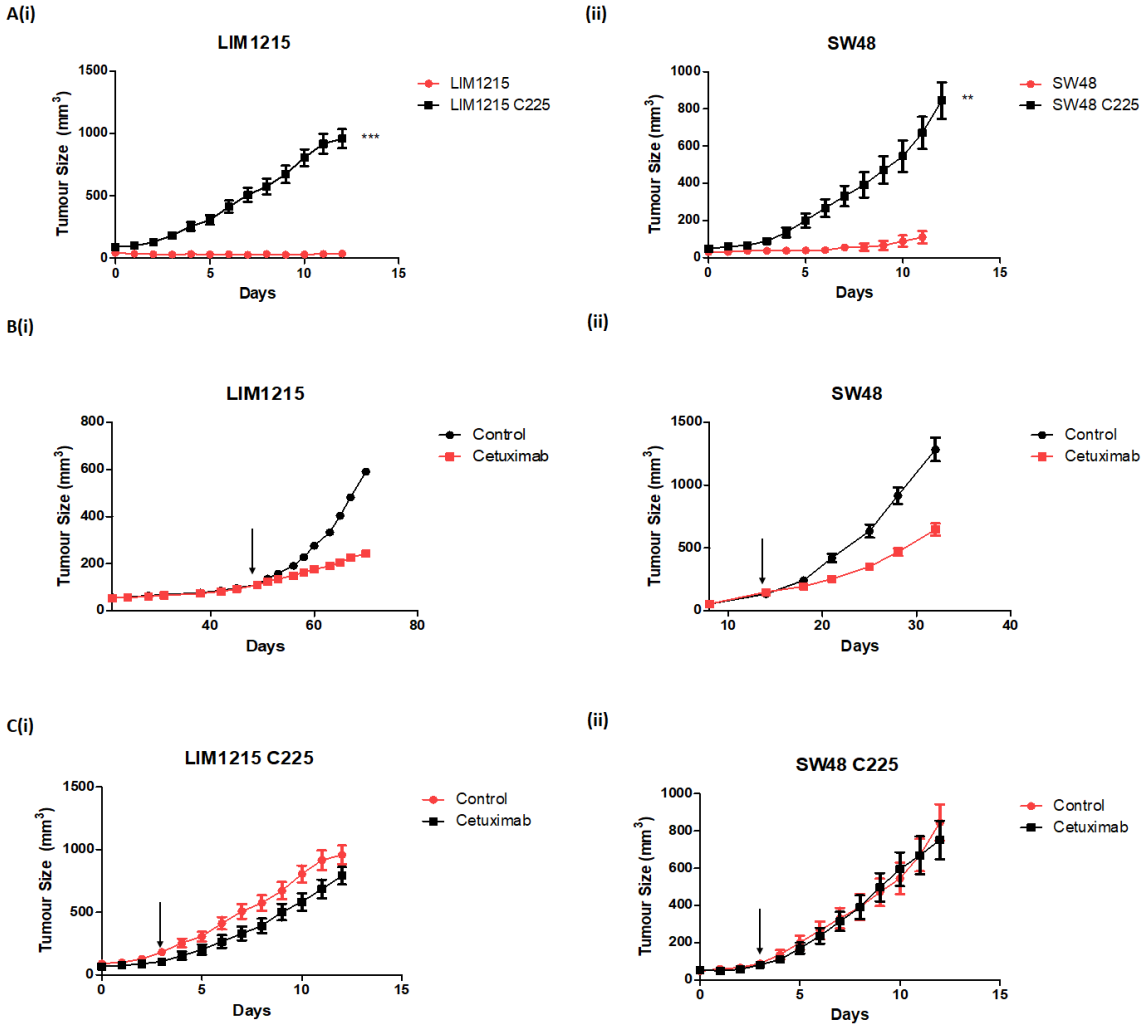

Figure 3.10: Subcutaneous xenograft mouse model of resistant cells

*Cell lines LIM1215 and LIM1215 C225 were inoculated into mice and grown until it reached approximately 1000mm^3. The mice were either treated with PBS as control or Cetuximab. The graph showed the tumor size from the first day the tumor was measured. (A(i-ii)) Comparison of tumor size between the parental (LIM1215 and SW48) and resistant (LIM1215 C225 and SW48 C225) cells. (B(i-ii)) Comparison of tumor size between control and Cetuximab treatment for LIM1215 and SW48 parental cells. (C(i-ii)) Comparison of tumor size between control untreated and Cetuximab treatment for LIM1215 C225 and SW48 C225. Arrows indicated the start of treatment; B(i) Day 49, B(ii) Day 14, C(i) Day 3, and C(ii) Day 3. Two-tailed student t-test was carried out for statistical significance. ** indicates p<0.01, *** indicates p<0.001. Error bars represented SEM. n=10*

3.3.6. Acquired Resistance Cell Lines Have Elevated STAT3 Activity

Several labs including ours have implicated that STAT3 signaling mediates resistance to EGFR-targeted therapy. Using both sensitive and resistant cell lines, the level of activated STAT3 was measured through Western Blot. At basal level, all resistant cell lines showed elevated STAT3 activity (**Figure 3.11**).

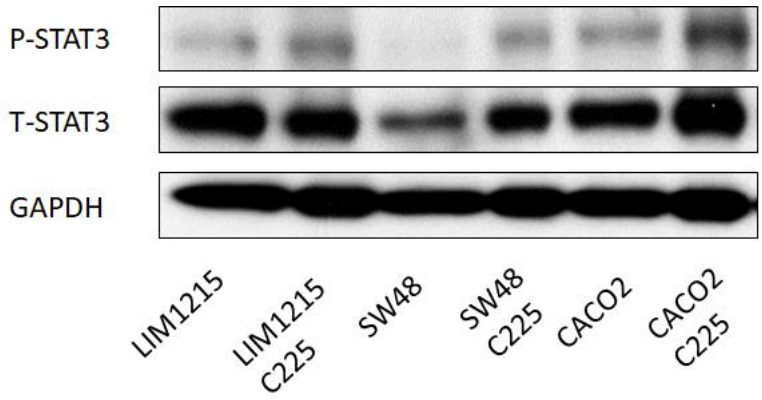

Figure 3.11: Western blot assay of STAT3.

Cell lines LIM1215, LIM1215 C225, SW48, SW48 C225, CACO2, and CACO2 C225 were probed with antibody P-STAT3, T-STAT3 and GAPDH as a control to check the basal level. The proteins were visualized using detection reagent and developed onto film. Cetuximab-resistant cell lines (C225) showed an increase in P-STAT3 level.

To further validate the data, quantitative PCR was performed. The gene expression of SOCS3 which is directly regulated by STAT3 was measured. The result showed significant increase of SOCS3 expression in LIM1215 C225 cell lines which was expected as elevated STAT3 activity would increase SOCS3 expression. The results for the other 2 cell lines, however, were not significant. The expression of IL-6, IL-6R, IL-11 and IL-11R were also measured as they played a role in activating STAT3 signaling. **Figure 3.12** showed the expression of IL-6R was up-regulated in LIM1215 C225 but the expressions of IL-6 and IL-6R for other cell lines were not significant. Similar results were observed in IL-11 and its receptor (**Figure 3.12**). IL-11 was shown to be the driver of tumorigenesis

more than IL-6 [75]. However, the downregulation of these receptors and ligands could suggest that STAT3 is activated through another pathway.

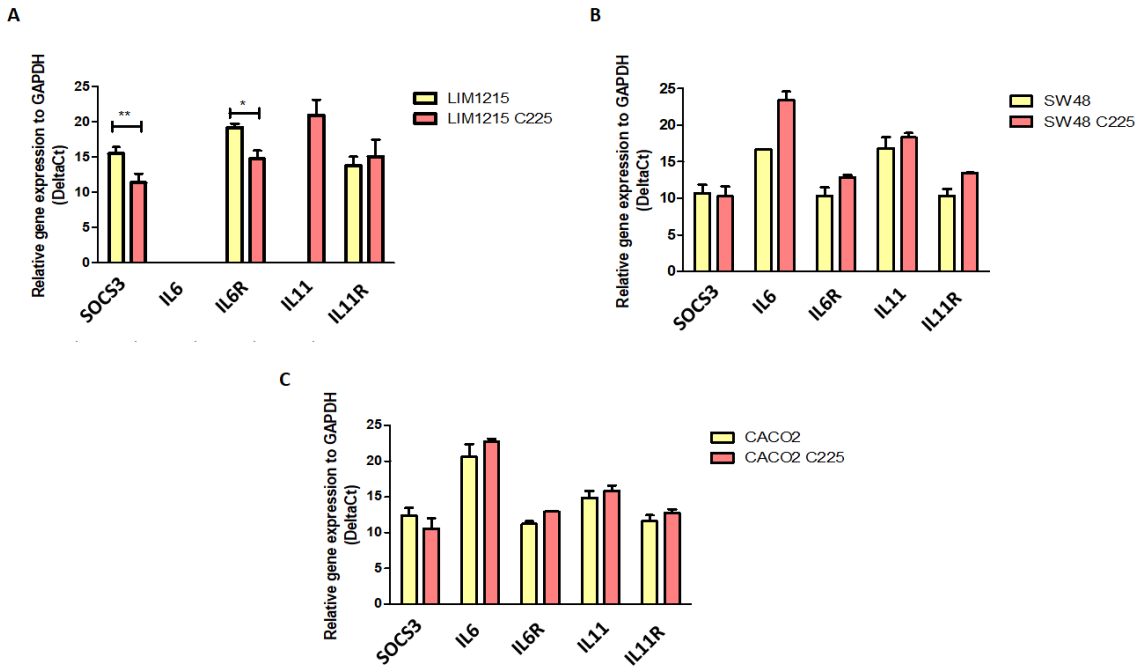

Figure 3.12: Quantitative PCR of STAT3-related genes.

*The expression of five genes (SOCS3, IL-6, IL-6R, IL-11, IL-11R) were analyzed using quantitative PCR in cell lines LIM1215, LIM1215 C225, SW48, SW48 C225, CACO2 and CACO2 C225. The graphs showed relative gene expression to housekeeping gene GAPDH represented by ΔCt. Lower ΔCt represented high expression and high ΔCt represented low expression. Empty graphs represented very low expression. Two-tailed student t-test was carried out for statistical significance. * indicates p<0.05, ** indicates p<0.01. Error bars represented SEM. LIM1215 C225, SW48 C225, and CACO2 C225 n=2*

3.3.7. STAT3 as a Resistance Biomarker

Due to enhanced growth capability of the resistant cells that can be attributed to elevated STAT3 activity, the expression of STAT3 was knocked down by siRNA to study its effect. All resistant cell lines were transfected with siRNA for 48h and treated with Cetuximab for 3 days. The cell lines were then assessed with Cell viability assay. All cell lines showed no reduction in viability of cells despite the successful STAT3 knockdown (**Figure 3.13**). This result suggested that STAT3 might not play a direct role in Cetuximab resistant in all three cell lines. Two other markers from important signaling pathway; AKT and Erk1/2 were also knocked down to study its effect. Like STAT3, there were no significant reduction in viability although it could be attributed to the unsuccessful knockdown (**Figure 3.14**).

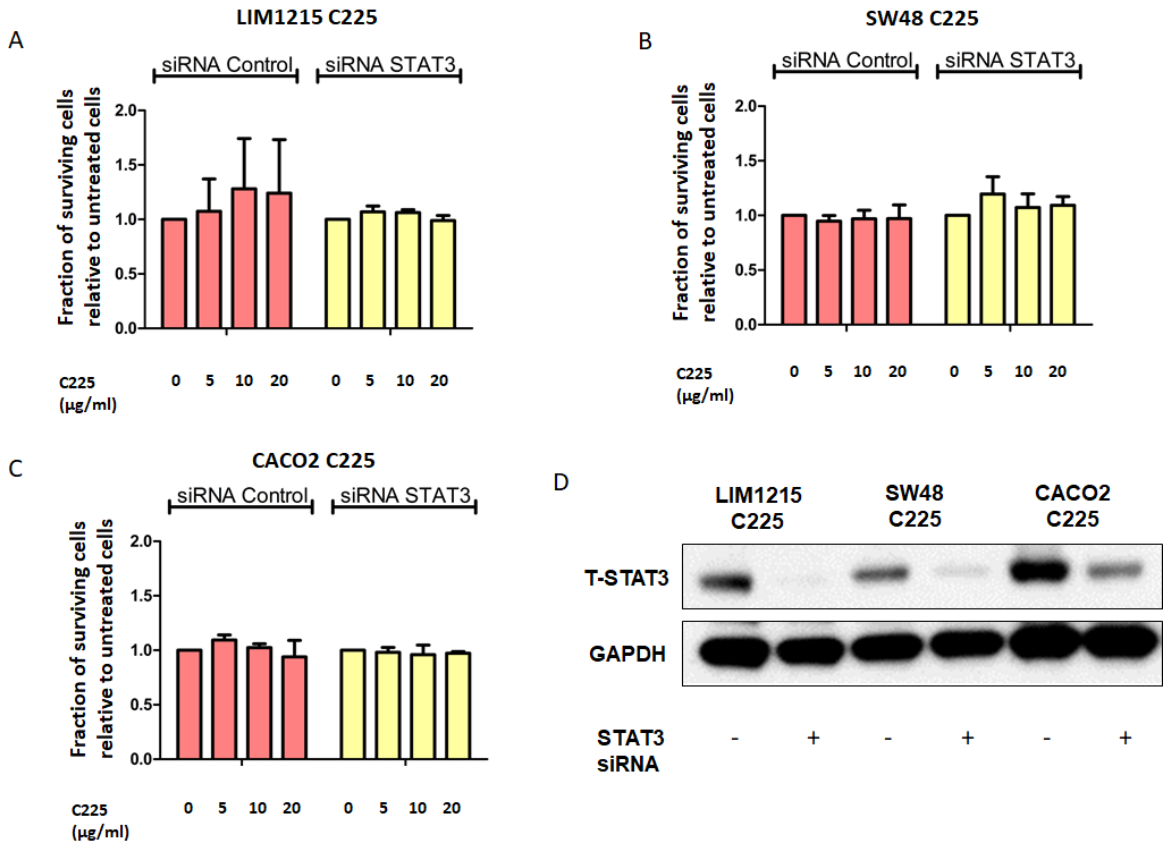

Figure 3.13: STAT3 siRNA knockdown in resistant cell lines.

Cell lines LIM1215 C225, SW48 C225 and CACO2 C225 were seeded and incubated with scramble siRNA (20nM) as control and STAT3 siRNA (20nM) for 48 hours. The cell lines were then treated with Cetuximab (5µg/ml, 10µg/ml and 20µg/ml) for 3 days. (A, B, C) Graphs representing the relative change of cell number to untreated cell lines. 2-way ANOVA was carried out for overall statistical significance. Post-hoc test, Bonferroni's test was performed for significance between untreated cell line group with other groups. Error bars represented SEM. P-value < 0.05 indicates significance. (D) Western blot analysis of the cell lines after 48 hours incubation to check for the knockdown efficiency. n=3

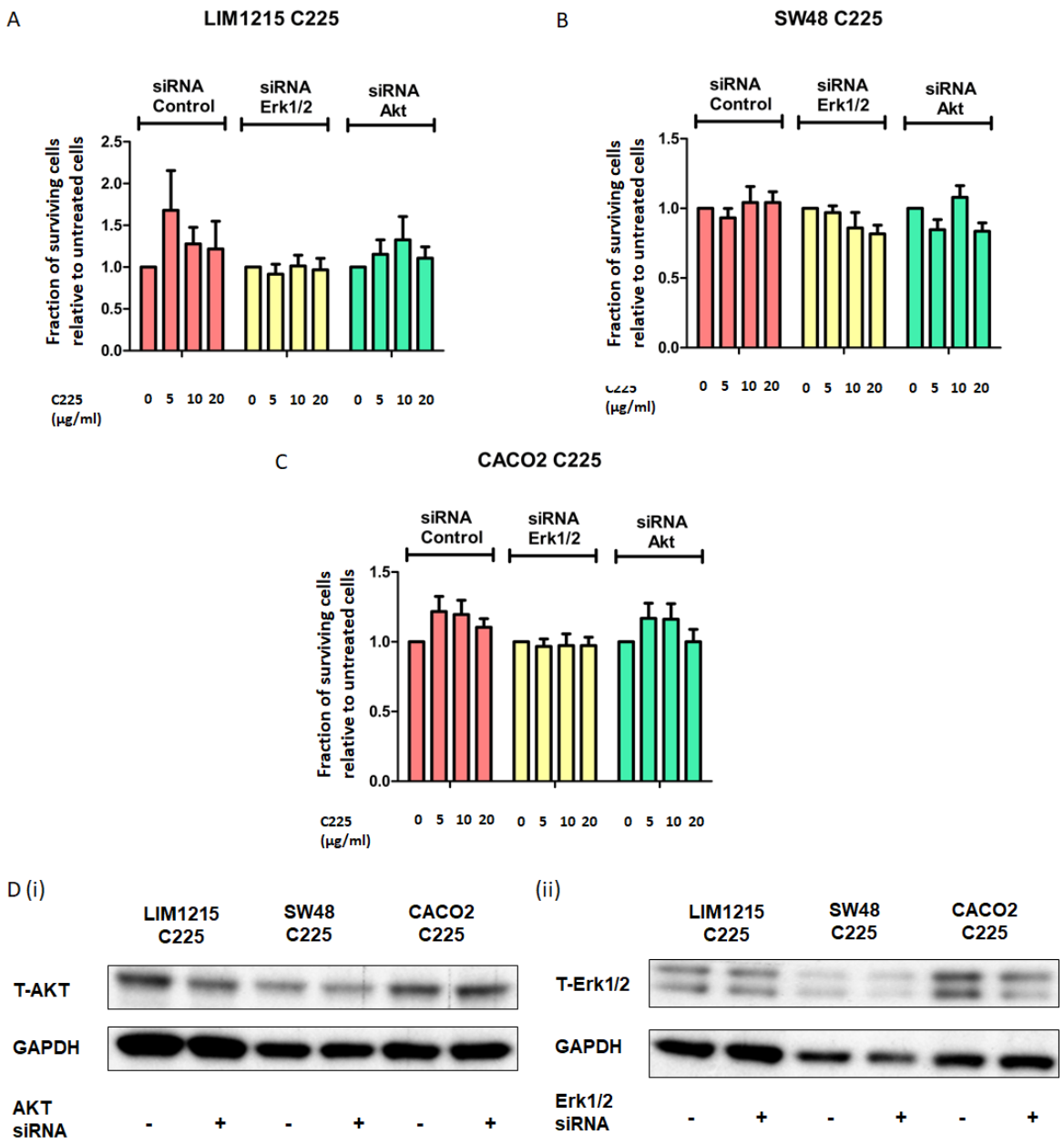

Figure 3.14: ERK and AKT siRNA knockdown in resistant cell lines.

Cell lines LIM1215 C225, SW48 C225 and CACO2 C225 were seeded and incubated with scramble siRNA (20nM) as control, ERK and AKT siRNA (20nM) for 48 hours. The cell lines were then treated with Cetuximab (5µg/ml, 10µg/ml and 20µg/ml) for 3 days. (A, B, C) Graphs representing the relative change of cell number to untreated cell lines. 2-way ANOVA was carried out for overall statistical significance. Post-hoc test, Bonferroni's test was performed for significance between untreated cell line group with other groups. Error bars represented SEM. P-value < 0.05 indicates significance. (D) Western blot analysis of the cell lines after 48 hours incubation to check for the knockdown efficiency. n=3

3.3.8. Proteomic analysis

As part of the characterization of our resistant cell lines, we also performed proteomic analysis on one of our resistant cell lines. The gene expression of SW48 and SW48 C225 were analyzed using bioinformatic tool Ingenuity pathway analysis (IPA). This tool uses build-in dataset that is available to perform gene expression analysis. To investigate the differences in gene expression profile, both SW48 and SW48 C225 were analyzed at their basal state. A total of 2908 proteins were identified in both cell lines. We observed 288 proteins which were significantly difference in their expression. 149 proteins were downregulated while 139 proteins were upregulated. **Figure 3.15** showed the heatmap of the genomic profile which displayed differences between SW48 (control) and SW48 C225 (C225). The full list of the differentially expressed proteins is listed in **Supplementary Table 3.1**.

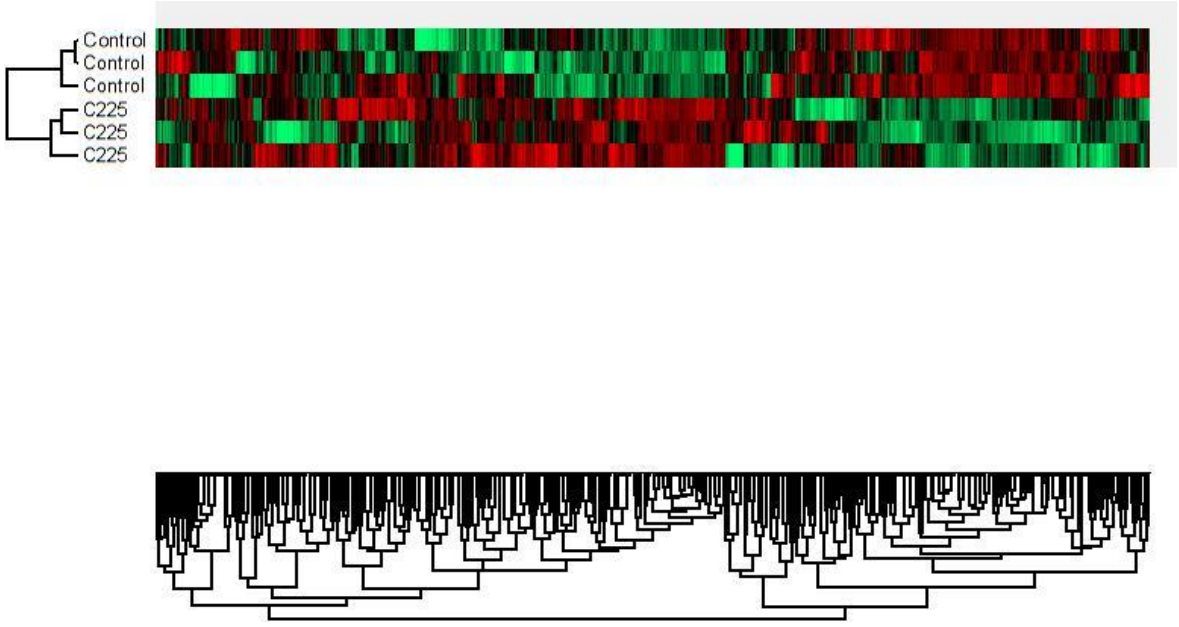

Figure 3.15: Heatmap and hierarchical clustering of proteins.

The expression levels of the genes were indicated by the color on the heatmap. Red color indicates increase expression while green color indicates decreased expression as compared to control.

To further this analysis, we obtained the data which categorized the differentially expressed proteins into related canonical pathways. Five top pathways were recognized having p-values lower than 10^{-6}. **Table 3.1** summarizes the top canonical pathways. Sirtuin signaling pathway has the lowest p-value at $1.5x10^{-11}$ with 22 overlapping proteins out of 291 proteins. This signaling pathway plays a role in several metabolic processes including apoptosis, mitochondrial biosynthesis, lipid metabolism, fatty acid oxidation and aging. The highest p-value at $3.6x10^{-6}$ is the hypoxia signaling in the cardiovascular system. It also has the second highest ratio of overlapping protein at 10.8% (8/74 proteins).

Table 3.1: Top canonical pathways.

Pathways	p-value	Overlap
Sirtuin Signaling Pathway	$1.5x10^{-11}$	7.6% 22/291
Remodeling of Epithelial Adherens Juntions	$1.5x10^{-07}$	13.2% 9/88
Huntington's Disease Signaling	$1.6x10^{-06}$	5.9% 14/237
Epithelial Adherens Junction Signaling	$3.14x10^{-06}$	7.2% 11/152
Hypoxia Signaling in the Cardiovascular System	$3.6x10^{-06}$	10.8% 8/74

Among the differentially expressed proteins, the analysis also provides the top upstream regulators between the two cell lines. **Table 3.2** showed the top five regulators that is differentially expressed. *TP53* has the lowest p-value at $5.9x10^{-28}$ followed by MAPT ($5.6x10^{-19}$), NFE2L2 ($2.26x10^{-16}$). 1,2-dithiol-3-thione ($3.02x10^{-16}$) and sirolimus ($4.3x10^{-15}$). *TP53* encodes p53 protein which act as a tumor suppressor while NFE2l2 involves in expression of leucine zipper protein that regulates expression of antioxidant. Furthermore, these two proteins were predicted to be inhibited in the resistant cell line. Given the aggressive growth of the resistant cell line, it is understandable that p53 is inhibited. No predicted activation state of other regulators was stated in the analysis.

Table 3.2: Top Upstream Regulators

Regulators	p-value	Predicted activation
TP53	$5.9x10^{-28}$	Inhibited
MAPT	$5.6x10^{-19}$	
NFE2L2	$2.26x10^{-16}$	Inhibited
1,2-dithiol-3-thione	$3.02x10^{-16}$	
sirolimus	$4.3x10^{-15}$	

In addition to the canonical pathways, the differentially expressed proteins are also categorized into related biological functions. Similar to the pathways, top five biological functions are listed in **Table 3.3**. Cell death and survival functions is the most significant cellular process that is related to the resistant cells. This is consistent with the results obtained for upstream regulator which *TP53* is the most significantly expressed gene with other 153 molecules. Furthermore, nucleic acid metabolism, protein synthesis and cellular development seems to be affected in the analysis. These three cellular functions may play an important role in the resistant cells.

Table 3.3: Top Biological Functions

Functions	p-value range	# Molecules
Cell Death and Survival	$2.07x10^{-09}$ - $8.57x10^{-24}$	154
Nucleic Acid Metabolism	$1.49x10^{-09}$ - $1.73x10^{-16}$	40
Small Molecule Biochemistry	$1.49x10^{-09}$ - $1.73x10^{-16}$	37
Protein Synthesis	$8.67x10^{-09}$ - $9.88x10^{-16}$	66
Cellular Development	$2.13x10^{-09}$ - $3.65x10^{-14}$	92

Consistent with the biological functions, the analysis revealed toxicity list related to the differentially expressed proteins. Renal Necrosis/Cell Death has the lowest p-value at $3.3x10^{-06}$ with 3.8% overlapping proteins (**Table 3.4**). The alteration in cell cycle specifically at G2/M DNA damage checkpoint also consistent with the affected cellular development functions. Furthermore, oxidative stress and oxidative stress response could be attributed to the protein NFE2L2.

Table 3.4: Top Toxicity List

Toxicity	p-value	Overlap
Renal Necrosis/Cell Death	$3.32x10^{-06}$	3.8% 22/577
Oxidative Stress	$6.37x10^{-06}$	12.3% 7/57
NRF2-mediated Oxidative Stress Response	$9.49x10^{-06}$	5.4% 13/239
Hypoxia-inducible Factor Signaling	$2.52x10^{-05}$	10.0% 7/70
Cell Cycle: G2/M DNA Damage Checkpoint Regulation	$4.27x10^{-05}$	11.5% 6/52

Other than the top canonical pathways and biological functions, gene networks were also incorporated into the analysis by associating the differentially expressed proteins with related disease and cellular functions. The top networks have a score of 62, 43, 41, 36 and 36 with higher score indicates more differentially expressed protein associated with that particular network (**Table 3.5**). In these networks, similar cellular function is observed to be involved such as Small Molecule Biochemistry. Other metabolic processes including amino acid, carbohydrate, vitamin, and mineral metabolisms were also determined in most of the networks. Protein synthesis as well as RNA damage and repair were also associated with the differentially expressed genes.

Table 3.5: Associated Network Functions

Network Functions	Score
Carbohydrate Metabolism, Small Molecule Biochemistry, Infectious Diseases	62
Amino Acid Metabolism, Small Molecule Biochemistry, Vitamin and Mineral Metabolism	43
Free Radical Scavenging, Small Molecule Biochemistry, Cellular Function and Maintenance	41
Amino Acid Metabolism, Small Molecule Biochemistry, Cancer	36
Protein Synthesis, RNA Damage and Repair, Hematological System Development and Function	36

3.4. Discussion

The primary care of a colorectal cancer patients involved surgery and chemotherapy. Often the treatment regiments are supplemented with targeted therapy agent such as Cetuximab. Despite the improvement in patient's prognosis, Cetuximab is only effective in some patients who has wild-type KRAS. Mutated KRAS protein caused important signaling pathway that govern multiple biological processes such proliferation and growth to be constitutively active. However, it is difficult to predict whether a patient with wild-type KRAS will respond to Cetuximab suggesting an internal resistance mechanism other than KRAS. This chapter focused on the production of Cetuximab-resistant cells and analyzing its characteristic when compared to Cetuximab-sensitive cells. We also explored a possible resistance mechanism driven by STAT3 activity in this set of cells.

The development of resistance cell lines provided a model of cancer that can be easily studied before extending to a model closer to humans such as mice. Parental cells were developed to become resistance to Cetuximab through selection of resistance population [217, 218]. This method was performed to generate cell lines that could mimic the Cetuximab-resistant population in wild-type KRAS patients. Then we chose cell lines that express wild-type KRAS. By isolating these resistant sub-population of cells, we would be able to culture these cells as a model of Cetuximab resistance.

Following the generation of the resistant cell lines, several assays were performed to investigate their characteristics. All resistant cell lines showed enhanced growth rate either in the presence or absence of Cetuximab. Cell viability and colony formation assays that was performed demonstrated significantly greater proliferation over 7 days. These results corroborate with our hypothesis that resistant cells have enhanced proliferative activity. The rate of growth was surprising as it was multiple times higher than the parental cancer cells. Other studies mainly focused on the respond of the cell line to Cetuximab rather than the growth rate of the resistant cells. Kjaer et al. 2016 and Antoni et al. 2015 showed the same level of resistance in their Cetuximab resistant cell lines as compared to our results [218, 219]. Furthermore, enhanced proliferative effect of the resistant cell lines translated well in the mice model. Cells that grow *in vitro* might not exhibit the same effect *in vivo* [220]. All resistant cell lines demonstrated significantly higher growth rate than the parental line (**Figure 3.9**). Napolitano et al. 2015 showed similar observation with their Cetuximab resistant cells [221]. The *in vivo* growth rate however was not as fast our cell lines. 9

days after treatment, our resistant cells reached 1000mm^3 while they need at least two weeks. Another study also observed similar observation with faster tumor growth in 4 weeks compared to control cells. Increased rate of tumor growth signifies the enhanced aggressiveness of resistant cells in patients. The results are reflected in patients where cancer that is resistant to treatment always has poorer prognosis [222]. Furthermore, based on the proteomic analysis performed on SW48 and SW48 C225, several genes involve in proliferation were differentially expressed (**Supplementary Table 3.1**). EGF receptor was downregulated in SW48 C225 cells which opposed the enhanced proliferation effect that the cells exhibit. We can speculate that the downstream signaling pathway of EGFR is activated through other pathways such as NFKB and HER2 signaling [223-225]. Our analysis also showed upregulation of *NFKB* gene in the resistant cell which make our hypothesis feasible. Moreover, the low level of EGF receptor would also explain the lack of response of Cetuximab on the resistant cell line.

One of the aspects of cancer is that their capability to metastasize to other organs. Besides enhanced proliferative activity, resistant cells also showed increase migratory effect as compared to parental cells. Under the challenge of Cetuximab, the scratch managed to close within 3 days of treatment (**Figure 3.6-3.8**). The wound closing speed indicates high potential for metastatic progression for the resistant cells. Our results also corroborate with other studies that looked at Cetuximab resistant cell lines. Although the cell lines used were different, they found that resistant cell line have stronger migratory capability [226]. However, migration assay only shows cells capability to migrate not invade. The cells need to be able to move and invade through extracellular matrix in order to metastasize (epithelial-mesenchymal transition (EMT)) [227]. One of the biomarkers for EMT is Vimentin which has been shown to play a role in mediating this process [228]. Overexpression of Vimentin was found in many cancers as mark of poor prognosis [229-231]. In our proteomic analysis, Vimentin is upregulated which suggest invasive characteristic in our resistant cells. Furthermore, Serpinb5 that has been associated with anti-metastatic activity [232], is downregulated which further supports the potential invasive properties. However, more assay needs to be done to validate this hypothesis. Assay such as invasion assay could be performed to further confirm the cells increased metastatic ability.

Tumor cells that become resistant to a certain drug and treatments because they have an abnormal change to signaling pathways that govern cells survival. Resistance to Cetuximab in CRC patients have often been related to *KRAS* mutations. Now that KRAS has been used as a clinical

marker of Cetuximab resistance, patient's outcome has improved. However, many patients who do not responded to Cetuximab despite having wild-type KRAS clearly indicate that other pathways are affected ensuring the cell's survival and resistance. Our focus revolved around the JAK/STAT3 signaling pathway. The JAK/STAT3 pathway has been associated with resistance to EGFR-treatment, either primary or acquired resistance. STAT3 activity was observed to be elevated in all resistant cells compared to the parental. These results correspond with multiple studies where higher STAT3 level/activity was observed [140, 141, 216]. Furthermore, our proteomic analysis also showed upregulation in STAT3 in resistant cell line. Enhanced level of STAT3 activity increased the activation of the signaling pathway thus elevating the cell's survival capability. Elevated level of SOCS3 also further validate our results as SOCS3 is involved in STAT3 negative feedback mechanism. SOCS3 overexpression was observed to be in line with STAT3 expression [233]. Although the result was only significant in one of the cell lines (LIM1215-C225), the trend was present in the other two cell lines ($CACO_2$-C225 and SW48-C225). The difference of SOCS3 expression between the cell lines might be attributed to the difference in the level of STAT3 activation [234]. Another study however showed the opposite where SOCS3 expression is lower when STAT3 expression is higher in tumor sections [235]. Both findings are true in a sense because while the level of SOCS3 increased with STAT3 expression, we did not analyze the differences between the expression of SOCS3 and STAT3 themselves.

STAT3 could be activated through several different pathways including IL-6, Pi3K/AKT, and Src signaling pathways. Activation of STAT3 through IL-6 signaling pathway has been shown in several studies and have been linked with resistance to treatment. Increase expression of the IL-6 and its receptor were shown to elevate the expression of STAT3 [216]. Our results showed no differences in the expression of IL-6/IL-6 receptor between parental and resistant cells (Figure 3.10). Previously shown higher phosphorylation of STAT3 does not seem to correlate with IL-6 expression. This implies that STAT3 activation might not be through the IL-6 signaling pathway. A much more recent studies looked at IL-11 signaling pathway and its role in STAT3 activation. In colorectal cancer, IL-11 has been shown to play a more significant role in driving tumorigenesis compared to IL-6. Our studies however showed a similar observation to IL-6 suggesting a similar role in resistance. Phosphorylation of the IL-6 and IL-11 receptors would activate the pathways and a good way to validate their roles in activating STAT3. Nevertheless, as our initial analysis of the expression of the genes itself showed no significant differences, we did not pursue this.

Many studies provide evidence on how STAT3 affects the growth of a tumor [133, 139]. Furthermore, STAT3 has also been linked to resistance in cancer treatment [140, 143]. The role of STAT3 as a biomarker for resistant was studied through knockdown assay. Our results showed successful knockdown, but no effect was observed on the cell's viability. STAT3 is important in regulating various cellular functions including cell growth which is one of the aspects in resistant cells. Reduction of STAT3 activity through less available protein itself should affect the cells capability to grow. However, based on our data, no significant changes in cell growth may indicate that STAT3 is not the main driver of Cetuximab resistance in these cell lines. Other studies showed different observation where STAT3 knockdown restore the cell's sensitivity towards Cetuximab [134, 135]. Alternatives to STAT3, EGFR activation can activate other signaling pathways that include AKT and ERK pathways. Both signaling molecules were knockdown to checked for the role of the pathways. Our results showed no significant changes in cell's viability similar to STAT3. However, the knockdown was not efficient for both AKT and ERK suggesting the results obtained might not be accurate.

3.5. Conclusion

Developing a model to investigate resistance towards treatment is a valuable method to study potential mechanism occurring in patients treated with such therapeutics. A new cell line model needs to be characterized to determine whether they are suitable to use. We showed that our resistant cell lines have enhanced capability in growth, migration, and elevated level of markers that involved in cellular activities through a series of assays including proteomic analysis designed to test these characteristics. A proteomic analysis provides a basic knowledge at the global protein level of the differences between matched Cetuximab-sensitive and Cetuximab acquired resistant cell lines. An association of the proteins gathered in the analysis and functional assays complete the characterization process. STAT3 was prominent in the proteomic analysis which supports our hypothesis. STAT3's role in regulating cellular activities related to proliferation, migration and survivability makes it a viable target. Despite elevated level of STAT3 activity that was observed, knockdown of STAT3 protein showed no effects in affecting cells survivability. Knockdown of other markers also showed no significant results suggesting that STAT3 might not be a major contributor to Cetuximab resistance in these cell lines. In the next chapter we will expand on these findings to further search for a novel biomarker that could potentially predict and possibly mediate resistance to Cetuximab.

CHAPTER 4:

Novel Biomarker of Resistance to EGFR-Targeted Therapy

4. Chapter 4: Novel Biomarker of Resistance to EGFR Targeted Therapy

4.1. Introduction

Targeted therapies have been widely used in treatment for cancer patients over the past decades in combination with chemotherapy/radiotherapy and when chemotherapies regiments were no longer sufficient [236]. These therapies target specific molecules within the cells that are involved in maintaining the cancer cell's survivability and progression and subsequently decreasing patient survival. One of the most studied targets is the Epidermal Growth Factor receptor (EGFR) which is part of an important signaling pathway that governs many critical cellular functions [89]. Two monoclonal antibodies that were developed to target this pathway are Cetuximab and Panitumumab [88, 237]. They function by inhibiting the binding of EGF to its receptor, subsequently inhibiting downstream signaling through prevention of receptor activation. A randomized Phase III study evaluating these drugs showed promising results on patients with wild-type KRAS [238, 239]. While the use of these therapies has been a success, many tumors developed resistance towards the drugs.

4.1.1. Resistance and Colorectal Cancer

The cause of resistance was often associated with mutations in one or more protein that involve in a signaling pathway including EGFR signaling pathway [114]. Mutated *KRAS* is an important biomarker for Cetuximab resistance in colorectal cancer. Mutation in exon 2 of the gene renders the protein to be constitutively active and activate downstream signaling molecule [113]. Thus, a screening of this mutation is performed before treatment is administered [84]. However, 40-60% of patients who express wild-type KRAS do not responded suggesting alternative mutations in the molecule downstream of EGFR [240]. Alterations in several signaling molecules including PTEN and PIK3CA have been suggested to play a role in this resistance [117, 119]. Besides downstream molecules, protein upstream of KRAS can also be involved in activating the MAPK/ERK pathway. A compensatory signaling through other receptors such as MET, IGF-1R, and HER2 could feed into the activation of the pathway [241-243]. Discovering several alternative resistance

mechanisms would further our understanding of the drug mechanics as well as patient's reaction. Furthermore, it would help in optimizing the right treatment required for the patients.

4.1.2. Screening for Biomarker

The process of discovering novel resistance mechanism involves studies that usually start with a screen. There are several screening techniques that could be applied to the study of resistance such as micro-array and RNA-sequencing [244, 245]. These are widely used transcriptome-based assays that study the changes of the sample at the transcriptomic level. While these methods were commonly used in research, having a wider variety of screening methods would far more beneficial. For example, a novel method utilizing transposon was developed to screen for genes involved in drug resistance [246]. Other than genomic-based screening, a simpler type of assay could also be utilized. High-throughput screening of potential agents can be performed using proliferative assay systems such as MTT or fluorescence based assays to observe the changes in cell proliferation upon treatment in order to study drug resistance have commonly been employed [247]. By employing these methods, we can discover and study the genes that could be responsible for causing resistance towards treatment.

4.1.3. Relevance and Importance of Study

Many studies that research treatment resistance have identified a signaling pathway that may drive resistance. Once the pathway is blocked using an inhibitor, the tumor sensitivity to the treatment is expected to be restored. Tumor heterogeneity makes it unlikely however for there to be only one driver of resistance across the whole tumor. The most established resistance marker to Cetuximab in colorectal cancer is *KRAS* mutations, where *KRAS* mutations render Cetuximab largely ineffective. Patients who has wild-type KRAS are eligible for Cetuximab as they some of these patients respond well. However, even in wild-type KRAS patients, some patients do not respond to Cetuximab suggesting alternative pathway or molecules are activated or over-expressed leading to the inhibition of Cetuximab's efficacy. This chapter will focus on the process of investigating alternative and novel molecules that might be involved in resistance mechanism to Cetuximab.

4.2. Results

4.2.1. Colorectal Cancer Cell Lines Screening

We selected a series of 13 colorectal cancer cell lines due to known wild-type KRAS status. All cell lines were subjected to treatment of Cetuximab to categorize them in order of sensitivity (**Figure 4.1**). We arbitrarily designated cells that had reduced viability by less than 50% as Cetuximab sensitive and cells that did not reduce in viability by 50% as Cetuximab resistant. Both Cetuximab concentrations (10 and 20µg/ml) demonstrated similar anti-proliferative effects for each cell line. Therefore, we decided to use the maximum concentration of Cetuximab (20µg/ml) in our further experiments. **Table 4.1** showed seven cell lines in the sensitive group and six cell lines in the resistant group after the assay. Among all 13 cell lines, C70 and DIFI were the most sensitive while Colo320 and HT115 were the most resistant to 20µg/ml of Cetuximab (**Figure 4.2**).

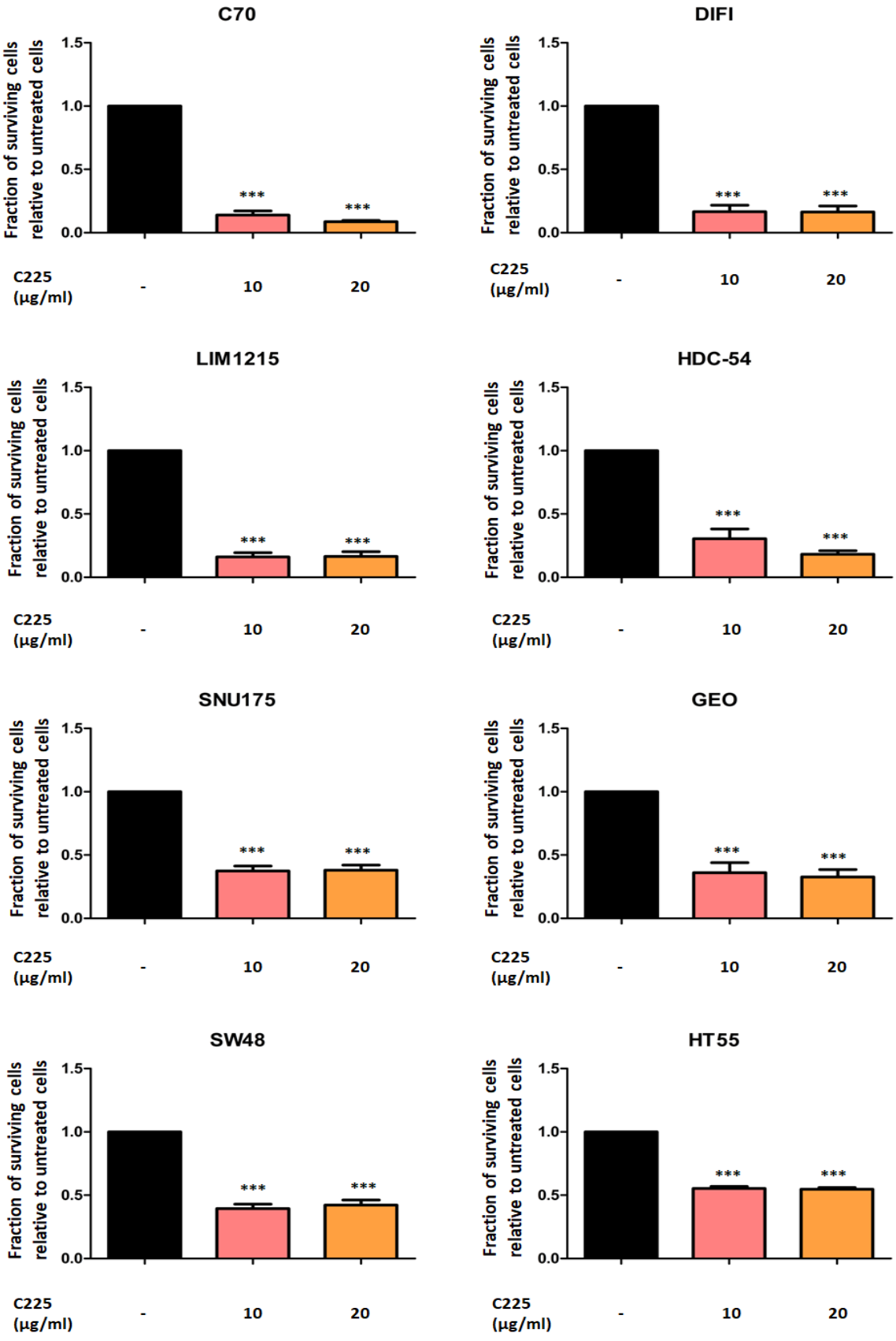
C70
DIFI
LIM1215
HDC-54
SNU175
GEO
SW48
HT55
Fraction of surviving cells relative to untreated cells
1.5
1.0
0.5
0.0
***
C225 (µg/ml)
-
10
20

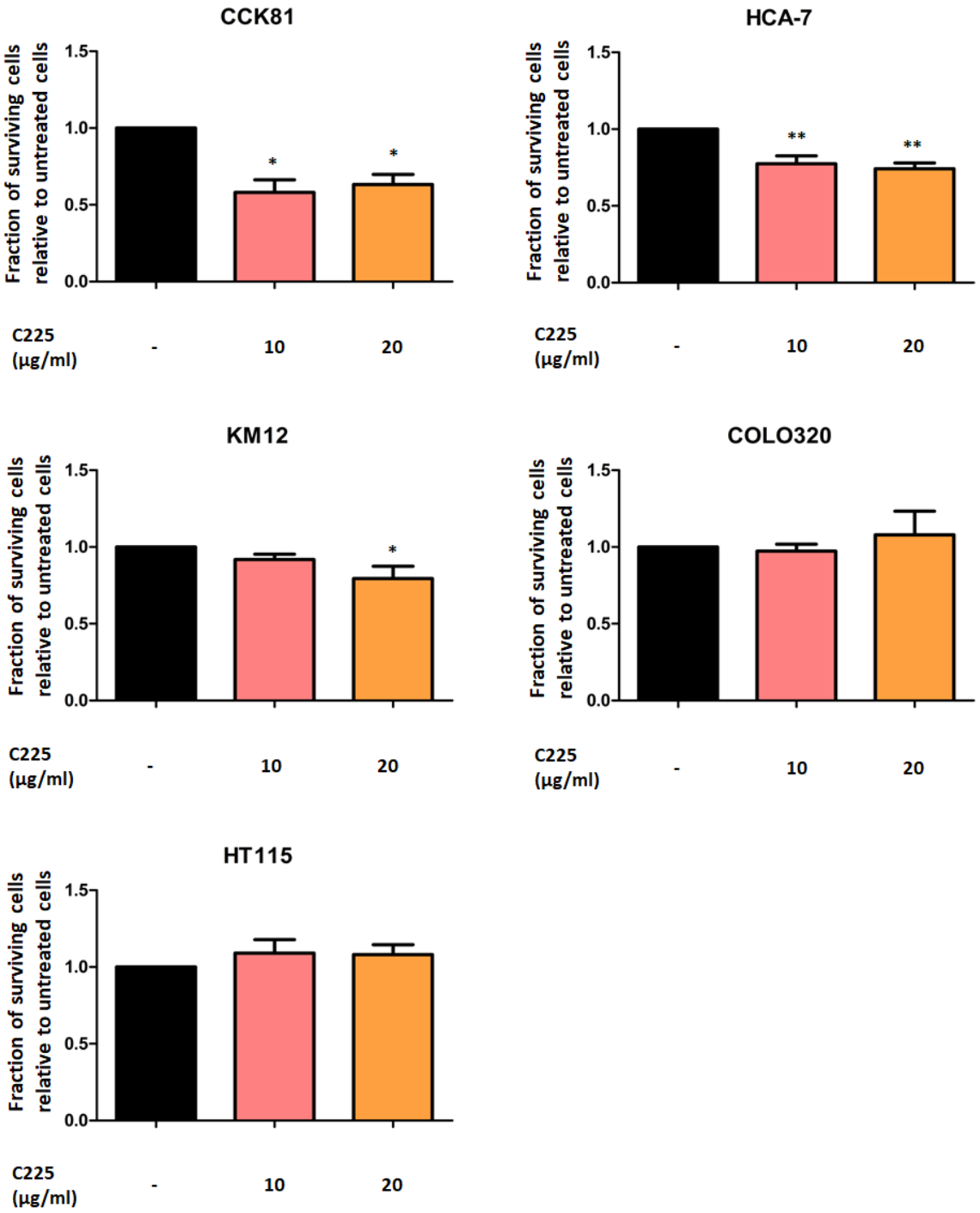

Figure 4.1: Cell viability assay for 13 colorectal cancer cell lines.

Cell Lines as listed in Table 1 were screened using Cell Viability Assay to determine its sensitivity to Cetuximab. All cell lines were treated with 10ug/ml and 20ug/ml of Cetuximab for 3 days before cell viability was measured. The data are presented as relative change of cell number to untreated cell line. Cell lines that show reduction of viability by more than 50% were categorized as sensitive. Error bars are represented by SEM. n=3.

Table 4.1: Categories of colorectal cancer cell lines.

Sensitive Cell Lines	Resistant Cell Lines
LIM1215	HCA-7
SW48	KM-12
DIFI	Colo320
SNU175	HT115
C70	CCK81
GEO	HT55
HDC-54	

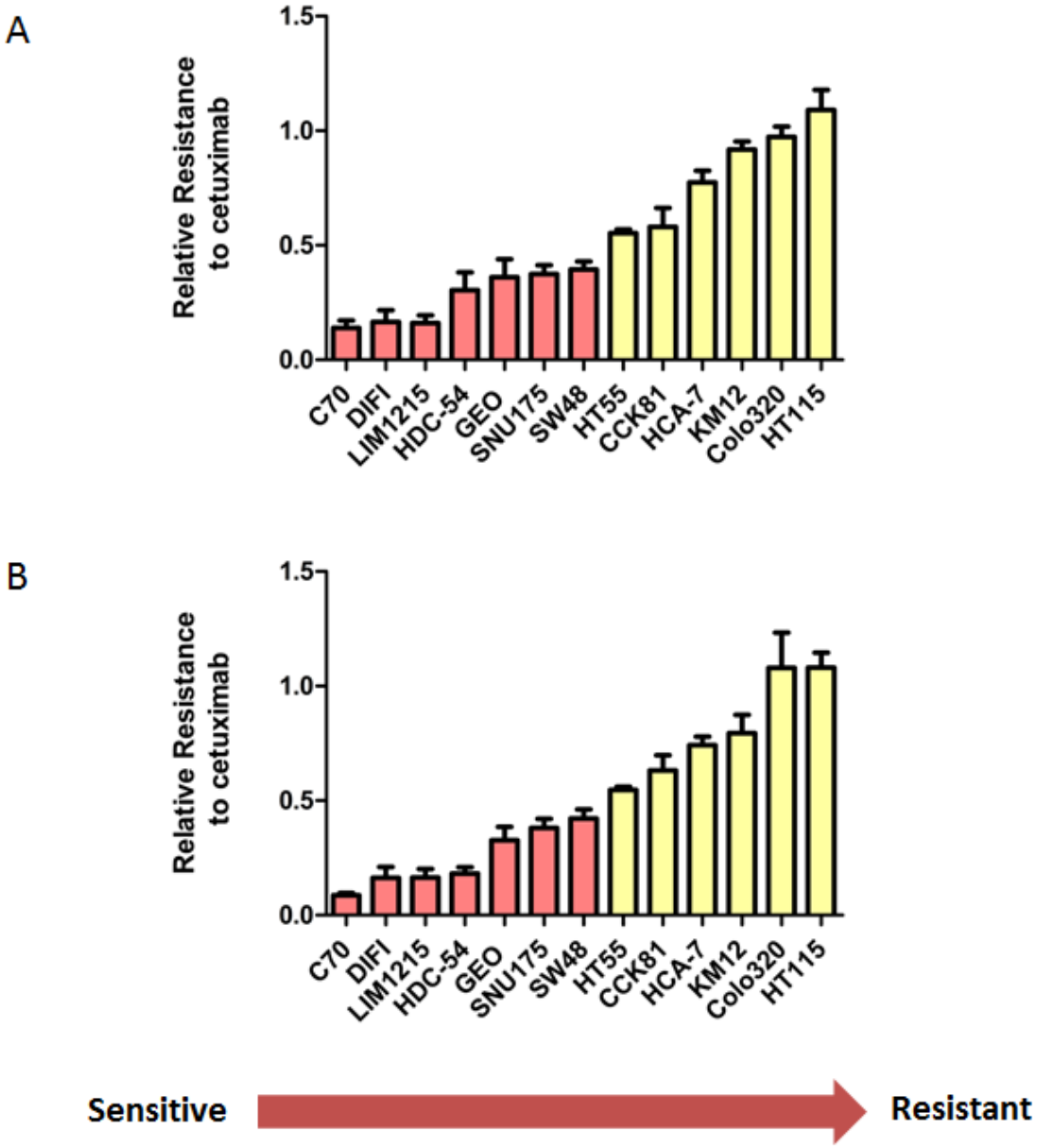

Figure 4.2: Sensitivity level of 13 colorectal cancer cell lines.

The data showed the resistance level of the cell lines to Cetuximab in increasing order from left to right. Cell lines with over 50% resistance to Cetuximab were categorized as Cetuximab-resistance group. (A) The cell lines were treated with 10ug/ml of Cetuximab while (B) were treated with 20ug/ml of Cetuximab. Pink bar represented sensitive cell lines while yellow bar represented resistance cell lines. Error bars are represented by SEM. n=3

4.2.2. Screening for Novel Biomarker for Cetuximab Resistance

After the cell lines have been categorized, we used RNA-sequencing data that was obtained from our collaborator (Prof John Moriadason, ONJCRI) to perform Differential Gene Expression analysis. The differences of gene expression between the sensitive and resistant group was determined. A total of 25371 genes were analyzed using the tool XLSTAT in Excel. The data was in the form of Reads per Kilobase of transcript per Million mapped reads (RPKM) and has been normalized to control dataset. The values were then used in Differential Gene Expression analysis by using XLSTAT software. This software is an add-on program to Microsoft Excel which used a one-way ANOVA to generate p-values. Prior to the analysis, a non-specific filtering was performed to eliminate genes that have low variability. A post-hoc correction, Benjamini-Hochberg procedure was performed to correct for false discovery. Next, Tukey's test was performed as multiple pair-wise comparisons for each gene. After analysis, the top five genes with lowest p-value were selected to proceed with further validation (Highlighted) (**Table 4.2**). Mann-Whitney test was performed on the five genes and showed significance difference between the sensitive and the resistant group (**Figure 4.3**). *CHAC2, NAA25, POLR2A and SF3A1* showed higher expression in resistant cell lines while *CRY2* was higher in sensitive cell lines. These five genes were chosen to be validated further.

Table 4.2. List of differentially expressed genes

Genes	P-value
CHAC2	0.298
CRY2	0.718
NAA25	0.718
POLR2A	0.718
SF3A1	0.718
NUDCD1	0.833
GRIN2D	0.833
CCDC183	0.833
PRPS1	0.833
TMEM120A	0.833
GART	0.833
RRP1B	0.833
LOC100862671	0.833

CENPU	0.833
HSP90AA1	0.833
CPSF2	0.833
FAM175B	0.833
ABCE1	0.833
SSH3	0.833
RIC8B	0.833
ATP2A2	0.833
LRRC40	0.833
PRMT9	0.833
DNAJB4	0.833
DEPDC1	0.833
CENPC	0.833
TRMT5	0.833
MALT1	0.833
CNOT7	0.833
GSE1	0.833

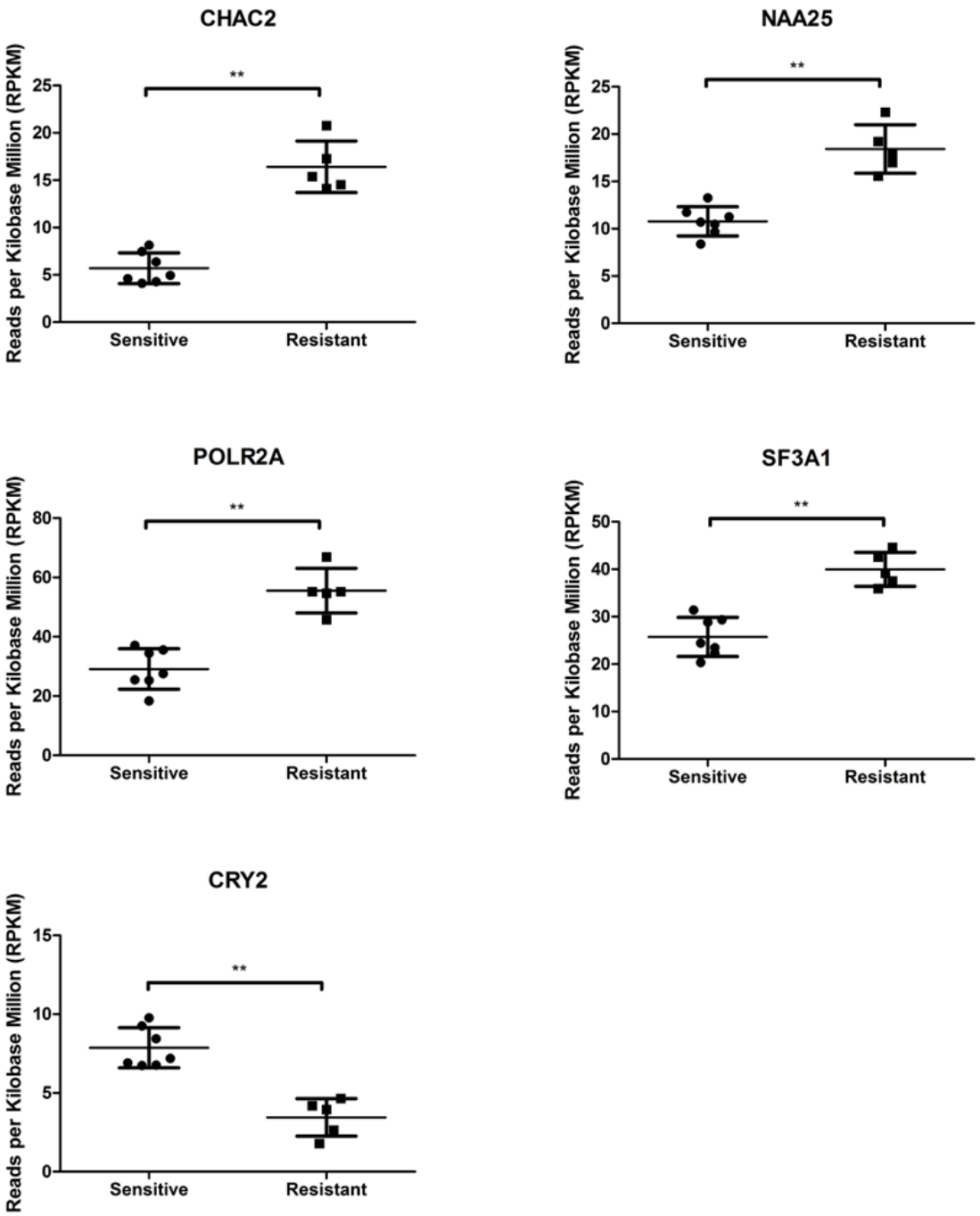

Figure 4.3: Differential Gene Expression Analysis (DGE).

*CHAC2, NAA25, POLR2A, SF3A1 and CRY2 were obtained from the DGE analysis performed in XLSTAT. A subsequent Mann-Whitney test was performed on each gene. ** indicates p<0.01. The data is represented by Reads per Kilobase Million (RPKM). Higher value of RPKM indicates higher expression.*

4.2.3. Five Genes Validation

4.2.3.1. Intrinsic Resistant Cell Lines

We next explored whether the differentiated changes seen at the gene expression level were also present at the protein level of the 5 genes. **Figure 4.4** showed the protein expression across all cell lines. The expressions were varied across all cell lines and genes. No clear differences can be observed between the sensitive and the resistant groups for all target genes. CHAC2 expression was very low across all cell lines such that no analysis can be performed. To further validate the genes, qPCR was performed to measure the RNA expression in all cell lines. There were no significant differences in expression between cell lines for all candidate genes (**Figure 4.5**). In addition, no differences were observed when specifically comparing between the sensitive and resistant group. However, *CRY2* gene was significantly different between the most sensitive cell line in the sensitive group and the most resistant in the resistant group (**Figure 4.5**).

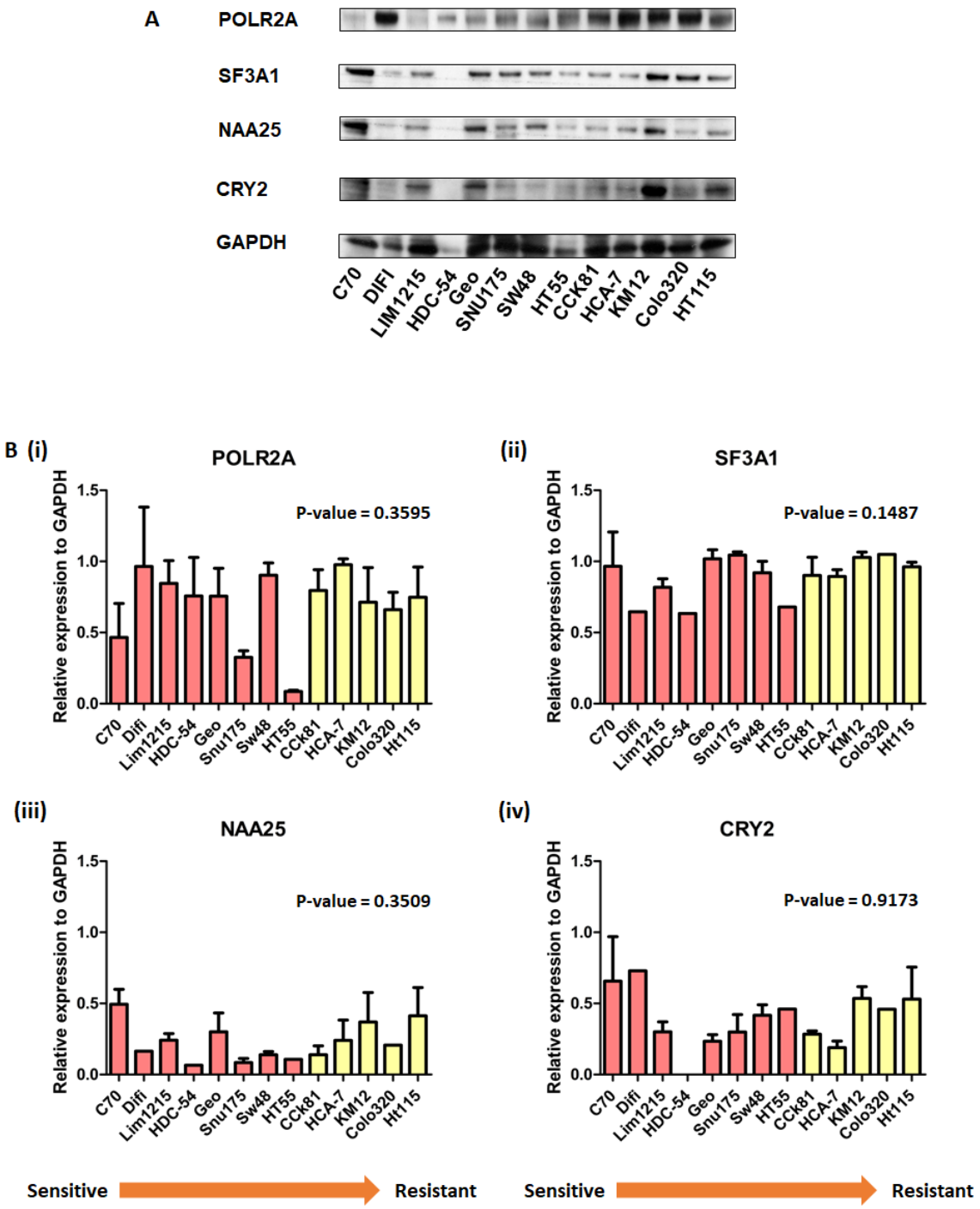

Figure 4.4: Candidate genes protein expression.

(A) The Western blot representative of the expression of POLR2A, SF3A1, NAA25 and CRY2. (B)(I-iv) The expression of POLR2A, SF3A1, NAA25 and CRY2 were presented as densitometry with the protein expression is shown as relative to loading control, GAPDH. The cell lines were arranged in increasing resistance to Cetuximab. Pink bar represented sensitive cell lines while yellow bar represented resistance cell lines. Error bars are represented by SEM. P-value < 0.05 indicates significance. n=3

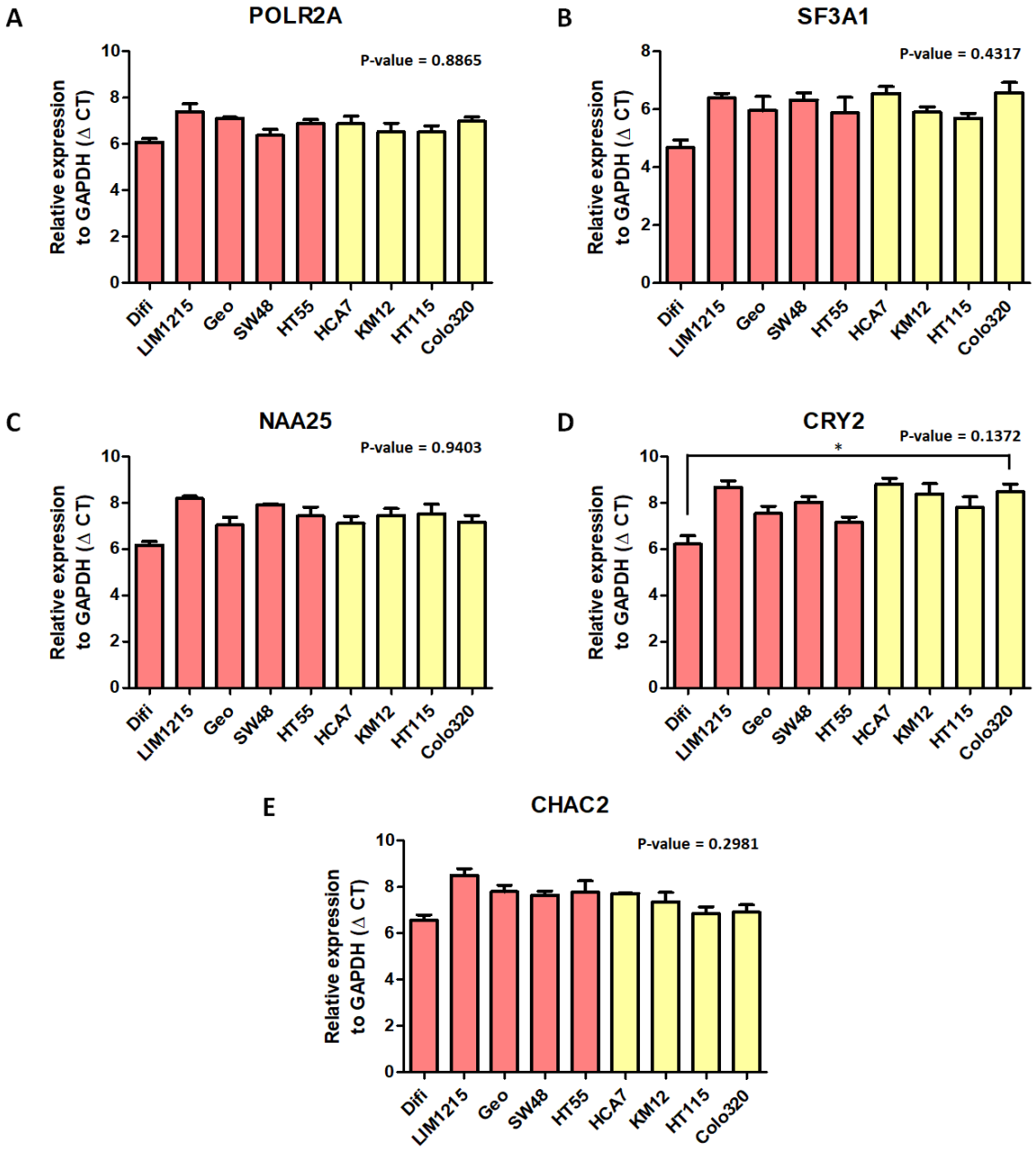

Figure 4.5: Quantitative PCR of candidate genes in intrinsic resistant cell lines.

*(A, B, C, D, E) The RNA expression of five candidate genes were measured using qPCR. The graphs were represented by the gene's relative expression to GAPDH (ΔCT). Higher ΔCT represented higher expression and vice versa. Pink bar represented sensitive cell lines while yellow bar represented resistance cell lines. The cell lines were arranged in increasing resistance to Cetuximab. Error bars are represented by SEM. P-value < 0.05 indicates signifance. * indicates p-value < 0.05. n=3*

4.2.3.2. Acquired Resistant Cell Lines

Next, we explored whether these 5 genes may be differentially expressed in the acquired resistant cells. Due to the low amount of CHAC2 in the cell lines, the protein was not included in the analysis. The protein expression between parental and resistant cells were compared under normal growth condition. Among all genes, NAA25 and CRY2 showed a significant change in protein expression between parental and resistant cells. The results were not consistent in all cell lines with LIM1215 C225 and SW48 C225 significantly expressed greater NAA25 protein than their parental counterpart while CRY2 expression was significant higher in LIM1215 C225 compared to LIM1215 parental cells. The trend where resistant cells expressed more protein can be observed for all genes except for SF3A1 where SW48 C225 expressed lower protein than its parental cells (**Figure 4.6**).

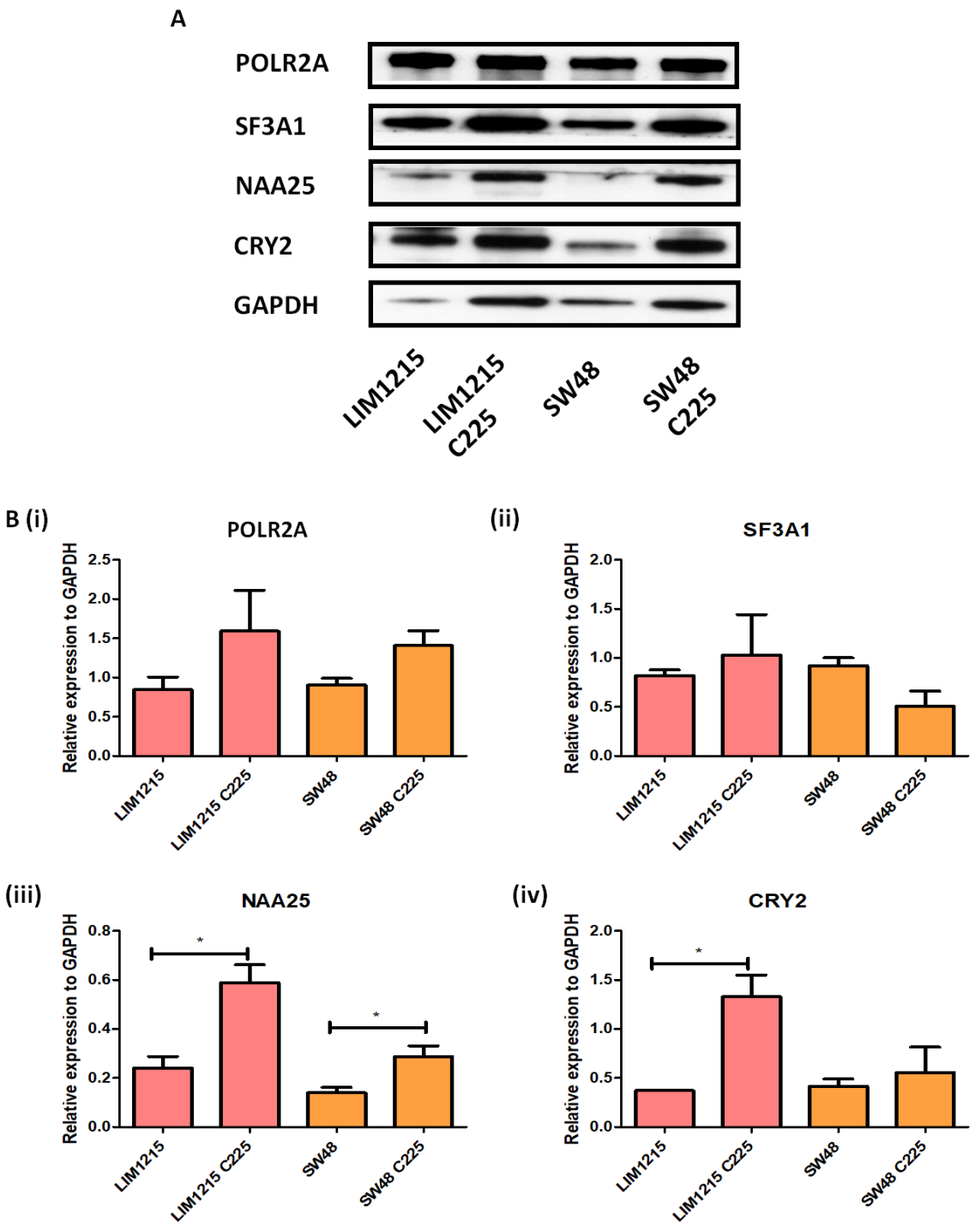

Figure 4.6: Western blot analysis of candidate genes in acquired resistant cell lines.

*(A) The Western blot representative of the expression of POLR2A, SF3A1, NAA25 and CRY2. (B(i-iv)) The expression of POLR2A, SF3A1, NAA25 and CRY2 were presented as densitometry with the protein expression is relative to loading control, GAPDH. Error bars are represented by SEM. * indicates p-value < 0.05. n=3*

Next, a qPCR was performed to measure the RNA expression level. **Figure 4.7** showed the relative RNA expression of the resistant cells compared with their parental counterpart. The expression of RNA differs from the protein expression. LIM1215 C225 and SW48 C225 that have higher NAA25 protein expression showed no differences in term of RNA expression. Similar results were observed with other genes for the other cells. *POLR2A* RNA expression was higher for SW48 C225 compared to its parental but not significant.

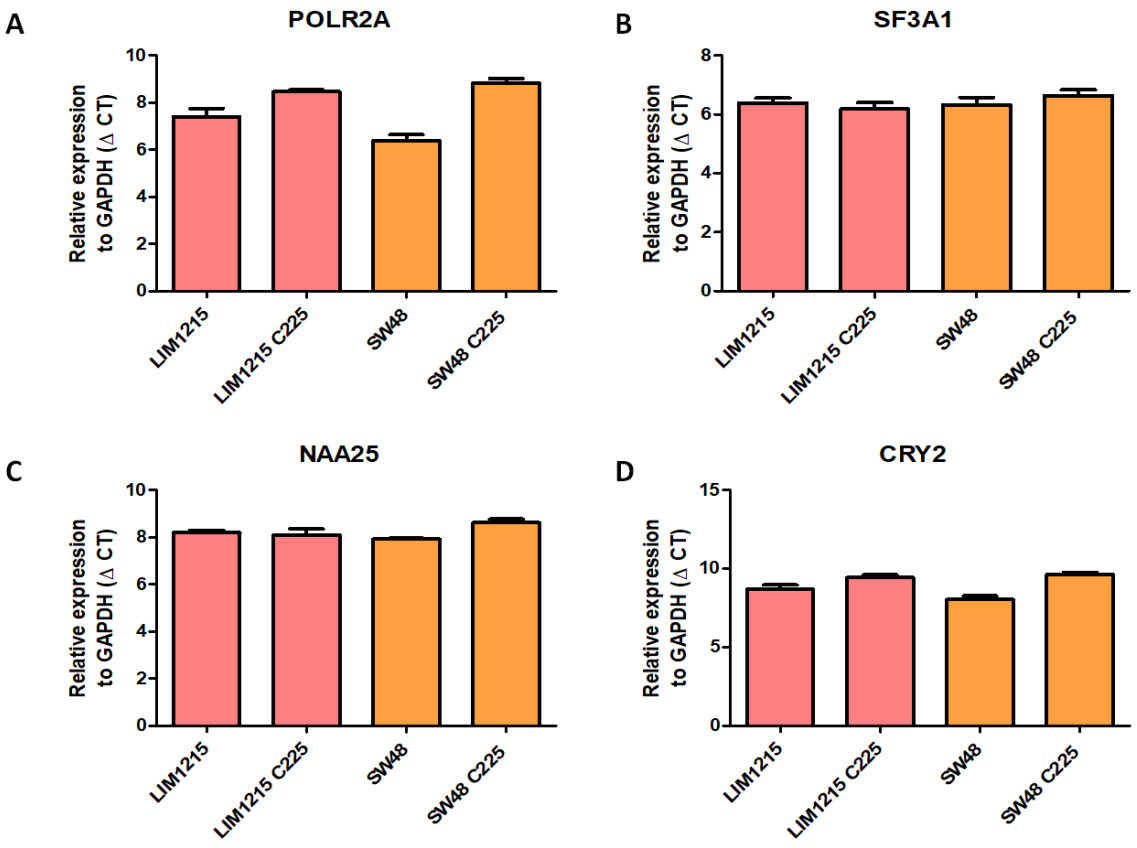

Figure 4.7: Quantitative PCR of candidate genes in acquired resistant cell lines.

The RNA expression of (A)POLR2A, (B)SF3A1, (C)NAA25, and (D)CRY2 genes were measured using qPCR. The graphs were represented by the gene's relative expression to GAPDH (ΔCT). Higher ΔCT represented higher expression and vice versa. The graph showed comparison between parental and resistant cell lines. Error bars are represented by SEM. n=3

4.2.3.3. CRY2 Knockdown

Our previous results showed a trend in CRY2 having a differential expression in both intrinsic and acquired resistant cells. Therefore, we knocked down *CRY2* using siRNA to study its role in Cetuximab resistance. *CRY2* was knocked down in all acquired resistant cell lines and cell viability was performed to study its effect. **Figure 4.8** showed the relative change of the cell number when treated with Cetuximab. No significant changes were observed across all cell lines at all level of Cetuximab concentrations.

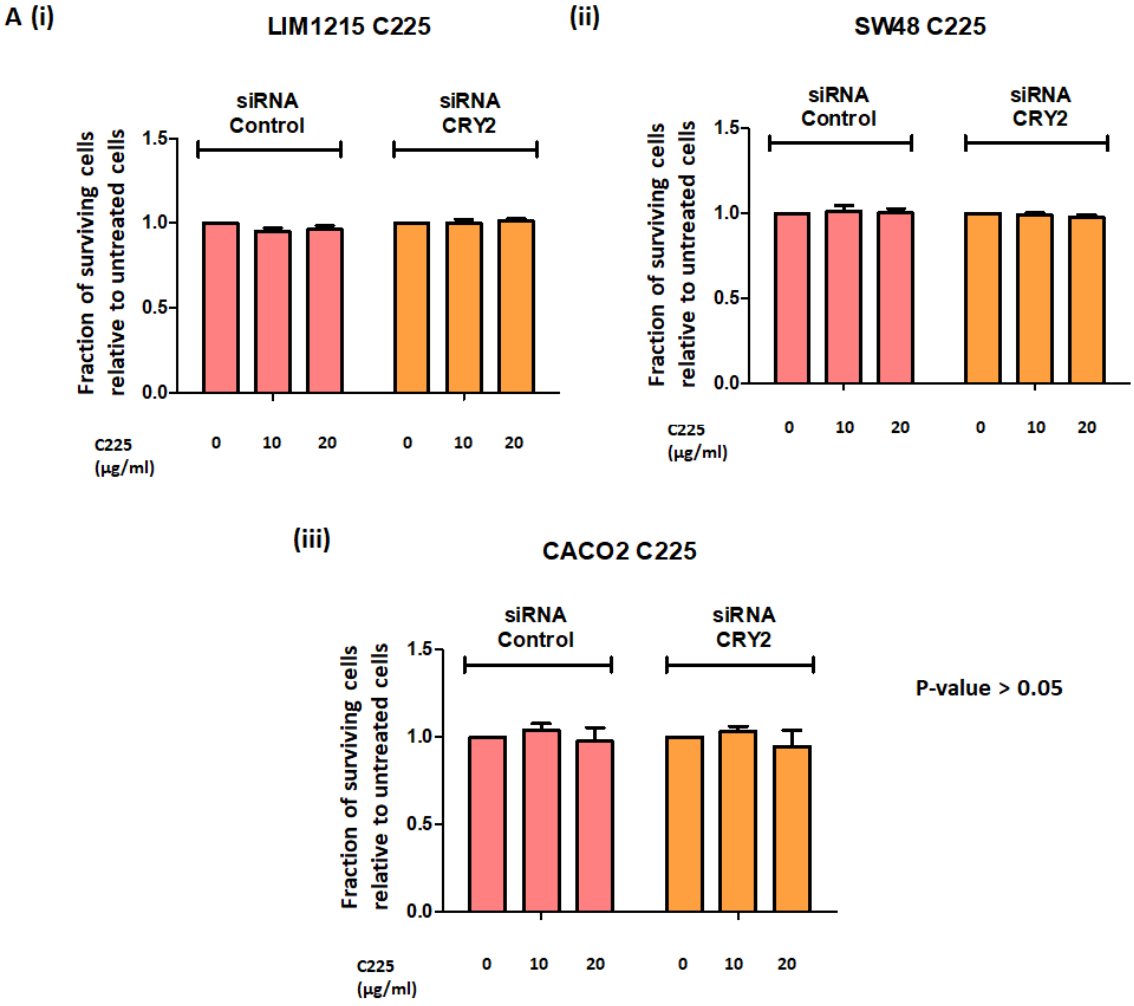
A (i)
LIM1215 C225
siRNA Control
siRNA CRY2
Fraction of surviving cells relative to untreated cells
1.5
1.0
0.5
0.0
C225 (µg/ml)
0 10 20 0 10 20
(ii)
SW48 C225
siRNA Control
siRNA CRY2
Fraction of surviving cells relative to untreated cells
1.5
1.0
0.5
0.0
C225 (µg/ml)
0 10 20 0 10 20
(iii)
CACO2 C225
siRNA Control
siRNA CRY2
Fraction of surviving cells relative to untreated cells
1.5
1.0
0.5
0.0
C225 (µg/ml)
0 10 20 0 10 20
P-value > 0.05

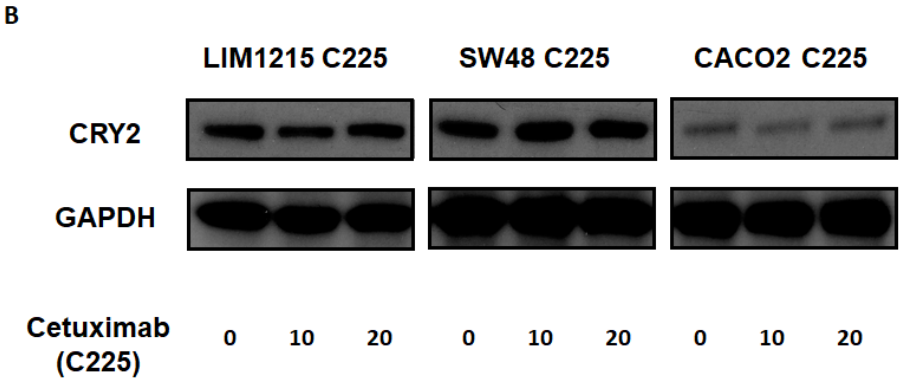
B
LIM1215 C225
SW48 C225
CACO2 C225
CRY2
GAPDH
Cetuximab (C225)
0 10 20 0 10 20 0 10 20

Figure 4.8: Cry knockdown in acquired resistant cell lines.

Cell lines LIM1215 C225, SW48 C225 and CACO2 C225 were seeded and incubated with scramble siRNA (20nM) as control and CRY2 siRNA (20nM) for 48 hours. The cell lines were then treated with Cetuximab (10µg/ml and 20µg/ml) for 3 days. (A(i-iii)) Graphs representing the relative change of cell number to untreated cell lines. (B) Western blot analysis of the cell lines after 48 hours incubation to check for the knockdown efficiency. 2-way ANOVA was carried out for overall statistical significance. Post-hoc test, Bonferroni's test was performed for significance between untreated cell line group with other groups. P-value < 0.05 indicates significance. Error bars represented SEM. n=3

4.3. Discussion

KRAS has long been the most studied biomarker for colorectal cancer patients when determining whether Cetuximab treatment is suitable. Mutated *KRAS* makes Cetuximab not effective on colorectal cancer patients leading to its being use only in patients with wild-type KRAS. However, a subset of those patients is refractory to Cetuximab which leads to our focus of this chapter. A novel biomarker for these patients is required to predict response to Cetuximab prospectively and thereby choose a more rationale alternative treatment if Cetuximab is likely to be ineffective. There are countless genes that could potentially be responsible for Cetuximab resistance in colorectal cancer patients. This chapter explored potential new biomarkers that could predict intrinsic and acquired resistance to Cetuximab.

Resistance towards Cetuximab can be categorized into two; intrinsic and acquired resistance. For acquired resistance, in the previous chapter, we have generated some cell lines that has become resistant to Cetuximab through long-term selection. In the case of intrinsic cell lines, a series of cell lines that have wild-type KRAS was procured and undergone treatment of Cetuximab to test their sensitivity. This method showed the sensitivity of the cells and allowed us to categorize the cells according their response to Cetuximab. The most resistant cells have the same level of resistant as compared to our acquired resistant cells.

The categorization of the cell lines gives us a way to filter through the many genes that could be a new biomarker for resistance and select rationale candidates. RNA-sequencing has been a method widely used to measure and find a predictive biomarker of clinical outcome. Nobili et al. used this method in their study to search for a biomarker that potentially predict clinical outcome in colorectal cancer patients [248]. Another study used RNA-sequencing as an alternative to standard histopathology for prognosis and treatment choice [249]. By using this method, we compared the two groups of cell lines; sensitive and resistant towards Cetuximab. The analysis we performed here is different compared to the usual analysis. The traditional analysis of RNA sequencing data uses the raw data, which undergoes several steps in a well establish pipeline designed for differential expression analysis [250]. Our RNA-sequencing data was already generated and normalized producing final data in RPKM format without any analysis. We used the data and performed differential expression analysis using XLSTAT. Among the 20,000 plus genes, the top five genes generated were selected and further validated.

The potential biomarkers are part of different pathways that govern specific cell functions. Not all of them has been explored thoroughly and only a small amount of knowledge has been obtained. Some of the pathways are obscure in term of its own functions and very little is known about their potential role in treatment resistance. Any findings on these biomarkers would add towards the current knowledge of the genes. Among all the biomarkers, four of them were significantly expressed more in the resistant cells while only *CRY2* was expressed more in the parental cells. Given that each of the biomarkers have their own functions, we can only speculate what is their role in the resistant cells. The results were further validated using the same type of cell lines that were used in the RNA-sequencing data. Our results showed the heterogeneity of the colorectal cancer cell lines. The protein expression for all the cell lines differ among each other and did not demonstrate any clear differences between the sensitive and the resistant group. Furthermore, the expression of each protein for each of the cell lines does not correspond with their sensitivity level towards Cetuximab. We can infer from the results that gene or protein expression alone is not enough to draw a conclusion. Among the five biomarkers, only CHAC2 protein was unable to be measured due to its low amount in all cell lines.

The differential expression analysis was performed on the RNA-sequencing data which comprised of RNA expression level for all cell lines. The data was obtained from an external source which required further validation on our part. qPCR was performed to measure the RNA expression level of the 5 biomarkers in our cell lines. Contrary to the RNA-sequencing data, no significant differences were observed between the sensitive and resistant group. Even though the cell lines are the same, there are other factors that could potentially affects the results. The two experiments were completed by different research teams at a different time which could lead to differences in the results. Nevertheless, the RNA-sequencing data worked as a reference on what biomarker could mark resistance to Cetuximab. Among the cell lines, the most resistance and sensitive cell lines showed a significant difference in *CRY2* RNA expression level. While the RNA-sequencing level showed lower level of *CRY2* in the resistant cells, our results appeared otherwise. However, this comparison is between individual cell lines as compared to multiple cell lines grouped together. Nevertheless, these differences provide a way forward in our study.

The characteristic of cell lines that is intrinsically resistant to Cetuximab might vary from cell lines that developed the resistance later. In colorectal cancer, *RAS* mutations has long been associated with primary resistance toward Cetuximab [251]. The same might not be the case with

acquired resistant cell lines. Similar assays were performed on our acquired resistant cells. While most of the biomarkers have higher level of protein expression in the resistant cells, not all of them had significant differences. NAA25 and CRY2 showed significant differences between LIM1215 C225 and its parental cells. Referring to previous RNA-sequencing data, there is more expression of the biomarkers in the resistant cells except for *CRY2*. Elevated expression of the genes generally translated into higher level of protein [252]. Though it was not significant, the trend can still be observed on the resistant cells. On the contrary, *CRY2* gene expression was lower in resistant cells but showed increase level in protein expression. The process of protein translation could involve multiple post-transcriptional mechanisms that are not yet well defined. Liu et al. 2016 stated that there could be a delay in protein synthesis after mRNA is transcribed. The level of the protein could be higher at a point where the mRNA level has already reduced over time [252]. We further looked at the RNA expression level of the resistant cells. For all biomarkers, no significant differences were observed between the parental and resistant cells. Our results showed that the mRNA of *CRY2* did not affect the level of protein expression. This could be due to the protein translation delay in the resistant cells. At the point of mRNA at the same level with parental cells, CRY2 protein increased in abundance. The results however need to be verified with further experiments.

A novel biomarker is needed to better characterize the Cetuximab resistant colorectal cancer. CRY2 which is a circadian clock protein might make a viable biomarker due to its role in degrading c-myc. The role of CRY2 was investigated by knocking down that protein using siRNA. However, we were unable to validate the role of CRY2 due to the failure in the knockdown assay. It has been shown in a study that CRY2 was found to be regulating genes involve in DNA damage checkpoint control [166]. Gery et al. 2010 stated that CRY1,2 knockout mice have slower liver degeneration by affecting the G_2/M checkpoint. We speculate that successful CRY2 knockdown would result in slower rate of proliferation, but more validation is needed.

4.4. Conclusion

The current biomarker for diagnosis and selecting a treatment for colorectal cancer patients is RAS mutations. Patients who have wild-type KRAS are eligible to receive Cetuximab. However, some of them still resist the treatment driving the need for a new biomarker. This chapter showed the process of analyzing a dataset and comparing sensitive and resistant group of cell lines to narrow down possible number of biomarkers. *POLR2A, SF3A1, NAA25, CRY2* and *CHAC2* were chosen as

they were the top listed in the differential gene expression analysis. The biomarkers were then validated, and one was chosen which was CRY2. The role of CRY2 was analyzed but the results were negative.

CHAPTER 5:

Screening agents to determine whether they can overcome Cetuximab Resistance in CRC.

5. Chapter 5: Screening agents to determine whether they can Overcome Cetuximab Resistance in CRC.

5.1. Introduction

The standard care of treatment for cancer patients involved the use of certain chemotherapeutic agents or a more targeted drug coupled with surgery and radiotherapy. The search for new and more effective drugs is a continuous journey due to the current agents not being optimal in colorectal cancer treatment and that resistance to these therapeutics is often observed. One potential target for treatment is the proteasome. The proteasome is a complex of proteases that processes protein that have been targeted for degradation through ubiquitin-dependent pathway [179]. Multiple cellular activities depend on this process and inhibition lead to accumulation of aberrated protein and eventually cell death [253]. Proteasome inhibitors have been used in cancer as one treatment option particularly in multiple myeloma. The success of first- and second-generation proteasome inhibitors such as Bortezomib and Carfilzomib have produced promising results in clinical trials [254, 255]. Following the resistance developed from Bortezomib treatment, Carfilzomib was developed to overcome Bortezomib resistance.

5.1.1. Carfilzomib in Cancer Treatment

Carfilzomib is an irreversible second-generation proteasome inhibitor. The drug selectively binds to the 20S proteasome and inhibits its chymotrypsin-like activity [253]. Carfilzomib has been approved by the FDA for treatment of recurrent multiple myeloma [256]. Compared to Bortezomib, a first-generation proteasome inhibitor, Carfilzomib has lower toxicity as well as minimal off-target effect [202]. In haemopoietic cancer, Carfilzomib has shown to be effective. In solid cancer however, their results were not very consistent. Clinical trials have been performed on some solid cancers revealing the efficacy of Carfilzomib [257, 258]. The current discovered mechanism of action involved several pathways. Inhibition of nuclear factor ĸB (NF-ĸB) signaling, interference of cell signaling and cellular apoptosis through tumor necrosis factor alpha (TNF-α) production were among the current known mechanism [259, 260]. While Carfilzomib has proven to be effective in

overcoming Bortezomib resistance in multiple myeloma, however, its efficacy in other types of cancer including colorectal cancer is not clear. Furthermore, Carfilzomib was also able to work in combination with other therapy such as lenalidomide and dexamethasone in myeloma patients [256]. Originally used in multiple myeloma, Carfilzomib showed significant single-agent activity in colorectal cancer as well as combination therapy with Irinotecan [261]. However, there is no reports determining whether Carfilzomib can overcome Cetuximab resistance in colorectal cancer.

5.1.2. Rationale and Significance of Study

Carfilzomib has been a great success in multiple myeloma being able to overcome tumor resistance to Bortezomib. The effect of Carfilzomib on solid cancers are inconsistent but overall shows great potential as a single-agent or as part of combination therapies. However, the mechanism used by Carfilzomib to overcome resistance is still not well understood especially in a Cetuximab resistant model. In this chapter, we will screen a series of FDA-approved agents for their ability to inhibit Cetuximab-resistant colorectal cancer cell lines. We identified Carfilzomib as our lead candidate. Furthermore, we investigated the mode of mechanism of how Carfilzomib can overcome the resistant caused by Cetuximab treatment.

5.2. Results

5.2.1. Novel Drug Screening

A set of 38 drugs consisting of chemotherapeutics and targeted agents were selected for our screening in search for a novel drug targeting Cetuximab resistance (**Table 5.1**). This set of drugs were chosen because it has been used previously in our laboratory. The method chosen to evaluate the effect of each drug on the resistant cells was cell viability assay. The acquired resistant cell lines; LIM1215 C225, SW48 C225 and CACO C225 and their parental counterparts were treated with the drugs at low concentration of 1uM over the period of 3 days. 1µM dose of the drugs was sufficient to exhibit an effect to the cell lines. The aim of screening for a novel drug was to search for a drug that is effective at low concentrations. The length of treatment was set to 3 days as it was the minimum amount of time that the drugs required to show its effect. **Figure 5.1** showed the responds of the cell lines to all drugs.

Table 5.1: List of 38 drugs that were used in cells screening.

38 Drugs		
Acadesine	Diclofenac	Nilotinib
Afatinib	Enzalutamide	Nystatin
Aminosalicylate sodium	Erlotinib HCL	Pazopanib HCL
Apatinib	Everolimus	Ponatinib
Axitinib	Evista	Regorafenib
Azelnidipine	Gefitinib	Reseveratrol
Bisoprolol	Ibrutinib	Ruxolitinib
Bosutinib	Imatinib Mesylate	Temsirolimus
Carbozantinib	Irinotecan	Tofacitinib Citrate
Carlfilzomib	Lapatinib	Vemurafenib
Crizotinib	Lenalinomide	Vismodegib
Dasatinib	Masitinib	Vorinostat
Dexamethasone	Niclosamide	

A (i)

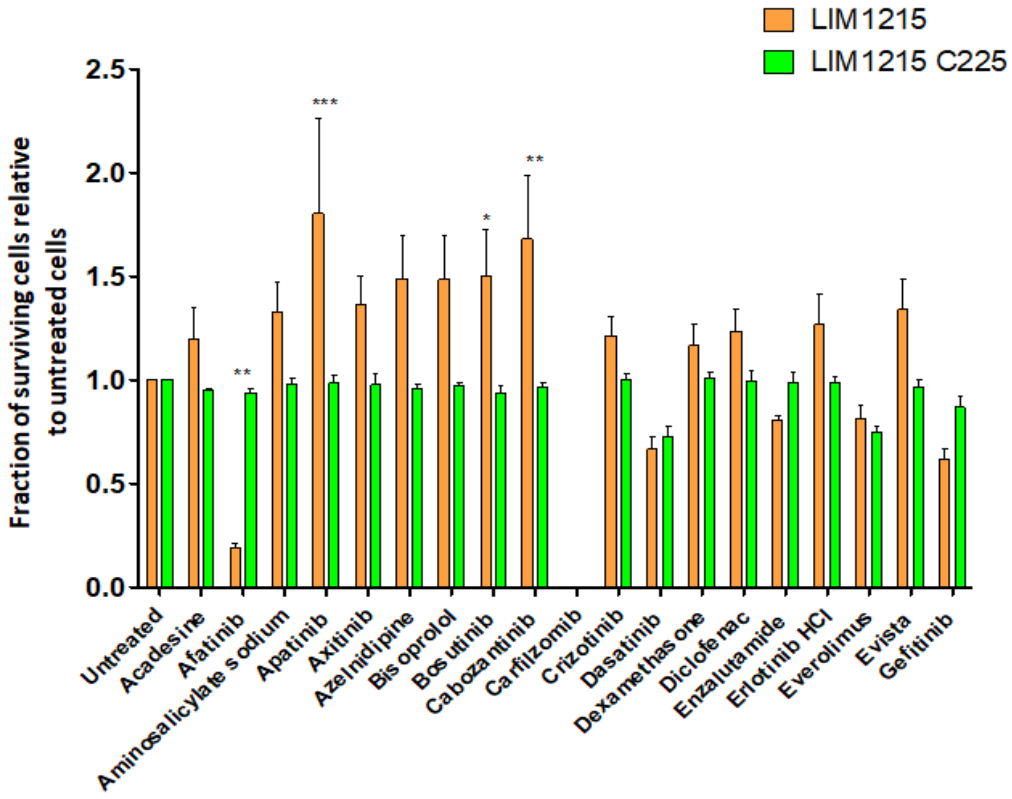
LIM1215
LIM1215 C225
Fraction of surviving cells relative to untreated cells
2.5
2.0
1.5
1.0
0.5
0.0
***
**
*
**
Untreated
Acadesine
Afatinib
Aminosalicylate sodium
Apatinib
Axitinib
Azelnidipine
Bisoprolol
Bosutinib
Cabozantinib
Carfilzomib
Crizotinib
Dasatinib
Dexamethasone
Diclofenac
Enzalutamide
Erlotinib HCl
Everolimus
Evista
Gefitinib

(ii)

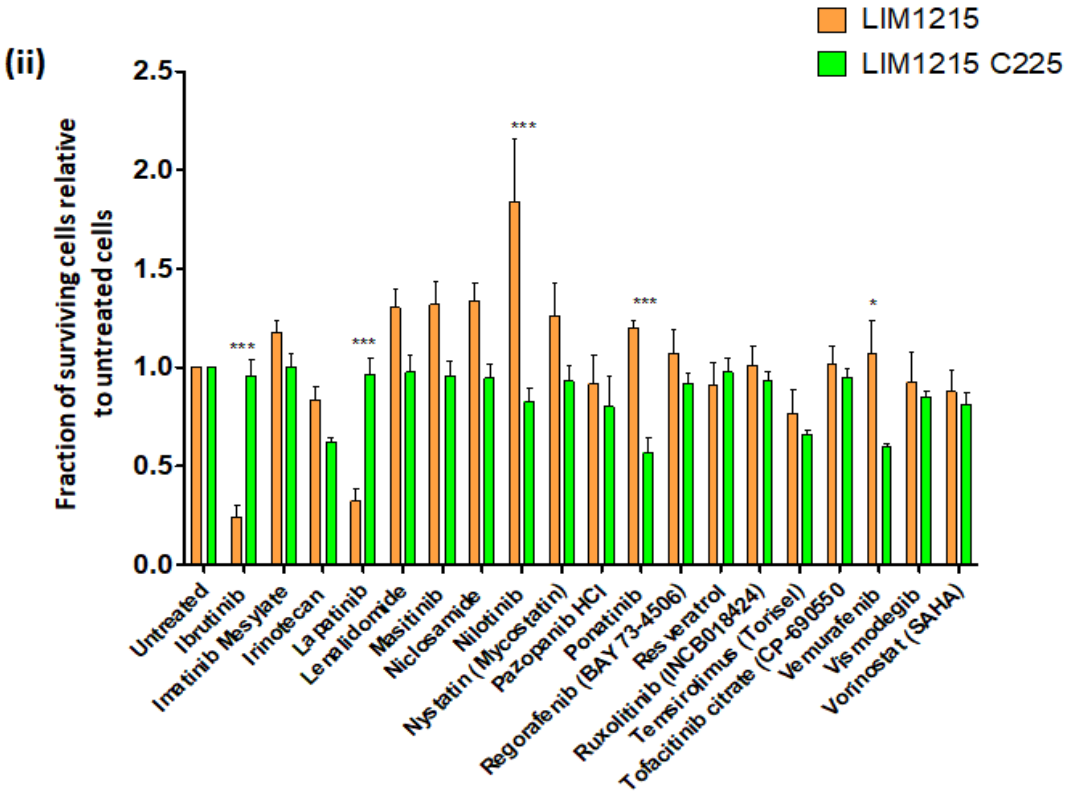
LIM1215
LIM1215 C225
Fraction of surviving cells relative to untreated cells
2.5
2.0
1.5
1.0
0.5
0.0
***
***
***
***
*
Untreated
Ibrutinib
Imatinib Mesylate
Irinotecan
Lapatinib
Lenalidomide
Masitinib
Niclosamide
Nilotinib
Nystatin (Mycostatin)
Pazopanib HCl
Ponatinib
Regorafenib (BAY 73-4506)
Resveratrol
Ruxolitinib (INCB018424)
Temsirolimus (Torisel)
Tofacitinib citrate (CP-690550
Vemurafenib
Vismodegib
Vorinostat (SAHA)

B (i)

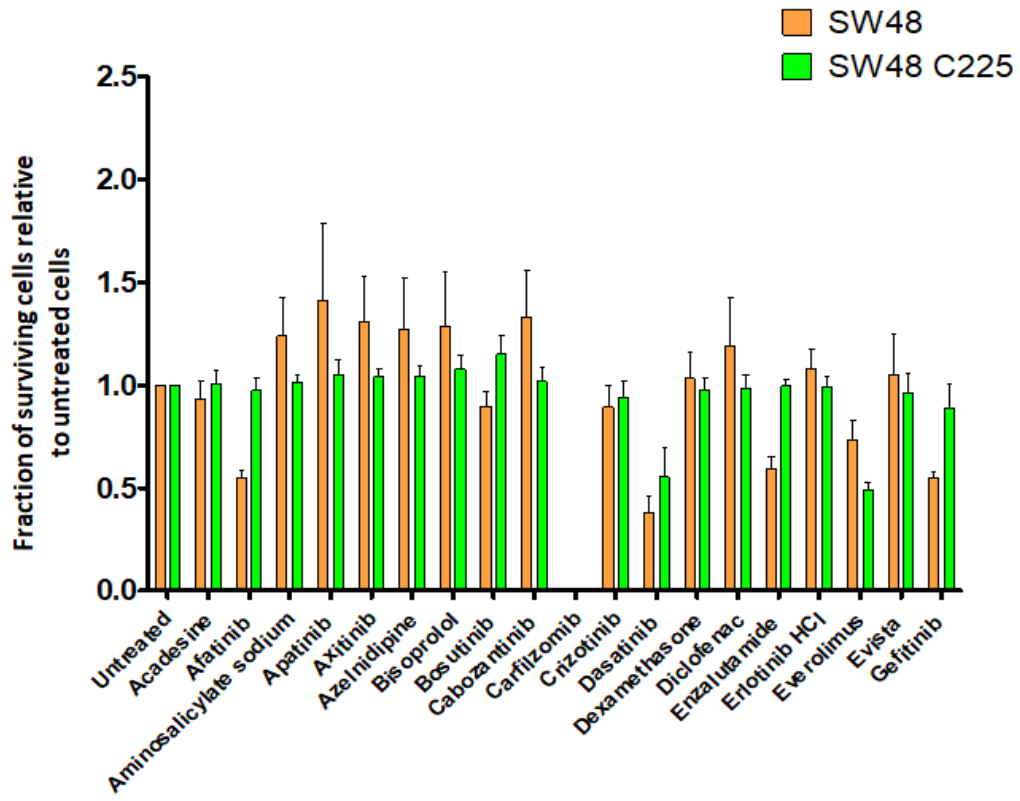
SW48
SW48 C225
Fraction of surviving cells relative to untreated cells
2.5
2.0
1.5
1.0
0.5
0.0
Untreated
Acadesine
Afatinib
Aminosalicylate sodium
Apatinib
Axitinib
Azelnidipine
Bisoprolol
Bosutinib
Cabozantinib
Carfilzomib
Crizotinib
Dasatinib
Dexamethasone
Diclofenac
Enzalutamide
Erlotinib HCl
Everolimus
Evista
Gefitinib

(ii)

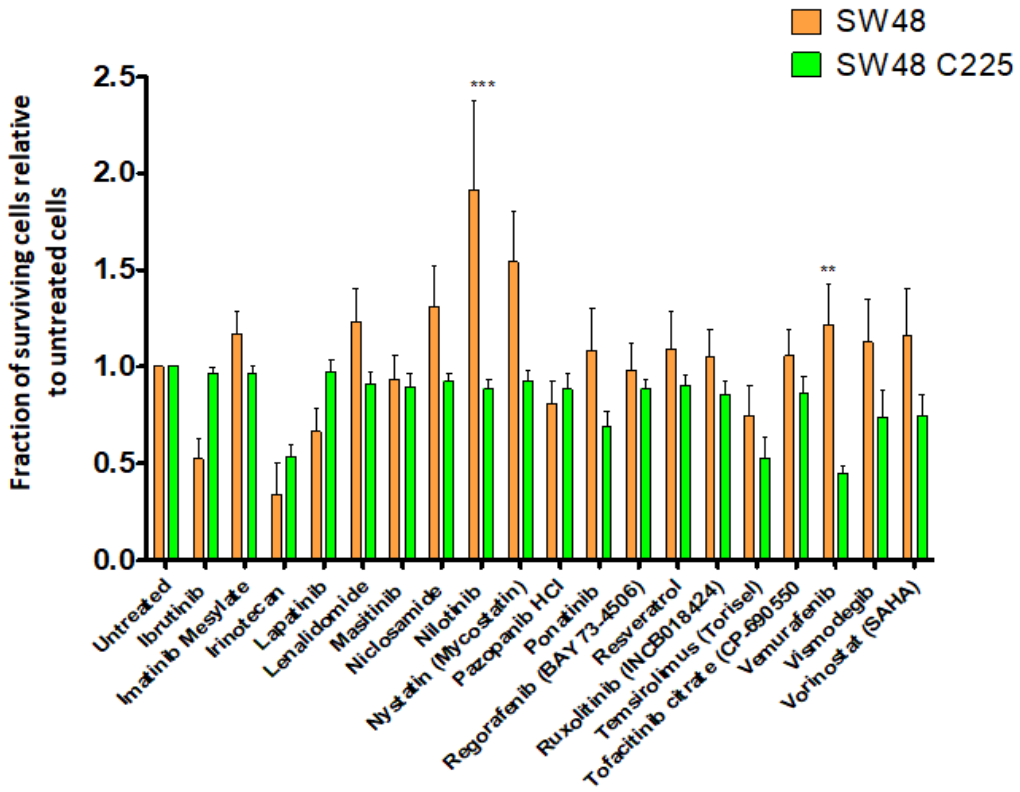
SW48
SW48 C225
Fraction of surviving cells relative to untreated cells
2.5
2.0
1.5
1.0
0.5
0.0
***
**
Untreated
Ibrutinib
Imatinib Mesylate
Irinotecan
Lapatinib
Lenalidomide
Masitinib
Niclosamide
Nilotinib
Nystatin (Mycostatin)
Pazopanib HCl
Ponatinib
Regorafenib (BAY 73-4506)
Resveratrol
Ruxolitinib (INCB018424)
Temsirolimus (Torisel)
Tofacitinib citrate (CP-690550)
Vemurafenib
Vismodegib
Vorinostat (SAHA)

C (i)

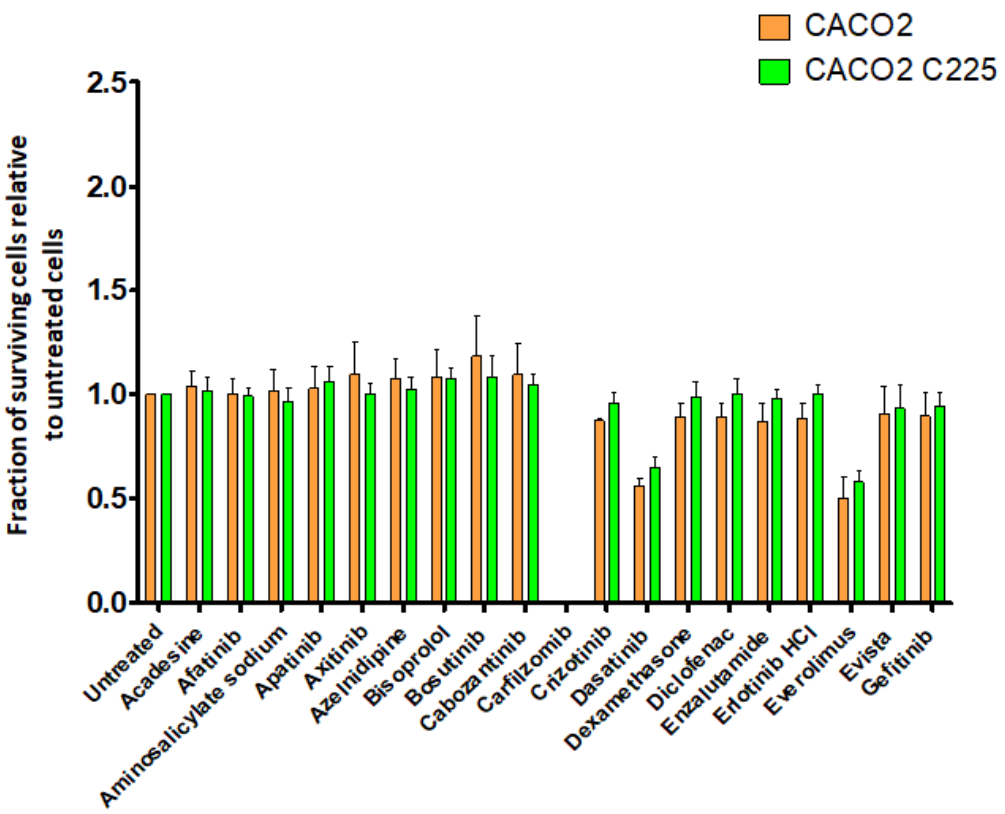
CACO2
CACO2 C225
Fraction of surviving cells relative to untreated cells
2.5
2.0
1.5
1.0
0.5
0.0
Untreated
Acadesine
Afatinib
Aminosalicylate sodium
Apatinib
Axitinib
Azelnidipine
Bisoprolol
Bosutinib
Cabozantinib
Carfilzomib
Crizotinib
Dasatinib
Dexamethasone
Diclofenac
Enzalutamide
Erlotinib HCl
Everolimus
Evista
Gefitinib

(ii)

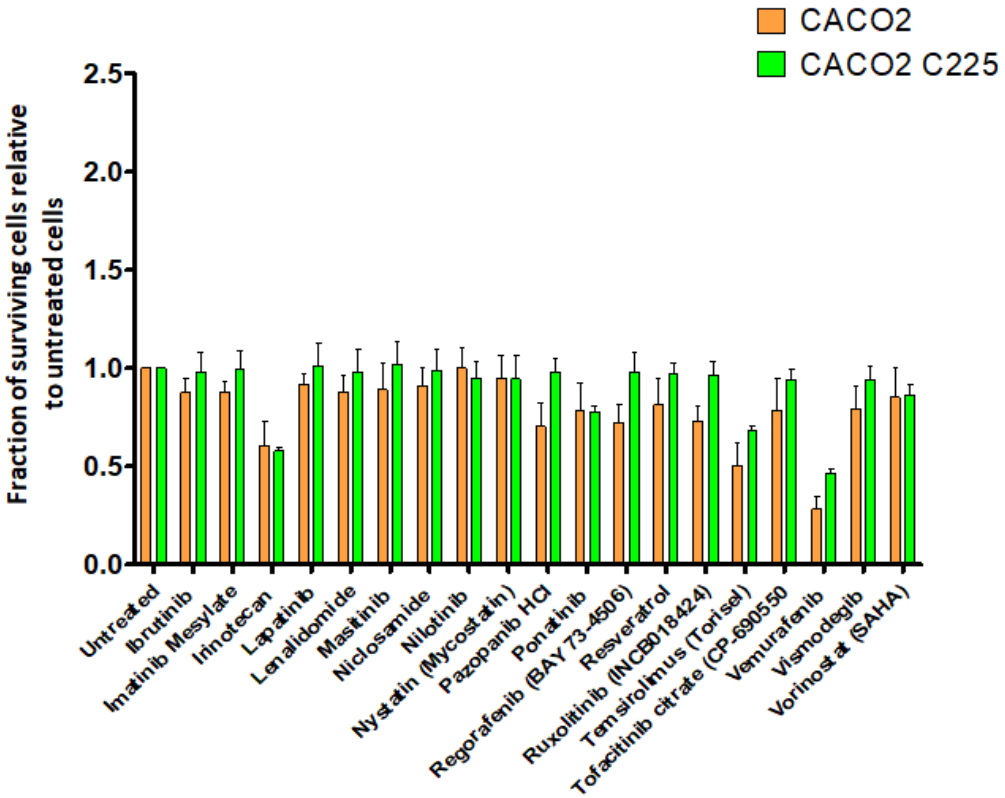
CACO2
CACO2 C225
Fraction of surviving cells relative to untreated cells
2.5
2.0
1.5
1.0
0.5
0.0
Untreated
Ibrutinib
Imatinib Mesylate
Irinotecan
Lapatinib
Lenalidomide
Masitinib
Niclosamide
Nilotinib
Nystatin (Mycostatin)
Pazopanib HCl
Ponatinib
Regorafenib (BAY 73-4506)
Resveratrol
Ruxolitinib (INCB018424)
Temsirolimus (Torisel)
Tofacitinib citrate (CP-690550
Vemurafenib
Vismodegib
Vorinostat (SAHA)

Figure 5.1: Drug screening.

Cell viability assay was performed to screen drug on acquired resistant cell lines. Acquire resistant cell lines were grown and treated with each drug individually at concentration of 1uM. After 3 days, cell's viability was measured using luminometer. The data presented as relative change of cell number to untreated cell line. 1-way ANOVA was carried out for overall statistical significance. Post-hoc test, Tukey's test was performed for significance between untreated cell line group with other groups. Error bars are represented by SEM. n=3

All three cell lines showed various responses to each of the drugs. Many of the drugs were not effective on the resistant cells as shown in the results where there were no significant changes to their cell viability. The results indicated that some of the drugs (i.e: Carbozantinib & Nilotinib) were able to increase the rate of cells proliferation (LIM1215 C225 & SW48 C225 respectively) more than others. However, not all cell lines behaved the same with the same drug i.e CACO2 C225. Among the drugs, a few were identified to be able to significantly reduce the cells' viability in all three resistant cells. They were Carfilzomib, Dasatinib, Everolimus, Irinotecan, Temsirolimus and Vemurafenib (**Figure 5.2**).

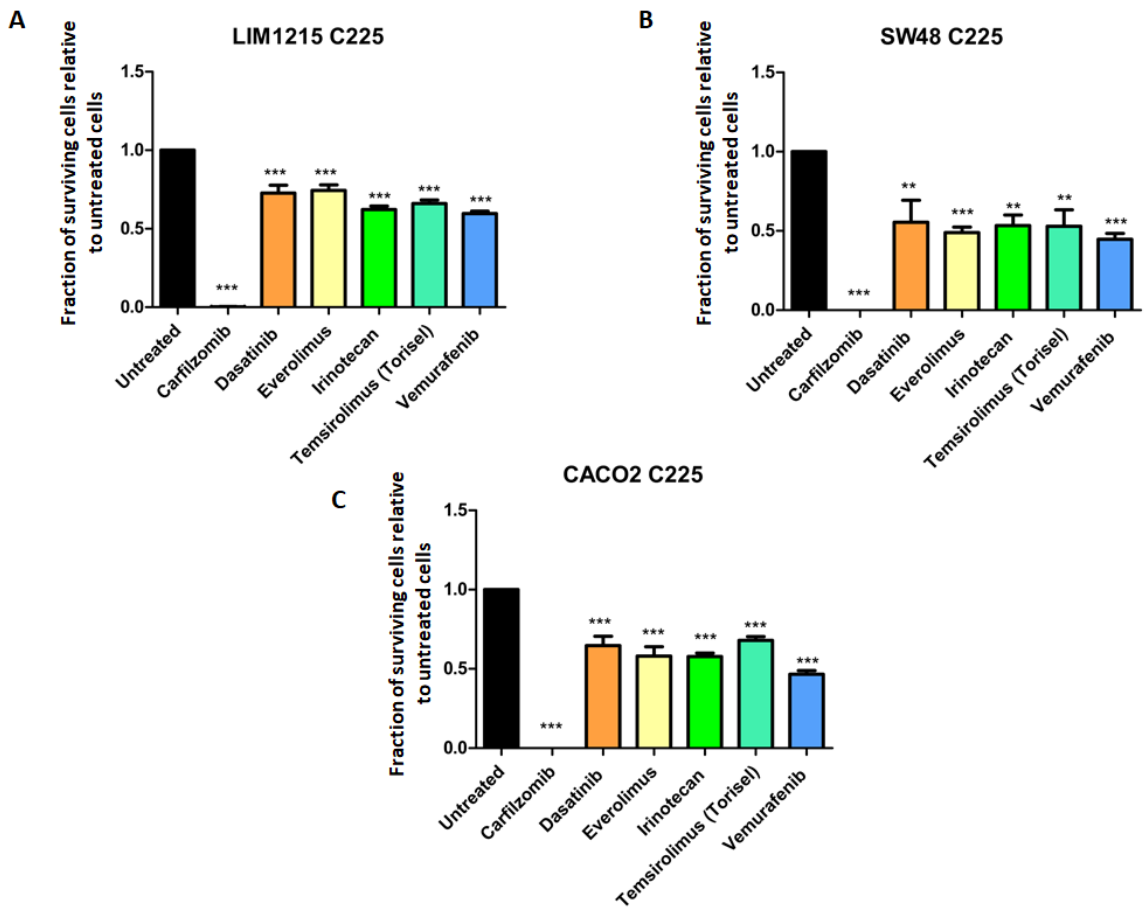

Figure 5.2: Cell viability assay for short-listed drug.

*(A-C) Cell lines LIM1215 C225, SW48 C225, and CACO2 C225 were treated with Carfilzomib, Dasatinib, Everolimus, Irinotecan, Temsirolimus and Vemurafenib at 1uM for 3 days. Cell viability was measured using Luminometer. The data are represented by relative change of cell number to untreated cell lines. 1-way ANOVA was performed for overall statistical significance. Tukey's post-test was performed for comparison between treated and untreated cell lines. ** indicates p<0.01, *** indicates p<0.001. Error bars are represented by SEM. n=3*

Though these drugs were able to significantly reduce the cell's viability, they have different level of efficacy in each cell lines. Most of the drugs were capable of inhibiting cells viability by about 40-50% in all 3 Cetuximab-resistant cell lines. However, among the six drugs, Carfilzomib showed a very potent effect on reducing viability by more than 90% in all Cetuximab-resistant cells. Next, we did a dose dependent assay to determine the IC_{50} of Carfilzomib. The doses that we used were 1.0nM, 2.5nM, 5.0nM, 7.5nM, 10.0nM, 17.5nM, 25.0nM, and 50.0nM. The data was analyzed using Graphpad Prism to determine the IC_{50}. The doses were transformed logarithmically followed by normalizing the data to a common scale using the normalizing function in Graphpad Prism. The IC_{50} of the drug for all cell lines were 5.3, 4.0 and 8.1nM for LIM1215 C225, SW48 C225 and CACO2 C225 respectively (**Figure 5.3**). As the highest IC_{50} is 8.1nM, we decided to use 5 and 10nM as the concentration for subsequent experiments.

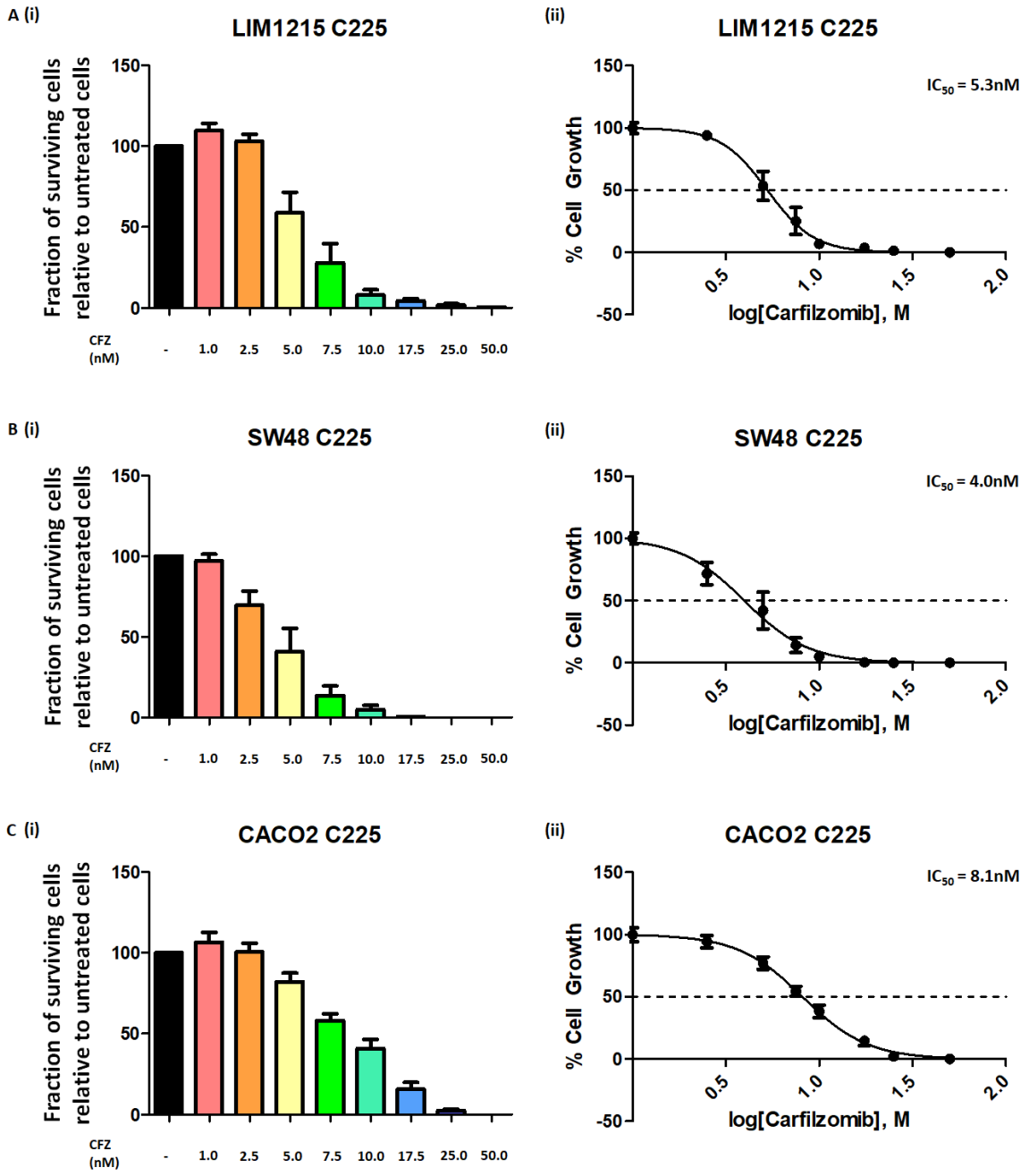

Figure 5.3: Dose dependent assay for Carfilzomib.

(A-C)(i) Cell lines LIM1215 C225, SW48 C225 and CACO2 C225 were treated with increasing concentration of Carfilzomib for 3 days. (A-C)(ii) The data are represented by the percentage of cell growth that was inhibited upon treatment with increasing concentration of Carfilzomib (1nM, 2.5nM, 5nM, 7.5nM, 10nM, 17.5nM, 25nM and 50nM) that has been logarithmic transformed. The IC_{50} determined for LIM1215 C225, SW48 C225 and CACO2 C225 were 5.3, 4.0 and 8.1nM respectively. Error bars are represented by SEM. n=3

5.2.2. Carfilzomib Reduced Viability

The IC_{50} for Carfilzomib was different according to cell lines. We used 5 and 10nM as the basis for subsequent experiments. The efficacy of Carfilzomib was tested on both intrinsic and acquired Cetuximab resistant cell lines via cell viability assay. **Figure 5.4** showed the effect of Carfilzomib on intrinsic resistant cells. All four cell lines responded to Carfilzomib treatment at both concentrations except for Colo320 which only responded at 10nM of Carfilzomib. HCA-7 and HT115 showed the biggest changes in viability with the reduction by more than 90%. KM12 has more modest reduction at 5nM and similar results at 10nM with the other cell lines. Colo320 proved to be the most resistant to Carfilzomib at 5nM but has approximately 50% reduction in viability at 10nM. Similar assay was performed on acquired resistant line model. All three resistant lines showed similar trend in responds to Carfilzomib (**Figure 5.5**). About 50% of cell's viability was reduced at 5nM and more at 10nM. All changes were statistically significant.

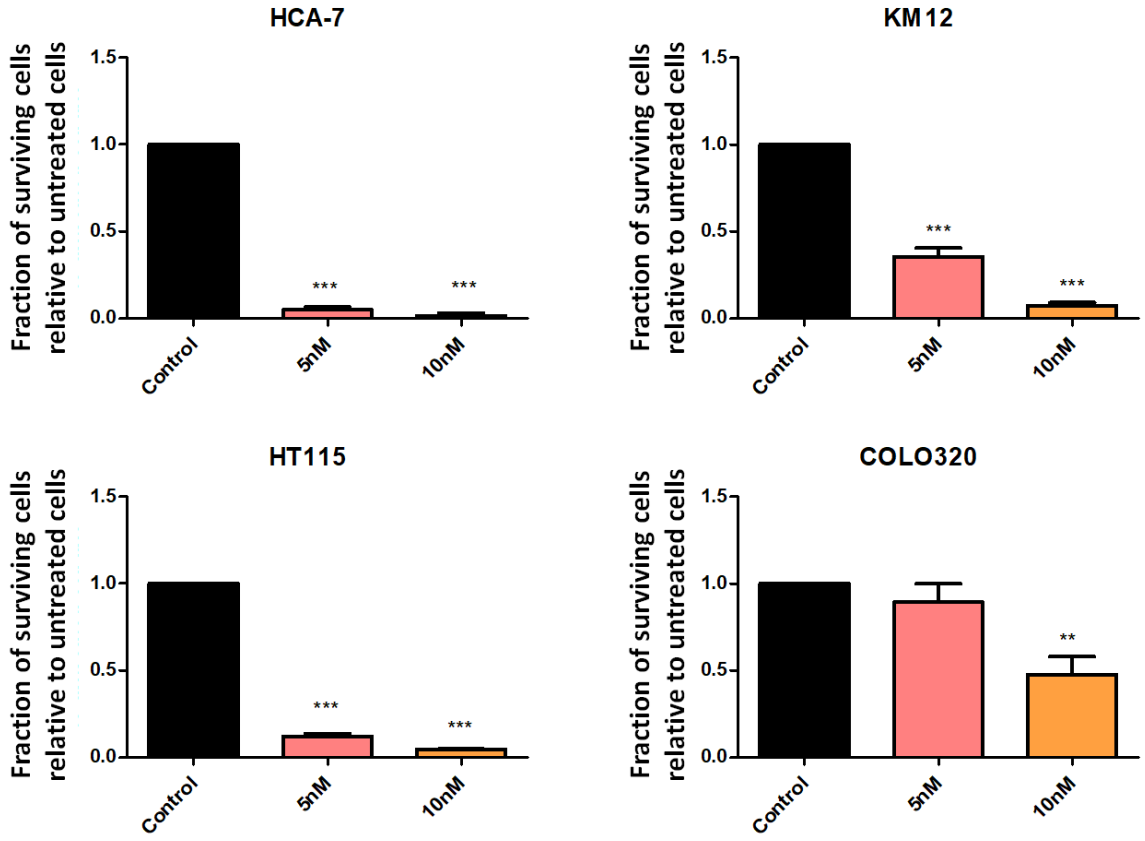

Figure 5.4: Cell viability assay of intrinsic Cetuximab-resistant cell lines.

*Intrinsic Cetuximab Resistant cell lines HCA7, KM12, HT115, and Colo320 were treated with Carfilzomib at 5 and 10nM for 3 days. Cell viability was measured using Luminometer. The data are represented by relative change of cell number to untreated cell lines. 1-way ANOVA was performed for overall statistical significance. Tukey's post-test was performed for comparison between treated and untreated cell lines. ** indicates p<0.01, *** indicates p<0.001. Error bars are represented by SEM. n=3*

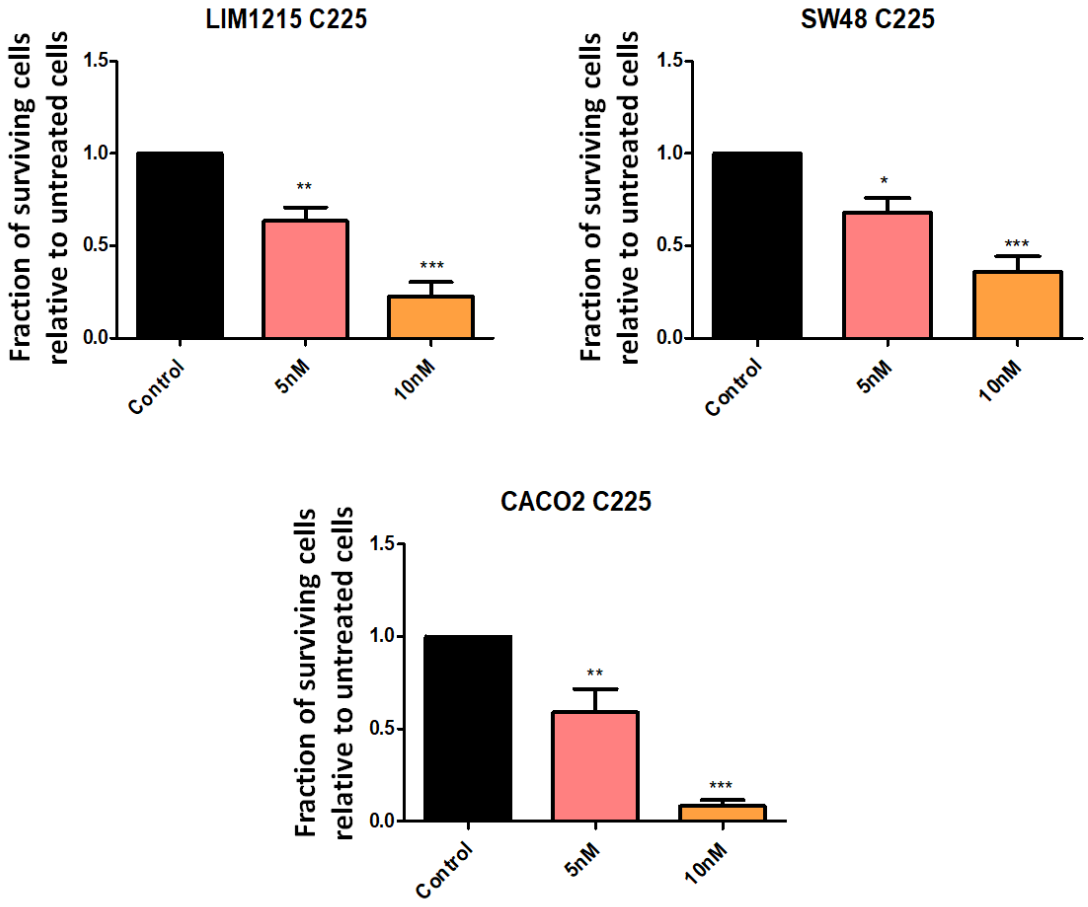

Figure 5.5: Cell viability assay of acquired Cetuximab-resistant cell lines.

*Acquired Cetuximab Resistant cell lines LIM1215 C225, SW48 C225 and CACO2 C225 were treated with Carfilzomib at 5 and 10nM for 3 days. Cell viability was measured using Luminometer. The data are represented by relative change of cell number to untreated cell lines. 1-way ANOVA was performed for overall statistical significance. Tukey's post-test was performed for comparison between treated and untreated cell lines. ** indicates p<0.01, *** indicates p<0.001. Error bars are represented by SEM. n=3*

5.2.3. Carfilzomib Reduce Colony Forming Ability

As Carfilzomib was able to inhibit proliferation very potently, we hypothesized that Carfilzomib would have similar inhibitory effect on colony formation. We further investigated this ability by performing colony formation assay. Two control groups were used which were untreated and Cetuximab treated cells. **Figure 5.6** showed the colonies formed under the challenged of Cetuximab and Carfilzomib. All resistant cells were unable to form any colonies when treated with Carfilzomib as compared to Cetuximab treated. The effect of Carfilzomib was similar across all cell lines.

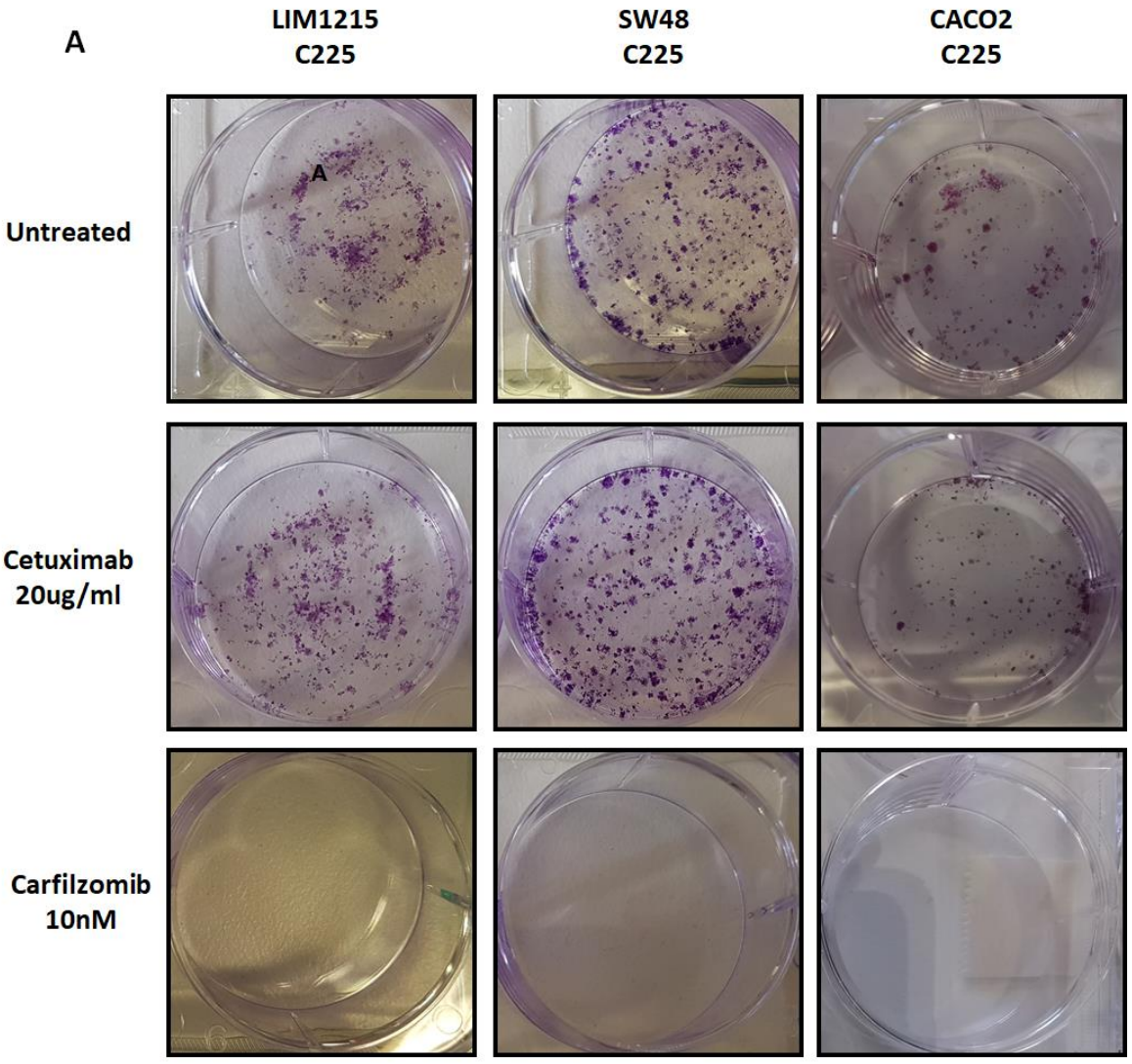
A
LIM1215 C225
SW48 C225
CACO2 C225
Untreated
Cetuximab 20ug/ml
Carfilzomib 10nM
A

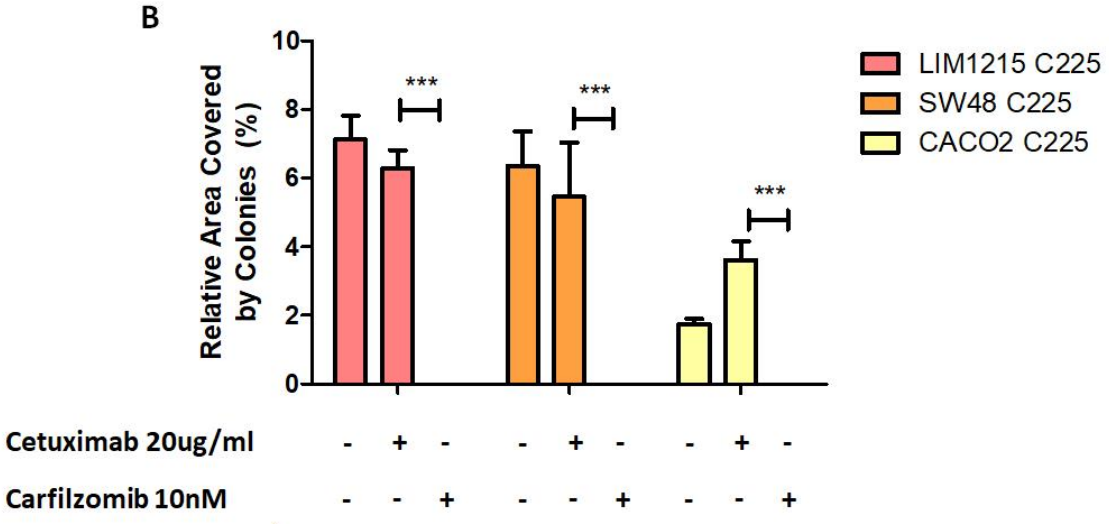
B
Relative Area Covered by Colonies (%)
10
8
6
4
2
0
***
***
***
LIM1215 C225
SW48 C225
CACO2 C225
Cetuximab 20ug/ml - + - - + - - + -
Carfilzomib 10nM - - + - - + - - +

Figure 5.6: Colony formation assay.

*(A) LIM1215 C225, SW48 C225, and CACO2 C225 were seeded at concentration of 1000 cells/ml and grown for 7 days. The colonies were treated with Cetuximab (20ug/ml) and Carfilzomib (10nM). Crystal violet staining was performed, and images were taken. (B) Analysis of colony efficiency was done using ImageJ. The data presented in form percentage of area covered by cells colony. 2-way ANOVA was carried out for overall statistical significance. Post-hoc test, Bonferroni's test was performed for significance parental and resistant cells; *** indicates p<0.05. Error bars are represented by SEM. n=3*

5.2.4. Carfilzomib have no effect on Cell Migration

Carfilzomib has shown to have anti-proliferative effect on all resistant cell lines. Next, its properties in affecting migration was investigated. Acquired resistant cells were seeded and treated with Carfilzomib and cell wound assay was performed to assess migration. Over the period of 7 days, no significant differences can be observed between the untreated and treated group (**Figure 5.7**). Furthermore, the rate of wound closing in all cell lines were relatively similar suggesting that Carfilzomib did not affect the migration capability of the resistant cells.

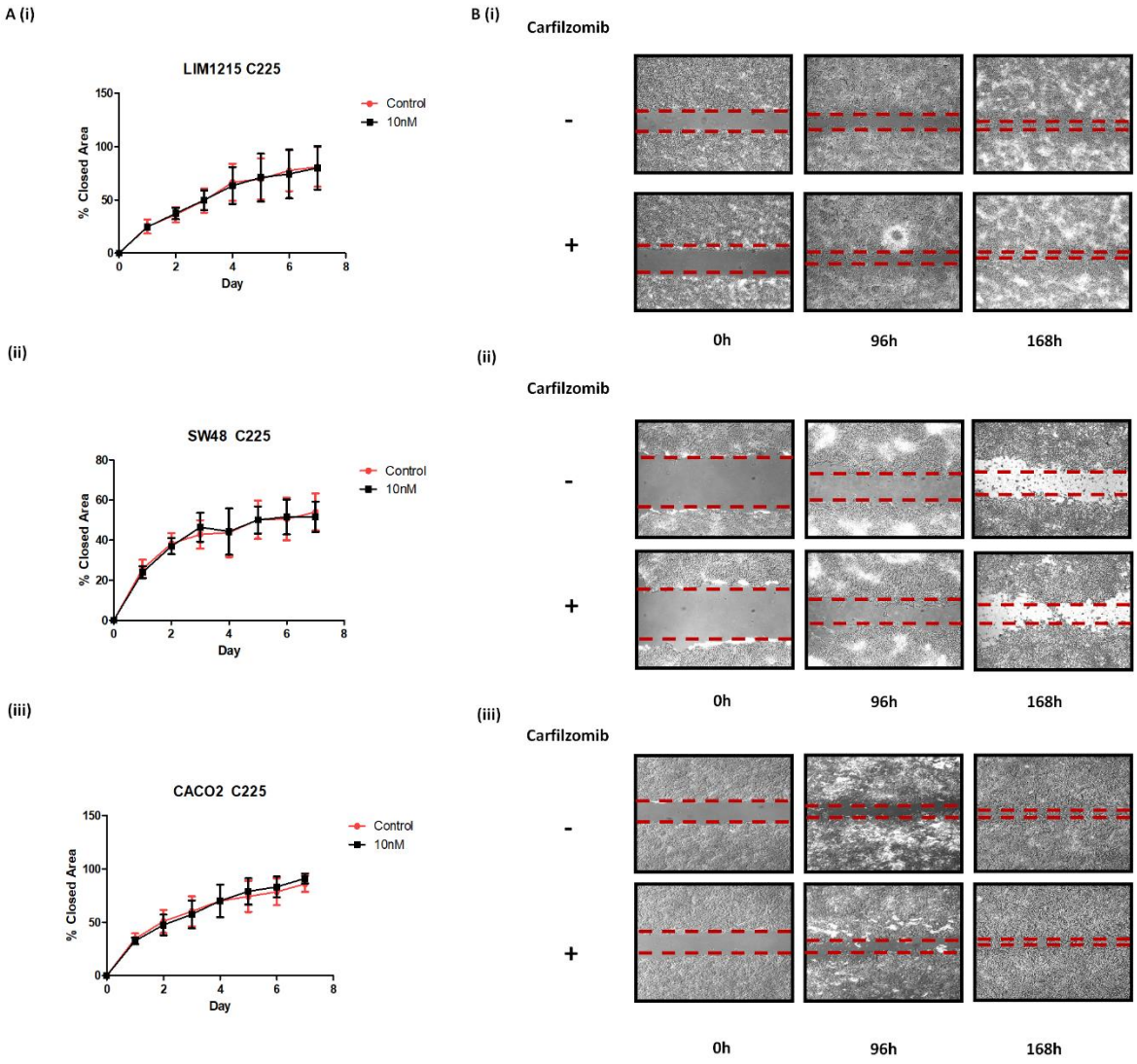

Figure 5.7: Cell scratch assay.

Cell lines LIM1215 C225, SW48 C225 and CACO2 C225 were seeded and grown until 100% confluent before a scratch was made. The cell lines were treated with Carfilzomib (20ug/ml) for 7 days. The area of scratch was measured every day. (A(i-iii)) The graphs represented the % of wound area closed over a period of 7 days between untreated and treated group for each cell lines. (B)(i-iii) The graphical representative of the area of wound closing from 0h to 168h. 2-way ANOVA was carried out for statistical significance. Error bars represented SEM. n=3.

5.2.5. *In vivo* effects of Carfilzomib

The effect of Carfilzomib *in vitro* has been shown to be promising. Next, we tested the efficiency of Carfilzomib using a subcutaneous xenograft mouse model. LIM1215 C225 and SW48 C225 as well as their parental counterpart were injected into mice subcutaneously. The mice were then treated with PBS or Carfilzomib (4mg/kg) as the treated group. **Figure 5.8** showed the growth of the tumor for each cell lines. LIM1215 C225 and SW48 C225 have higher rate of proliferation and achieved maximum tumor growth faster than their parental counterpart (**Figure 5.8 A(i-ii)**). The results corroborate with *in vitro* data where resistant cells grow quicker than parental cells. However, Carfilzomib did not inhibit the growth of either LIM1215 C225 or SW48 C225. This data is contradictory to our *in vitro* results where Carfilzomib had high inhibition of cell growth.

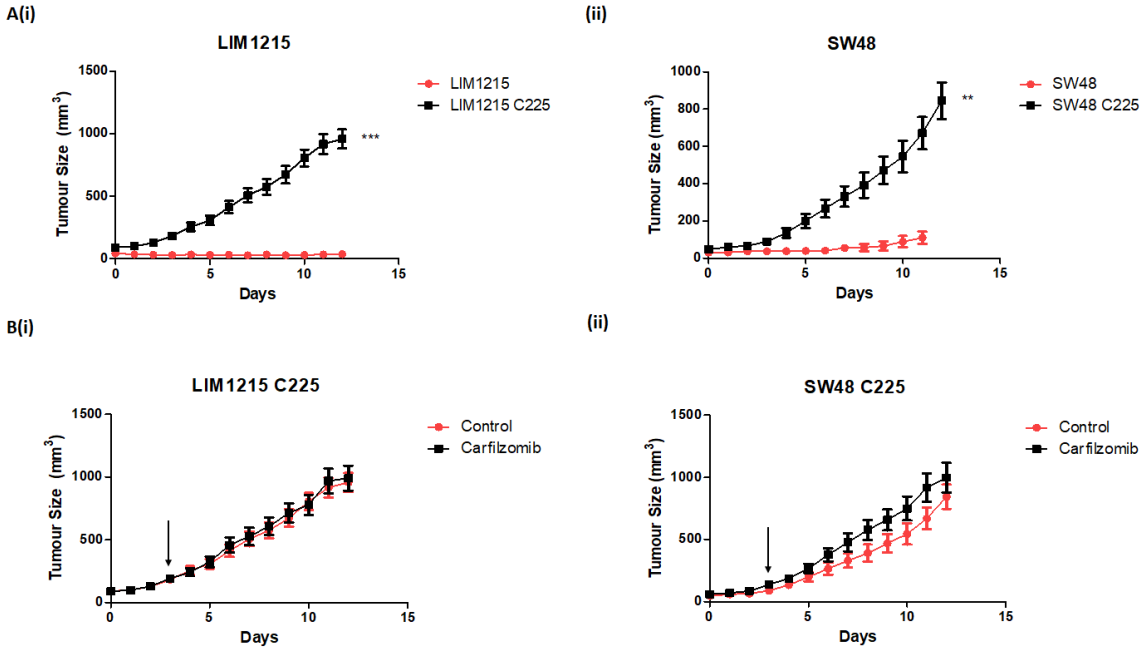

Figure 5.8: Subcutaneous xenograft mouse model.

Cell lines LIM1215 and SW48 (Parental) and LIM1215 C225 and SW48 C225 (Resistant) were injected subcutaneously into mice to observe tumor growth. The mice were either treated with PBS as control or Carfilzomib. The graph showed the tumor size from the first day the tumor was measured. A(i-ii) Graphs comparing between Parental and Resistant cells. B(i-ii) Graphs comparing control group and Carfilzomib treated mice in resistant cells. Arrows indicated the start of treatment. Treatment was administered every 2 days 3 times a week. Error bars represented SEM. n=10

5.2.6. The effect of the combination Cetuximab and Carfilzomib on cell viability.

Our *in vitro* experiments have displayed great inhibitory effect of Carfilzomib on the resistant cells. As Carfilzomib worked even on its own, we aimed to investigate the effect of combination treatment of Cetuximab with Carfilzomib. All resistant cells were treated with Cetuximab and Carfilzomib on their own as control and the combination of both. Cell viability assay was performed to measure their response. The resistant cells showed similar trend for each treatment (**Figure 5.9**). Two doses of Cetuximab and Carfilzomib were used to study the drug treatment efficacy. The combination of Carfilzomib and Cetuximab did not reveal a synergistic effect. The results showed that at two concentrations of Cetuximab and Carfilzomib, Cetuximab did not have an additive effect in inhibiting cell proliferation. It could be suggested that Carfilzomib acts through a different pathway than Cetuximab and they are independent of each other.

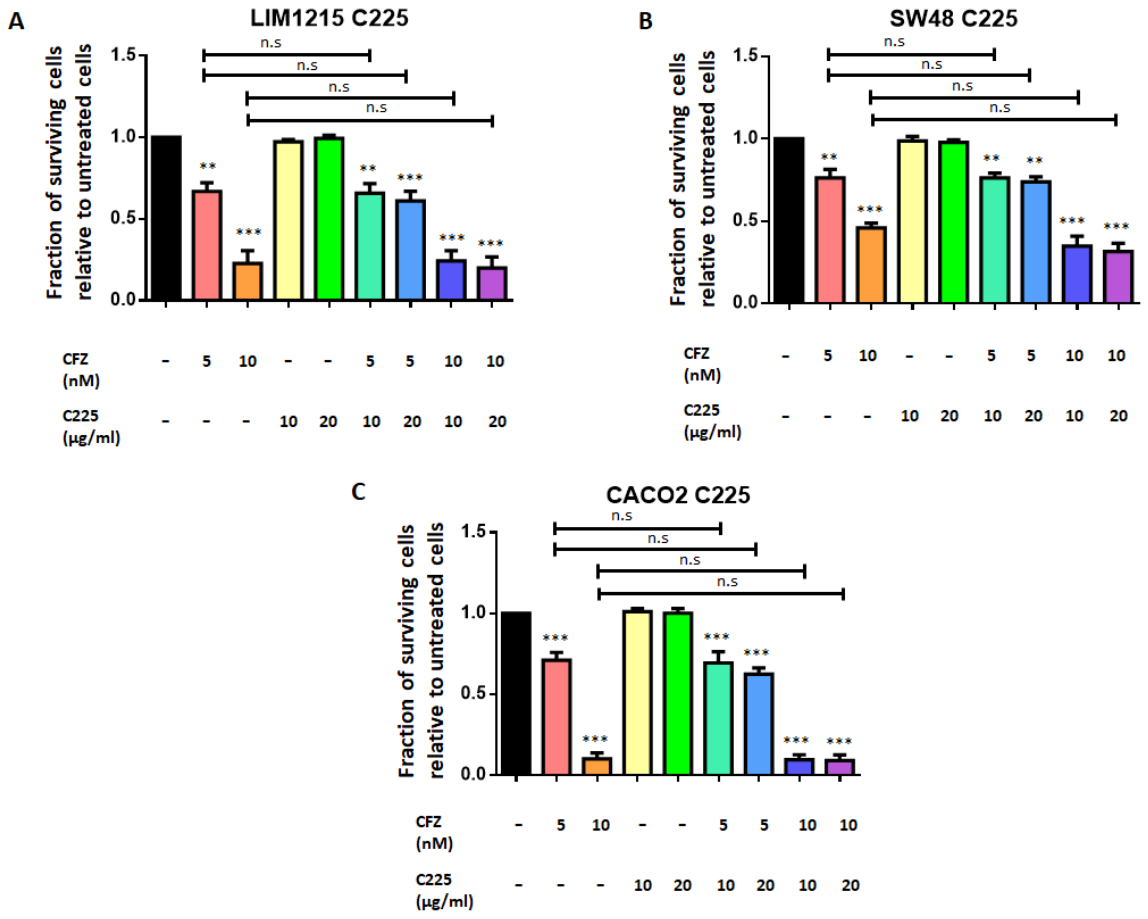

Figure 5.9: Cell viability assay on combination treatment of Carfilzomib and Cetuximab.

*(A-C) Cell lines LIM1215 C225, SW48 C225, and CACO2 C225 were treated with Carfilzomib (CFZ), Cetuximab (C225) and Carfilzomib + Cetuximab for 3 days. Cell viability was measured using Luminometer. The data are represented by relative change of cell number to untreated cell lines. 1-way ANOVA was performed for overall statistical significance. Tukey's post-test was performed for comparison between groups. P-value < 0.05 indicates significance. ** indicates p<0.01, *** indicates p<0.001, n.s indicates not significant. Error bars are represented by SEM. n=3*

5.2.7. The effect of Carfilzomib on our Five Novel Biomarkers

In the previous chapter, we established five potential novel biomarkers that could potentially predict tumor resistance to Cetuximab. As Carfilzomib could inhibit Cetuximab-resistant cells, we next investigated the effect of Carfilzomib on these biomarkers to better elucidate its mechanism of action. All resistant cells were treated with Carfilzomib and protein expression of these five biomarkers are analyzed. Various concentrations of Carfilzomib were used to cover the possible responses of the biomarkers towards the drug. The resistant cells showed different response to Carfilzomib (**Figure 5.10**). The level of NAA25 and CRY2 decreased in LIM1215 after treatment with Carfilzomib. In the other cell lines, the effects were not as significant. SW48 C225 showed a significant reduction in SF3A1 proteins upon treatment compared to the other two cell lines. POLR2A has the most consistent protein expression across the resistant cells. CHAC2 protein expression however was very low for all resistant cells leading to the absence of densitometry analysis. These results displayed the heterogeneity of colorectal cancer cell lines. Next, qPCR was performed to measure the level of RNA expression with concentration of 5nM and 10nM were used in the assay (**Figure 5.11**). No significant differences were observed for all biomarkers in all cell lines at both concentrations. The level of RNA expressed did not corresponded with the amount of protein expressed.

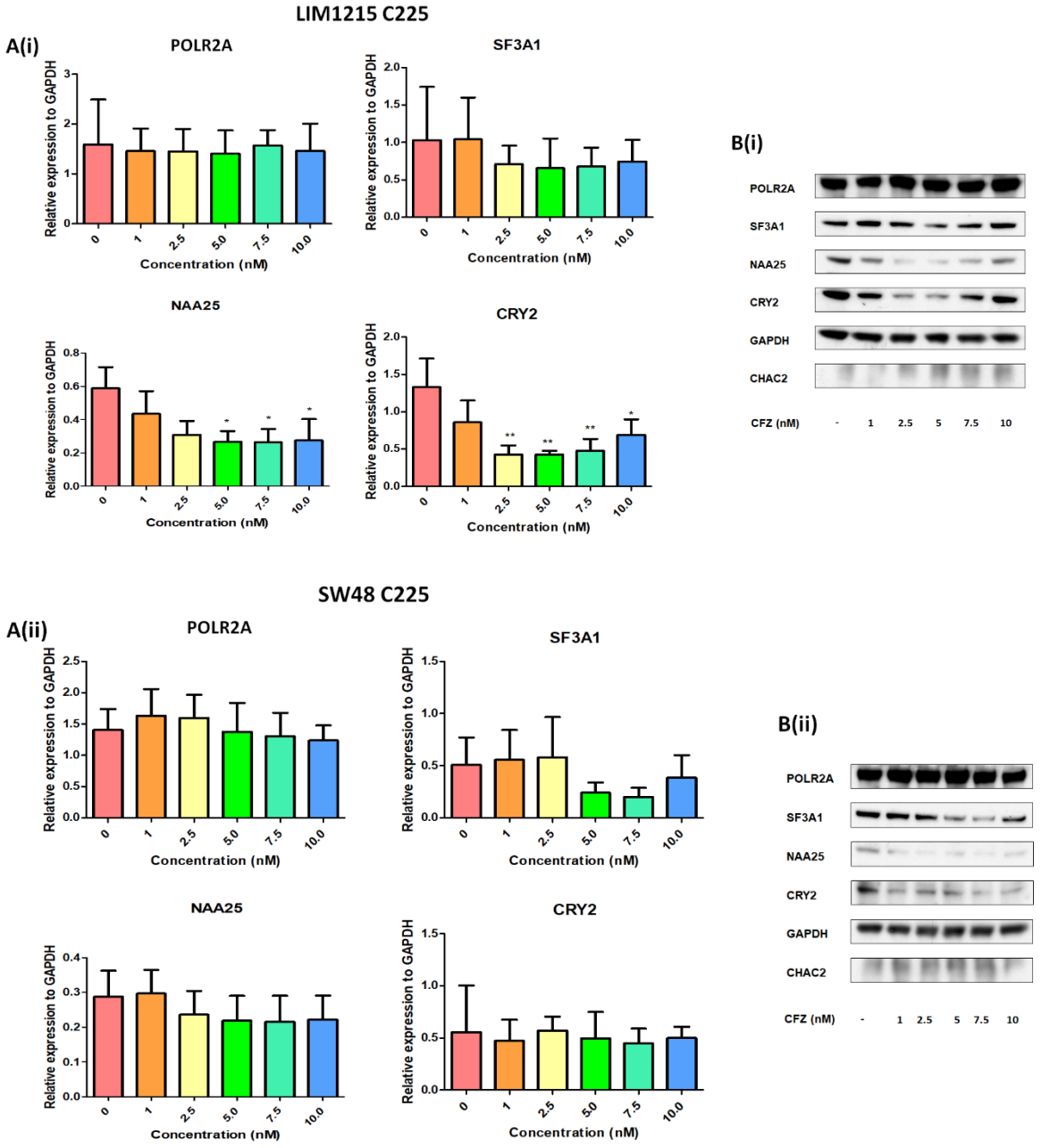
LIM1215 C225
A(i)
POLR2A
SF3A1
NAA25
CRY2
Relative expression to GAPDH
Concentration (nM)
0
1
2.5
5.0
7.5
10.0
B(i)
POLR2A
SF3A1
NAA25
CRY2
GAPDH
CHAC2
CFZ (nM) - 1 2.5 5 7.5 10
SW48 C225
A(ii)
POLR2A
SF3A1
NAA25
CRY2
Relative expression to GAPDH
Concentration (nM)
B(ii)
POLR2A
SF3A1
NAA25
CRY2
GAPDH
CHAC2
CFZ (nM) - 1 2.5 5 7.5 10

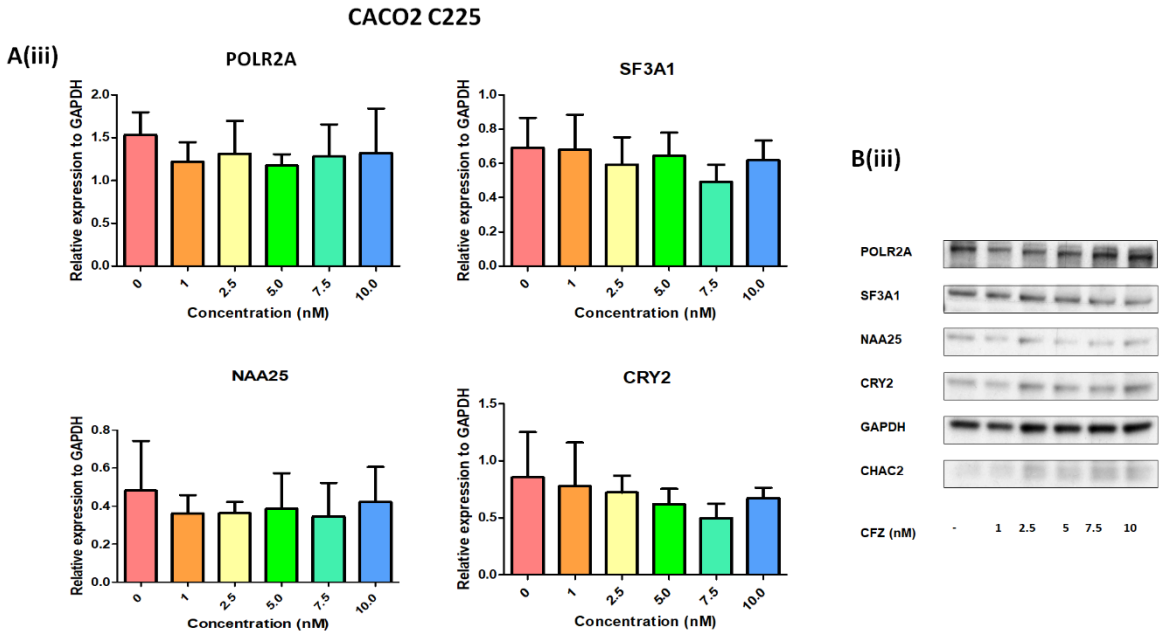

Figure 5.10: The effect of Carfilzomib treatment on five biomarkers.

*(A)(i-iii)) The expression of RPB1, SF3A1, NAA25 and CRY2 were presented as densitometry with the protein expression is relative to loading control, GAPDH. (B)(i-iii) The Western blot representative of the expression of POLR2A, SF3A1, NAA25 and CRY2. The cell lines were treated with Carfilzomib in dose dependent manner. 1-way ANOVA was performed for overall statistical significance. Tukey's post-test was performed for comparison between treated and untreated cell lines. P-value < 0.05 indicates significance. * indicates p<0.05, ** indicates p<0.01. Error bars are represented by SEM. n=3*

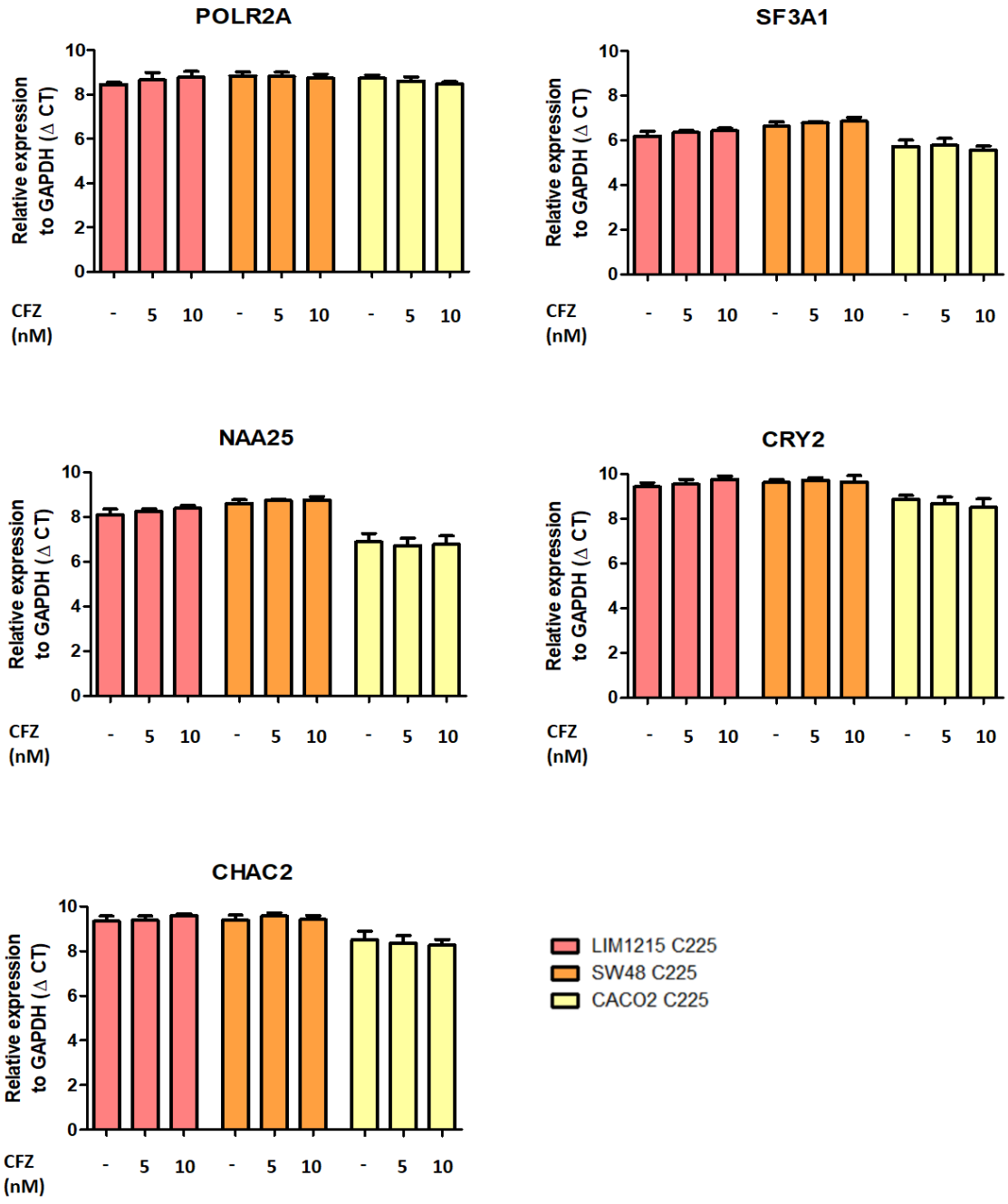

Figure 5.11: Quantitative PCR on five biomarkers.

The expression of five genes (POLR2A, SF3A1, NAA25, CRY2 and CHAC2) were analyzed using quantitative PCR in cell lines LIM1215 C225, SW48 C225 and CACO2 C225. The graphs showed relative gene expression to housekeeping gene GAPDH represented by ΔCt. Lower ΔCt represented high expression and high ΔCt represented low expression. 1-way ANOVA was performed for overall statistical significance for each cell lines. Tukey's post-test was performed for comparison between treated and untreated cell lines. Error bars represented SEM. n=3.

5.3. Discussion

The current treatment for colorectal cancer involves the combination of surgery, chemotherapies, and targeted therapies. Among the targeted agents, Cetuximab is commonly used and approved for the treatment of colorectal cancer and head and neck cancer patients. However, most patients develop resistance to Cetuximab and therefore an alternative drug that could overcome tumor resistance to Cetuximab is needed. This chapter investigated the process of drug screening, validations, and verification of the possible drug mechanism through novel biomarkers previously discussed (**Chapter 4**) for Cetuximab resistance.

The process of discovering new drugs for cancer treatment could be divided into screening a well-established drug that has been approved by the FDA or creating a novel drug from scratch. Developing a drug would take time and requires a significant amount of pre-clinical and clinical evaluation before it can be approved. Screening a library of approved drug will shorten the time and save regulatory costs and time. Repurposing a drug for cancer treatment has been performed previously [262] and we employed a similar method here. A set of drugs that consists of chemotherapeutic and targeted agent were selected for our screen. The cell viability assay was used as the screening method since cancer cells usually has enhanced proliferation. Growth inhibition is an important characteristic for a drug. The concentration of the drugs used in our screen is low to determine the efficacy of the drug at clinically relevant doses. Lower dose is more favorable to patients when translated into clinical trial. The resistant cell lines showed various responses towards the drug. In general, the resistant cells showed no response towards most of the drugs (**Figure 5.1**). Higher doses might influence cell's viability, but it could be because of toxicity of drug not by inhibiting specific function of the cell's specific pathways and those doses may not be relevant to treatment of patients. Certain drugs were able to elevate the proliferation of parental cell lines and lower it in resistant cells. An over-active pathway might be present in the resistant cells that the drugs were able to inhibit thus affecting cell growth. Six drugs were able to achieve this by inhibiting their target(s). Though their ability to reduce viability was significantly higher than other drugs, Carfilzomib was shown to be the most effective.

Carfilzomib has been used as a therapy in treating multiple myeloma with great success. Its use in solid tumor treatment is currently being studied. A proteasome inhibitor could potentially inhibit several cellular processes as the proteasome is vital in removing unwanted cellular debris as well

as regulating specific proteins [255, 259]. Our analysis showed that at a very low concentration, Carfilzomib was able to inhibit cell proliferation by more than 90%. Given the primary function of the drug is to inhibit the proteasome, it could be hypothesized that an accumulation of cellular debris in the cell might cause some toxicity in the cell leading to cell death. The actual mechanism of this process however is still unknown. As lower concentration is more favorable in clinical settings, a dose response curve was performed to determine its IC_{50}. The concentrations for resistant cells were in the nanomolar range which is low and potentially has minimal side effects if applied clinically. Proliferation of all Cetuximab intrinsic and acquired resistant cell lines was inhibited when treated with Carfilzomib at concentrations of 10nM. Other studies had used higher doses of Carfilzomib to inhibit the growth of the cancer cells [261, 263]. However, different cell lines could have different response to Carfilzomib as shown in our results (**Figure 5.4 & 5.5**). Acquired resistant cells have higher tolerance to Carfilzomib at 5nM compared to some of the intrinsic resistant cells.

The effect of Carfilzomib was studied using resistant cells as our model and various *in vitro* analysis was performed. Enhanced proliferative activity of the resistant cell lines marked one of the hallmarks for cancer. Based on our results, the proliferation of resistant cells could be inhibited significantly with Carfilzomib (**Figure 5.5**). Study performed by Tang et al. 2014 showed anti-proliferative effect of Carfilzomib in colorectal cancer [261]. In breast as well as head and neck cancers, Carfilzomib had cytotoxic and apoptotic effect on the cancer cells [253, 264]. Furthermore, the potency of Carfilzomib could be observed in colony formation assays. Our results displayed high inhibition of colony formation under the challenge of Carfilzomib (**Figure 5.6**). Other than proliferation, the migratory capability was also analyzed using a wound healing assay. Upon treatment with Carfilzomib, the resistant cells however showed no differences in the rate of which the wound healed (**Figure 5.7**). Although Carfilzomib managed to inhibit proliferation, it did not affect migration, indicating that it may potentially act on a pathway that only regulates cell proliferation but not motility. This assay, however, was limited in accuracy as proliferation might affects the measurement for cell migration. Although the cells have had its proliferation inhibited by Mitomycin C, the effects might not last the whole period of the experiments.

The growth of the resistant cells is highly elevated when compared to parental cells. Despite that, Carfilzomib was able to inhibit their growth significantly. To better mimic the effect of the drug in man, we tested Carfilzomib in subcutaneous xenograft mouse models. The result obtained

was contradictory to our hypothesis. No reduction was observed in the size of tumor in Carfilzomib treated mice. Several studies have used Carfilzomib in treating solid tumors *in vivo* and they showed significant response towards the drug [257, 258]. Similar method was employed in our study but revealed different results. This difference may be attributed to the properties of the drug itself as well as the characteristic of the resistant cells.

The success of Carfilzomib *in vitro* in our study was significant. While single agent treatments have occasionally been efficacious, combination treatment with other drugs could produce additive or synergistic effects. Bortezomib has been shown to be effective in combination with anti-estrogen agents in estrogen-receptor positive breast cancer [265]. In contrast, a combination of marizomib (Proteasome inhibitor) and vorinostat (Histone deacetylase inhibitor) administered clinically in pancreatic cancer patients was not successful [266]. We hypothesized that a combination of Cetuximab and Carfilzomib would have a synergistic effect on resistant cells. The results however, showed differently. Carfilzomib can significantly reduce the resistant cell's viability however the addition of Cetuximab did not increase cell cytotoxicity. As the pathway for the drug mechanism might be different, inhibition by Carfilzomib did not manage to enhance the effect or restored the function of Cetuximab.

Dissecting the pathway that leads to Cetuximab resistance is important in understanding the drug and the disease itself. The most established biomarker in Cetuximab resistance is KRAS which is a regulator of many important cellular processes. Cells that are resistant to Cetuximab can still express wild-type KRAS. Therefore, another biomarker is needed. 5 novel biomarkers that were discovered previously (**Chapter 4**) were studied further. Carfilzomib mechanism of action involves the inhibition of proteasome leading to inhibition of cell function which eventually leads to cell death. The effect of Carfilzomib on these 5 biomarkers was studied at protein and RNA level. No changes in RNA expression were observed for all cell lines at all level of concentration (**Figure 5.11**). This result showed that Carfilzomib did not work at RNA level but probably at the protein level. The results obtained for protein expression revealed various level of protein response to Carfilzomib. Only one cell line showed a difference in two of the biomarkers when treated with Carfilzomib. All biomarkers have their own specific pathways that may intersect with other pathways that are affected by Carfilzomib. Furthermore, the differences observed in each cell lines could be attributed to heterogeneity of the cell itself. Extensive study must be performed to elucidate this mechanism.

5.4. Conclusion

This chapter focused on the discovery of potential novel drug that could be used to abolish Cetuximab resistance in patients. Cetuximab has been used as one of the standard treatments for colorectal cancer patients but resistance eventually developed. The discovery of a novel drug that has been approved by the FDA would hasten the process of translation to clinical settings. Carfilzomib, a proteasome inhibitor, originally used for treating Multiple Myeloma has potent inhibiting effect on resistant cells. Although the drug was effective *in vitro,* our *in vivo* experiment showed otherwise. Furthermore, combination treatment between Cetuximab and Carfilzomib had no synergistic effect on the resistant cells. In the process of analyzing the resistance mechanism, 5 biomarkers previously discovered showed no significant differences in protein and RNA level when challenged with Carfilzomib. Further investigation is needed to show potential Cetuximab resistance mechanism.

CHAPTER 6:

Overall Discussion and Conclusion

6 Chapter 6: Overall Discussion and Conclusion.

6.1 Overall Discussion

In cancer, many treatments have been trialed with the ultimate aim of successful anti-tumor activity in patients. A combination of surgery, chemotherapy and radiotherapy is the most common treatment for cancer patients. These treatment regiments are often improved when combined with more recent targeted therapy agents. These drugs target potentially critical molecules involved in promoting cancer cell proliferation, invasion, and increased survival. Some patients show good response towards these treatments, but a subset of patients does not response because their tumors are inherently resistant to the treatment. Furthermore, many patients that originally respond develop or acquire resistance often within months thereby rendering the original therapeutic agent ineffective. In colorectal cancer, Cetuximab is currently being used as a treatment option for patients with tumors that express wild-type KRAS, as patients with tumors that harbor mutated *KRAS* do not respond to Cetuximab. Nevertheless, some wild-type KRAS patients are resistance towards Cetuximab. This raises the question: What other pathways or proteins are involved in this Cetuximab resistance? This thesis investigated the possible mechanism that contributes to this resistance and explores a panel of novel drug that could overcome it.

There are many studies that utilize *in vitro* and/or *in vivo* cellular models to evaluate drug resistance mechanisms. [267-269]. Using *in vitro* models initially before proceeding with *in vivo* models is the most common method used although there are studies that only focused on *in vitro* analysis. Our study employed both *in vitro* and *in vivo* models to study the mechanism. This study started with the development of resistant cell lines for *in vitro* analysis. The method for generating resistant cell lines has been used in other studies and have shown to successfully resemble biological properties clinically [270, 271]. Our cell lines were Cetuximab-resistant after 6 months of continuous exposure to Cetuximab in culture. (**Chapter 3, Figure 3.1**). Long-term treatment is required to select for drug-resistance populations. The sub-population that we generated after long-term exposure to Cetuximab could be a combination of intrinsically resistant cells in the original population and resistant cells that have acquired potential alterations and/or mutations

due to the challenge of Cetuximab. These differences could be determined by performing genome sequencing comparing the Cetuximab-sensitive parental and Cetuximab-resistant cells. Nevertheless, the composition of the cells genetically would not matter as we were trying to mimic the cells found in patients after Cetuximab treatment. Therefore, the genetic profile of our resistance cells could theoretically be similar to those found in Cetuximab resistant patients. By developing these resistant cell lines, we have created our own cellular models of tumor resistance to Cetuximab, which we have utilized here and in future experiments.

The hallmarks of cancer include the capability of the cancer cells to sustain proliferation, activating invasion and metastasis and resisting cell death [272]. Changes to these features were assessed in this study in order to characterize potential differences in the Cetuximab-resistant cell lines. Resistant cells are expected to maintain proliferation, migration, and growth in the presence of an inhibitor; in this case Cetuximab. Our results support this hypothesis showing an increase in growth, migration, and colony formation ability and importantly a reduced effect of Cetuximab. (**Chapter 3, Figure 3.3-3.10).** There are many studies that have developed resistant cell lines to study resistance mechanism [218, 219, 271]. However, they did not perform a thorough characterization of their resistant cells. Antoni et al. 2015 generated Cetuximab resistant cell lines for colorectal cancer cells and did only dose-dependent curves as comparison between parental and resistant cells [220]. Similarly, Boeckx et al. 2015 showed the enhanced proliferative effect in resistance cells through proliferation assay [271]. Nevertheless, they did a genome-wide profiling of the resistant cells as part of the characterization which provided a variety of information on the properties of the cells. Our study includes a thorough *in vitro* characterization of our Cetuximab-resistant cell's properties using three genetically differing human colon cancer cell lines. Even though a proteomic analysis was performed on one of the cell lines, a genome-wide analysis on other cell line would provide an improved global understanding of the molecular differences between resistant and Cetuximab-sensitive parental cells. Overall, this study lay out more characteristics of a Cetuximab resistant cells for a more complete profile which could serve as a foundation for future studies (explored in subsequent chapters of this thesis).

As mention previously, some wild-type KRAS patients do not respond to Cetuximab despite no mutation being detected in the KRAS protein [251]. Therefore, other signaling pathways/or alternative mechanisms must be activated as an alternative pathway in inhibiting the activity of Cetuximab. Our hypothesis was that STAT3 plays a role in mediating Cetuximab resistance in

colorectal cancer. We tested this hypothesis in **Chapter 3** and initially, the elevated level of phospho-STAT3 protein level supports our hypothesis (**Chapter 3, Figure 3.11**). However, further investigation using STAT3 knocked down methodology showed that STAT3 did not play a role in mediating Cetuximab resistance in these three resistance cell lines (**Chapter 3, Figure 3.13**). Our results were partly different when compared to other studies. A study on Cetuximab resistance head and neck cancer showed similar results in term of elevated phospho-STAT3 but cell growth of their resistance cells was inhibited by using STAT3 decoy [273]. Another study on head and neck cancer also revealed that knocking down STAT3 resulted in increased apoptosis even in the absence of Cetuximab in their resistant cells [274]. In addition, STAT3 inhibition reduced the growth of the resistant cells and displayed synergistic effect with Cetuximab treatment. Our study successfully knocked down *STAT3* expression, but this reduced *STAT3* expression did not change cell viability with or without Cetuximab treatment, suggesting that STAT3 may not play a key role in the Cetuximab resistance seen in our cells and that an alternative pathway(s) may be responsible for this resistance. However, more assays targeting several parameters such as migration and colony formation need to be performed to further confirmed this hypothesis. Besides the JAK/STAT3 signaling pathway, PI3K-AKT and RAS-MAPK signaling pathways are the 2 well-studied signaling pathways downstream of EGFR. According to De Roock et al. 2010 mutations in *PIK3CA* has been shown to be a predictive marker for Cetuximab resistance [113]. Analyzing the changes of the protein involved could potentially shed more light on the mechanism. Despite our attempts to knockdown AKT and ERK1/2 in our study (**Chapter 3, Figure 3.14**), the results were not conclusive thereby requiring future investigation. We can only speculate the possible pathways that drive tumor cell resistance to Cetuximab. For instance, there are studies that report activation and amplification of MET receptor as a possible mechanism of resistance to Cetuximab [241, 275]. Similar to EGF receptor, MET transmits its cellular signal through RAS/MAPK and PI3K/AKT pathways [276]. Furthermore, HER2 which is part of the EGFR family was also shown to be amplified and associated with Cetuximab resistance in tumor xenograft model [277].

The heterogeneity of cancer cells has led to many proposed mechanisms for tumor resistance caused by a therapeutic agent such as Cetuximab [117, 241, 278, 279]. In our study, we discovered several genes that were differentially expressed in intrinsically Cetuximab-resistant cells compared to Cetuximab-sensitive cells using RNA-seq methodology (**Chapter 4, Figure 4.4**). However, there are limitations that were determined in this analysis. The data was obtained externally from a collaborator which could have affected our gene expression analysis. Although the cell lines used

were the same, some conditions could play a role in influencing the results such as the way the cell lines were maintained including varying media constituents, cell confluency and serum concentration that may have differed to our conditions when performing our validation experiments. Furthermore, the data obtained has been normalized, taking out the sequencing depth from the analysis. This would affect the comparison between samples given that sequencing depth can be different according to samples. Highly heterogenous samples can skew the count distribution thus normalizing method such as TMM, DESeq and UpperQuartile would be used as they ignore highly variable features [280-282]. However, these pipeline methods require raw data before being normalized and analyzed for gene expression, so we were restricted with our analytical methodology. Through this study, we have utilized XLSTAT which is an addition to the Microsoft XL software that allowed us to perform differential gene expression analysis using the normalized data. As this method could also exclude the highly variable features for the analysis, it was the most appropriate protocol.

Among the five genes that were selected for further analysis, our subsequent cell biology-based analysis demonstrated that only *CRY2* could act as a potential biomarker for Cetuximab resistance. CRY2 is part of the circadian clock protein which is not widely studied in the area of cancer. Mocellin et al. 2018 performed a pathway analysis using adaptive rank truncated product (ARTP) method and discovered CRY2 to be associated with the risk of breast and lung cancer [283]. A study conducted on colorectal cancer patients revealed that overexpression of *CRY2* correlate with patient's poor survival [165]. The association of CRY2 with cancer which was discovered in several studies subsequently examined the function(s) of CRY2 in the cancer setting. *CRY2* knock down by siRNA facilitated the differentiation of osteoblasts by down-regulating several important genes [284]. However, the role of CRY2 in mediating resistance to targeted therapeutics such as Cetuximab has not been reported. We can only speculate on the exact mechanism of how CRY2 is involved in mediating Cetuximab resistance. Given that CRY2 was shown to have some effect in regulating genes involved in cell cycle progression [166], any alteration in the gene could affect cell proliferation. In addition, Fang et al. 2015 showed that knocking down *CRY2* increase the cell's sensitivity towards oxaliplatin suggesting a potential role in resistance to chemotherapy. [165]. In osteosarcoma cells, *CRY2* knockdown led to the inhibition of cell proliferation and migration [285]. In contrast, Huber et al. 2016 showed elevated level of proliferation and colony formation in the absence of *CRY2* expression in fibroblasts [168]. These two studies gave two contradictory observations regarding the abolishment of CRY2 functions. It could be due to fact that it was

performed in two different models. Enhancement of proliferation and CRY2 level are the characteristics of our resistant cells which would predict that *CRY2* knockdown would result in a lower proliferation rate. However, unsuccessful knockdown became the barrier in studying the function of CRY2 (**Chapter 4, Figure 4.9**). The roles of CRY2 in cancer are still being studied but the disparity found in previous reports makes it a very obscure area of research. Nevertheless, our study in the role of CRY2 specifically in cancer would expand the current knowledge that we have regarding the molecule.

In addition to aiming to identify novel biomarkers for tumor resistance to Cetuximab, we also explored possible novel drug(s) that could overcome or bypass Cetuximab resistance. In **Chapter 5**, a screen of 38 FDA-approved drugs was conducted which revealed Carfilzomib as the most potent agent in blocking Cetuximab-resistant cell proliferation. The original rationale behind the development of Carfilzomib was to overcome Bortezomib resistance in multiple myeloma [203, 256]. However, Carfilzomib has been repurposed to treat other types of cancer. Zarei et al. 2019 demonstrated synergistic effect of Carfilzomib in combination with cisplatin in cisplatin-resistance ovarian carcinoma cancer cells [269]. In KRAS mutant colorectal cancer, Carfilzomib was shown to be effective in combination with Bcl-xl antagonist in inducing apoptosis [286]. In addition, Carfilzomib and Bortezomib both caused cell death in lapatinib-resistance breast cancer cells [287]. The effect of Carfilzomib was promising both in combination with other drugs and as a single agent. Our study showed significant anti-proliferation effect on Cetuximab resistant cells as a monotherapy though no synergistic effect was observed when in combination with Cetuximab (**Chapter 5, Figure 5.9**). The results, however, could not be replicated in our xenograft model using two different Cetuximab resistant cell lines. The drug delivery method used in our study was via the intraperitoneal route using the normalized dose used in patients. Similar method was employed by Jarauta et al. 2016 in their study demonstrating the effect of Carfilzomib on tumor size [288]. Other studies utilized intravenous injection as the method of delivery yielding similar anti-tumor results [261, 289]. There are two reasons which we hypothesized could be the reasons of the drug failed to show any effect. Firstly, the method of delivery for Carfilzomib was not ideal. Carfilzomib is a water-insoluble drug which needs to be diluted in a proper solvent before it can be administered. Solubility plays an important role in achieving the required amount of drug in the systemic circulation of the body. The drug needs to be in an aqueous form before it can be absorbed. Thus, water-insoluble drugs have limitations regarding slow absorption leading to low bioavailability of the drug [290]. One method that is currently being used to improve drug delivery to the tumor is

to package the drug into nanoparticles. Nanoparticles can be designed to control the release of water-insoluble drug such as Carfilzomib over a period of time to ensure prolonged exposure to the drug [291]. By employing this method, the delivery of Carfilzomib could be improved, and the effect could be shown. The second reason is that our resistant cells might be too aggressive. The growth of our Cetuximab-resistant cell lines were many times higher than the parental cells (**Chapter 3, Figure 3.2**). We theorized that the growth of the resistant cells in the xenograft mouse model was potentially too quick for the drug to take effect. We can either increase the dose that was used or increase the frequency of which the treatment is being administered. However, both methods would have significant effect on the mouse which would not be recommended and would not be appropriate clinically. Nevertheless, this study successfully showed significant anti-proliferative effect of Carfilzomib on Cetuximab-resistant cells *in vitro* which would prove to be beneficial to patients with more research.

In this study, we also speculate the resistance mechanism for Cetuximab by hypothesizing that the expression of CRY2 would be affected by Carfilzomib treatment. As discussed previously, CRY2 showed a role in regulating genes related to cell proliferation and is regulated by the F-box protein, FBXW7 that function by targeting CRY2 with ubiquitin for degradation by the proteasome [165, 166]. Carfilzomib inhibits the activity of the proteasome, affecting cellular processes [185] including the function of CRY2. By inhibiting the function of CRY2, two studies showed different results in proliferation. A study performed by Yu et al. 2018 showed that proliferation was inhibited upon *CRY2* knockdown [285] while another study showed losing CRY2 enhances cell' proliferation and stabilizes c-MYC [168]. The relation of CRY2 and Carfilzomib has yet to be studied and our work here discussed potential interaction between them. The proliferation of our resistant cells was inhibited when treated with Carfilzomib and the expression of CRY2 was significantly reduced. Based on the study performed by Yu et al. 2018, we hypothesized that the anti-proliferative effect of Carfilzomib is affected by the low level of CRY2. However, inhibition of proteasome by Carfilzomib should have caused CRY2 protein to be accumulated instead of reduced thus increasing cell apoptosis. Furthermore, Huber et al. 2016 showed that loss of *CRY2* enhances cell proliferation which differs from our observations. They discovered that CRY2 in tandem with FBXL3 protein stimulate c-MYC ubiquitination. We speculate that through c-MYC stabilization when CRY2 is inhibited, it will continuously be activating genes related to cell proliferation [292] thus ensuring cell survival. Therefore, the decrease of CRY2 after Carfilzomib treatment as observed in our study would not have caused the resistant cells to undergo apoptosis but rather survive. Gathered, we

postulate that while Carfilzomib can block proliferation in cells that are resistant to Cetuximab, the mechanism of this reduced proliferation does not involve CRY2. Carfilzomib's mode of action can be further hypothesized through a combination of 1) Inhibition of proteasome leading to accumulation of protein targeted for degradation and 2) Proteins that supposed to be degraded were constitutively active/not active. The proteasome has been known to play a role in regulating several basic cellular processes including proliferation, apoptosis, and differentiation [293]. Regulation of cell cycle involves degradation of proteins including p27, cyclin A, D, and E which are all required for the progression of the cell cycle [294]. Inhibition of the proteasome by Carfilzomib would block the degradation of these proteins thus preventing cells from proliferating. Furthermore, enhancement of cell apoptosis through bcl-2 stabilization would further supports Carfilzomib's mode of action [295]. Therefore, it is likely that Carfilzomib anti-tumor effect is through another mechanism which is independent of CRY2.

6.2 Overall Conclusion

In this study, we have developed and characterized a set of colorectal cell lines that are resistant to Cetuximab. The thorough characterization of these cells provides us the foundation for future studies to investigate tumor resistance to Cetuximab. A much thorough analysis in genomic, proteomics and metabolomics could be done to complete the global profile of Cetuximab-resistant cells. Furthermore, in order to search for biomarkers that predict Cetuximab resistance, we examined the role of STAT3 in resistance. Although other studies showed the potential of STAT3 as a Cetuximab-resistance biomarker, we observed contradicting results. We have determined that STAT3 did not play a major role in mediating tumor resistance in the cells we generated. More investigation needs to be performed to study the exact function of STAT3 in Cetuximab-resistance cells as we did see elevated levels of phosphorylated STAT3 in our Cetuximab-resistant cells compared to the matched Cetuximab-sensitive parental cells. After disproving the STAT3 hypothesize, more novel biomarkers were discovered using RNA-sequencing data. CRY2 was shown to be a potential resistance biomarker but more detailed biochemical and cell biological research needs to be done. Besides that, the other four biomarkers POLR2A, SF3A1, NAA25 and CHAC2 also have the potential of being a Cetuximab resistance biomarker. Each gene has their own specific function and has yet to be investigated in term of treatment resistance. As patients who developed resistant no longer responded to current treatment, we discovered a novel drug, Carfilzomib that is currently being used in the treatment of Multiple myeloma. This drug proved to significantly inhibit Cetuximab-resistant cells *in vitro* but not *in vivo.* More suitable method(s) needs to be used to deliver the drug effectively into the mouse model to exhibit the full effect of Carfilzomib. Taken together, this study provides a Cetuximab resistant model that can be used for further studies coupled with possible resistance mechanism as well as a novel drug to overcome Cetuximab resistance.

7. References

1. Bray, F., et al., *Global cancer statistics 2018: GLOBOCAN estimates of incidence and mortality worldwide for 36 cancers in 185 countries*. 2018. p. 394-424.
2. Australian Inst Hlth, W., *Cancer in Australia: Actual incidence data from 1982 to 2013 and mortality data from 1982 to 2014 with projections to 2017*. 2018. p. 5-15.
3. Glover, M., et al., *Epidemiology of Colorectal Cancer in Average Risk Adults 20-39 Years of Age: A Population-Based National Study.* Digestive Diseases And Sciences, 2019.
4. Marley, A.R. and H. Nan, *Epidemiology of colorectal cancer.* International Journal Of Molecular Epidemiology And Genetics, 2016. **7**(3): p. 105-114.
5. Zhou, Q., et al., *Risk of Colorectal Cancer in Ulcerative Colitis Patients: A Systematic Review and Meta-Analysis.* Gastroenterology Research & Practice, 2019: p. 1-11.
6. Canavan, C., K.R. Abrams, and J. Mayberry, *Meta-analysis: colorectal and small bowel cancer risk in patients with Crohn's disease.* Alimentary Pharmacology & Therapeutics, 2006. **23**(8): p. 1097-1104.
7. Roos, V.H., et al., *Effects of Family History on Relative and Absolute Risks for Colorectal Cancer: A Systematic Review and Meta-Analysis.* Clinical Gastroenterology and Hepatology, 2019. **17**(13): p. 2657-2667.
8. Aleksandrova, K., et al., *Combined impact of healthy lifestyle factors on colorectal cancer: a large European cohort study.* BMC Medicine, 2014. **12**(1): p. 168.
9. Slattery, M.L., *Physical Activity and Colorectal Cancer.* Sports Medicine, 2004. **34**(4): p. 239-252.
10. Robertson, D.J. *ABC of Colorectal Cancer*. 2012. United States: ELSEVIER SCIENCE B.V. AMSTERDAM.
11. Martinez-Useros, J. and J. Garcia-Foncillas, *Obesity and colorectal cancer: molecular features of adipose tissue.* Journal Of Translational Medicine, 2016. **14**: p. 12.
12. Kinzler, K.W. and B. Vogelstein, *Lessons from hereditary colorectal cancer.* Cell, 1996. **87**(2): p. 159-170.
13. Petersen, G.M., J. Slack, and Y. Nakamura, *Screening guidelines and premorbid diagnosis of familial adenomatous polyposis using linkage.* Gastroenterology, 1991. **100**(6): p. 1658-1664.
14. Lamlum, H., et al., *The type of somatic mutation at APC in familial adenomatous polyposis is determined by the site of the germline mutation: a new facet to Knudson's `two-hit' hypothesis.* Nature Medicine, 1999(9): p. 1071.
15. Fearon, E.R. and B. Vogelstein, *A genetic model for colorectal tumorigenesis.* Cell, 1990. **61**(5): p. 759-767.
16. Jarno, D., et al., *Sequential cancer mutations in cultured human intestinal stem cells.* Nature, 2015(7550): p. 43.
17. Fumagalli, A., et al., *Genetic dissection of colorectal cancer progression by orthotopic transplantation of engineered cancer organoids.* Proceedings of the National Academy of Sciences of the United States, 2017(12): p. 2357.
18. Sansom, O.J., et al., *Loss of Apc in vivo immediately perturbs Wnt signaling, differentiation, and migration.* Genes & Development, 2004. **18**(12): p. 1385-1390.
19. Reya, T. and H. Clevers, *Wnt signalling in stem cells and cancer*. 2005, Nature Publishing Group: Great Britain. p. 843.

20. Komiya, Y. and R. Habas, *Wnt signal transduction pathways*. 2008, LANDES BIOSCIENCE: United States. p. 68.
21. Minde, D.P., et al., *Messing up disorder: how do missense mutations in the tumor suppressor protein APC lead to cancer?* Molecular Cancer, 2011. **10**: p. 101-101.
22. Clevers, H., *Wnt/beta-catenin signaling in development and disease.* Cell, 2006. **127**(3): p. 469-480.
23. Hampel, H., et al., *Feasibility of screening for Lynch syndrome among patients with colorectal cancer.* Journal Of Clinical Oncology: Official Journal Of The American Society Of Clinical Oncology, 2008. **26**(35): p. 5783-5788.
24. Brosens, L.A.A., G.J.A. Offerhaus, and F.M. Giardiello, *Hereditary Colorectal Cancer: Genetics and Screening.* The Surgical clinics of North America, 2015. **95**(5): p. 1067-1080.
25. H T, L., et al., *Review of the Lynch syndrome: history, molecular genetics, screening, differential diagnosis, and medicolegal ramifications.* Clinical Genetics, 2009(1): p. 1.
26. Rustgi, A.K., *The genetics of hereditary colon cancer.* Genes & Development, 2007. **21**(20): p. 2525-2538.
27. Markowitz, A.J. and S.J. Winawer, *Management of colorectal polyps.* CA: A Cancer Journal for Clinicians, 1997. **47**(2): p. 93-112.
28. Edelstein, D.L., et al., *Rapid Development of Colorectal Neoplasia in Patients With Lynch Syndrome.* Clinical Gastroenterology and Hepatology, 2011. **9**(4): p. 340-343.
29. E, V.C., et al., *Metastatic colorectal cancer: ESMO Clinical Practice Guidelines for diagnosis, treatment and follow-up†.* Annals of Oncology, 2014(suppl_3 Suppl 1): p. iii1.
30. Yang, Y.-F., et al., *Overall survival of patients with KRAS wild-type tumor treated with FOLFOX/FORFIRI±cetuximab as the first-line treatment for metastatic colorectal cancer: A meta-analysis.* Medicine, 2017. **96**(12): p. e6335-e6335.
31. Munker, S., et al., *Chemotherapy for metastatic colon cancer: No effect on survival when the dose is reduced due to side effects.* BMC Cancer, 2018. **18**(1): p. 455.
32. Douillard, J.-Y., et al., *Panitumumab-FOLFOX4 treatment and RAS mutations in colorectal cancer.* The New England Journal Of Medicine, 2013. **369**(11): p. 1023-1034.
33. Chen, D., et al., *FOLFOX plus anti-epidermal growth factor receptor (EGFR) monoclonal antibody (mAb) is an effective first-line treatment for patients with RAS-wild left-sided metastatic colorectal cancer: A meta-analysis.* Medicine (Baltimore), 2018. **97**(10): p. e0097.
34. Andre, T., et al., *Multicenter phase II study of bimonthly high-dose leucovorin, fluorouracil infusion, and oxaliplatin for metastatic colorectal cancer resistant to the same leucovorin and fluorouracil regimen.* J Clin Oncol, 1999. **17**(11): p. 3560-8.
35. Jonker, D., et al., *Role of oxaliplatin combined with 5-fluorouracil and folinic acid in the first- and second-line treatment of advanced colorectal cancer.* Current oncology (Toronto, Ont.), 2006. **13**(5): p. 173-184.
36. Pitot, H.C., et al., *N9841: A randomized phase III equivalence trial of irinotecan (CPT-11) versus oxaliplatin/5-fluorouracil (5FU)/leucovorin (FOLFOX4) in patients (pts) with advanced colorectal cancer (CRC) previously treated with 5FU.* Journal of Clinical Oncology, 2005. **23**(16_suppl): p. 3506-3506.
37. Cassidy, J., et al., *Randomized phase III study of capecitabine plus oxaliplatin compared with fluorouracil/folinic acid plus oxaliplatin as first-line therapy for metastatic colorectal cancer.* J Clin Oncol, 2008. **26**(12): p. 2006-12.
38. Haller, D.G., et al., *Capecitabine plus oxaliplatin compared with fluorouracil and folinic acid as adjuvant therapy for stage III colon cancer.* J Clin Oncol, 2011. **29**(11): p. 1465-71.

39. Mamo, A., et al., *Retrospective analysis of the effect of CAPOX and mFOLFOX6 dose intensity on survival in colorectal patients in the adjuvant setting.* Curr Oncol, 2016. **23**(3): p. 171-7.
40. Dela Cruz, C.S., L.T. Tanoue, and R.A. Matthay, *Lung cancer: epidemiology, etiology, and prevention.* Clin Chest Med, 2011. **32**(4): p. 605-44.
41. Warner, K.E. and D. Mendez, *Tobacco control policy in developed countries: yesterday, today, and tomorrow.* Nicotine Tob Res, 2010. **12**(9): p. 876-87.
42. Wynder, E.L., *Tobacco as a cause of lung cancer: some reflections.* Am J Epidemiol, 1997. **146**(9): p. 687-94.
43. Office of the Surgeon, G., S. Office on, and Health, *Reports of the Surgeon General*, in *The Health Consequences of Smoking: A Report of the Surgeon General*. 2004, Centers for Disease Control and Prevention (US): Atlanta (GA).
44. Papadopoulos, A., et al., *Heavy smoking and lung cancer: Are women at higher risk? Result of the ICARE study.* British Journal of Cancer, 2014. **110**(5): p. 1385-1391.
45. Zang, E.A. and E.L. Wynder, *Differences in lung cancer risk between men and women: examination of the evidence.* J Natl Cancer Inst, 1996. **88**(3-4): p. 183-92.
46. Flanders, W.D., et al., *Lung Cancer Mortality in Relation to Age, Duration of Smoking, and Daily Cigarette Consumption.* Cancer Research, 2003. **63**(19): p. 6556.
47. Pesch, B., et al., *Cigarette smoking and lung cancer--relative risk estimates for the major histological types from a pooled analysis of case-control studies.* International journal of cancer, 2012. **131**(5): p. 1210-1219.
48. Varghese, A.M., et al., *Lungs Don't Forget: Comparison of the KRAS and EGFR Mutation Profile and Survival of Collegiate Smokers and Never Smokers with Advanced Lung Cancers.* Journal of Thoracic Oncology, 2013. **8**(1): p. 123-125.
49. Herbst, R.S., J.V. Heymach, and S.M. Lippman, *Lung cancer.* N Engl J Med, 2008. **359**(13): p. 1367-80.
50. Goldstraw, P., et al., *Non-small-cell lung cancer.* Lancet, 2011. **378**(9804): p. 1727-40.
51. Pelosi, G., et al., *Large cell carcinoma of the lung: a tumor in search of an author. A clinically oriented critical reappraisal.* Lung Cancer, 2015. **87**(3): p. 226-31.
52. Le Calvez, F., et al., *TP53 and KRAS mutation load and types in lung cancers in relation to tobacco smoke: distinct patterns in never, former, and current smokers.* Cancer Res, 2005. **65**(12): p. 5076-83.
53. Ridanpaa, M., et al., *Genetic alterations in p53 and k-ras in lung-cancer in relation to histopathology of the tumor and smoking history of the patient.* Int J Oncol, 1994. **5**(5): p. 1109-17.
54. Rudin, C.M., et al., *Lung cancer in never smokers: molecular profiles and therapeutic implications.* Clin Cancer Res, 2009. **15**(18): p. 5646-61.
55. Shigematsu, H., et al., *Clinical and biological features associated with epidermal growth factor receptor gene mutations in lung cancers.* J Natl Cancer Inst, 2005. **97**(5): p. 339-46.
56. Zhang, Z., et al., *Late occurrence of K-ras gene mutations in the pathogenesis of squamous cell carcinoma of the lung: analysis in sputum.* Anal Quant Cytol Histol, 1996. **18**(6): p. 501-2.
57. Testa, U., G. Castelli, and E. Pelosi, *Lung Cancers: Molecular Characterization, Clonal Heterogeneity and Evolution, and Cancer Stem Cells.* Cancers (Basel), 2018. **10**(8): p. 248.
58. Ooi, A.T., et al., *Molecular profiling of premalignant lesions in lung squamous cell carcinomas identifies mechanisms involved in stepwise carcinogenesis.* Cancer Prev Res (Phila), 2014. **7**(5): p. 487-95.
59. Shen, C., et al., *Microsatellite alteration in multiple primary lung cancer.* Journal of thoracic disease, 2014. **6**(10): p. 1499-1505.

60. Jones, G.S. and D.R. Baldwin, *Recent advances in the management of lung cancer.* Clinical medicine (London, England), 2018. **18**(Suppl 2): p. s41-s46.
61. *Chemotherapy in non-small cell lung cancer: a meta-analysis using updated data on individual patients from 52 randomised clinical trials. Non-small Cell Lung Cancer Collaborative Group.* Bmj, 1995. **311**(7010): p. 899-909.
62. Masters, G.A., et al., *Systemic Therapy for Stage IV Non-Small-Cell Lung Cancer: American Society of Clinical Oncology Clinical Practice Guideline Update.* J Clin Oncol, 2015. **33**(30): p. 3488-515.
63. Fakiris, A.J., et al., *Stereotactic body radiation therapy for early-stage non-small-cell lung carcinoma: four-year results of a prospective phase II study.* Int J Radiat Oncol Biol Phys, 2009. **75**(3): p. 677-82.
64. Jorissen, R.N., et al., *Epidermal growth factor receptor: mechanisms of activation and signalling.* Experimental Cell Research, 2003. **284**(1): p. 31-53.
65. Harris, R.C., E. Chung, and R.J. Coffey, *EGF receptor ligands.* Experimental Cell Research, 2003. **284**(1): p. 2-13.
66. Adrain, C. and M. Freeman, *Regulation of receptor tyrosine kinase ligand processing.* Cold Spring Harbor Perspectives In Biology, 2014. **6**(1).
67. Mark A. Lemmon, J.S., and Kathryn M. Ferguson, *The EGFR Family: Not So Prototypical Receptor Tyrosine Kinases.* Cold Spring Harbor Perspectives In Biology, 2014. **4**(6).
68. Kim, J.E., et al., *STAT3 Activation in Glioblastoma: Biochemical and Therapeutic Implications.* Cancers, 2014. **6**(1): p. 376-395.
69. Yang, J., et al., *Novel roles of unphosphorylated STAT3 in oncogenesis and transcriptional regulation.* Cancer Res, 2005. **65**(3): p. 939-47.
70. Braunstein, J., et al., *STATs dimerize in the absence of phosphorylation.* The Journal Of Biological Chemistry, 2003. **278**(36): p. 34133-34140.
71. Xiaokui ZhangBlenis, J., *Requirement of serine phosphorylation for formation of STAT-promoter complexes.* Science, 1995. **267**(5206): p. 1990.
72. Putoczki, T. and M. Ernst, *More than a sidekick: the IL-6 family cytokine IL-11 links inflammation to cancer.* Journal Of Leukocyte Biology, 2010. **88**(6): p. 1109-1117.
73. Auernhammer, C.J., C. Bousquet, and S. Melmed, *Autoregulation of pituitary corticotroph SOCS-3 expression: characterization of the murine SOCS-3 promoter.* Proceedings Of The National Academy Of Sciences Of The United States Of America, 1999. **96**(12): p. 6964-6969.
74. Babon, J.J., L.N. Varghese, and N.A. Nicola, *Inhibition of IL-6 family cytokines by SOCS3.* Seminars in Immunology, 2014. **26**(1): p. 13-19.
75. Duval, D., et al., *The 'PINIT' motif, of a newly identified conserved domain of the PIAS protein family, is essential for nuclear retention of PIAS3L.* FEBS Letters, 2003. **554**(1–2): p. 111-118.
76. Kluge, A., et al., *Protein inhibitor of activated STAT3 expression in lung cancer.* Molecular Oncology, 2011. **5**: p. 256-264.
77. Rajalingam, K., et al., *Ras oncogenes and their downstream targets.* Biochimica et Biophysica Acta (BBA) - Molecular Cell Research, 2007. **1773**(8): p. 1177-1195.
78. McKay, M.M. and D.K. Morrison, *Integrating signals from RTKs to ERK/MAPK.* Oncogene, 2007. **26**(22): p. 3113-3121.
79. Samuels, Y. and K. Ericson, *Oncogenic PI3K and its role in cancer.* Current Opinion In Oncology, 2006. **18**(1): p. 77-82.
80. Miao, B., et al., *Small molecule inhibition of phosphatidylinositol-3,4,5-triphosphate (PIP3) binding to pleckstrin homology domains*. 2010, National Academy of Sciences. p. 20126.

81. Li, H., J. Zeng, and K. Shen, *PI3K/AKT/mTOR signaling pathway as a therapeutic target for ovarian cancer.* Archives Of Gynecology And Obstetrics, 2014. **290**(6): p. 1067-1078.
82. Maehama, T. and J.E. Dixon, *The tumor suppressor, PTEN/MMAC1, dephosphorylates the lipid second messenger, phosphatidylinositol 3,4,5-trisphosphate.* The Journal Of Biological Chemistry, 1998. **273**(22): p. 13375-13378.
83. Françoso, A. and P.U. Simioni, *Immunotherapy for the treatment of colorectal tumors: focus on approved and in-clinical-trial monoclonal antibodies.* Drug Design, Development and Therapy, 2017. **11**: p. 177-184.
84. Van Cutsem, E., et al., *Cetuximab and chemotherapy as initial treatment for metastatic colorectal cancer.* N Engl J Med, 2009. **360**(14): p. 1408-17.
85. Van Cutsem, E., et al., *Fluorouracil, leucovorin, and irinotecan plus cetuximab treatment and RAS mutations in colorectal cancer.* J Clin Oncol, 2015. **33**(7): p. 692-700.
86. Bokemeyer, C., et al., *FOLFOX4 plus cetuximab treatment and RAS mutations in colorectal cancer.* Eur J Cancer, 2015. **51**(10): p. 1243-52.
87. Jonker, D.J., et al., *Cetuximab for the treatment of colorectal cancer.* N Engl J Med, 2007. **357**(20): p. 2040-8.
88. Gibson, T.B., A. Ranganathan, and A. Grothey, *Randomized phase III trial results of panitumumab, a fully human anti-epidermal growth factor receptor monoclonal antibody, in metastatic colorectal cancer.* Clinical Colorectal Cancer, 2006. **6**(1): p. 29-31.
89. Yazdi, M.H., et al., *A comprehensive review of clinical trials on EGFR inhibitors such as cetuximab and panitumumab as monotherapy and in combination for treatment of metastatic colorectal cancer.* Avicenna Journal of Medical Biotechnology (AJMB), 2015. **7**(4): p. 134-145.
90. Herbst, R.S., et al., *Gefitinib in combination with paclitaxel and carboplatin in advanced non-small-cell lung cancer: a phase III trial--INTACT 2.* J Clin Oncol, 2004. **22**(5): p. 785-94.
91. Kris, M.G., et al., *Efficacy of Gefitinib, an Inhibitor of the Epidermal Growth Factor Receptor Tyrosine Kinase, in Symptomatic Patients With Non–Small Cell Lung Cancer: A Randomized Trial.* JAMA: Journal of the American Medical Association, 2003. **290**(16): p. 2149-2158.
92. Cohen, M.H., et al., *United States Food and Drug Administration Drug Approval summary: Gefitinib (ZD1839; Iressa) tablets.* Clinical Cancer Research: An Official Journal Of The American Association For Cancer Research, 2004. **10**(4): p. 1212-1218.
93. Fukuoka, M., et al., *Multi-institutional randomized phase II trial of gefitinib for previously treated patients with advanced non-small-cell lung cancer (The IDEAL 1 Trial) [corrected].* Journal Of Clinical Oncology: Official Journal Of The American Society Of Clinical Oncology, 2003. **21**(12): p. 2237-2246.
94. Thatcher, N., et al., *Gefitinib plus best supportive care in previously treated patients with refractory advanced non-small-cell lung cancer: results from a randomised, placebo-controlled, multicentre study (Iressa Survival Evaluation in Lung Cancer).* The Lancet, 2005. **366**(9496): p. 1527.
95. Kim, E.S., et al., *Gefitinib versus docetaxel in previously treated non-small-cell lung cancer (INTEREST): a randomised phase III trial.* Lancet, 2008. **372**(9652): p. 1809-1818.
96. Yoshioka, H., et al., *Final overall survival results of WJTOG3405, a randomized phase III trial comparing gefitinib versus cisplatin with docetaxel as the first-line treatment for patients with stage IIIB/IV or postoperative recurrent EGFR mutation-positive non-small-cell lung cancer.* Ann Oncol, 2019. **30**(12): p. 1978-1984.
97. Inoue, A., et al., *Updated overall survival results from a randomized phase III trial comparing gefitinib with carboplatin-paclitaxel for chemo-naive non-small cell lung cancer with sensitive EGFR gene mutations (NEJ002).* Ann Oncol, 2013. **24**(1): p. 54-9.

98. Han, J.Y., et al., *First-SIGNAL: first-line single-agent iressa versus gemcitabine and cisplatin trial in never-smokers with adenocarcinoma of the lung.* J Clin Oncol, 2012. **30**(10): p. 1122-8.
99. Mok, T.S., et al., *Gefitinib or carboplatin-paclitaxel in pulmonary adenocarcinoma.* N Engl J Med, 2009. **361**(10): p. 947-57.
100. Pérez-Soler, R., et al., *Determinants of tumor response and survival with erlotinib in patients with non--small-cell lung cancer.* Journal Of Clinical Oncology: Official Journal Of The American Society Of Clinical Oncology, 2004. **22**(16): p. 3238-3247.
101. Shepherd, F.A., et al., *Erlotinib in previously treated non-small-cell lung cancer.* N Engl J Med, 2005. **353**(2): p. 123-132.
102. Rossi, D., et al., *Activity and safety of erlotinib as second- and third-line treatment in elderly patients with advanced non-small cell lung cancer: a phase II trial.* Targeted Oncology, 2010. **5**(4): p. 231-235.
103. Ng, R., et al., *Brief report: retrospective review of efficacy of erlotinib or gefitinib compared to docetaxel as subsequent line therapy in advanced non-small cell lung cancer (NSCLC) following failure of platinum-based chemotherapy.* Lung Cancer (Amsterdam, Netherlands), 2008. **61**(2): p. 262-265.
104. Chen, X., et al., *Clinical perspective of afatinib in non-small cell lung cancer.* Lung Cancer, 2013. **81**(2): p. 155-161.
105. Yap, T.A. and S. Popat, *Toward precision medicine with next-generation EGFR inhibitors in non-small-cell lung cancer.* Pharmacogenomics and Personalized Medicine, 2014. **7**: p. 285-295.
106. Miller, V.A., et al., *Afatinib versus placebo for patients with advanced, metastatic non-small-cell lung cancer after failure of erlotinib, gefitinib, or both, and one or two lines of chemotherapy (LUX-Lung 1): a phase 2b/3 randomised trial.* The Lancet. Oncology, 2012. **13**(5): p. 528-538.
107. Ribeiro Gomes, J. and M.R. Cruz, *Combination of afatinib with cetuximab in patients with EGFR-mutant non-small-cell lung cancer resistant to EGFR inhibitors.* OncoTargets and Therapy, 2015. **8**: p. 1137-1142.
108. Yang, J.C.-H., et al., *Afatinib versus cisplatin-based chemotherapy for EGFR mutation-positive lung adenocarcinoma (LUX-Lung 3 and LUX-Lung 6): analysis of overall survival data from two randomised, phase 3 trials.* The Lancet. Oncology, 2015. **16**(2): p. 141-151.
109. Siegel, R., et al., *Cancer treatment and survivorship statistics, 2012*. 2012, American Cancer Society, Inc. p. 220.
110. Mármol, I., et al., *Colorectal Carcinoma: A General Overview and Future Perspectives in Colorectal Cancer.* International Journal of Molecular Sciences, 2017. **18**(1): p. 1-39.
111. Grady, W.M. and J.M. Carethers, *Genomic and Epigenetic Instability in Colorectal Cancer Pathogenesis*. 2008, Elsevier B.V. p. 1079.
112. Bos, J.L., *ras oncogenes in human cancer: a review.* Cancer Research, 1989. **49**(17): p. 4682-4689.
113. De Roock, W., et al., *Effects of KRAS, BRAF, NRAS, and PIK3CA mutations on the efficacy of cetuximab plus chemotherapy in chemotherapy-refractory metastatic colorectal cancer: a retrospective consortium analysis.* The Lancet. Oncology, 2010. **11**(8): p. 753-762.
114. Lièvre, A., et al., *KRAS mutation status is predictive of response to cetuximab therapy in colorectal cancer.* Cancer Research, 2006. **66**(8): p. 3992-3995.
115. Heinemann, V., et al., *FOLFIRI plus cetuximab versus FOLFIRI plus bevacizumab as first-line treatment for patients with metastatic colorectal cancer (FIRE-3): a randomised, open-label, phase 3 trial.* The Lancet. Oncology, 2014. **15**(10): p. 1065-1075.

116. Pietrantonio, F., et al., *Predictive role of BRAF mutations in patients with advanced colorectal cancer receiving cetuximab and panitumumab: A meta-analysis.* European Journal of Cancer. **51**(5): p. 587-594.
117. Sartore-Bianchi, A., et al., *PIK3CA mutations in colorectal cancer are associated with clinical resistance to EGFR-targeted monoclonal antibodies.* Cancer Research, 2009. **69**(5): p. 1851-1857.
118. Seymour, M.T., et al., *Panitumumab and irinotecan versus irinotecan alone for patients with KRAS wild-type, fluorouracil-resistant advanced colorectal cancer (PICCOLO): a prospectively stratified randomised trial.* Lancet Oncology, 2013. **14**(8): p. 749-759.
119. Sansal, I. and W.R. Sellers, *The biology and clinical relevance of the PTEN tumor suppressor pathway.* Journal Of Clinical Oncology: Official Journal Of The American Society Of Clinical Oncology, 2004. **22**(14): p. 2954-2963.
120. Karapetis, C.S., et al., *PIK3CA, BRAF, and PTEN status and benefit from cetuximab in the treatment of advanced colorectal cancer--results from NCIC CTG/AGITG CO.17.* Clinical Cancer Research: An Official Journal Of The American Association For Cancer Research, 2014. **20**(3): p. 744-753.
121. Okugawa, Y., W.M. Grady, and A. Goel, *Epigenetic Alterations in Colorectal Cancer: Emerging Biomarkers.* Gastroenterology, 2015. **149**(5): p. 1204-1225.e12.
122. Samowitz, W.S., *The CpG island methylator phenotype in colorectal cancer.* The Journal of molecular diagnostics : JMD, 2007. **9**(3): p. 281-283.
123. Toyota, M., et al., *Aberrant methylation in gastric cancer associated with the CpG island methylator phenotype.* Cancer research, 1999. **59**(21): p. 5438-5442.
124. Jover, R., et al., *5-Fluorouracil adjuvant chemotherapy does not increase survival in patients with CpG island methylator phenotype colorectal cancer.* Gastroenterology, 2011. **140**(4): p. 1174-1181.
125. Ouchi, K., et al., *DNA methylation status as a biomarker of anti-EGFR treatment for metastatic colorectal cancer.* Cancer science, 2015. **106**(12): p. 1722-1729.
126. Kita, Y., et al., *Epigenetically regulated microRNAs and their prospect in cancer diagnosis.* Expert Rev Mol Diagn, 2014. **14**(6): p. 673-83.
127. Lu, Y., et al., *lncRNA MIR100HG-derived miR-100 and miR-125b mediate cetuximab resistance via Wnt/β-catenin signaling.* Nat Med, 2017. **23**(11): p. 1331-1341.
128. Sun, L., et al., *miR-302a Inhibits Metastasis and Cetuximab Resistance in Colorectal Cancer by Targeting NFIB and CD44.* Theranostics, 2019. **9**(26): p. 8409-8425.
129. Dobi, E., et al., *Impact of STAT3 phosphorylation on the clinical effectiveness of anti-EGFR-based therapy in patients with metastatic colorectal cancer.* Clinical Colorectal Cancer, 2013. **12**(1): p. 28-36.
130. Haura, E.B., et al., *A pilot study of preoperative gefitinib for early-stage lung cancer to assess intratumor drug concentration and pathways mediating primary resistance.* Journal Of Thoracic Oncology: Official Publication Of The International Association For The Study Of Lung Cancer, 2010. **5**(11): p. 1806-1814.
131. Deeken, J.F., et al., *A phase 1 study of cetuximab and lapatinib in patients with advanced solid tumor malignancies*. 2015, J.B. Lippincott Company. p. 1645.
132. Li, Q., et al., *Nuclear PKM2 contributes to gefitinib resistance via upregulation of STAT3 activation in colorectal cancer.* Scientific Reports, 2015. **5**: p. 16082-16082.
133. Li, L., et al., *Metformin sensitizes EGFR-TKI-resistant human lung cancer cells in vitro and in vivo through inhibition of IL-6 signaling and EMT reversal.* Clinical Cancer Research: An Official Journal Of The American Association For Cancer Research, 2014. **20**(10): p. 2714-2726.

134. Kijima, T., et al., *STAT3 activation abrogates growth factor dependence and contributes to head and neck squamous cell carcinoma tumor growth in vivo.* Cell Growth & Differentiation: The Molecular Biology Journal Of The American Association For Cancer Research, 2002. **13**(8): p. 355-362.
135. Bonner, J.A., et al., *Inhibition of STAT-3 results in greater cetuximab sensitivity in head and neck squamous cell carcinoma.* Radiotherapy and Oncology, 2011. **99**(3): p. 339-343.
136. Chen, W., et al., *NSC 74859-mediated inhibition of STAT3 enhances the anti-proliferative activity of cetuximab in hepatocellular carcinoma.* Liver International: Official Journal Of The International Association For The Study Of The Liver, 2012. **32**(1): p. 70-77.
137. Ung, N., et al., *Anti-EGFR therapeutic efficacy correlates directly with inhibition of STAT3 activity.* Cancer Biology & Therapy, 2014. **15**(5): p. 623-632.
138. Looyenga, B.D., et al., *STAT3 Is Activated by JAK2 Independent of Key Oncogenic Driver Mutations in Non-Small Cell Lung Carcinoma.* PLoS ONE, 2012. **7**(2): p. 1-12.
139. Gao, S.P., et al., *JAK2 inhibition sensitizes resistant EGFR-mutant lung adenocarcinoma to tyrosine kinase inhibitors.* Science Signaling, 2016. **9**(421): p. ra33-ra33.
140. Li, R., et al., *Niclosamide overcomes acquired resistance to erlotinib through suppression of STAT3 in non-small cell lung cancer.* Molecular Cancer Therapeutics, 2013. **12**(10): p. 2200-2212.
141. Yao, Z., et al., *TGF-beta IL-6 axis mediates selective and adaptive mechanisms of resistance to molecular targeted therapy in lung cancer.* Proc Natl Acad Sci USA, 2010. **107**(35): p. 15535-15541.
142. Jung, M.J., et al., *Upregulation of CXCR4 is functionally crucial for maintenance of stemness in drug-resistant non-small cell lung cancer cells.* Oncogene, 2013. **32**(2): p. 209-221.
143. Ioannou, N., et al., *Acquired resistance of pancreatic cancer cells to treatment with gemcitabine and HER-inhibitors is accompanied by increased sensitivity to STAT3 inhibition.* International Journal of Oncology, 2016. **48**(3): p. 908-919.
144. Kaur, A., et al., *ChaC2, an Enzyme for Slow Turnover of Cytosolic Glutathione.* Journal of Biological Chemistry, 2017. **292**(2): p. 638-651.
145. Fujiwara, S., et al., *RipAY, a Plant Pathogen Effector Protein, Exhibits Robust γ-Glutamyl Cyclotransferase Activity When Stimulated by Eukaryotic Thioredoxins.* The Journal Of Biological Chemistry, 2016. **291**(13): p. 6813-6830.
146. Kim, I., W. Xu, and J.C. Reed, *Cell death and endoplasmic reticulum stress: disease relevance and therapeutic opportunities.* Nature Reviews Drug Discovery, 2008. **7**(12): p. 1013-1030.
147. Liu, S., et al., *CHAC2, downregulated in gastric and colorectal cancers, acted as a tumor suppressor inducing apoptosis and autophagy through unfolded protein response.* Cell Death and Disease, 2017. **8**(8): p. e3009.
148. Yasuda, K., et al., *Mdm20 Stimulates PolyQ Aggregation via Inhibiting Autophagy Through Akt-Ser473 Phosphorylation.* PloS One, 2013. **8**(12): p. e82523.
149. Yasuda, K., M. Takahashi, and N. Mori, *Mdm20 Modulates Actin Remodeling through the mTORC2 Pathway via Its Effect on Rictor Expression.* PLoS ONE, 2015. **10**(11): p. 1-19.
150. Hampsey, M., *Molecular genetics of the RNA polymerase II general transcriptional machinery.* Microbiology and molecular biology reviews : MMBR, 1998. **62**(2): p. 465-503.
151. Litingtung, Y., et al., *Growth retardation and neonatal lethality in mice with a homozygous deletion in the C-terminal domain of RNA polymerase II.* Mol Gen Genet, 1999. **261**(1): p. 100-105.
152. He, X., et al., *TP53 loss creates therapeutic vulnerability in colorectal cancer.* Nature, 2015. **520**(7549): p. 697-701.

153. Liu, Y., et al., *A new way to target p53-defective colorectal cancer.* Future Oncology, 2015. **11**(23): p. 3101-3104.
154. Liu, Y., et al., *TP53 loss creates therapeutic vulnerability in colorectal cancer.* Nature, 2015. **520**(7549): p. 697-701.
155. Krämer, A., *The structure and function of proteins involved in mammalian pre-mRNA splicing.* Annual Review Of Biochemistry, 1996. **65**: p. 367-409.
156. Angela Krämer, a., et al., *Combined Biochemical and Electron Microscopic Analyses Reveal the Architecture of the Mammalian U2 snRNP.* The Journal of Cell Biology, 1999. **145**(7): p. 1355-1368.
157. Tian, J., et al., *SF3A1 and pancreatic cancer: new evidence for the association of the spliceosome and cancer.* Oncotarget, 2015. **6**(35): p. 37750-37757.
158. Chen, X., et al., *The Associations between RNA Splicing Complex Gene SF3A1 Polymorphisms and Colorectal Cancer Risk in a Chinese Population.* PLoS ONE, 2015. **10**(6): p. 1-10.
159. Song, W., et al., *[Research on the association between U2-dependent spliceosome gene and hepatocellular cancer].* Zhonghua Liu Xing Bing Xue Za Zhi = Zhonghua Liuxingbingxue Zazhi, 2015. **36**(6): p. 634-638.
160. O'Connor, B.P., et al., *Regulation of Toll-like Receptor Signaling by the SF3a mRNA Splicing Complex.* PLoS Genetics, 2015. **11**(2): p. 1-27.
161. Mostafaie, N., et al., *Correlated downregulation of estrogen receptor beta and the circadian clock gene Per1 in human colorectal cancer*. 2009, John Wiley & Sons, Ltd: United States. p. 642.
162. Ibsal, S. and A. Balmain, *Deletion of the PER3 Gene on Chromosome 1p36 in Recurrent ER-Positive Breast Cancer.* Journal of Clinical Oncology, 2010. **28**(23): p. 3770-3778.
163. Cao, Q., et al., *A Role for the Clock Gene Per1 in Prostate Cancer*. 2009, AMERICAN ASSOCIATION FOR CANCER RESEARCH: United States. p. 7619.
164. Lowrey, P.L. and J.S. Takahashi, *MAMMALIAN CIRCADIAN BIOLOGY: Elucidating Genome-Wide Levels of Temporal Organization.* Annual Review of Genomics & Human Genetics, 2004. **5**(1): p. 407-C-1.
165. Fang, L., et al., *Circadian Clock Gene CRY2 Degradation Is Involved in Chemoresistance of Colorectal Cancer.* Molecular Cancer Therapeutics, 2015. **14**(6): p. 1476-1487.
166. Gery, S. and H.P. Koeffler, *Circadian rhythms and cancer.* Cell Cycle (Georgetown, Tex.), 2010. **9**(6): p. 1097-1103.
167. Nuri, O., et al., *Loss of Cryptochrome Reduces Cancer Risk in p53 Mutant Mice.* Proceedings of the National Academy of Sciences of the United States of America, 2009(8): p. 2841.
168. Huber, A.-L., et al., *CRY2 and FBXL3 Cooperatively Degrade c-MYC.* Molecular Cell, 2016. **64**(4): p. 774-789.
169. Zheng, N., W. Wenyi, and W. Zhiwei, *Ubiquitination-mediated degradation of cell cycle-related proteins by F-box proteins.* international journal of biochemistry & cell biology, 2016. **73**: p. 99-110.
170. Kitajima, Y., et al., *The Ubiquitin-Proteasome System Is Indispensable for the Maintenance of Muscle Stem Cells.* Stem Cell Reports, 2018. **11**(6): p. 1523-1538.
171. Vlachostergios, P.J., et al., *The ubiquitin-proteasome system in cancer, a major player in DNA repair. Part 1: post-translational regulation*. 2009, CAROL DAVILA UNIVERSITY PRESS: Great Britain. p. 3006.
172. Vlachostergios, P.J., et al., *The ubiquitin-proteasome system in cancer, a major player in DNA repair. Part 2: transcriptional regulation*. 2009. p. 3019-3031.
173. Rahimi, N., *The Ubiquitin-Proteasome System Meets Angiogenesis.* Molecular Cancer Therapeutics, 2012. **11**(3): p. 538-548.

174. Bax, M., et al., *The Ubiquitin Proteasome System Is a Key Regulator of Pluripotent Stem Cell Survival and Motor Neuron Differentiation.* Cells, 2019. **8**(6): p. 581.
175. Dipankar, N., et al., *The ubiquitin-proteasome system.* Journal of Biosciences, 2006. **31**(1): p. 137-155.
176. Gorica, e., e. Wei-Ling, and V.T. Sokol, *An Optimal Ubiquitin-Proteasome Pathway in the Nervous System: The Role of Deubiquitinating Enzymes.* Frontiers in Molecular Neuroscience, 2014. **7**: p. 72.
177. Sun, L. and Z.J. Chen, *The novel functions of ubiquitination in signaling.* Current Opinion in Cell Biology, 2004. **16**(2): p. 119-126.
178. Braten, O., et al., *Numerous proteins with unique characteristics are degraded by the 26S proteasome following monoubiquitination.* Proceedings of the National Academy of Sciences of the United States of America, 2016. **113**(32): p. E4639.
179. Keiji, T., *The proteasome: Overview of structure and functions.* Proceedings of the Japan Academy, Series B, 2009. **85**(1): p. 12.
180. Pickart, C.M. and R.E. Cohen, *Proteasomes and their kin: proteases in the machine age*. 2004, Nature Publishing Group: Great Britain. p. 177.
181. Ido Livneh Victoria Cohen-Kaplan Chen Cohen-Rosenzweig Noa Avni Aaron, C., *The life cycle of the 26S proteasome ： from birth, through regulation and function, and onto its death.* Cell Research, 2016. **26**(8): p. 869-885.
182. Hu, X.-T., et al., *The proteasome subunit PSMA7 located on the 20q13 amplicon is overexpressed and associated with liver metastasis in colorectal cancer.* Oncology Reports, 2008. **19**(2): p. 441-446.
183. Arlt, A., et al., *Increased proteasome subunit protein expression and proteasome activity in colon cancer relate to an enhanced activation of nuclear factor E2-related factor 2 (Nrf2).* Oncogene, 2009. **28**(45): p. 3983-3996.
184. An, B., et al., *Novel dipeptidyl proteasome inhibitors overcome Bcl-2 protective function and selectively accumulate the cyclin-dependent kinase inhibitor p27 and induce apoptosis in transformed, but not normal, human fibroblasts*. 1998, GREENGATE PUBLISHING SERVICES: Great Britain. p. 1062.
185. Lisa J, C., W. Brian, and I. Alexandra E, *Proteasome inhibitors in cancer therapy.* Journal of Cell Communication and Signaling, 2011. **5**(2): p. 101-110.
186. Soave, C.L., et al., *Targeting the ubiquitin-proteasome system for cancer treatment: discovering novel inhibitors from nature and drug repurposing.* Cancer and Metastasis Reviews, 2017. **36**(4): p. 717-736.
187. Adams, J., et al., *Proteasome Inhibitors: A Novel Class of Potent and Effective Antitumor Agents*. 1999, WAVERLY PRESS INC: United States. p. 2615.
188. Teicher, B.A., et al., *The Proteasome Inhibitor PS-341 in Cancer Therapy*. 1999, AMERICAN ASSOCIATION FOR CANCER RESEARCH, INC.: United States. p. 2638.
189. Hideshima, T., et al., *The proteasome inhibitor PS-341 inhibits growth, induces apoptosis, and overcomes drug resistance in human multiple myeloma (MM) cells.* Cancer Research, 2000. **61**(7): p. 3071-3077.
190. Sunwoo, J.B., et al., *Novel proteasome inhibitor PS-341 inhibits activation of nuclear factor-kappa B, cell survival, tumor growth, and angiogenesis in squamous cell carcinoma.* Clinical Cancer Research: An Official Journal Of The American Association For Cancer Research, 2001. **7**(5): p. 1419-1428.
191. Yang, Y., et al., *Proteasome inhibitor PS-341 induces growth arrest and apoptosis of non-small cell lung cancer cells via the JNK/c-Jun/AP-1 signaling*. 2004, JAPANESE CANCER ASSOCIATION: Japan. p. 176.

192. Williams, S.A. and D.J. McConkey, *The Proteasome Inhibitor Bortezomib Stabilizes a Novel Active Form of p53 in Human LNCaP-Pro5 Prostate Cancer Cells*. 2003, AMERICAN ASSOCIATION FOR CANCER RESEARCH: United States. p. 7338.
193. Richardson, P.G., et al., *Extended follow-up of a phase 3 trial in relapsed multiple myeloma: final time-to-event results of the APEX trial.* Blood, 2007. **110**(10): p. 3557-3560.
194. Paul G, R., et al., *A Phase 2 Study of Bortezomib in Relapsed, Refractory Myeloma.* The New England Journal of Medicine, 2003. **348**(26): p. 2609-2617.
195. S, J., et al., *A phase 2 study of two doses of bortezomib in relapsed or refractory myeloma.* British Journal of Haematology, 2004. **127**(2): p. 165-172.
196. Kane, R.C., et al., *United States Food and Drug Administration Approval Summary: Bortezomib for the Treatment of Progressive Multiple Myeloma after One Prior Therapy*. 2006, AMERICAN ASSOCIATION FOR CANCER RESEARCH, INC.: United States. p. 2955.
197. O'Donnell, E.K., et al., *A phase 2 study of modified lenalidomide, bortezomib and dexamethasone in transplant-ineligible multiple myeloma.* British Journal of Haematology, 2018. **182**(2): p. 222-231.
198. Moreau, P., et al., *Bortezomib, thalidomide, and dexamethasone with or without daratumumab before and after autologous stem-cell transplantation for newly diagnosed multiple myeloma (CASSIOPEIA): a randomised, open-label, phase 3 study.* The Lancet, 2019. **394**(10192): p. 29-38.
199. Wang, S., et al., *Leucovorin Enhances the Anti-cancer Effect of Bortezomib in Colorectal Cancer Cells.* Sci Rep, 2017. **7**(1): p. 682.
200. Kretowski, R., A. Stypulkowska, and M. Cechowska-Pasko, *Efficient apoptosis and necrosis induction by proteasome inhibitor: bortezomib in the DLD-1 human colon cancer cell line.* Mol Cell Biochem, 2015. **398**(1-2): p. 165-73.
201. Kuhn, D.J., et al., *Potent activity of carfilzomib, a novel, irreversible inhibitor of the ubiquitin-proteasome pathway, against preclinical models of multiple myeloma*. 2007, AMERICAN SOCIETY OF HEMATOLOGY: United States. p. 3281.
202. Arastu-Kapur, S., et al., *Nonproteasomal targets of the proteasome inhibitors bortezomib and carfilzomib: a link to clinical adverse events.* Clinical Cancer Research: An Official Journal Of The American Association For Cancer Research, 2011. **17**(9): p. 2734-2743.
203. Demo, S.D., et al., *Antitumor Activity of PR-171, a Novel Irreversible Inhibitor of the Proteasome*. 2007, AMERICAN ASSOCIATION FOR CANCER RESEARCH: United States. p. 6383.
204. Alsina, M., et al., *A phase I single-agent study of twice-weekly consecutive-day dosing of the proteasome inhibitor carfilzomib in patients with relapsed or refractory multiple myeloma or lymphoma.* Clinical Cancer Research: An Official Journal Of The American Association For Cancer Research, 2012. **18**(17): p. 4830-4840.
205. Siegel, D.S., et al., *A phase 2 study of single-agent carfilzomib (PX-171-003-A1) in patients with relapsed and refractory multiple myeloma.* Blood, 2012. **120**(14): p. 2817-2825.
206. Jagannath, S., et al., *An Open-Label Single-Arm Pilot Phase II Study (PX-171-003-A0) of Low-Dose, Single-Agent Carfilzomib in Patients With Relapsed and Refractory Multiple Myeloma.* Clinical Lymphoma Myeloma and Leukemia, 2012. **12**(5): p. 310-318.
207. Fostier, K., A. De Becker, and R. Schots, *Carfilzomib: a novel treatment in relapsed and refractory multiple myeloma.* OncoTargets and Therapy, 2012. **5**: p. 237-244.
208. Dimopoulos, M.A., et al., *Carfilzomib and dexamethasone versus bortezomib and dexamethasone for patients with relapsed or refractory multiple myeloma (ENDEAVOR): a randomised, phase 3, open-label, multicentre study.* Lancet Oncology, 2016. **17**(1): p. 27-38.

209. Miller, A. *Analyzing gels and western blots with ImageJ*. 2010 [cited 2019 October 20]; Available from: https://lukemiller.org/index.php/2010/11/analyzing-gels-and-western-blots-with-image-j/.
210. Franken, N.A., et al., *Clonogenic assay of cells in vitro.* Nat Protoc, 2006. **1**(5): p. 2315-9.
211. Guzmán, C., et al., *ColonyArea: An ImageJ Plugin to Automatically Quantify Colony Formation in Clonogenic Assays.* PLOS ONE, 2014. **9**(3): p. e92444.
212. Rosa, R., et al., *In vitro and in vivo models for analysis of resistance to anticancer molecular therapies.* Current medicinal chemistry, 2014. **21**(14): p. 1595-1606.
213. Eichhorn, P.J.A., et al., *Phosphatidylinositol 3-Kinase Hyperactivation Results in Lapatinib Resistance that Is Reversed by the mTOR/Phosphatidylinositol 3-Kinase Inhibitor NVP-BEZ235*. 2008, AMERICAN ASSOCIATION FOR CANCER RESEARCH: United States. p. 9221.
214. Li, J., et al., *A chemical and phosphoproteomic characterization of dasatinib action in lung cancer.* Nature Chemical Biology, 2010. **6**(4): p. 291-299.
215. Ciardiello, F., et al., *Antitumor Activity of ZD6474, a Vascular Endothelial Growth Factor Receptor Tyrosine Kinase Inhibitor, in Human Cancer Cells with Acquired Resistance to Antiepidermal Growth Factor Receptor Therapy*. 2004, AMERICAN ASSOCIATION FOR CANCER RESEARCH, INC.: United States. p. 784.
216. Gao, S.P., et al., *Mutations in the EGFR kinase domain mediate STAT3 activation via IL-6 production in human lung adenocarcinomas.* The Journal Of Clinical Investigation, 2007. **117**(12): p. 3846-3856.
217. McDermott, M., et al., *In vitro Development of Chemotherapy and Targeted Therapy Drug-Resistant Cancer Cell Lines: A Practical Guide with Case Studies.* Frontiers in oncology, 2014. **4**: p. 40-40.
218. Ines De, P., et al., *Overcoming Intrinsic and Acquired Cetuximab Resistance in RAS Wild-Type Colorectal Cancer: An In Vitro Study on the Expression of HER Receptors and the Potential of Afatini.* Cancers, 2019. **11**(1): p. 98.
219. Kjaer, I., et al., *Cetuximab Resistance in Squamous Carcinomas of the Upper Aerodigestive Tract Is Driven by Receptor Tyrosine Kinase Plasticity: Potential for mAb Mixtures*. Molecular Cancer Therapeutics, 2016. **15**(7)p. 1614-1626.
220. Antoni, D., et al., *Three-Dimensional Cell Culture: A Breakthrough in Vivo.* International Journal of Molecular Sciences, 2015. **16**(3): p. 5517-5527.
221. Napolitano, S., et al., *Primary and Acquired Resistance of Colorectal Cancer to Anti-EGFR Monoclonal Antibody Can Be Overcome by Combined Treatment of Regorafenib with Cetuximab*. Clinical Cancer Research, 2015. **21**(13): p. 2975-2983.
222. Sato, H., et al., *Clinical outcomes of platinum-based chemotherapy plus cetuximab for recurrent or metastatic squamous cell carcinoma of the head and neck: comparison between platinum-sensitive and platinum-resistant patients.* Acta Oto-Laryngologica, 2019. **139**(2): p. 201-205.
223. Park, M.H. and J.T. Hong, *Roles of NF-κB in Cancer and Inflammatory Diseases and Their Therapeutic Approaches.* Cells, 2016. **5**(2): p. 15.
224. Brantley, D.M., et al., *Nuclear factor-kappaB (NF-kappaB) regulates proliferation and branching in mouse mammary epithelium.* Mol Biol Cell, 2001. **12**(5): p. 1445-55.
225. Wolf-Yadlin, A., et al., *Effects of HER2 overexpression on cell signaling networks governing proliferation and migration.* Molecular systems biology, 2006. **2**: p. 54-54.
226. Boeckx, C., et al., *Establishment and characterization of cetuximab resistant head and neck squamous cell carcinoma cell lines: focus on the contribution of the AP-1 transcription factor*. American Journal of Cancer Research, 2015. **5**(6): p. 1921-1938.

227. Calvin R. Justus, a., et al., *In vitro Cell Migration and Invasion Assays.* Journal of Visualized Experiments, 2014(88).
228. Satelli, A. and S. Li, *Vimentin in cancer and its potential as a molecular target for cancer therapy.* Cell Mol Life Sci, 2011. **68**(18): p. 3033-46.
229. Takemura, K., et al., *Expression of vimentin in gastric cancer: a possible indicator for prognosis.* Pathobiology, 1994. **62**(3): p. 149-54.
230. Gilles, C., et al., *Transactivation of vimentin by beta-catenin in human breast cancer cells.* Cancer Res, 2003. **63**(10): p. 2658-64.
231. Al-Saad, S., et al., *The prognostic impact of NF-kappaB p105, vimentin, E-cadherin and Par6 expression in epithelial and stromal compartment in non-small-cell lung cancer.* Br J Cancer, 2008. **99**(9): p. 1476-83.
232. Tamazato Longhi, M., et al., *EGFR Signaling Regulates Maspin/SerpinB5 Phosphorylation and Nuclear Localization in Mammary Epithelial Cells.* PloS one, 2016. **11**(7): p. e0159856-e0159856.
233. Zhou, H., et al., *Reciprocal regulation of SOCS 1 and SOCS3 enhances resistance to ionizing radiation in glioblastoma multiforme.* Clinical Cancer Research: An Official Journal Of The American Association For Cancer Research, 2007. **13**(8): p. 2344-2353.
234. Chaves de Souza, J., et al., *SOCS3 Expression Correlates with Severity of Inflammation, Expression of Proinflammatory Cytokines, and Activation of STAT3 and p38 MAPK in LPS-Induced Inflammation In Vivo.* Mediators of Inflammation, 2013. **2013**: p. 10.
235. Shang, A.-Q., et al. *Relationship between HER2 and JAK/STAT-SOCS3 signaling pathway and clinicopathological features and prognosis of ovarian cancer*. 2017. Great Britain: LANDES BIOSCIENCE.
236. Luca, F., S. Salvatore, and L. Massimo, *Evolution of Cancer Pharmacological Treatments at the Turn of the Third Millennium.* Frontiers in Pharmacology, 2018. **9**: p. 1300.
237. David, C., et al., *Cetuximab Monotherapy and Cetuximab plus Irinotecan in Irinotecan-Refractory Metastatic Colorectal Cancer.* The New England Journal of Medicine, 2004. **351**(4): p. 337-346.
238. Saltz, L.B., et al., *Phase II trial of cetuximab in patients with refractory colorectal cancer that expresses the epidermal growth factor receptor.* J Clin Oncol, 2004. **22**(7): p. 1201-8.
239. Van Cutsem, E., et al., *Open-label phase III trial of panitumumab plus best supportive care compared with best supportive care alone in patients with chemotherapy-refractory metastatic colorectal cancer.* J Clin Oncol, 2007. **25**(13): p. 1658-64.
240. Allegra, C.J., et al., *American Society of Clinical Oncology provisional clinical opinion: testing for KRAS gene mutations in patients with metastatic colorectal carcinoma to predict response to anti-epidermal growth factor receptor monoclonal antibody therapy.* J Clin Oncol, 2009. **27**(12): p. 2091-6.
241. Bardelli, A., et al., *Amplification of the MET receptor drives resistance to anti-EGFR therapies in colorectal cancer.* Cancer Discov, 2013. **3**(6): p. 658-73.
242. Weber, M.M., et al., *Overexpression of the insulin-like growth factor I receptor in human colon carcinomas.* Cancer, 2002. **95**(10): p. 2086-95.
243. Wheeler, D.L., et al., *Mechanisms of acquired resistance to cetuximab: role of HER (ErbB) family members.* Oncogene, 2008. **27**(28): p. 3944-56.
244. Januchowski, R., et al., *Microarray-based detection and expression analysis of new genes associated with drug resistance in ovarian cancer cell lines.* Oncotarget, 2017. **8**(30): p. 49944-49958.
245. Shaheen, S., et al., *Differential Expression and Pathway Analysis in Drug-Resistant Triple-Negative Breast Cancer Cell Lines Using RNASeq Analysis.* Int J Mol Sci, 2018. **19**(6).

246. Tsutsui, M., et al., *Comprehensive screening of genes resistant to an anticancer drug in esophageal squamous cell carcinoma.* Int J Oncol, 2015. **47**(3): p. 867-74.
247. Sargent, J.M., *The use of the MTT assay to study drug resistance in fresh tumour samples.* Recent Results Cancer Res, 2003. **161**: p. 13-25.
248. Mini, E., et al., *RNA sequencing reveals PNN and KCNQ1OT1 as predictive biomarkers of clinical outcome in stage III colorectal cancer patients treated with adjuvant chemotherapy.* International Journal of Cancer, 2019(9): p. 2580.
249. Brueffer, C., et al., *On the development and clinical value of RNA-sequencing-based classifiers for prediction of the five conventional breast cancer biomarkers: A report from the population-based multicenter SCAN-B study*. 2018.
250. Conesa, A., et al., *A survey of best practices for RNA-seq data analysis.* Genome Biology, 2016. **17**(1): p. 13.
251. Allegra, C.J., R.B. Rumble, and R.L. Schilsky, *Extended RAS Gene Mutation Testing in Metastatic Colorectal Carcinoma to Predict Response to Anti-Epidermal Growth Factor Receptor Monoclonal Antibody Therapy: American Society of Clinical Oncology Provisional Clinical Opinion Update 2015 Summary.* Journal of Oncology Practice, 2016. **12**(2): p. 180-181.
252. Liu, Y., A. Beyer, and R. Aebersold, *On the Dependency of Cellular Protein Levels on mRNA Abundance.* Cell, 2016. **165**(3): p. 535-550.
253. Shi, Y., et al., *Second-generation proteasome inhibitor carfilzomib enhances doxorubicin-induced cytotoxicity and apoptosis in breast cancer cells.* Oncotarget, 2016. **7**(45): p. 73697-73710.
254. McBride, A., J.O. Klaus, and K. Stockerl-Goldstein, *Carfilzomib: a second-generation proteasome inhibitor for the treatment of multiple myeloma.* American Journal Of Health-System Pharmacy: AJHP: Official Journal Of The American Society Of Health-System Pharmacists, 2015. **72**(5): p. 353-360.
255. Guerrero-Garcia, T.A., et al., *The power of proteasome inhibition in multiple myeloma.* Expert Review Of Proteomics, 2018. **15**(12): p. 1033-1052.
256. Jakubowiak, A.J., *Evolution of carfilzomib dose and schedule in patients with multiple myeloma: A historical overview.* Cancer Treatment Reviews, 2014. **40**(6): p. 781-790.
257. Baker, A.F., et al., *Carfilzomib demonstrates broad anti-tumor activity in pre-clinical non-small cell and small cell lung cancer models.* Journal of Experimental & Clinical Cancer Research (17569966), 2014. **33**(1): p. 1-22.
258. Mehta, A., et al., *Carfilzomib is an effective anticancer agent in anaplastic thyroid cancer.* Endocrine-related Cancer, 2015. **22**(3): p. 319-329.
259. Driscoll, J.J. and E.S. Woodle, *Targeting the Ubiquitin plus Proteasome System in Solid Tumors.* Seminars in Hematology, 2012. **49**(3): p. 277-283.
260. Hoeller, D. and I. Dikic, *Targeting the ubiquitin system in cancer therapy.* Nature, 2009. **458**(7237): p. 438-444.
261. Tang, W., et al., *Enhanced anti-colorectal cancer effects of carfilzomib combined with CPT-11 via downregulation of nuclear factor-κB in vitro and in vivo.* International Journal Of Oncology, 2014. **45**(3): p. 995-1010.
262. Tan, F.H., et al., *The role of STAT3 signaling in mediating tumor resistance to cancer therapy.* Curr Drug Targets, 2014. **15**(14): p. 1341-53.
263. Mañas, A., et al., *BaxΔ2 sensitizes colorectal cancer cells to proteasome inhibitor-induced cell death.* Biochemical and biophysical research communications, 2018. **496**(1): p. 18-24.
264. Zang, Y., et al., *Carfilzomib and ONX 0912 Inhibit Cell Survival and Tumor Growth of Head and Neck Cancer and Their Activities Are Enhanced by Suppression of Mcl-1 or Autophagy.*

Clinical Cancer Research: An Official Journal Of The American Association For Cancer Research, 2012. **18**(20): p. 5639-5649.
265. Maynadier, M., et al., *Combination treatment with proteasome inhibitors and antiestrogens has a synergistic effect mediated by p21WAF1 in estrogen receptor-positive breast cancer.* Oncology Reports, 2016. **36**(2): p. 1127-1134.
266. Millward, M., et al., *Phase 1 clinical trial of the novel proteasome inhibitor marizomib with the histone deacetylase inhibitor vorinostat in patients with melanoma, pancreatic and lung cancer based on in vitro assessments of the combination.* Investigational New Drugs, 2012. **30**(6): p. 2303-2317.
267. Lee, J.E., et al., *Hippo pathway effector YAP inhibition restores the sensitivity of EGFR-TKI in lung adenocarcinoma having primary or acquired EGFR-TKI resistance.* Biochemical and Biophysical Research Communications, 2016. **474**(1): p. 154-161.
268. Troiani, T., et al., *Increased TGF-α as a mechanism of acquired resistance to the anti-EGFR inhibitor cetuximab through EGFR-MET interaction and activation of MET signaling in colon cancer cells.* Clinical Cancer Research: An Official Journal Of The American Association For Cancer Research, 2013. **19**(24): p. 6751-6765.
269. Zarei, S., et al., *Effects of carfilzomib alone and in combination with cisplatin on the cell death in cisplatin-sensitive and cisplatin-resistant ovarian carcinoma cell lines.* Bratisl Lek Listy, 2019. **120**(6): p. 468-475.
270. Mohr, L., et al., *Generation of Prostate Cancer Cell Models of Resistance to the Anti-mitotic Agent Docetaxel.* Journal of visualized experiments : JoVE, 2017. **127**(127): p. 56327.
271. Boeckx, C., et al., *Establishment and characterization of cetuximab resistant head and neck squamous cell carcinoma cell lines: focus on the contribution of the AP-1 transcription factor.* American journal of cancer research, 2015. **5**(6): p. 1921-1938.
272. Hanahan, D. and R.A. Weinberg, *Hallmarks of cancer: the next generation.* Cell, 2011. **144**(5): p. 646-74.
273. Sen, M., et al., *Targeting Stat3 abrogates EGFR inhibitor resistance in cancer.* Clinical cancer research : an official journal of the American Association for Cancer Research, 2012. **18**(18): p. 4986-4996.
274. Willey, C.D., et al., *Differential escape mechanisms in cetuximab-resistant head and neck cancer cells.* Biochemical and Biophysical Research Communications, 2019. **517**(1): p. 36-42.
275. Liska, D., et al., *HGF Rescues Colorectal Cancer Cells from EGFR Inhibition via MET Activation.* Clinical Cancer Research, 2011. **17**(3): p. 472-482.
276. Gherardi, E., et al., *Targeting MET in cancer: rationale and progress.* Nature reviews. Cancer, 2012. **12**(2): p. 89-103.
277. Bertotti, A., et al., *A Molecularly Annotated Platform of Patient-Derived Xenografts ("Xenopatients") Identifies HER2 as an Effective Therapeutic Target in Cetuximab-Resistant Colorectal Cancer.* Cancer Discovery, 2011. **1**(6): p. 508-523.
278. Moroni, M., et al., *Gene copy number for epidermal growth factor receptor (EGFR) and clinical response to antiEGFR treatment in colorectal cancer: a cohort study.* Lancet Oncology, 2005. **6**(5): p. 279-286.
279. De Roock, W., et al., *Association of KRAS p.G13D mutation with outcome in patients with chemotherapy-refractory metastatic colorectal cancer treated with cetuximab.* JAMA, 2010. **304**(16): p. 1812-1820.
280. Bullard, J.H., et al., *Evaluation of statistical methods for normalization and differential expression in mRNA-Seq experiments.* BMC bioinformatics, 2010. **11**: p. 94.

281. Yan, Z., et al., *A statistical normalization method and differential expression analysis for RNA-seq data between different species.* BMC Bioinformatics, 2019. **20**(1): p. 1-10.
282. Anders, S. and W. Huber, *Differential expression analysis for sequence count data.* Genome Biology, 2010. **11**(10): p. 2483.
283. Mocellin, S., et al., *Circadian pathway genetic variation and cancer risk: evidence from genome-wide association studies.* BMC medicine, 2018. **16**(1): p. 20.
284. Tang, Z., et al., *Inhibition of CRY2 by STAT3/miRNA-7-5p Promotes Osteoblast Differentiation through Upregulation of CLOCK/BMAL1/P300 Expression.* Molecular Therapy - Nucleic Acids, 2020. **19**: p. 865-876.
285. Yu, Y., et al., *Cryptochrome 2 (CRY2) Suppresses Proliferation and Migration and Regulates Clock Gene Network in Osteosarcoma Cells.* Medical science monitor : international medical journal of experimental and clinical research, 2018. **24**: p. 3856-3862.
286. Okamoto, K., et al., *Reversal of Mutant KRAS-Mediated Apoptosis Resistance by Concurrent Noxa/Bik Induction and Bcl-2/Bcl-xL Antagonism in Colon Cancer Cells.* Mol Cancer Res, 2015. **13**(4): p. 659-69.
287. Thaler, S., et al., *Proteasome inhibitors prevent bi-directional HER2/estrogen-receptor cross-talk leading to cell death in endocrine and lapatinib-resistant HER2+/ER+ breast cancer cells.* Oncotarget, 2017. **8**(42): p. 72281-72301.
288. Jarauta, V., et al., *Inhibition of autophagy with chloroquine potentiates carfilzomib-induced apoptosis in myeloma cells in vitro and in vivo.* Cancer Lett, 2016. **382**(1): p. 1-10.
289. Zhang, L., et al., *In vitro and in vivo therapeutic efficacy of carfilzomib in mantle cell lymphoma: targeting the immunoproteasome.* Mol Cancer Ther, 2013. **12**(11): p. 2494-504.
290. Savjani, K.T., A.K. Gajjar, and J.K. Savjani, *Drug solubility: importance and enhancement techniques.* ISRN pharmaceutics, 2012. **2012**(1): p. 195727-195727.
291. Jyoti, A., et al., *An in vitro assessment of liposomal topotecan simulating metronomic chemotherapy in combination with radiation in tumor-endothelial spheroids.* Sci Rep, 2015. **5**: p. 15236.
292. Farrell, A.S. and R.C. Sears, *MYC degradation.* Cold Spring Harb Perspect Med, 2014. **4**(3).
293. Naujokat, C. and S. Hoffmann, *Role and Function of the 26S Proteasome in Proliferation and Apoptosis.* Laboratory Investigation, 2002. **82**(8): p. 965-980.
294. Barnum, K.J. and M.J. O'Connell, *Cell cycle regulation by checkpoints.* Methods in molecular biology (Clifton, N.J.), 2014. **1170**: p. 29-40.
295. Yip, K.W. and J.C. Reed, *Bcl-2 family proteins and cancer.* Oncogene, 2008. **27**(50): p. 6398-6406.

8. Supplementary Tables and Figures

Supplementary Table 3.1: List of Differentially Expressed proteins from our Proteomics analysis (SW48-C225 vs SW48)

Gene names	Protein names	Expression Value (-ve = downregulation, +ve = upregulation)
Abhd14b	Alpha/beta hydrolase domain-containing protein 14B	-1.185369492
Ptma	Prothymosin alpha;Prothymosin alpha, N-terminally processed;Thymosin alpha	-1.016953786
Bzw1	Basic leucine zipper and W2 domain-containing protein 1	3.377185186
Lrrfip1	Leucine-rich repeat flightless-interacting protein 1	1.192747116
Tuba4a	Tubulin alpha-4A chain	-1.264493942
Lrba	Lipopolysaccharide-responsive and beige-like anchor protein	-2.097447077
Cdk5	Cyclin-dependent-like kinase 5	1.030009588
S100a4	Protein S100-A4	-1.918312709
Ube2k	Ubiquitin-conjugating enzyme E2 K	0.700332006
Eno2	Gamma-enolase;Enolase	-1.510478973
Pdia4	Protein disulfide-isomerase A4	-1.104814529
Dbn1	Drebrin	0.801160177
Slc3a2	4F2 cell-surface antigen heavy chain	-2.63825353
Rpl13a	60S ribosomal protein L13a	5.278285344
Arfip2	Arfaptin-2	0.667046229
Ldha	L-lactate dehydrogenase;L-lactate dehydrogenase A chain	0.728661855

Ctsd	Cathepsin D	-2.784800847
Gys1	Glycogen [starch] synthase, muscle	1.002151489
Myof	Myoferlin	1.08313179
Camk2g;Camk2b	Calcium/calmodulin-dependent protein kinase type II subunit gamma;Calcium/calmodulin-dependent protein kinase type II subunit beta	-1.720769882
Xpo7	Exportin-7	-1.358728409
Eppk1	Epiplakin	-1.762388229
Nup155	Nuclear pore complex protein Nup155	1.070278804
Cul4b	Cullin-4B	1.367647171
Ube2c	Ubiquitin-conjugating enzyme E2 C	1.48340416
septin-9	Septin-9	0.650990804
Yars	Tyrosine--tRNA ligase;Tyrosine--tRNA ligase, cytoplasmic;Tyrosine--tRNA ligase, cytoplasmic, N-terminally processed	1.324473063
Ppp1r8	Nuclear inhibitor of protein phosphatase 1	-1.99164327
Hsd17b10	3-hydroxyacyl-CoA dehydrogenase type-2	-0.805627823
Bcl2l1	Bcl-2-like protein 1	0.883090337
Pir	Pirin	-2.26031812
Atp5c1	ATP synthase subunit gamma;ATP synthase subunit gamma, mitochondrial	-3.073059718
Asph	Aspartyl/asparaginyl beta-hydroxylase	0.972614924
Nckap1	Nck-associated protein 1	-0.474907557
Dync1i2	Cytoplasmic dynein 1 intermediate chain 2	-0.518511454
Pabpc4	Polyadenylate-binding protein	2.184317271
Prdx1	Peroxiredoxin-1	-0.805488586
Flna	Filamin-A	-0.929649989
Nap1l4	Nucleosome assembly protein 1-like 4	0.854700089

Tjp1	Tight junction protein ZO-1	-1.150740306
Ddah1	N(G),N(G)-dimethylarginine dimethylaminohydrolase 1	-2.65682284
Pfn2	Profilin;Profilin-2	-2.993269602
Tmed7		1.417027791
Ctnnd1	Catenin delta-1	2.456123988
Pdcd5	Programmed cell death protein 5	-1.643405914
Tyms	Thymidylate synthase	3.018360138
Pcmt1	Protein-L-isoaspartate O-methyltransferase;Protein-L-isoaspartate(D-aspartate) O-methyltransferase	1.700061162
Acsl3	Long-chain-fatty-acid--CoA ligase 3	1.149263382
Arhgef1	Rho guanine nucleotide exchange factor 1	-1.268052419
Slc25a22;Slc25a18	Mitochondrial glutamate carrier 1;Mitochondrial glutamate carrier 2	2.367378871
Myo6	Unconventional myosin-VI	0.692811966
Rps6ka1	Ribosomal protein S6 kinase;Ribosomal protein S6 kinase alpha-1	-0.577563604
Lmo7		-2.586266836
Atl3	Atlastin-3	-1.625808716
Oxr1	Oxidation resistance protein 1	-4.376340866
Hsph1	Heat shock protein 105 kDa	-2.742766062
Sec23a	Protein transport protein Sec23A	-1.353640238
Adsl	Adenylosuccinate lyase	1.926452001
Alcam	CD166 antigen	2.571329117
Dsp	Desmoplakin	-2.416680654
Ahnak		-0.757407506
Sec22b	Vesicle-trafficking protein SEC22b	-1.026524226
Pfdn4	Prefoldin subunit 4	1.694707235

Slc12a2	Solute carrier family 12 member 2	-2.407907486
Ptbp3	Polypyrimidine tract-binding protein 3	1.304224014
Psme1	Proteasome activator complex subunit 1	0.768373489
Gtf2i	General transcription factor II-I	-1.034772237
Pfdn6	Prefoldin subunit 6	2.225906372
Shmt1	Serine hydroxymethyltransferase;Serine hydroxymethyltransferase, cytosolic	-1.528624217
Prdx5	Peroxiredoxin-5, mitochondrial	0.850025813
Psme2	Proteasome activator complex subunit 2	1.360802968
Atp2b1	Plasma membrane calcium-transporting ATPase 1	-1.097454071
Cyb5a	Cytochrome b5	-3.270346959
Cct8	T-complex protein 1 subunit theta	0.470482508
Arpc3	Actin-related protein 2/3 complex subunit 3	-0.896882375
Arrb1	Beta-arrestin-1	-0.820654551
Capn2	Calpain-2 catalytic subunit	1.090559006
Dpysl2	Dihydropyrimidinase-related protein 2	-2.932701747
Aip	AH receptor-interacting protein	-0.916685104
Hdac1;Gm10093	Histone deacetylase 1;Histone deacetylase	1.18628184
Scarb2	Lysosome membrane protein 2	-2.539943059
Emg1	Ribosomal RNA small subunit methyltransferase NEP1	1.399272283
Exoc4	Exocyst complex component 4	-0.440038045
Anxa3	Annexin A3;Annexin	2.501558304
Calu	Calumenin	-2.109759013
Smarce1	SWI/SNF-related matrix-associated actin-dependent regulator of chromatin subfamily E member 1	0.972995758
Supt5h	Transcription elongation factor SPT5	1.479299545

Sfn	14-3-3 protein sigma	-2.904422124
Ugdh	UDP-glucose 6-dehydrogenase	-1.529936473
Zfr	Zinc finger RNA-binding protein	1.635283152
Idh1	Isocitrate dehydrogenase [NADP] cytoplasmic	-0.626363754
Hprt1	Hypoxanthine-guanine phosphoribosyltransferase	-0.991415024
Ca2	Carbonic anhydrase 2	2.452917099
H3f3a;H3f3c	Histone H3.3;Histone H3.3C;Histone H3	-1.080780029
Got2	Aspartate aminotransferase, mitochondrial	-1.10312144
Rrm1	Ribonucleoside-diphosphate reductase large subunit	-1.366312663
Hsp90b1	Endoplasmin	-1.236576716
S100a10	Protein S100-A10	-3.28527832
Mdh2	Malate dehydrogenase, mitochondrial	-0.808168411
P4hb	Protein disulfide-isomerase	-0.907909393
Calm1;Calml3	Calmodulin-like protein 3	-0.870864232
Anxa1	Annexin A1	-1.968730927
Txn	Thioredoxin	-5.849562963
Cdk1	Cyclin-dependent kinase 1	1.651474635
Hsp90ab1	Heat shock protein HSP 90-beta	1.067808787
Pfkl	ATP-dependent 6-phosphofructokinase, liver type	-0.768334707
Atp1b1	Sodium/potassium-transporting ATPase subunit beta-1	-1.717624029
Rpsa	40S ribosomal protein SA	0.715988795
Calr	Calreticulin	-0.850519816
Lgals3	Galectin;Galectin-3	-2.701066971
Hmga1	High mobility group protein HMG-I/HMG-Y	3.169912338
Hmga1	High mobility group protein HMG-I/HMG-Y	2.694886525

Slc2a1	Solute carrier family 2, facilitated glucose transporter member 1	-2.318007787
Hspa1a;Hspa1b	Heat shock 70 kDa protein 1A;Heat shock 70 kDa protein 1B	0.697822571
Tmsb4x	Thymosin beta-4;Hematopoietic system regulatory peptide	1.366552353
Vim	Vimentin	1.987710317
Cat	Catalase	-1.653533936
Ezr	Ezrin	1.524459203
Msn	Moesin	4.935460409
Ctnna1	Catenin alpha-1	0.957602183
Pdia3	Protein disulfide-isomerase A3	-1.558506648
Apex1	DNA-(apurinic or apyrimidinic site) lyase;DNA-(apurinic or apyrimidinic site) lyase, mitochondrial	0.72213618
Fkbp4	Peptidyl-prolyl cis-trans isomerase FKBP4;Peptidyl-prolyl cis-trans isomerase FKBP4, N-terminally processed;Peptidyl-prolyl cis-trans isomerase	1.733669281
Cpox	Oxygen-dependent coproporphyrinogen-III oxidase, mitochondrial	-2.89885203
Stat3	Signal transducer and activator of transcription 3;Signal transducer and activator of transcription	2.740074158
Hist1h1e	Histone H1.4	-1.025764465
Stt3a	Dolichyl-diphosphooligosaccharide--protein glycosyltransferase subunit STT3A	-0.843609492
Aldh3a1	Aldehyde dehydrogenase, dimeric NADP-preferring	-6.823120117
Pfkm	ATP-dependent 6-phosphofructokinase, muscle type	-0.714340846
Lmna	Prelamin-A/C;Lamin-A/C	-1.113861084
Cbr1	Carbonyl reductase [NADPH] 1	-3.427728017
S100a11	Protein S100-A11	-2.441742579
Slc25a5	ADP/ATP translocase 2;ADP/ATP translocase 2, N-terminally processed	0.951053619

Tst	Thiosulfate sulfurtransferase	1.912115097
Pkm	Pyruvate kinase PKM	-1.020753225
Idh2	Isocitrate dehydrogenase [NADP], mitochondrial	-2.000218709
Slc16a3	Monocarboxylate transporter 4	1.452981949
Opa1	Dynamin-like 120 kDa protein, mitochondrial;Dynamin-like 120 kDa protein, form S1	-1.575267792
Eif5	Eukaryotic translation initiation factor 5	1.725870768
Arpc4	Actin-related protein 2/3 complex subunit 4	-1.054702759
Ruvbl1	RuvB-like 1	1.245564143
Nploc4	Nuclear protein localization protein 4 homolog	-0.792996724
Cirbp	Cold-inducible RNA-binding protein	-2.135060628
Cks1brt;Cks1b	Cyclin-dependent kinases regulatory subunit;Cyclin-dependent kinases regulatory subunit 1	1.375775655
Ube2n	Ubiquitin-conjugating enzyme E2 N	-0.82365036
Vbp1	Prefoldin subunit 3	1.403630575
Nutf2	Nuclear transport factor 2	-1.162699382
Ywhag	14-3-3 protein gamma;14-3-3 protein gamma, N-terminally processed	-0.918899536
Psmc1	26S protease regulatory subunit 4	0.664941152
Rps8	40S ribosomal protein S8	0.4604098
Rps11	40S ribosomal protein S11	0.482859294
Eef1a2	Elongation factor 1-alpha 2	3.653432846
Vsnl1	Visinin-like protein 1	-4.573549906
Mtpn	Myotrophin	-2.214583079
Hist1h4a	Histone H4	-0.78116862
Ran;1700009N14Rik	GTP-binding nuclear protein Ran	-0.627092997

Gnb1	Guanine nucleotide-binding protein G(I)/G(S)/G(T) subunit beta-1	-3.062351227
Gnb2	Guanine nucleotide-binding protein G(I)/G(S)/G(T) subunit beta-2	-1.401170095
Actg1;Actb	Actin, cytoplasmic 2;Actin, cytoplasmic 2, N-terminally processed;Actin, cytoplasmic 1;Actin, cytoplasmic 1, N-terminally processed	-0.546151479
Rala;Ralb	Ras-related protein Ral-A;Ras-related protein Ral-B	-2.105714798
Rps10	40S ribosomal protein S10	1.668891271
Ppp3ca	Serine/threonine-protein phosphatase 2B catalytic subunit alpha isoform	-1.107041677
Rpl22	60S ribosomal protein L22	6.029586156
Serpinb5	Serpin B5	-2.077781041
Naca	Nascent polypeptide-associated complex subunit alpha;Nascent polypeptide-associated complex subunit alpha, muscle-specific form	1.163086573
Urod	Uroporphyrinogen decarboxylase	1.890880585
Prkdc	DNA-dependent protein kinase catalytic subunit	-0.663030624
Csrp1	Cysteine and glycine-rich protein 1	-0.721536636
G3bp2	Ras GTPase-activating protein-binding protein 2	-0.942860285
Anxa4	Annexin A4;Annexin	-5.636772156
Gclc	Glutamate--cysteine ligase catalytic subunit	-2.551165899
Smarcc1	SWI/SNF complex subunit SMARCC1	1.554854075
G3bp1	Ras GTPase-activating protein-binding protein 1	1.134945552
Egfr	Epidermal growth factor receptor	-1.777962367
Vcp	Transitional endoplasmic reticulum ATPase	0.472113291
Ckb	Creatine kinase B-type	5.474826813
Top1	DNA topoisomerase 1	0.570701599
Col17a1	Collagen alpha-1(XVII) chain;120 kDa linear IgA disease antigen homolog	-1.901775996

Cbfb	Core-binding factor subunit beta	-1.212540309
Npepps	Puromycin-sensitive aminopeptidase	0.490581512
Acly	ATP-citrate synthase	1.717308044
Gnat3	Guanine nucleotide-binding protein G(t) subunit alpha-3	-4.828833262
Mthfd1l	Monofunctional C1-tetrahydrofolate synthase, mitochondrial	2.393877665
Ddx46	Probable ATP-dependent RNA helicase DDX46	1.155245463
Akap8l	A-kinase anchor protein 8-like	0.790770849
Ogdh	2-oxoglutarate dehydrogenase, mitochondrial	-2.659437815
Cttn	Src substrate cortactin	-0.686978022
Rbbp4	Histone-binding protein RBBP4	1.249253591
Asns	Asparagine synthetase [glutamine-hydrolyzing]	2.398107529
Bcap31	B-cell receptor-associated protein 31	-0.793476105
Fscn1	Fascin	-3.16881752
Fxr1	Fragile X mental retardation syndrome-related protein 1	2.037222544
Ddx5	Probable ATP-dependent RNA helicase DDX5	0.598960241
Nnt	NAD(P) transhydrogenase, mitochondrial	-3.077504476
Ddx3x;Ddx3y	ATP-dependent RNA helicase DDX3X;ATP-dependent RNA helicase DDX3Y	0.390374502
Sptbn1	Spectrin beta chain, non-erythrocytic 1	0.595769246
Trim28	Transcription intermediary factor 1-beta	1.53168869
Tsn	Translin	-0.722482681
Supt6h	Transcription elongation factor SPT6	0.881121953
Fkbp3	Peptidyl-prolyl cis-trans isomerase FKBP3	-1.050245921
Top2b	DNA topoisomerase 2-beta	-1.50833257
Hist2h2ac;Hist2h2aa1	Histone H2A type 2-C;Histone H2A type 2-A	-0.644659678

Nqo1	NAD(P)H dehydrogenase [quinone] 1	-3.730345408
Gart	Trifunctional purine biosynthetic protein adenosine-3;Phosphoribosylamine--glycine ligase;Phosphoribosylformylglycinamidine cyclo-ligase;Phosphoribosylglycinamide formyltransferase	3.523539861
Nop58	Nucleolar protein 58	0.668396632
Cltb	Clathrin light chain B	-1.149697622
Snx1	Sorting nexin-1	-0.614756266
Clpx	ATP-dependent Clp protease ATP-binding subunit clpX-like, mitochondrial	1.768865585
Dcaf13	DDB1- and CUL4-associated factor 13	1.621135076
Rcc1	Regulator of chromosome condensation	0.590672811
Mlec	Malectin	-1.058811188
Snd1	Staphylococcal nuclease domain-containing protein 1	-0.940498352
Syncrip	Heterogeneous nuclear ribonucleoprotein Q	0.821582794
Tubb2a;Tubb2b	Tubulin beta-2A chain;Tubulin beta-2B chain	-1.039213816
Flnb	Filamin-B	2.166229248
H1fx		-3.319665273
Vapb	Vesicle-associated membrane protein-associated protein B	-1.012865702
Ganab	Neutral alpha-glucosidase AB	0.524529775
Nceh1	Neutral cholesterol ester hydrolase 1	-1.726918538
Srp68	Signal recognition particle subunit SRP68	1.008265177
Ckap4	Cytoskeleton-associated protein 4	-0.880446116
Hadha	Trifunctional enzyme subunit alpha, mitochondrial;Long-chain enoyl-CoA hydratase;Long chain 3-hydroxyacyl-CoA dehydrogenase	-0.836735408
Efhd2	EF-hand domain-containing protein D2	2.484165827

Polr2b	DNA-directed RNA polymerase II subunit RPB2	1.027057012
Ogt	UDP-N-acetylglucosamine--peptide N-acetylglucosaminyltransferase 110 kDa subunit	1.813751221
Pdlim5	PDZ and LIM domain protein 5	-2.838061015
Hmgcs1	Hydroxymethylglutaryl-CoA synthase, cytoplasmic	3.008804957
Afg3l2	AFG3-like protein 2	-1.1448644
Slc25a1	Tricarboxylate transport protein, mitochondrial	2.628494898
Gfm1	Elongation factor G, mitochondrial	0.795063019
Hpgd	15-hydroxyprostaglandin dehydrogenase [NAD(+)]	-2.115217845
Rnpep	Aminopeptidase B	-1.111710866
Atp1a1	Sodium/potassium-transporting ATPase subunit alpha-1	-1.142976125
Flnc	Filamin-C	1.46927007
Ndufs1	NADH-ubiquinone oxidoreductase 75 kDa subunit, mitochondrial	3.672290802
Eif3h	Eukaryotic translation initiation factor 3 subunit H	0.715641658
Rpn1	Dolichyl-diphosphooligosaccharide--protein glycosyltransferase subunit 1	-0.940685272
Dars	Aspartate--tRNA ligase, cytoplasmic	1.940743764
Pycr2	Pyrroline-5-carboxylate reductase 2	0.793860118
Atad3	ATPase family AAA domain-containing protein 3	1.038368225
Sar1a	GTP-binding protein SAR1a	-1.615252177
Aco2	Aconitate hydratase, mitochondrial	-0.823734283
Nampt	Nicotinamide phosphoribosyltransferase	1.4914608
Hibadh	3-hydroxyisobutyrate dehydrogenase, mitochondrial	-1.564733505
Mrpl15	39S ribosomal protein L15, mitochondrial	1.835666021
Rps21	40S ribosomal protein S21	1.815513611
Rpl14	60S ribosomal protein L14	-3.449358622

Slc25a11	Mitochondrial 2-oxoglutarate/malate carrier protein	0.888594309
Smc3	Structural maintenance of chromosomes protein 3	0.554861069
Atic	Bifunctional purine biosynthesis protein PURH;Phosphoribosylaminoimidazolecarboxamide formyltransferase;IMP cyclohydrolase	-1.246859233
Rrs1	Ribosome biogenesis regulatory protein homolog	1.636969884
Pbdc1	Protein PBDC1	-1.45150884
Dimt1	Probable dimethyladenosine transferase	1.050111135
Pgm1;Pgm2	Phosphoglucomutase-1	2.127451579
Tars	Threonine--tRNA ligase, cytoplasmic	1.483244578
Ppil1	Peptidyl-prolyl cis-trans isomerase-like 1	1.688128789
Chordc1	Cysteine and histidine-rich domain-containing protein 1	2.372676214
Rpl34	60S ribosomal protein L34	0.676570892
Dlst	Dihydrolipoyllysine-residue succinyltransferase component of 2-oxoglutarate dehydrogenase complex, mitochondrial	-1.819494247
Atad1	ATPase family AAA domain-containing protein 1	1.10117658
Ndufv2	NADH dehydrogenase [ubiquinone] flavoprotein 2, mitochondrial	2.058582942
Rpl22l1	60S ribosomal protein L22-like 1	-1.243289948
U2af1	Splicing factor U2AF 35 kDa subunit	1.387233734
Itpa	Inosine triphosphate pyrophosphatase	0.925391515
Chmp4b	Charged multivesicular body protein 4b	-0.645785014
Ebna1bp2	Probable rRNA-processing protein EBP2	3.259344101
Prpf4	U4/U6 small nuclear ribonucleoprotein Prp4	0.947041829
Prkar1a	cAMP-dependent protein kinase type I-alpha regulatory subunit;cAMP-dependent protein kinase type I-alpha regulatory subunit, N-terminally processed	2.417814255

Pgam1	Phosphoglycerate mutase 1	-0.492620468
Atp5h	ATP synthase subunit d, mitochondrial	2.16292127
Sacm1l	Phosphatidylinositide phosphatase SAC1	-1.01671346
Tubb3	Tubulin beta-3 chain	-0.979939143
Lima1	LIM domain and actin-binding protein 1	-2.412229538
Rtn3	Reticulon-3	-2.267805735
Ivd	Isovaleryl-CoA dehydrogenase, mitochondrial	-1.860891342
Aldh1a3	Aldehyde dehydrogenase family 1 member A3	5.732103984
Prmt1	Protein arginine N-methyltransferase 1	0.994005203
Akr1a1	Alcohol dehydrogenase [NADP(+)]	-0.80557251
Sh3bgrl	SH3 domain-binding glutamic acid-rich-like protein	-3.090478261
Tomm40	Mitochondrial import receptor subunit TOM40 homolog	2.409690221
Gda	Guanine deaminase	2.378440857
Nfkb2	Nuclear factor NF-kappa-B p100 subunit;Nuclear factor NF-kappa-B p52 subunit	2.305530548
Ruvbl2	RuvB-like 2	1.01911672
Eif4h	Eukaryotic translation initiation factor 4H	-0.775741577
Tagln2	Transgelin-2	-1.183851242
Twf2	Twinfilin-2	1.538225174
Tfg		0.576126099
Letm1	LETM1 and EF-hand domain-containing protein 1, mitochondrial	-3.154640834